# Three-Dimensional Printing of Regulatory T-Cells: A Novel Immunotherapy to Prevent Transplantation Rejection

Juewan Kim

School of Biological Sciences
Department of Molecular & Biomedical Science


February 2020

# CONTENTS

# ABSTRACT

The work presented in this thesis explores the encapsulation of human natural and induced regulatory T-cells (nTregs and iTregs), and the generation of phenotypically stable iTregs for application in 3D-bioprinting with pancreatic islets. 3D-bioprinting of Tregs with islets could serve as an alternative method of islet transplantation to tackle current challenges associated with intra-hepatic islet transplantation such as side-effects of immunosuppressive drugs and sub-optimal characteristics of liver as the site of islet implantation. Paper one explores in vitro evaluation of nTregs and iTregs encapsulated in alginate-gelatin methacryloyl (GelMA) hydrogel. While encapsulation of islets has been extensively investigated since the 1950s, encapsulation of Tregs has never been done, thus this paper aimed to examine whether Tregs can viably be encapsulated. In this study, the alginate-GelMA hydrogel was supplemented with Treg-specific bioactive factors IL-2 and CCL1, to evaluate the effect of IL-2 on encapsulated Tregs and to investigate the potential of CCL1 to recruit recipient Tregs upon transplantation. This study demonstrated that encapsulated nTregs and iTregs are viable, phenotypically stable and functional. Furthermore, encapsulation prevented migration of Tregs out of the hydrogel structure in the presence of potent chemotactic signals. Supplementation of the hydrogel with IL-2 and CCL1 improved encapsulated Treg viability, phenotype and function, and recruited Tregs to the hydrogel structure, respectively. Moreover, peripheral blood CD4+ T-cells expressing the chemokine receptor for CCL1, CCR8, were highly enriched with Tregs, and selective recruitment of these Tregs from peripheral blood mononuclear cells was demonstrated using CCL1. Paper two investigates the generation of stable human iTregs. Most trials of Treg-therapy have been focusing on nTregs, as iTregs are unstable and can differentiate into pro-inflammatory Th17 cells. For applications in transplantation, iTregs could be an attractive alternative to nTregs given their TCR repertoire and the ease of generating enough iTregs for clinical dosage. In this study, an iTreg differentiation method was optimized and demonstrated to generate superior iTregs to a commercially available kit in terms of viability, and CD25 and FOXP3 expression. In-house generated iTregs were stable in the absence of IL-2 and in the presence of Th17-polarizing cytokines without upregulation of Th17 signature genes, even though demethylation of the Treg-specific demethylation region (TSDR) was not demonstrated. Moreover, they were stable and highly suppressive when re-stimulated without iTreg differentiation components.

# DECLARATION

I certify that this work contains no material which has been accepted for the award of any other degree or diploma in my name, in any university or other tertiary institution and, to the best of my knowledge and belief, contains no material previously published or written by another person, except where due reference has been made in the text. In addition, I certify that no part of this work will, in the future, be used in a submission in my name, for any other degree or diploma in any university or other tertiary institution without the prior approval of the University of Adelaide and where applicable, any partner institution responsible for the joint-award of this degree.

I acknowledge that copyright of published works contained within this thesis resides with the copyright holder(s) of those works.

I also give permission for the digital version of my thesis to be made available on the web, via the University's digital research repository, the Library Search and also through web search engines, unless permission has been granted by the University to restrict access for a period of time.

Juewan Kim

February 2020

To my grandfathers,
I dedicate this thesis.
In honour of your loving memories.

# ACKNOWLEDGEMENTS

First, I would like to thank my principal supervisor, Professor Toby Coates. He has been a truly amazing supervisor, providing me with many opportunities and resources. Professor Coates has been nothing but encouraging and supportive throughout my PhD, making sure I can spread my wings under his tutelage. I will always be grateful for what he has done for me.

I'd also like to thank my co-supervisors, Professor Simon Barry and Associate Professor Robert Carroll and Dr Christopher Hope for their supervision and assistance. In particular, Dr Hope has been essential for my experimental designs and data interpretation. I sincerely enjoyed all the discussions we had together, and I appreciate all the critical feedbacks he has given me.

I want to thank my best friends and laboratory colleagues, Mr Griffith Perkins, Mr Francis Kette and Dr Sebastian Stead. I cannot thank them enough for their assistance in experiments and manuscript writing, and the scientific discussions we had together whether beers were involved or not. I will definitely cherish these memories throughout my life.

I would like to thank the members of the renal laboratory, Mr. Christopher Drogemuller, Mrs. Julie Johnston, Mrs. Svjetlana Kireta, Ms. Daniella Penko, Mrs. Jodie Nitschke, Mr. Ernesto Hurtado, Dr. Plinio Hurtado, Miss. Jacqueline Scaffidi and Mr. Denghao Wu. They facilitated my PhD research by helping me with many aspects of my work. I could not have asked for better workplace environment full of such amazing people.

I would like to thank our collaborators at University of Wollongong, Professor Gordon Wallace, Dr. Zhilian Yue, Dr. Xiao Liu and Miss Narangerel Gantumur. Their expertise in biomaterials and 3D bioprinting has been crucial for my project.

I would like to thank my partner, Roma Suarez, for her endless love and encouragement. She has always believed in me and has been proud of me for what I do. She cheered me up at difficult times, she celebrated with me at good times and she motivated me at all times. I cannot thank her enough for all the support she has given me throughout my PhD.

Lastly, I would like to thank my parents and my sisters. They made me who I am today, and they have been constant sources of motivation throughout my PhD. I am truly grateful for their love, care and support. Thank you so much for always listening to me talking about my research even though I cannot explain it very well in Korean.

# LITERATURE REVIEW

## *Introduction*

Diabetes mellitus (DM), is a chronic disorder characterized by hyperglycaemia due to failing of glucose metabolism, which causes long-term complications in multiple organs including retinopathy, nephropathy, neuropathy, and vasculopathy[1]. DM is a serious public health problem, causing significant cost to both the health care system and the economy, with an estimation of 673 billion USD per annum worldwide. Globally, DM is the eighth leading cause of death causing over 5 million deaths. In 2015, there were an estimated 415 million adults with diabetes worldwide with the global prevalence of 8.8% and it is predicted to increase to 642 million by 2040[2].

Type 1 diabetes mellitus (T1DM), also known as juvenile diabetes, accounts for 5-10% of the population with diabetes[3]. Symptoms of T1DM include polyuria, polydipsia, polyphagia, weight loss, blurry vision and extreme fatigue. T1DM may occur at virtually any age but is most common in children and young adults and occurs as a consequence of an autoimmune destruction of the insulin-producing β cells of the islets of Langerhans in the pancreas, leading to absolute insulin deficiency[1,4]. The autoimmune destruction is caused by islet-specific T cell response[5] by various autoantibodies such as autoantibodies to insulin[1,3]. Recent studies suggest T1DM is triggered by environmental factors such as exposure to pathogens or environmental antigens in individuals who are genetically predisposed to diabetes by particular genes such as the HLA genes, which contribute to 50% of the genetic susceptibility to T1DM[3,4].

Currently, patients with T1DM are treated with daily exogenous insulin administration[6,7]. However, despite advances in medicine, there has not yet been a development of an insulin therapy that can mimic the physiological rhythms or a mechanical replacement for pancreatic β cells. An intensive monitoring of blood glucose level accompanied by exogenous insulin therapy via insulin injection or pump represents the current state of treatments for T1DM. Although these treatments are able to delay the progression of diabetic complications including neuropathy and retinopathy, it is not sufficient to prevent these complications[8]. The replacement of β-cell function through whole pancreas transplantation is presently the only permanent alternative for re-establishing endogenous insulin secretion in patients with T1DM[9].

## *Current approaches for β-cell replacement*

Pancreas transplantation is reserved and performed in patients with T1DM and advanced or end-stage renal disease. As a result, over three quarters of the whole pancreas is transplanted in conjunction with kidney transplantation as either simultaneous kidney-pancreas transplantation or alternatively pancreas after kidney transplantation[10]. Furthermore, the surgical procedure is associated with significant mortality risk, accompanied with clinically significant complications such as pancreatitis, bleeding, re-occurrence of autoimmunity, and rejection post-transplantation, which motivates the urgent need for the search of an alternative therapy[11].

A logical alternative to whole-organ transplantation is to transplant the cells that have been destroyed. Pancreatic islet transplantation is a minimally invasive approach where purified allogeneic donor islets, isolated from deceased organ donor pancreata are currently percutaneously infused into recipient liver through the portal vein (**Figure 1**)[12–14]. This procedure has lower risk compared to pancreas transplantation as major surgery is not required and a differing immunosuppression regimen is employed. A cellular approach was first tried unsuccessfully in man in 1894 using fragmented sheep pancreas in a subject with diabetes[13,15]. The successful application of islet transplantation as a treatment for diabetes was not realized for many decades until reversal of diabetes was initially observed in rodents and in a patient with chronic pancreatitis who underwent pancreatectomy followed by islet auto-transplantation[16–18]. Following these findings, intensive research has been conducted in the field of islet transplantation. In 2000, the Edmonton immunosuppression protocol, which utilized a corticosteroid-free immunosuppression regimen and multiple islet infusions from different donors was established[19]. An insulin independence rate of 100% was achieved in seven patients following one year of islet transplantation and partial graft function was observed in most of the seven patients after five years[19,20] which represented a significant improvement from the success rate of 10% prior to the protocol [13,21,22]. Critically long-term insulin independence has been difficult to achieve, and most patients require at least two infusions to achieve insulin independence[20]. Islet transplantation has been adopted as a treatment option for T1DM in a number of countries and has proved an attractive method of β-cell replacement[22].

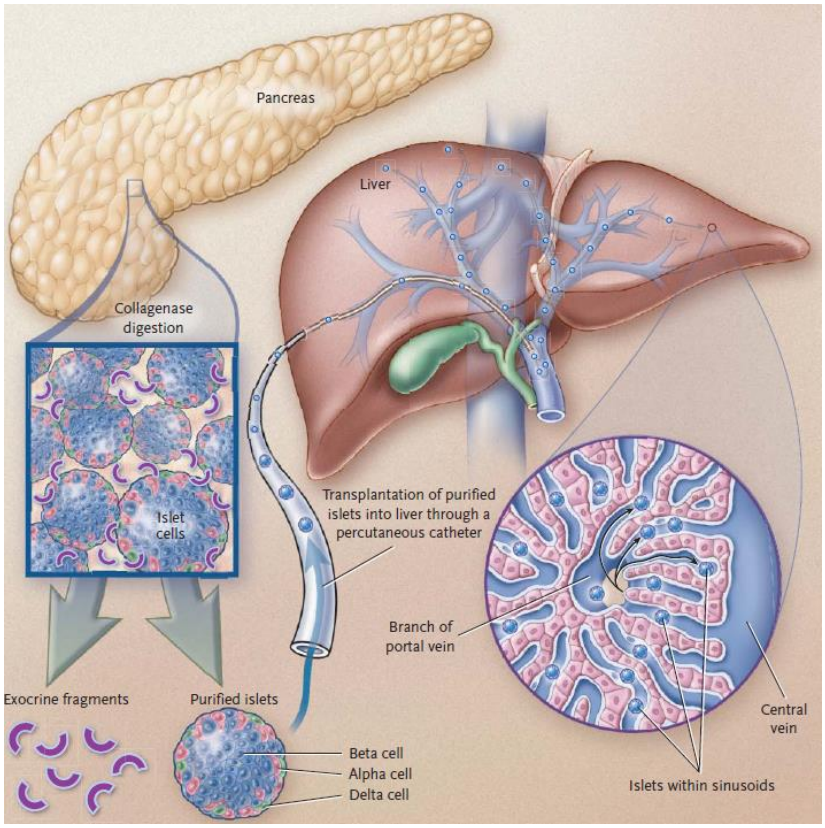


**Figure 1.** Current procedure of pancreatic islet transplantation. Islets are purified from the donor pancreas then infused into the recipient's liver via hepatic portal vein. Image adapted from R. P. Robertson[13].

Despite the significant progress in islet transplantation procedures, numerous obstacles remain that currently limit its clinical application[9,23]. The current clinical standard of care involves the infusion of islets into the patient liver via the portal vein where islets encounter a sub-optimal non-pancreatic environment: high glucose concentration, lower oxygen tension, and higher level of toxins[24]. Moreover, infusion of islets via hepatic portal vein triggers an innate immune reaction upon contact with blood, known as the instant blood mediated inflammatory reaction [25]. The hypoxic islets secrete chemokines and express tissue factors, which activates a thrombotic reaction[26]. Platelets are attracted to the islet surface, recruiting leukocytes and macrophages to infiltrate and destroy the islet cells[25,27]. Together these factors kill up to 70% of transplanted islets in the first 48 hours[28,29] and consequentially islets from up to three donor pancreata are required for clinical benefit, limiting the availability of the transplantation. Additionally, the obligatory use of immunosuppressive regimen is another major challenge of islet transplantation. Immunosuppressive drugs used for islet transplantation

are associated with many side effects including risks of infection, higher rate of malignancy, β-cell toxicity and organ toxicity, significantly decreasing the individual's quality of life[21].

## *Immunosuppression*

Upon transplantation, recipient T cells recognize alloantigens of the allograft, which activates recipient T cells to induce inflammation at the site of the allograft, as part of the alloresponse (**Figure 2**)[30]. Allogeneic major histocompatibility complex (MHC) molecules are the major drivers of this response[31].These molecules are presented to the recipient T cells through a number of pathways (**Figure 3**)[32]. In the direct pathway, donor antigen presenting cells (APCs) migrate from the allograft to the secondary lymphoid organ, in which they mature and present donor MHC molecules to naïve T cells[30,32]. In the indirect pathway, recipient APCs obtain donor MHC molecules from donor cells that have undergone necrosis and apoptosis, and present the processed peptides on self-MHC molecules to naïve T cells[33]. In the semi-direct pathway, recipient APCs acquire intact donor MHC molecules via direct contact with donor APCs or MHC-containing endosomes released from donor APCs, presenting donor MHC molecules on their surface to naïve T cells[33]. The direct pathway has been associated with acute graft rejection early on while the indirect and the semi-direct pathways have been tied to chronic graft rejection in later stages of the disease[30].

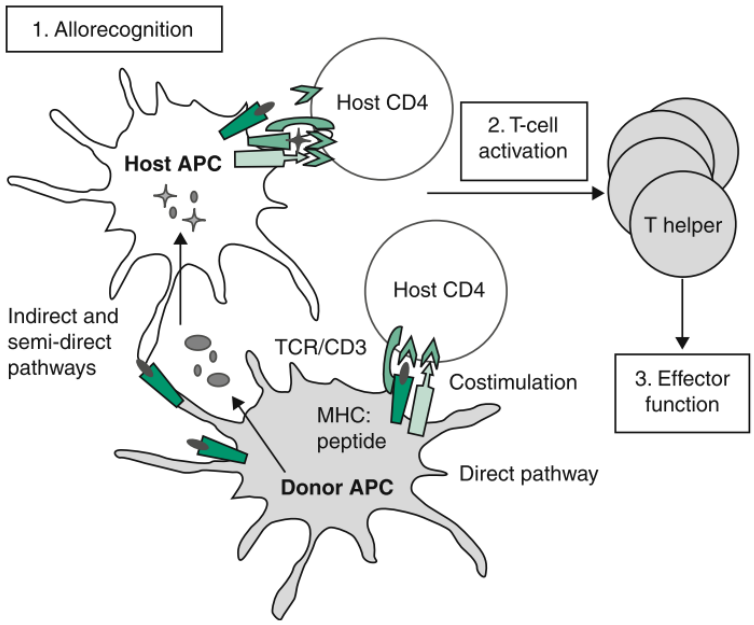


**Figure 2.** Overview of allorecognition and alloresponse. Image is adapted from Golshayan *et al.*[30].

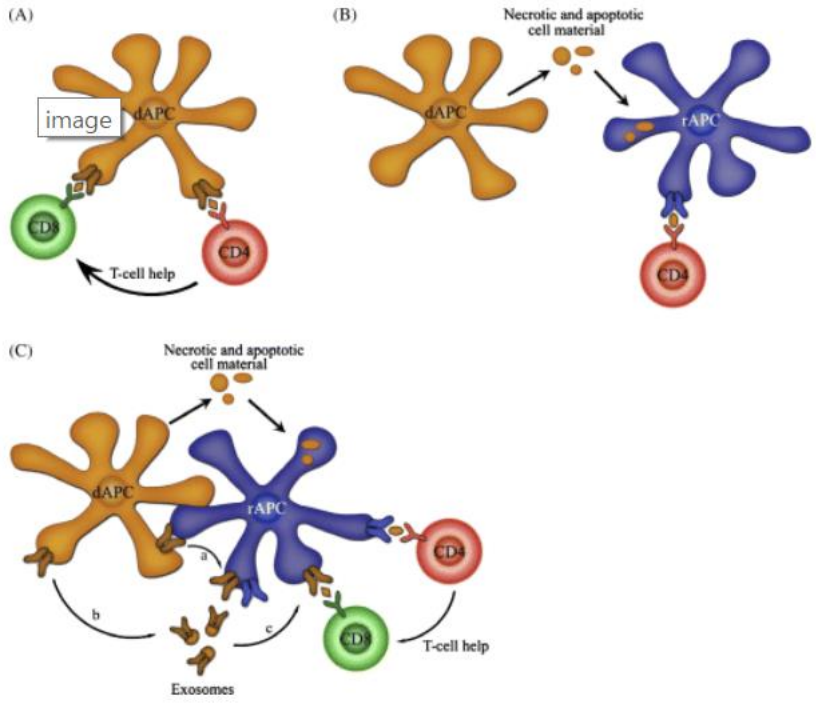


**Figure 3.** Different pathways of allorecognition. (A) The direct pathway involves interactions of donor APCs with recipient T-cells. (B) The indirect pathway involves presentation of processed donor MHC peptides on recipient APCs to recipient T-cells. (C) The semi-direct pathway involves transfer of intact donor MHC molecules via cell-to-cell contact or endosomes on recipient APCs and interactions with recipient T-cells. Image adapted from Afzali *et al.*[33].

In the 1950s it was discovered that antimetabolite 6-mercaptopurine possesses immunosuppressive properties that prolong survival of kidney transplants in dogs[34]. Since this discovery, many immunosuppressants with different properties and mechanisms of action have been developed[35–39]. The use of immunosuppressants has significantly improved the early rate of graft and patient survival by preventing allorecognition and consequent acute graft rejection[30]. However, long-term survival is still a major issue due to chronic graft dysfunction and the side effects of immunosuppression regimen being deleterious, causing high mortality and morbidity. In the case of pancreatic islet transplantation, sirolimus and tacrolimus are the immunosuppressants of choice. They are however associated with infections, selective organ toxicity and increased risk of cancer. The most common sites of infection are the upper respiratory, skin and urinary tract; most of which have mild symptoms and are entirely treatable. Multi-organ toxicity caused by sirolimus and tacrolimus ranges from minor acne to severe neurologic side effects such as tremor and higher risks of malignancy in various cell lines (notably

squamous cells of skin). Additionally, β-cells of the transplanted islets are directly affected by sirolimus and tacrolimus. Sirolimus diminishes β-cell proliferation and causes apoptosis of β-cells, while tacrolimus inhibits transcription of the insulin gene, decreasing insulin secretion and increasing insulin resistance[21]. Thus, in order to improve long-term outcomes of islet transplantation, there is a need for novel immunotherapies able to prevent allorecognition and alloresponse without the need for immunosuppressants.

## *Alternative transplantation sites*

Many studies in recent years have explored alternative sites for islet transplantation with the following key characteristics (**Figure 4**): (a) sufficient space for islet engraftment; (b) close proximity to vascular network to provide optimal oxygen tension, sensing and release of insulin; (c) allow real time communication between cellular graft and the circulation; and (d) offer minimal inflammatory potential to support long term graft survival. A few sites with immunological privileges such as testis or thymus have been tested in small animals, however, to date they remained clinically irrelevant due to limited space for islet engraftment[40,41]. Among many sites explored, the skin site received attention as it offers a readily accessible site via a minimally invasive surgical procedure. The only drawback is that unlike the liver or kidney capsule, dermal poor vascularization limits the integration and functionality of engrafted islets[42]. The pancreas, the native home of islets, has also been explored as a site of islet transplantation. However, it is not considered for a transplantation site due to the metabolic complications such as pancreatitis (potentially induced after embolization) and limited vascular supply. At this point in time for clinical islet transplantation, intra-portal infusion remains the gold standard[43].

As no suitable alternative transplantation site in the human body has been found, one option to explore is the fabrication of an artificial transplantation site. The recent advancements in bio-engineering technology now enable constructing of such sites. Hydrogels are a multi-component system comprised of a tri-dimensional network of polymer chains with absorbed water filling the space between the macromolecules, within which various biomaterials may be incorporated to mimic tissue-like properties. The main approach of incorporating such technology in islet transplantation is via islet encapsulation

(**Figure 5**). Pancreatic islets are embedded within a hydrogel, and this "mini organ" hold pores which allow bidirectional diffusion of small molecules such as insulin (~6 kDa), nutrients and glucose, and at the same time, protects islets from immune attack by restricting the access of immune cells or antibodies (~150-900 kDa)[44].

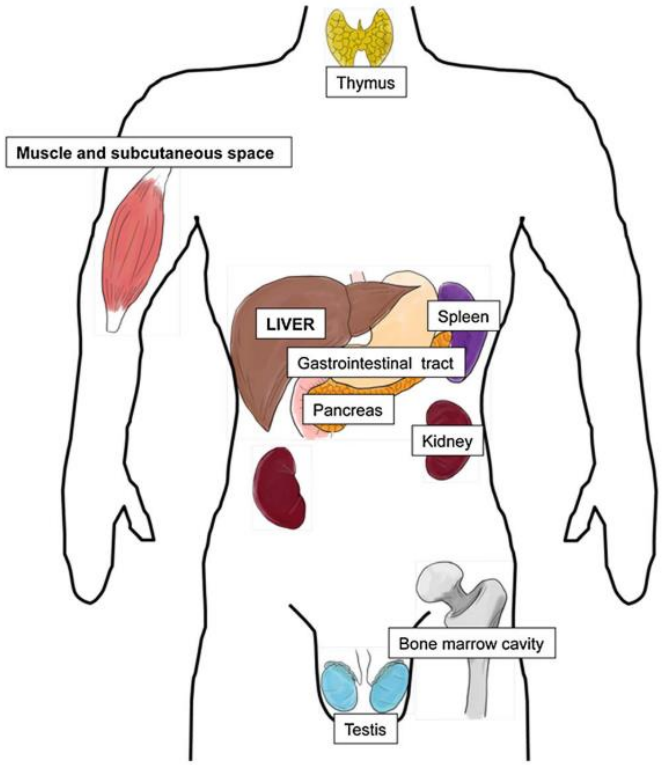


**Figure 4.** Candidates for alternative transplantation sites for pancreatic islets. Image adapted from Sakata *et al.*[45]

The pivotal point in this field of research has been the search for a suitable hydrogel. To date, various types of naturally derived polymers such as alginate, collagen, gelatin, fibrin, and fibronectin and synthetic polymers such as poly(lactic-co-glycolic acid), polysulphone, poly(lactic acid), poly(vinyl alcohol) have been evaluated[46]. Amongst all, alginate-based hydrogels have been the most extensively investigated polymers for their utility with pancreatic islets to treat T1DM. Alginate is a naturally occurring anionic polymer typically obtained from brown seaweed. Due to its anionic properties, alginate readily cross-links to form a polymer upon exposure to divalent cations such as $Ca^{2+}$[47]. Additionally, alginate is biocompatible and biosafe with non-toxic degradation products and a relatively low production cost[48]. Alginate has several limitations including an inability to

biodegrade, a lack of interaction with cells, and a tendency to induce foreign body reactions in recipients. These limitations can be easily overcome by partially oxidizing alginate to confer biodegradability, by copolymerizing alginate with gelatin or gelatin derivatives to which cells can adhere and by utilising high purity alginate.

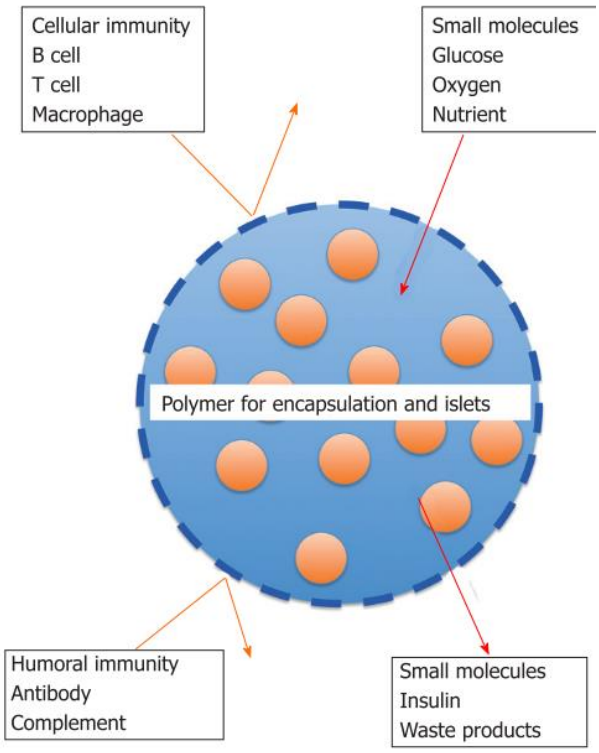


**Figure 5.** Encapsulation of pancreatic islets. Bidirectional diffusion of nutrients, oxygen, insulin and waste products is allowed while physical immune isolation is achieved. Image adapted from Sakata *et al.*[49]

Another aspect that must be considered is the degree of cross-linking. Mechanical stability, the pore size and the rate of diffusion and degradation are directly linked to the degree of cross-linking and these must be finely balanced[47]. In the case of alginate, the degree of cross-linking can be altered by varying the exposure time and concentration of divalent cations. While this is straightforward in theory, several challenges were observed in numerous small animal models. Islet encapsulation was demonstrated to improve glucose homeostasis for a short term, but no permanent restoration of euglycemia was observed[50–54]. One challenge arises as physical irregularities from fabricating hydrogel result in an incomplete coverage of the islets within the capsules. This may trigger a pericapsular fibrotic overgrowth (PFO) which blocks the diffusion of nutrients and oxygen, resulting in islet necrosis[55,56].

Even the successfully encapsulated islets suffer from hypoxia due to the restricting hydrogel permeability and increased distance from the surrounding blood vessels reduces the availability of oxygen by diffusion. This introduces a challenge in scaling up into a large animal model or clinically relevant dose of islets. Moreover, encapsulation prevents immediate re-vascularization post-transplantation, subjecting the islets to further hypoxic stress. As hypoxia hampers the function and responsiveness of islets to glucose, even larger number of islets are needed to restore normoglycemia.

## *3D-Bioprinting*

One approach to address hypoxia involves "seeding" of islets onto degradable 3D scaffold structures[57]. Scaffolds are made of similar biopolymers to mimic the pancreatic microenvironment. The construct provides increased surface area to volume ratio compared to the hydrogel capsules, and even allows for vascular ingrowth, thereby providing increased oxygen and nutrient supply[58]. Upon slow degradation of the scaffold, the extracellular matrix proteins are deposited by surrounding tissues and engrafted islets, gradually re-building the suitable environment required for islet survival[59]. Even though immune isolation is not achieved through this method, the scaffolds can prevent direct contact of embedded islets to circulating immune cells to reduce the inflammatory response until the scaffolds eventually degrades[25]. The efficacy of such device have been demonstrated in animal studies[60–62]. Moreover, utilization of 3D bioprinting technology with higher accuracy could provide highly controlled seeding of islets, thereby minimizing the onset of PFO arising with conventional techniques.

The concept of 3D printing was first introduced in 1986 by Charles W. Hull, and has become increasingly prominent over the past decades[63]. 3D printing technology allows printing of a 3D structure, typically through stacking successive thin layers in a layer-by-layer fashion. Advances in engineering technology have now opened up the possibility of using 3D printing to "print" spatially controlled biomaterial structures with embedded bioactive factors and cells into a functional tissue construct[64]. Such automated printing allows for the precise control of architecture, pore interconnectivity, and a high degree of reproducibility necessary for commercial clinical application and regulation. Furthermore, bioprinting allows the deposition of a wide array of cell types and bioactive

factors in a precise order to simulate native tissue environment and support cell survival[65–67].

The current varieties of 3D bioprinting techniques including inkjet bioprinting, extrusion bioprinting, laser-assisted and stereolithography bioprinting (**Figure 6**)[68,69]. Inkjet bioprinting was the first bioprinting technique to be developed. It often utilizes conventional inkjet printers which have been modified and customized to enable deposition of bioinks instead of inks. Inkjet bioprinting is driven by thermal or piezoelectric actuation which results in drop-by-drop deposition of the bioinks. Inkjet bioprinting allows rapid deposition of bioinks, however, only low viscosity bioinks with low cell densities can be used. Extrusion bioprinting has derived from inkjet bioprinting to enable printing of high viscosity bioinks with high cell densities. Extrusion bioprinting is driven by continuous pneumatic or manual force, depositing bioink filaments in a layer-by-layer fashion. One drawback of extrusion bioprinting is that cells are exposed to mechanical stresses such as shear forces, which could affect the viability of printed cells. Laser-assisted bioprinting employs laser-direct write and laser-induced transfer technologies. In laser-assisted bioprinting systems, a laser pulse is applied to the donor layer, often made of gold or titanium, which induces vaporization of the donor layer. Following vaporization, a bubble is generated between the donor layer and the underlining bioink layer, triggering deposition of the bioinks on to the receiving substrate. Laser-assisted bioprinting can print moderate viscosity bioinks with moderate cell densities with minimal mechanical stresses, however, is associated with high cost and complexity of operation. Finally, stereolithography bioprinting utilizes a light source to selectively crosslinks and deposit bioinks in a layer-by-layer fashion. Stereolithography bioprinting can rapidly generate high resolution structure with minimal mechanical stresses.

Among these, extrusion bioprinting has been most extensively investigated for the generation of artificial tissue constructs such as cartilages[70,71], liver[72] and neural tissues[73], as most existing commercial bioprinters uses extrusion bioprinting[68,69]. Extrusion bioprinting has also been explored for the generation of artificial pancreata using various sources of islets. A rat β-cell line, mouse and human islets were printed into a predefined 3D scaffold using alginate-based bioinks and the subsequent cell viability and morphology were found to be unaffected[74]. Furthermore, rat islets were printed into macroporous 3D constructs using an alginate/methylcellulose bioink. These printed rat islets retained

their viability, morphology and function, for up to 7 days in culture[75].

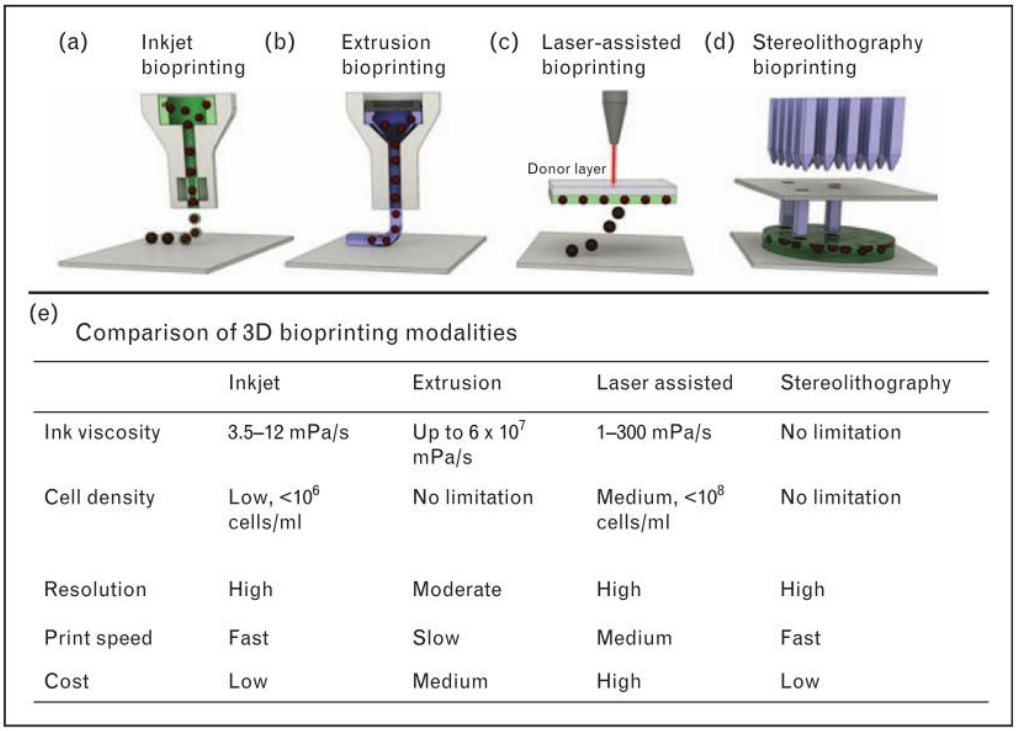


(e) Comparison of 3D bioprinting modalities

| | Inkjet | Extrusion | Laser assisted | Stereolithography |
|---|---|---|---|---|
| Ink viscosity | 3.5–12 mPa/s | Up to 6 x $10^7$ mPa/s | 1–300 mPa/s | No limitation |
| Cell density | Low, <$10^6$ cells/ml | No limitation | Medium, <$10^8$ cells/ml | No limitation |
| Resolution | High | Moderate | High | High |
| Print speed | Fast | Slow | Medium | Fast |
| Cost | Low | Medium | High | Low |

**Figure 6.** Different types of bioprinting techniques. (a) Inkjet bioprinting involves deposition of bioink droplets via thermal or piezoelectric actuation. (b) Extrusion bioprinting involves layer-by-layer deposition of pneumatically or manually extruded bioink filaments. (c) Laser-assisted bioprinting involves vaporization of the donor layer via a laser which causes formation of bubbles followed by deposition of bioinks. (d) Stereolithography bioprinting involves layer-by-layer deposition of selectively crosslinked bioinks using a digital light source. (e) Comparison of the different techniques. Adapted from Yue *et al*. [68]

Beyond the modification of the bioinks to support islet cells, bioprinting also enables the co-transplantation of islets with supporting cells that could enhance islet survival[76]. Recently, our group developed a extrusion bioprinter equipped with a co-axial extruder nozzle and two separate ink chambers (**Figure 7**)[77]. Different bioinks tailored with cell-type specific bioactive molecules can be utilized in each chamber, allowing co-printing of islets with supporting cells. These geometries have the advantage that more delicate components can be strategically placed within the core with a surrounding protective layer, referred to as the shell. The use of a co-axial structure has been shown to significantly improve islet encapsulation by minimizing material volume per islet and reducing the risk of PFO[55]. For co-axial printing of islets, alginate-gelatin methacryloyl (GelMA) bioink was formulated.

Modification of gelatin with methacryloyl moieties enabled photo-crosslinking of GelMA molecules using visible light. Alginate-GelMA bioink showed mechanical stability, optimal macroscopic and rheological properties, shear-thinning behavior, and capacity to support cell survival. Indeed, co-axially printed mouse islets and endothelial progenitor cells demonstrated high viability[77]. Together, co-axial 3D bioprinting has the potential to enable the embedding of clinically relevant doses of islets with support for islet survival, including supporting cells and bioactive factors. Regulatory T-cells (Tregs) are a key candidate for this, given their natural ability to mediate immune regulation and suppression. Incorporation of Tregs, in conjunction with Treg-specific bioactive factors may provide local immune-protection to co-printed islets, achieving graft tolerance without the use of systemic immunosuppression.

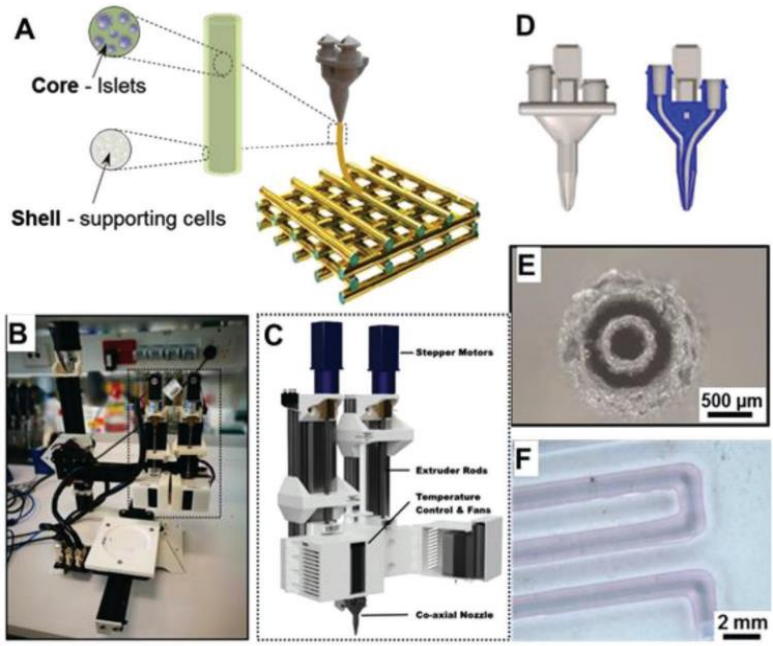


**Figure 7.** 3D co-axial extrusion bioprinter. (A) Schematic of the 3D structure printed with the bioprinter. Pancreatic islets will be localized to the core while supporting cells surround islets in the shell. (B,C) Image of the bioprinter. (D) Co-axial nozzle for the bioprinter. (E) Microscope image of the co-axial nozzle. (F) Brightfield image of co-axially printed strands using lutrol bioink coloured with red (shell) and blue (core) for visualization.

## *Regulatory T-cells (Tregs)*

The immune system can respond to a broad range of pathogens while being unresponsive to specific antigens. This state of unresponsiveness is termed immunological tolerance and is crucial for one's health. Immunological tolerance is tightly regulated by several mechanisms, breakdown of which can be deleterious and result in autoimmunity, allergy, and failure to clear tumour cells and pathogens. Mechanisms of immunological tolerance can be classified based on their site of establishment. Central tolerance is established in the primary lymphoid organs, such as bone marrow and the thymus during lymphocyte development, through clonal deletion of self-reactive lymphocytes as required for tolerance to self-antigen. Peripheral tolerance occurs in peripheral tissue, suppressing immune responses to environmental antigens and inhibiting activation of self-reactive lymphocytes that escaped central tolerance. Peripheral tolerance is achieved through several mechanisms including anergy, deletion, clonal ignorance and suppression (**Figure 8**)[78,79].

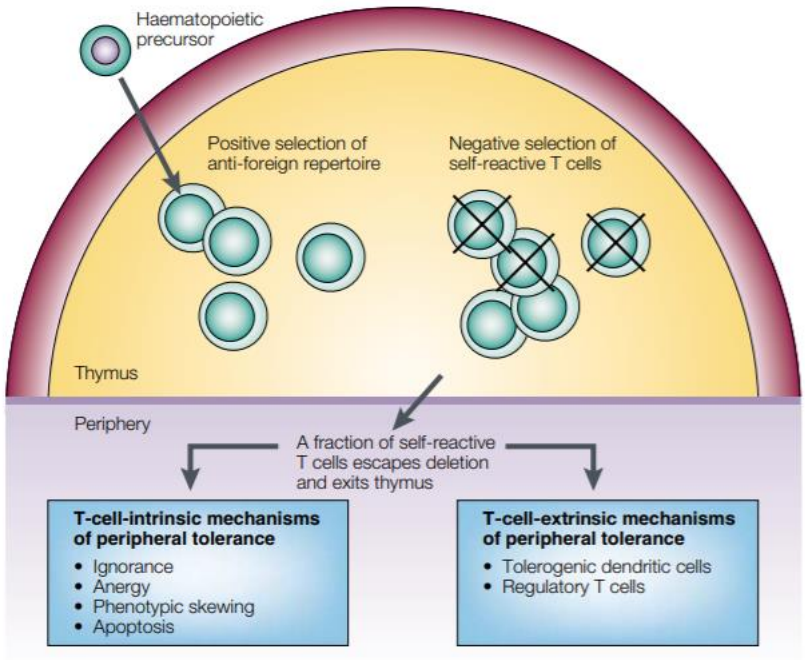


**Figure 8.** Central and peripheral tolerance of T-cells. During thymic development, self-reactive T-cells are negatively selected. In the periphery, self-reactive T-cells which have escaped central tolerance are neutralized via various mechanisms including anergy, clonal ignorance, deletion and suppression. Image adapted from Walker *et al.*[79]

Regulatory T cells (Tregs) are a sub-population of T cells that specialize in immune suppression. The idea of Tregs arose when, in 1970, Gershon and Kondo discovered that a subset of T cells diminish immune responses[80]. This T cell population was named suppressor T cells at the time and was intensely investigated[81,82]. $CD4^+$ $CD25^{hi}$ T cells were defined as Tregs in mice[83] and humans in 1995 and 2001[84–87], respectively. In later years, forkhead box p3 (FOXP3)[88–90] was identified as the master regulator of Tregs and the absence of CD127[91,92] found to be a complementary marker, eventually defining Tregs as $CD4^+$ $FOXP3^+$ $CD25^{hi}$ $CD127^-$ T cells. To date, two types of natural Tregs (nTregs) have been identified with the $CD4^+$ $FOXP3^+$ $CD25^{hi}$ $CD127^-$ profile. Thymic Tregs (tTregs) arise from highly self-reactive T cells in the thymus during T cell development and establishment of central tolerance[93]. tTregs are characterized by complete demethylation of the *FOXP3* promoter region and Treg-specific demethylation region (TSDR) in conserved non-coding sequence 2 (CNS2), which results in stable expression of FOXP3 and a suppressive phenotype[94,95]. On the other hand, peripheral Tregs (pTregs) are generated from naïve CD4+ T cells in the periphery upon stimulation of the T cell receptor (TCR), transforming growth factor beta (TGF-β), retinoic acid (RA) and IL-2, which can be mimicked *in vitro* to generate induced Tregs (iTregs)[96,97]. The *FOXP3* promoter region and TSDR of pTregs and iTregs are not demethylated leading to their functional instability[94,95]. Besides the canonical $CD4^+$ $FOXP3^+$ $CD25^{hi}$ $CD127^-$ Tregs, there are other types of Tregs found in the periphery, including Th3 Tregs, Tr1 Tregs and $CD8^+$ $FOXP3^+$ Tregs[98].

Treg-mediated suppression is the main mechanism of peripheral tolerance. Thus, Tregs are a vital component of the immune system[78,99]; loss of Tregs is lethal in humans, causing immunodysregulation polyendocrinopathy enteropathy X-linked syndrome (IPEX), a fatal multi-organ autoimmune disorder[100]. Tregs play many roles in the immune system including downregulation of immune responses once pathogens have been cleared, maintaining tolerance to self, gut microbiota, new chemicals, environmental and food antigens and the fetus in cases of pregnancy. Treg-mediated suppression targets a broad spectrum of immune cells such as other T cell subsets, B cells, APCs and natural killer (NK) cells[101]. Suppression is achieved via several circumstance dependent mechanisms, including inhibitory cytokines, cytolysis, metabolic disruption and modulation of dendritic cells (DCs) (**Figure 9**)[99]. Given such versatility, Tregs are a promising candidate for novel immunotherapies.

Downregulation and upregulation of Tregs could be utilized for the treatment of cancer and autoimmunity/allergy, respectively. Furthermore, Treg cell therapy could be used to establish graft tolerance in transplant recipients, potentially tackling the issues of organ scarcity and the long-term side effects of immunosuppression in transplantation.

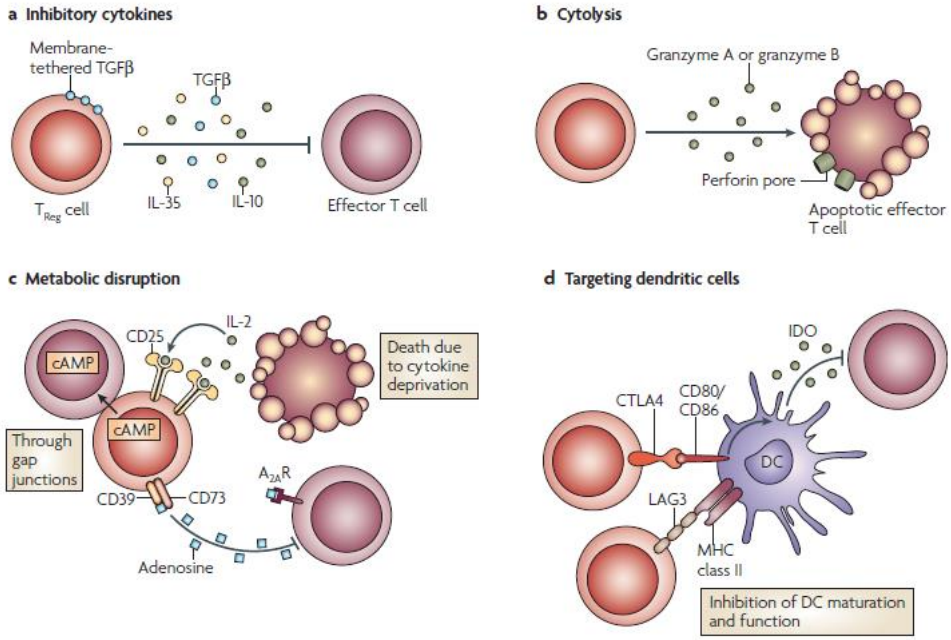


**Figure 9.** Suppression mechanisms of Tregs. (a) Inhibitory cytokines such as TGF-β, IL10 and IL35. (b)Cytolysis via perforin/granzyme pathway. (c) Metabolic disruption via CD25-mediated IL-2 deprivation, transfer of cAMP and CD39/73-mediated generation of pericellular adenosine. (d) Targeting of dendritic cells via co-inhibitory molecules such as CTLA-4 and LAG3.

Since the first organ transplantation clinical trials, spontaneous graft tolerance(the acceptance of allograft without immunosuppressive regimen) has been observed, mostly in liver transplant recipients[102–104]. The exact factors underlying this phenomenon have not yet been fully identified, however, it has been shown that Tregs play a major role in spontaneous graft tolerance in mice liver allograft models[105,106] and there is elevation of Treg proportion in spontaneously tolerant patients[107]. Additionally, it has been demonstrated that Tregs mediate infectious tolerance against allografts, a phenomenon in which tolerance in one population of lymphocytes is transferred to another population[108,109]. Together, these properties promise a Treg-based immunotherapy with the goal of long-term graft tolerance. To date, several different approaches have been attempted. In vivo augmentation/induction of Tregs has proven problematic as there was a lack of specificity towards Tregs

resulting in ineffective or adverse outcomes[110–112]. Alternatively, Treg cell therapy utilizing adoptive transfer of *ex vivo* expanded Tregs has a number of advantages compared with the *in vivo* approach, including greater control over the expansion/generation of Tregs, the possibility of functional and phenotypical analysis prior to delivery and finer control of dosage and delivery time[111,112]. Adoptive transfer of *ex vivo* expanded nTregs has been extensively investigated with most clinical trials utilizing this method[113]. It has proved promising in many animal transplantation models[114–118], including murine islet transplantation models[119,120] and clinical liver[121] and kidney[122] transplantation trials. One challenge of adoptive transfer is generation of sufficient numbers of Tregs for clinically significant results. As the frequency of nTregs in the human peripheral blood is low, the expansion protocols can be extremely time-consuming and costly[123,124]. Recent clinical trials have used up to 5 billion nTregs per patient, taking up to 36 days for expansion[124]. Thus, more targeted approaches and alternative ways to generate large number of Tregs in shorter amount of time could be beneficial[123]. These could be achieved by encapsulating Tregs through 3D-bioprinting to serve as a localised immunosuppression and utilizing iTregs which are induced from naïve $CD4^+$ T-cells with significantly higher frequency in human peripheral blood than nTregs, respectively. Moreover, studies have shown that while TCR repertoire diversity of nTregs is similar to conventional T-cells, TCR repertoire of nTregs is distinct from conventional T-cells and is skewed towards self-antigens[125–130]. Thus, given that iTregs are generated from conventional T-cells, TCR repertoire of iTregs would be skewed towards non-self-antigens which could be advantageous in allogeneic transplantation[131]. As mentioned above, iTregs exhibit phenotypic instability and can transit into Th17 cells in pro-inflammatory environments[132]. Thus, the key to utilization of iTregs for adoptive transfer is stabilisation of their phenotype.

## *Treg-specific bioactive factors*

Interleukin-2 (IL-2) is a T cell stimulatory cytokine, largely produced by $CD4^+$ T helper cells. IL-2 signalling is crucial for activation and clonal expansion T cells[133]. While $CD4^+$ T helper cells can produce IL-2 for autocrine signalling upon T-cell receptor stimulation, Treg cells cannot and thus are reliant on IL-2 produced by other cells[81,134]. IL-2 is crucial for Treg function as well as their survival.

Tregs highly express CD25, the α-chain of the high affinity IL-2 receptor complex [135] and the interaction of IL-2 and CD25 induces high expression of FOXP3 and inhibits Th17 polarization thereby reinforcing Treg phenotype and function[131,136–138]. Moreover, with high expression of CD25, Tregs can respond to low concentrations of IL-2 and bind to IL-2 with high affinity[139], which can lead to sequestration of IL-2 from effector T cells, depriving them of survival signal[99]. Administration of exogenous IL-2 in autoimmunity and organ transplantation has been investigated to augment Treg numbers and function[140]. Particularly, low-dose IL-2 therapy has shown promising results in hematopoietic stem cell transplantation graft-versus-host disease, selectively increasing Treg numbers[141–144]. Thus, incorporation of IL-2 in the bioink may enhance survival and function of printed Tregs and create a Treg-rich microenvironment around the 3D bioprinted scaffold.

Chemokine ligand 1 (CCL1) is a chemotactic protein which only binds to chemokine receptor 8 (CCR8). CCR8 is pre-dominantly expressed on Tregs and Th2 cells in the peripheral blood with the main function of CCL1-CCR8 interactions being trafficking of Tregs and Th2 cells[145,146]. Pathologically, CCL1 is produced in various human tumour tissues to exploit the CCL1-CCR8 axis by recruiting Tregs to the tumour sites to create immunosuppressive microenvironments and inhibit anti-tumour responses mediated by effector $CD4^+$ and $CD8^+$ T-cells, natural killer T-cells and natural killer cells[147–149]. Indeed, blockade of CCL1 was shown to augment anti-tumour responses by specifically inhibiting Treg function in tumour sites[147]. Thus, mimicking of CCL1-induced immune evasion of tumour cells via incorporation of CCL1 in the bioink may be beneficial as it could recruit recipient Tregs and create Treg-enriched microenvironment to establish a long-lasting recipient-driven tolerance to the islets. Furthermore, the CCL1-CCR8 axis has been shown to upregulate expression Treg-suppression molecules and augment suppressive activities of Tregs, suggesting that Tregs recruited to the transplantation site via CCL1-mediated chemotaxis would have augmented suppressive activities[150]. One drawback of CCL1 incorporation may be the unintended recruitment of Th2 cells, however, Th2 cells could be beneficial with their ability to inhibit Th1 responses, which are implicated in acute rejection[151].

Transforming growth factor-β (TGF-β) is a highly pleiotropic cytokine involved in many biological

processes. In the context of adaptive immunity, TGF-β is an immunosuppressive cytokine secreted by Tregs. It also plays an essential role for differentiation and development of Tregs[152]. It was the first factor to be used for generation of iTregs from murine naïve $CD4^+$ T-cells[153]. Furthermore, the gut environment has particularly large population of pTregs due to TGF-β secreted by $CD103^+$ intestinal dendritic cells (DCs). TGF-β induces binding of transcription factors, Smad2 and Smad3, to conserved non-coding DNA sequence 1 (CNS1) region of *fopx3* locus[97,131], which is required for FOXP3 induction in pTregs and iTregs[154]. In addition, similar to TGF-β, all trans retinoic acid (ATRA), a vitamin A derivative, is highly versatile with the ability to inhibit cytokine production of memory T-cells[155]. ATRA is also secreted by $CD103^+$ intestinal DCs and works in conjunction with TGF-β to enhance TGF-β-mediated binding of Smad3 to CNS1 region through histone acetylation of the Smad3 binding region. This prevents Th17 polarization, which also requires TGF-β signalling[97,131,156]. Moreover, TGF-β and ATRA are important for the maintenance of the Treg phenotype in iTregs post-differentiation, as well as the stability of nTregs under pro-inflammatory conditions[155,157,158]. Thus, incorporation of TGF-β and ATRA into the bioink may stabilise the phenotype of printed nTregs and iTregs, induce differentiation of circulating naïve $CD4^+$ T-cells into pTregs via infectious tolerance to further augment the immunosuppressive milieu around the printed structure[152,159], and directly suppress effector T-cells in the vicinity.

Rapamycin is a macrocyclic lactone product of *Streptomyces hygroscopicus*, which was originally isolated as an antifungal antibiotic[160]. In humans, rapamycin binds to immunophilin FKBP-12 and inhibits the mTOR (mammalian target of rapamycin) pathway[161]. The mTOR pathway is involved in cell growth and proliferation,[162] thus, inhibition of the mTOR pathway results in cell cycle arrest at G1 and S phase[163]. In particular, inhibition of the mTOR pathway in T-cells disrupts IL-2 signalling, which is required for T-cell activation and proliferation[164]. Due to this property, rapamycin is a common immunosuppressive drug used in allogeneic transplantation to prevent allograft rejection[165]. Interestingly, it has been shown that rapamycin promotes preferential expansion of Tregs over conventional T-cells[166], as Tregs utilize IL-2R-depedent STAT5 pathway for IL-2 signalling instead of mTOR pathway[167,168]. As such, rapamycin enhances the purity of iTreg differentiation and expansion through selective inhibition of effector T-cell differentiation[96]. Furthermore, rapamycin

has been shown to stabilise FOXP3 expression to reinforce Treg phenotype and Treg-lineage commitment, in both nTregs and iTregs[169,170]. Thus, incorporation of rapamycin into the bioink may serve as a local immunosuppressant by selectively inhibiting conventional T-cells and promoting growth of local Tregs and stabilising the phenotype of printed nTregs and iTregs.

## *Conclusion*

Pancreatic islet transplantation is a promising curative cell therapy for T1DM. The field is limited by human cadaveric islet cell sources at present. The current procedure of islet infusion into liver may not be optimal, and so alternative transplant strategies such as 3D bioprinting may provide new strategies. Modifications of the bioinks with local immunosuppression and bioactive factors to support the cells, are new directions for the field. The recent 3D bioprinting technology, especially with the development of the co-axial bioprinter, thus has potential to change the current pancreatic islet transplantation paradigm. The possibility of co-printing islets with supporting cells and bioactive factors potentiates direct improvement of engraftment condition, and thus survival and function of transplanted islets. Incorporation of Tregs via 3D-bioprinting could provide localized immune protection to islets. Bioactive factors such IL-2, CCL1, TGF-β, ATRA and rapamycin could enhance the survival, stability and function of printed cells to maximize the efficacy of the graft and augment the local immunosuppressive milieu through the recruitment of recipients Tregs, induction of pTregs, and promotion of Treg expansion. Furthermore, generation of phenotypically stable iTregs have an important clinical potential as it could significantly reduce the duration of *ex vivo* expansion required to generate enough Tregs for clinically relevant doses. Together, extra-hepatic islet transplantation without the use of immunosuppression might be clinically achieved by utilizing 3D bioprinting technology and phenotypically stable iTregs.

## *Thesis Hypotheses*

This thesis aims to develop and evaluate the encapsulation of two types of human regulatory T-cells, natural and induced regulatory T-cells (nTregs and iTregs), in alginate-GelMA hydrogel supplemented with IL-2 and CCL1, and the generation of stable iTregs for application in 3D-bioprinting with pancreatic islets as an alternative to the immunosuppressive regimens necessitated by current pancreatic islet transplantation methods. In order to achieve these, several hypotheses need to be addressed.

1. Encapsulation will not compromise Treg viability, phenotype and function.
2. Encapsulated Tregs will be spatially restricted to the hydrogel structure.
3. Supplementation of the alginate-GelMA hydrogel with IL2 will improve Treg viability, phenotype and function.
4. Supplementation of the alginate-GelMA hydrogel with CCL1 will recruit Tregs to the hydrogel structure.
5. iTregs generated with the optimised protocol will exhibit stability.

This thesis explores four main aims – which are covered by manuscript 1 & 2:

1. To evaluate the effect of encapsulation on the viability, phenotype and function of Tregs using IL-2-supplemented alginate-GelMA bioink
2. To assess migration capacity of encapsulated Tregs and recruit Tregs to the hydrogel structure using CCL1-supplemented alginate-GelMA bioink
3. To compare encapsulation of natural Tregs and induced Tregs to determine more suitable cell-type for 3D-bioprinting and maximise the efficacy of Treg incorporation.
4. To generate stable induced Tregs which could be utilized for 3D-bioprinting.

# Statement of Authorship

| | |
|---|---|
| Title of Paper | Encapsulation of Human Natural and Induced Regulatory T-cells in IL-2 and CCL1 Supplemented Alginate-GelMA Hydrogel for 3D-Bioprinting |
| Publication Status | Published on 20th of Feb 2020 |
| Publication Details | Advanced Functional Materials<br>Impact Factor 15.621 (2018) |

## Principal Author

| | | | |
|---|---|---|---|
| Name of Principal Author (Candidate) | Juewan Kim | | |
| Contribution to the Paper | Experiment design<br>Laboratory work<br>Data analysis<br>Manuscript writing/editing | | |
| Overall percentage (%) | 75 | | |
| Certification: | This paper reports on original research I conducted during the period of my Higher Degree by Research candidature and is not subject to any obligations or contractual agreements with a third party that would constrain its inclusion in this thesis. I am the primary author of this paper. | | |
| Signature | | Date | September 2019 |

## Co-Author Contributions

By signing the Statement of Authorship, each author certifies that:

i. the candidate's stated contribution to the publication is accurate (as detailed above);

ii. permission is granted for the candidate in include the publication in the thesis; and

iii. the sum of all co-author contributions is equal to 100% less the candidate's stated contribution.

| | | | |
|---|---|---|---|
| Name of Co-Author | Christopher M. Hope | | |
| Contribution to the Paper | Assisted experimental design<br>Assisted with chemokine receptor phenotyping (figure 8)<br>Manuscript editing | | |
| Signature | | Date | September 2019 |

| | | | |
|---|---|---|---|
| Name of Co-Author | Griffith B. Perkins | | |
| Contribution to the Paper | Assisted with CD154 suppression assay (figure 6)<br>Manuscript editing | | |
| Signature | | Date | September 2019 |

Please cut and paste additional co-author panels here as required.

| Name of Co-Author | Sebastian O. Stead | | |
|---|---|---|---|
| Contribution to the Paper | Assisted with encapsulated Treg phenotyping (figure 4 & 5)<br>Manuscript editing and figure editing | | |
| Signature | | Date | September 2019 |

| Name of Co-Author | Zhilian Yue | | |
|---|---|---|---|
| Contribution to the Paper | Assisted with synthesis of hydrogel precursor<br>Manuscript editing | | |
| Signature | | Date | September 2019 |

| Name of Co-Author | Xiao Liu | | |
|---|---|---|---|
| Contribution to the Paper | Assisted with synthesis of hydrogel precursor | | |
| Signature | | Date | September 2019 |

| Name of Co-Author | Narangerel Gantumur | | |
|---|---|---|---|
| Contribution to the Paper | Assisted with synthesis of hydrogel precursor | | |
| Signature | | Date | September 2019 |

| Name of Co-Author | Francis D. Kette | | |
|---|---|---|---|
| Contribution to the Paper | Assisted with encapsulated Treg phenotyping (Figure 4 & 5)<br>Manuscript editing | | |
| Signature | | Date | September 2019 |

| | | | |
|---|---|---|---|
| Name of Co-Author | Christopher J. Drogemuller | | |
| Contribution to the Paper | Supervision of the study<br>Conceptualisation of the project | | |
| Signature | | Date | September 2019 |

| | | | |
|---|---|---|---|
| Name of Co-Author | Robert P. Carroll | | |
| Contribution to the Paper | Supervision of the study<br>Manuscript editing | | |
| Signature | | Date | September 2019 |

| | | | |
|---|---|---|---|
| Name of Co-Author | Simon C. Barry | | |
| Contribution to the Paper | Supervision of the study<br>Manuscript editing | | |
| Signature | | Date | September 2019 |

| | | | |
|---|---|---|---|
| Name of Co-Author | Gordon G. Wallace | | |
| Contribution to the Paper | Supervision of the study<br>Conceptualisation of the project<br>Attained funding<br>Manuscript editing | | |
| Signature | | Date | September 2019 |

| | | | |
|---|---|---|---|
| Name of Co-Author | P. Toby Coates | | |
| Contribution to the Paper | Supervision of the study<br>Conceptualisation of the project<br>Attained funding<br>Manuscript editing | | |
| Signature | | Date | September 2019 |

PUBLICATION 1

# Encapsulation of Human Natural and Induced Regulatory T-cells in IL-2 and CCL1 Supplemented Alginate-GelMA Hydrogel for 3D-Bioprinting

**Encapsulation of Human Natural and Induced Regulatory T-cells in IL-2 and CCL1 Supplemented Alginate-GelMA Hydrogel for 3D-Bioprinting**

Juewan Kim[a], Christopher M. Hope[b,g], Griffith B. Perkins[a], Sebastian O. Stead[c,d], Zhilian Yue[e], Xiao Liu[e], Narangerel Gantumur[e], Francis D. Kette[c,d], Christopher J. Drogemuller[d,f], Robert P. Carroll[d,f], Simon C. Barry[b,g], Gordon G. Wallace[e,*], P. Toby Coates[d,f,*]

Affiliations:

a. The Department of Molecular & Cellular Biology, The School of Biological Sciences, The Faculty of Sciences, The University of Adelaide, Adelaide, South Australia
b. Department of Gastroenterology, Women's and Children's Hospital, Adelaide, South Australia
c. College of Medicine and Public Health, Discipline of Medicine, Flinders University, Bedford Park, South Australia
d. Discipline of Medicine, School of Medicine, The University of Adelaide, Adelaide, South Australia
e. Intelligent Polymer Research Institute, ARC Centre of Excellence for Electromaterial Science, University of Wollongong, Wollongong, New South Wales
f. Central Northern Adelaide Renal and Transplantation Service (CNARTS), The Royal Adelaide Hospital, Adelaide, South Australia
g. Molecular Immunology Group, Robinson Research Institute, School of Medicine, The University of Adelaide, Adelaide, South Australia

*Co-responding authors. Email: toby.coates@sa.gov.au & gwallace@uow.edu.au

Keywords: regulatory t-cells, encapsulation, hydrogel, immunotherapy, 3d-bioprinting

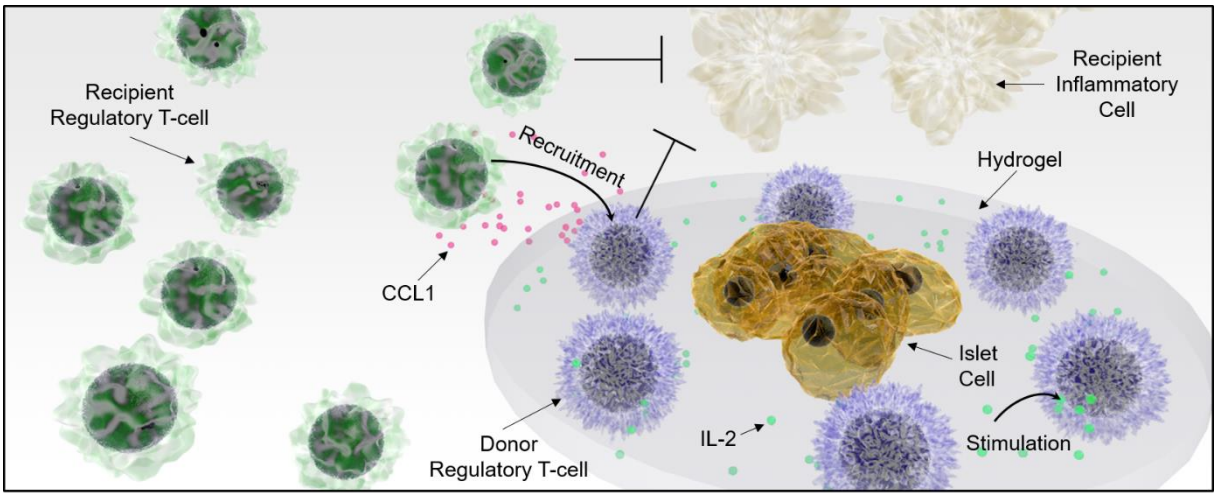


Regulatory T-cells (Tregs) are important modulators of the immune system through their intrinsic suppressive functions. Systemic adoptive transfer of *ex vivo* expanded Tregs has been extensively investigated for allogeneic transplantation. Due to the time-consuming and costly expansion protocols of Tregs, more targeted approaches could be beneficial. Here, we describe for the first time the encapsulation of human natural and induced Tregs for localized immunosuppression. Tregs encapsulated in alginate-GelMA hydrogel remained viable, phenotypically stable, and functional. Furthermore, encapsulation was sufficient to prevent migration of Tregs. Supplementation of the hydrogel with the Treg-specific bioactive factors IL-2 and CCL1 improved Treg viability, suppressive phenotype and function, and attracted to the structure $CCR8^+$ T-cells enriched with anti-inflammatory subpopulations, including Tregs, from human peripheral blood. This work establishes the co-encapsulation of Tregs by co-axial 3D-bioprinting as a valid option for providing local immune protection to allogeneic cellular transplants such as pancreatic islets.

## 1. Introduction

Regulatory T-cells (Tregs) constitute a vital $CD4^+$ T-cell sub-population specialized in immune suppression and regulation[1]. Tregs were initially reported in 1970 as suppressor T-cells, a subset of T-cells with the ability to abrogate the pro-inflammatory immune responses[2]. Since then, intensive investigations led to the discoveries of Treg-defining surface markers, $CD4^+$, $CD25^{hi}$ and $CD127^-$, and the master transcriptional regulator of Treg-lineage, FOXP3[3–8]. To date, two main subgroups of natural Tregs (nTregs) exhibit the $CD4^+$ $CD25^{hi}$ $CD127^-$ $FOXP3^+$ profile: thymic-derived Tregs (tTregs), which stably express FOXP3, and $CD4^+$ T cells that acquire FOXP3 expression in the periphery, called pTregs. pTregs generated *in vitro* are named induced Tregs (iTregs)[9,10].

Tregs are a crucial component of immunological tolerance and homeostasis, playing many roles in the immune system, including establishing tolerance to self and selected foreign antigens, and regulating the duration of immune responses to minimize self-damage[1]. Tregs mediate suppression via the secretion of anti-inflammatory cytokines, cytolysis of target cells, metabolic disruption, and modulation of dendritic cells[11]. Treg-mediated suppression, thus, targets a broad range of immune cells including other T-cell subsets, B cells, antigen presenting cells, and natural killer cells[12]. With such versatility in modes and targets of action, immunotherapies utilizing Tregs have been extensively investigated for the treatment of autoimmunity and allogeneic transplantation[13].

In particular, Treg-therapy could establish allograft tolerance in transplant recipients, overcoming challenges associated with the requirement for life-long systemic immunosuppression to prevent allograft rejection, such as an increased risk of infection, malignancy, and organ toxicity[14]. Furthermore, spontaneous allogeneic organ tolerance, a phenomenon in which transplant recipients accept the allografts without the use of immunosuppressive regimen, has been observed in liver transplant recipients with elevated Treg levels[15]. Currently, most clinical trials of Treg-therapies

utilize systemic adoptive transfer of *ex vivo* expanded Tregs[16]. While this method has shown promising results in clinical trials[17,18], *ex vivo* expansion of Tregs requires extremely time-consuming and costly protocols to generate appropriate numbers of cells for clinically significant results, due to the low frequency of Tregs in human peripheral blood[19,20]. Thus, it would be advantageous to employ more targeted approaches, such as hydrogel encapsulation to provide localized immunosuppression.

Pancreatic islet transplantation is currently the only curative cell therapy for type 1 diabetes mellitus. Islet transplantation is unique, compared to solid organ transplantation, as it involves the isolation and purification of islets from a donor pancreas, which are then infused into the recipient liver via the hepatic portal vein[21]. Due to such characteristics, it is possible to co-transplant islets with other cell types beneficial to their survival[22,23]. As rejection by the immune system remains a major hurdle, co-encapsulation of islets with Tregs could be of great benefit. This could be achieved via 3D-bioprinting using a recently developed customized co-axial bioprinter, equipped with dual bioink chambers, to generate a scaffold containing a core of islets surrounded by a shell of Tregs, providing localized immune-protection[24–26].

Here, we encapsulated human nTregs and iTregs in an alginate-GelMA (gelatin methacryloyl) hydrogel, a bioink that we recently developed for co-axial bioprinting of islets with supporting cells[25]. While islets have been routinely encapsulated since 1980[27], Tregs have never previously been encapsulated. Therefore, this study investigated the impact of encapsulation on human nTregs and iTregs. Furthermore, the hydrogel was supplemented with Treg-specific bioactive factors, interleukin-2 (IL-2) and chemokine ligand 1 (CCL1), to enhance the encapsulation of Tregs. IL-2 is a T-cell stimulatory cytokine which is crucial for Treg survival and function[28] The effect of IL-2 on the encapsulated Tregs was evaluated. CCL1 is a ligand for chemokine receptor 8 (CCR8) which is

preferentially expressed on Tregs[29]. The capability of CCL1 to recruit additional Tregs to the hydrogel structure was examined, as well as the composition of the lymphocyte population that would actively be recruited from human peripheral blood.

## 2. Materials and Methods

### *2.1. Preparation of alginate-GelMA hydrogel precursor*

Gelatin (porcine skin, type A, gel strength ~175 g Bloom, Sigma-Aldrich) was dissolved in phosphate buffered saline (PBS; 10% w/v) for one hour at 50 °C. Methacrylic anhydride (Sigma-Aldrich) was added to the 10% w/v gelatin solution in a drop-wise manner with stirring (final concentration of 7.4% v/v). The reaction continued for 3 hours and then terminated by diluting the solution four times with PBS. 1% v/v of Chloroform was added, and the mixture was dialyzed against distilled water for seven days at 40 °C (cellulose membrane, molecular weight cut off (MWCO): ~12 kDa). The dialyzed GelMA solution was lyophilized to white porous foam (stored at -20 °C until further use). The above process was undertaken under sterile conditions. The degree of functionalization (DoF) of GelMA was measured by a ninhydrin assay as described by Loessner et al[30]. Alginate (medium viscosity, Sigma-Aldrich) was sterilized by UV for 20 minutes then dissolved in PBS (2% w/v) for two days at 37 °C. GelMA was added to the alginate solution at a concentration of 7.5% w/v, resulting in 2%|7.5% w/v alginate-GelMa. The alginate-GelMA hydrogel precursor was incubated at 37 °C with occasional shaking until a homogenous formulation was formed.

### *2.2. Cell isolation and in vitro expansion*

Human buffy coat (Australian Red Cross) was treated with a RossetteSep Human CD4+ T cell enrichment cocktail (STEMCELL Technologies) for 20 minutes on a platform mixer at 80 rpm. Treated buffy coat was diluted with PBS (+2% foetal calf serum (FCS), Bovogen) prior to isolation

of $CD4^+$ T cells by density-gradient centrifugation over Lymphoprep (STEMCELL Technologies). Enriched $CD4^+$ T cells were surface-stained for CD4, CD25, CD127 and CD45RA. $CD4^+$ $CD25^+$ $CD127^-$ T cells (natural regulatory T cells or nTregs) and $CD4^+$ $CD25^-$ $CD127^+$ $CD45RA^+$ T cells (naïve $CD4^+$ T-cells) were sorted by fluorescence-activated cell sorting (FACS; BD FACSAria Fusion, BD Biosciences; Fig. S1A). Sorted nTregs and naïve $CD4^+$ T-cells were rested overnight in a complete X-vivo medium (cX-vivo: serum-free with gentamycin and phenol red, Lonza, supplemented with 2% HEPES, 1% L-glutamine and 5% human serum (Gibco, HyClone and Sigma-Aldrich, respectively) with 500 U/mL of IL-2 (Novartis Vaccines and Diagnostics). After overnight resting, these cells were checked for purity by staining for CD4, CD25 and FOXP3 (Foxp3/ Transcription factor staining buffer set, eBioscience; Fig. S1B). nTregs were cultured in an expansion medium consisting of cX-vivo and a 1:1 ratio of Human T-expander CD3/CD28 Dynabeads™ (Thermo Fisher Scientific). Naïve CD4+ T-cells were cultured in an induction medium composed of the expansion medium supplemented with 5 ng/mL of human TGF-β (eBioscience), 10 nM/mL of all-trans retinoic acid (Sigma-Aldrich) and 2 nM/mL rapamycin (LC Laboratories) for the generation of induced regulatory T cells (iTregs). nTreg expansion and iTreg generation were verified by expression of CD4, CD25 and FOXP3 (Fig. S1C). Following expansion, the expander beads were removed and Tregs were rested in cX-vivo (+500 U/mL of IL-2) for two days prior to use.

*2.3. Encapsulation of Tregs*

Rested Tregs were mixed well with 2%|7.5% w/v alginate-GelMa hydrogel precursor at $2 \times 10^6$ cells/mL, and then lithium phenyl-2,4,6-trimethylbenzoylphosphinate (LAP, Tocris Bioscience; a final concentration of 0.06% w/v) was added. For some experiments, IL-2 (500 U/mL) or CCL1 (10 µg/mL) was directly added to the above cell suspension. The hydrogel precursor-cell suspension was injected into a disc-mold (8 mm diameter with 1 mm height; approximately 50 µL in volume per

disc) using a drawing-up needle (BD Biosciences), which was then photo-crosslinked at 400 nm (Omnicure LX505, Excelitas) for 1 minute and then further crosslinked in 2% w/v $CaCl_2$ (BDH) solution for 10 minutes. The cell-laden discs were cultured in cX-vivo medium (no IL-2) for 24 or 72 hours at 37 ˚C with 5% $CO_2$ prior to downstream assays. Non-encapsulated Tregs were prepared by suspending Tregs at 2 $\times 10^6$ cells/mL in cX-vivo medium (+ 500U/mL of IL-2). Some discs made with IL-2-free 2%|7.5% w/v alginate-GelMa were cultured in cX-vivo medium (+ 500U/mL of IL-2); these were dubbed "Encapsulated (+IL-2 in media)". For viability, phenotype, functionality and CD154 suppression assay, the encapsulated Tregs were recovered by digesting the hydrogel constructs in TrypLE Express (Thermo Fisher Scientific) for 10 minutes at 37˚C and then washed twice with PBS (non-encapsulated Tregs were treated the same way).

*2.4. Viability, Treg phenotype and Treg functionality assay*

Unstained control and compensation controls were used when required. For assessment of viability, a positive dead control was prepared by three cycles of rapid freeze-thaw (at -80 ℃ and 37 ℃, respectively). For viability, propidium iodide (PI; 50 μg/mL) was added to the samples to a final concentration of 2.5 μg/mL. For Treg phenotype and functionality, recovered cells were stained for viability (fixable viability stain; supplementary table 1) then surface-stained for CD4 and CD25 before being fixed, permeabilized and intracellularly stained for FOXP3. Stained cells were divided into four groups: the first group was stained for CD69, the second for TGF-β, the third for CD39, and the fourth for CTLA-4. All samples were analyzed on a BD FACS Canto II flow cytometer (BD Biosciences), and the data analyzed with FCS Express 6 (De Novo Software).

*2.5. CD154 suppression assay*

Human peripheral blood mononuclear cells (PBMCs) cells were isolated from a fresh buffy coat by density gradient centrifugation as described above. Naïve $CD4^+$ T-cells were isolated using

EasySep™ Human Naïve CD4+ T Cell Isolation kit (STEMCELL Technologies). Naïve $CD4^+$ T-cells were labelled with 3,30-dioctadecyloxacarbocyanine perchlorate ($DiOC_{18}(3)$ (Thermo Fisher Scientific; a final concentration of 2 μg/mL) by incubation at 37 ˚C with 5% $CO_2$ for 45 minutes. 96-well round bottom plates were seeded with $DiOC_{18}(3)$-labelled naïve $CD4^+$ T-cells ($5 \times 10^4$ cells per well; "Teffector") and Tregs were added to the wells at various ratios of Treg:Teffector (1:1, 1:2, 1:4 and 1:8). Human T-expander CD3/CD28 Dynabeads™ (bead:Teffector ratio of 1:4) and anti-CD154 antibody were added to each well. $DiOC_{18}(3)$-labelled naïve CD4+ T-cells with and without Tregs were used as positive and negative controls, respectively. The plate was incubated at 37 ˚C with 5% $CO_2$ for 7 hours then analyzed for expression of CD154 by flow cytometry (FACS Canto II). Percentage suppression was calculated as follows: 100 × [1 - (%$CD154^+$ in the experiment sample divided by %$CD154^+$ in the positive control)].

*2.6. Transmission electron microscopy (TEM)*

Encapsulated Tregs and non-encapsulated controls were fixed overnight in electron microscopy fixative (4% paraformaldehyde/1.25% glutaraldehyde in PBS, + 4% sucrose, pH 7.2). Fixed samples were washed in washing buffer (PBS + 4% sucrose) for 5 minutes then stained with 2% $OsO_4$ solution for 1 hour. Stained samples were dehydrated through a series of washes (two washes in 70% ethanol for 15 minutes each, two washes in 90% ethanol for 15 minutes each, three washes in 100% ethanol for 15 minutes each then one wash in propylene oxide for 15 minutes). Dehydrated samples underwent resin infiltration (50% propylene oxide 50% epoxy resin for 1 hour, two washes in 100% resin for 1 hour each then 100% resin overnight). After overnight incubation, samples were embedded in fresh 100% resin then polymerized at 70 °C for at least 24 hours. Sections were cut from the polymerized samples and analyzed by FEI Tencai G2 Spirit Biotwin TEM at 100kV after appropriate staining.

*2.7. Whole blood chemokine receptor phenotyping*

Human peripheral blood mononuclear cells (PBMCs) were isolated from a fresh whole blood by density gradient centrifugation, as above. PBMCs were stained for CD3, CD4, CD45RA, CD25, CD127, CXCR3, CCR4, CCR6, CCR8 and CCR10 then analyzed on BD FACSymphony (BD Biosciences). Additionally, PBMCs were stained for CD4, CD45RA, CD25, CD127, CCR8 and FOXP3 for assessment of FOXP3 expression by $CCR8^+$ and $CCR8^-$ Tregs.

*2.8. Chemotaxis assay*

Chemotaxis assays were performed with either 96-well or 24-well transwell plates with 5 μm polycarbonate membranes (Corning). All chemokines and cells were resuspended in a chemotaxis buffer composed of RPMI 1640 medium (Gibco) with 0.5% w/v bovine serum albumin (Sigma-Aldrich) and 2.5% HEPES. 96-well plates employed 150 μL in the lower chamber and 50 μL in the upper chamber. 24-well plates employed 600 μL in the lower chamber and 100 μL in the upper chamber. To generate a migration response profile for CCL1 (96-well), various concentrations of CCL1 ranging from 100 ng/mL to 10 μg/mL (3-fold increments) were placed in the lower chambers, and Tregs ($2 \times 10^6$ cells/mL) were placed in the upper chambers. CXCL12 (30 ng/mL) was utilized as a positive control. For assessment of encapsulated Treg migration (24-well), 10 μg/mL of CCL1 was placed in the lower chamber and encapsulated ($2 \times 10^6$ cells/mL) and non-encapsulated ($1 \times 10^6$ cells/mL) Tregs were placed in the upper chamber. For assessment of CCL1 addition to the hydrogel (24-well), CCL-1-added hydrogel disc (no cells) and 10 μg/mL of CCL1 were placed in the lower chamber and Tregs ($2 \times 10^6$ cells/mL) were placed in the upper chamber. For all transwell migration assays, a spontaneous migration control with no chemokine in the lower chamber was included. The plates were incubated for 3 hours at 37 ˚C with 5% $CO_2$, and then migrated cells in the lower chamber were analyzed by flow cytometry (BD LSRFortessa for the 96 well set up and BD FACS Canto II for the 24 well set up; BD Biosciences) using counting beads (CountBright Absolute

Counting Beads; Thermo Fisher Scientific). Migration index was calculated as follows: number of cells in the experimental sample per 1000 beads divided by number of cells in the spontaneous migration control per 1000 beads. For immune phenotyping post-chemotaxis with CCL1, human PBMCs ($2 \times 10^6$ cells/mL) were placed in the upper chambers with 10 μg/mL of CCL1 in the lower chamber (24-well). After 3-hour incubation, cells in the lower chamber were stained as described in whole blood chemokine receptor phenotyping.

*2.9. Statistics*

Statistical significance ($p<0.05$) was analyzed using the GraphPad Prism 7. One-way ANOVA with Tukey's multiple comparisons test, Two-way ANOVA with Tukey's multiple comparisons test and paired two-tailed T-test were used to identify statistical significance. All replicates are biological replicates. All experiments utilized triplicates as technical replicates except for whole blood chemokine receptor phenotyping which used no technical replicates.

*2.10. Antibodies*

Antibody details are listed in the supplementary table 1.

*2.11. 3D-bioprinting of Tregs and viability staining*

Human nTregs and iTregs were 3D-bioprinted as described previously at $2 \times 10^6$ cells/mL.[25] 3D-bioprinted nTregs and iTregs were cultured in cX-vivo medium (+ 500U/mL of IL-2) overnight at 37 ˚C with 5% $CO_2$. 3D-bioprinted nTregs and iTregs were stained with Calcein AM (final concentration 1 μM; Thermo Fisher Scientific) and DAPI (300 ng/mL; Thermo Fisher Scientific) for 30 minutes at 37 ˚C with 5% $CO_2$ in dark. 3D-bioprinted cells were washed in PBS then imaged with Olympus FV3000 confocal laser scanning microscope (Olympus).

## 3. Results

### 3.1. Preparation of alginate-GelMA hydrogel precursor and Treg encapsulation

Alginate-GelMA hydrogel precursor was generated by the addition of GelMA to an alginate solution. GelMA was prepared from porcine gelatin by the addition of methacrylic anhydride (Fig. 1A). The degree of functionalization (DoF) was measured by a ninhydrin assay quantifying absorbance at 570 nm. The concentration of unfunctionalized gelatin remaining in the GelMA was interpolated from gelatin standards ranging from 0 mg/mL to 100 mg/mL, confirming successful methacryloyl functionalization with a DoF of 82 ± 5%. The hydrogel precursor was then used to encapsulate Tregs via photo- and chemical- crosslinking (Fig. 1B). Successful encapsulation was demonstrated by transmission electron microscopy (Fig. 2). In some experiments, Tregs were recovered via enzymatic dissolution of the hydrogel discs using TrypLE, which targets peptide bonds on the C-termini of lysine and arginine of GelMA.

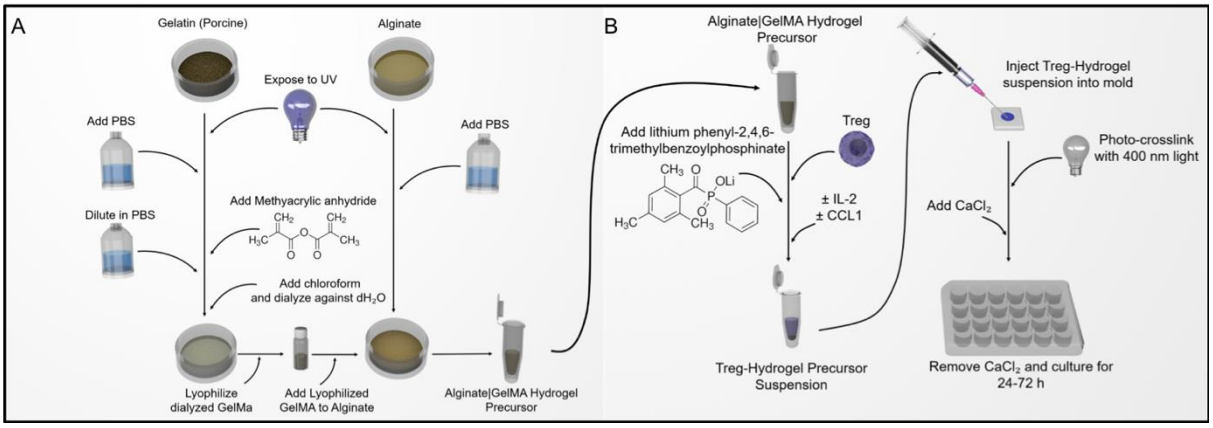


**Fig. 1.** (A) Schematics for preparation of alginate-GelMA hydrogel precursor and (B) Treg encapsulation.

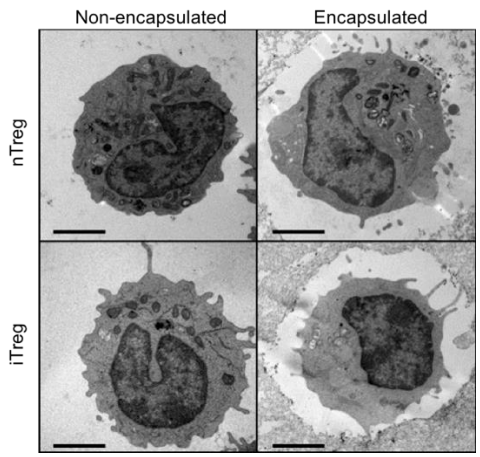


**Fig. 2.** Treg encapsulation in alginate-gelMA hydrogel.TEM images of non-encapsulated and encapsulated nTregs and iTregs. Scale bar represents 2 µm at 11500× magnification.

### 3.2. Viability of encapsulated Tregs

The viability of encapsulated or control non-encapsulated Tregs at days 1 and 3 was evaluated by measuring dye exclusion, based on % Propidium Iodide$^{+}$ (100% - %PI$^{+}$; Fig. 3A). On Day 1, encapsulated Treg viability was significantly reduced in both nTregs and iTregs (8% and 10%; $p=0.0034$ and $p=0.0038$, respectively) in the absence of IL-2, while there was no significant decrease in viability upon encapsulation in the presence of IL-2. Non-encapsulated and encapsulated Tregs without IL-2 displayed significantly lower viability than those with IL-2, a 9% ($p=0.0012$) and 12% ($p<0.0001$) decrease in nTregs and 16% ($p<0.0001$) and 23% ($p<0.0001$) decrease in iTregs, respectively. At day 3, viability of non-encapsulated and encapsulated Tregs without IL-2 decreased by 23% and 41% in nTregs and 29% and 40% in iTregs ($p<0.0001$), compared with those IL-2. The viability of encapsulated Tregs with IL-2 was significantly lower than non-encapsulated Tregs with IL-2 (18% decreases in both nTregs and iTregs, $p=0.0001$ and 0.0042 respectively; Fig. 3B and Fig. S2A, B). These decreases were reversed by supplementing the media with IL-2 ('encapsulated with IL-2 in media') instead of the hydrogel. The viability of encapsulated Tregs with IL-2 in the media displayed no significant differences from non-encapsulated Tregs with IL-2 (Fig. 3C and Fig. S2C).

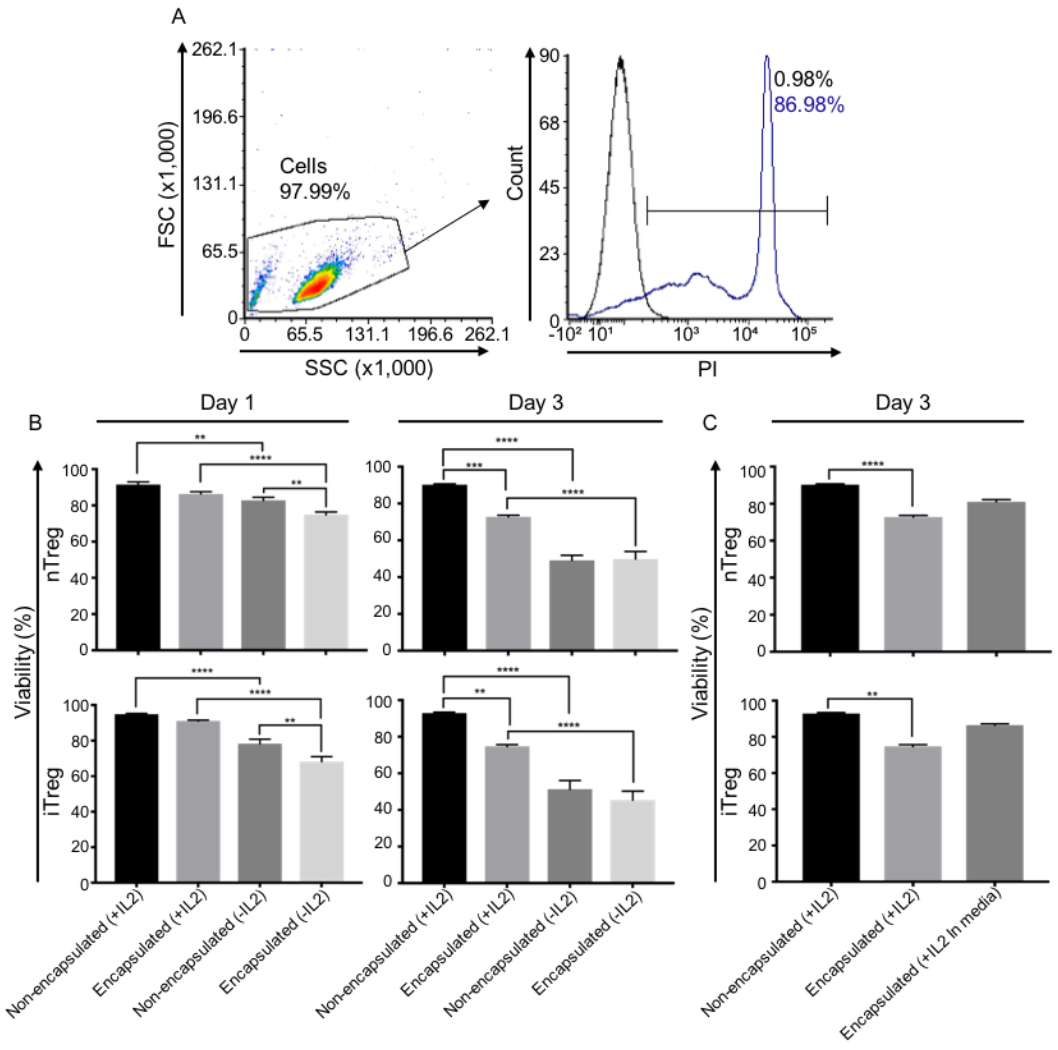


**Fig. 3.** Viability of Tregs encapsulated in alginate-GelMA hydrogel at day 1 and 3. (A) Gating strategy to determine the percentage of dead cells. Propidium iodide (PI) was used to stain dead cells (black line: unstained control; Indigo line: positive dead control). (B) Viability at day 1 and 3 for both nTregs and iTregs. Non-encapsulated Tregs were cultured in either IL-2-supplemented media "non-encapsulated (+IL-2) or IL-2-free media "non-encapsulated (-IL-2). Encapsulated Tregs were made with either IL-2-supplemented hydrogel "encapsulated (+IL-2) or IL-2-free hydrogel "encapsulated (-IL-2) then cultured in IL-2-free media. (C) Day 3 viability of encapsulated Tregs upon supplementation of the media with IL-2 instead of the hydrogel "encapsulated (+IL2 in media)". Data represented as mean ± SEM, n=3, statistical significance identified by One-way ANOVA with Tukey's multiple comparisons test *P<0.05, **0.01, ***0.001, ****0.0001.

### 3.3. Phenotype of encapsulated Tregs

Tregs are classically defined as $CD4^+$ $CD25^+$ $FOXP3^+$ cells. Expression of CD25 and FOXP3 was measured as mean fluorescence intensity (MFI) in viable $CD4^+$ populations (Fig. 4A). Analysis showed no significant differences in the MFI of CD25 expression between non-encapsulated and encapsulated Tregs. CD25 MFI of non-encapsulated and Tregs encapsulated with IL-2 were higher

than Tregs without IL-2 for nTregs (non-encapsulated: $p=0.0305$) and iTregs ($p<0.0001$). Tregs encapsulated with IL-2 showed significantly lower FOXP3 MFI than non-encapsulated Tregs cultured with IL-2 ($p=0.0006$ for nTregs and $p<0.0001$ for iTregs). This was in contrast to Tregs encapsulated without IL-2 which showed no significant decrease in FOXP3 MFI compared with non-encapsulated Tregs cultured without IL-2. Moreover, FOXP3 MFI of non-encapsulated and encapsulated Tregs without IL-2 were significantly reduced compared with those with IL-2 in both nTregs ($p<0.0001$ and $p=0.0069$) and iTregs ($p<0.0001$ and $p=0.0001$; Fig. 4B and Fig. S3A). Treg functional markers CD69, transforming growth factor beta (TGF-β), CD39 and cytotoxic T-lymphocyte-associated protein 4 (CTLA-4), which are surrogates for activation status and suppressive functionality (inhibitory cytokines, metabolic disruption and dendritic cell (DC) targeting)[11,31], were also assessed (Fig. 5A). There were no significant differences in CD69, CD39 and CLTA-4 MFI between non-encapsulated and encapsulated Tregs. Non-encapsulated Tregs without IL-2 showed significantly lower CD69 ($p=0.0472$) and CD39 ($p=0.0062$) MFI in iTregs and CTLA-4 ($p=0.0062$) MFI in nTregs while there were significant differences between encapsulated Tregs with and without IL-2. TGF-β expression mimicked that of FOXP3, showing significant differences between non-encapsulated and encapsulated Tregs with IL-2 ($p=0.0001$ in nTregs and $p=0.0011$ in iTregs) and between non-encapsulated and encapsulated Tregs with and without IL-2 ($p<0.0001$ and $p=0.0023$ in nTregs and $p<0.0001$ in iTregs; encapsulated Tregs showed n.s in iTregs; Fig. 5B and Fig. S3A). Again, upon supplementation of the media with IL-2, FOXP3 and TGF-β MFI expression was equivalent to non-encapsulated Tregs, showing significantly higher MFI (FOXP3: $p<0.0001$ in both nTregs and iTregs. TGF-β: $p=0.0044$ in nTregs and $p=0.0003$ in iTregs) than encapsulated Tregs with IL-2 (Fig. 5C and Fig. S3B). Percentage positive of each markers showed similar trends to MFI of the markers (Fig. S3C).

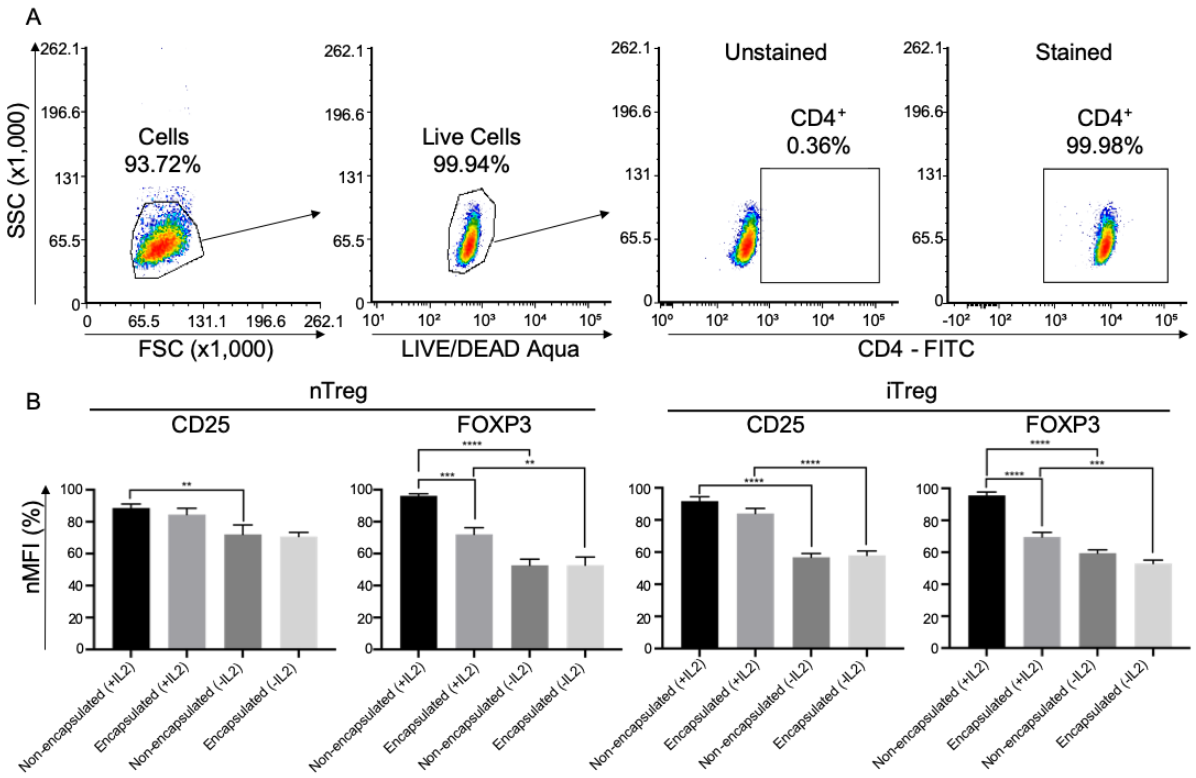


**Fig. 4.** Expression of Treg phenotype markers upon encapsulation in alginate-GelMA hydrogel. (A) Gating strategy for $CD4^+$ cells using an unstained population. Mean fluorescence intensity (MFI) for CD25 and FOXP3 were measured from this $CD4^+$ population. MFI was normalized to the maximum raw value in each marker and experiment. (B) CD25 and FOXP3 MFI in non-encapsulated and encapsulated nTregs and iTregs (±IL-2). Data represented as mean ± SEM, n=3, statistical significance identified by One-way ANOVA with Tukey's multiple comparisons test *P<0.05, **0.01, ***0.001, ****0.0001.

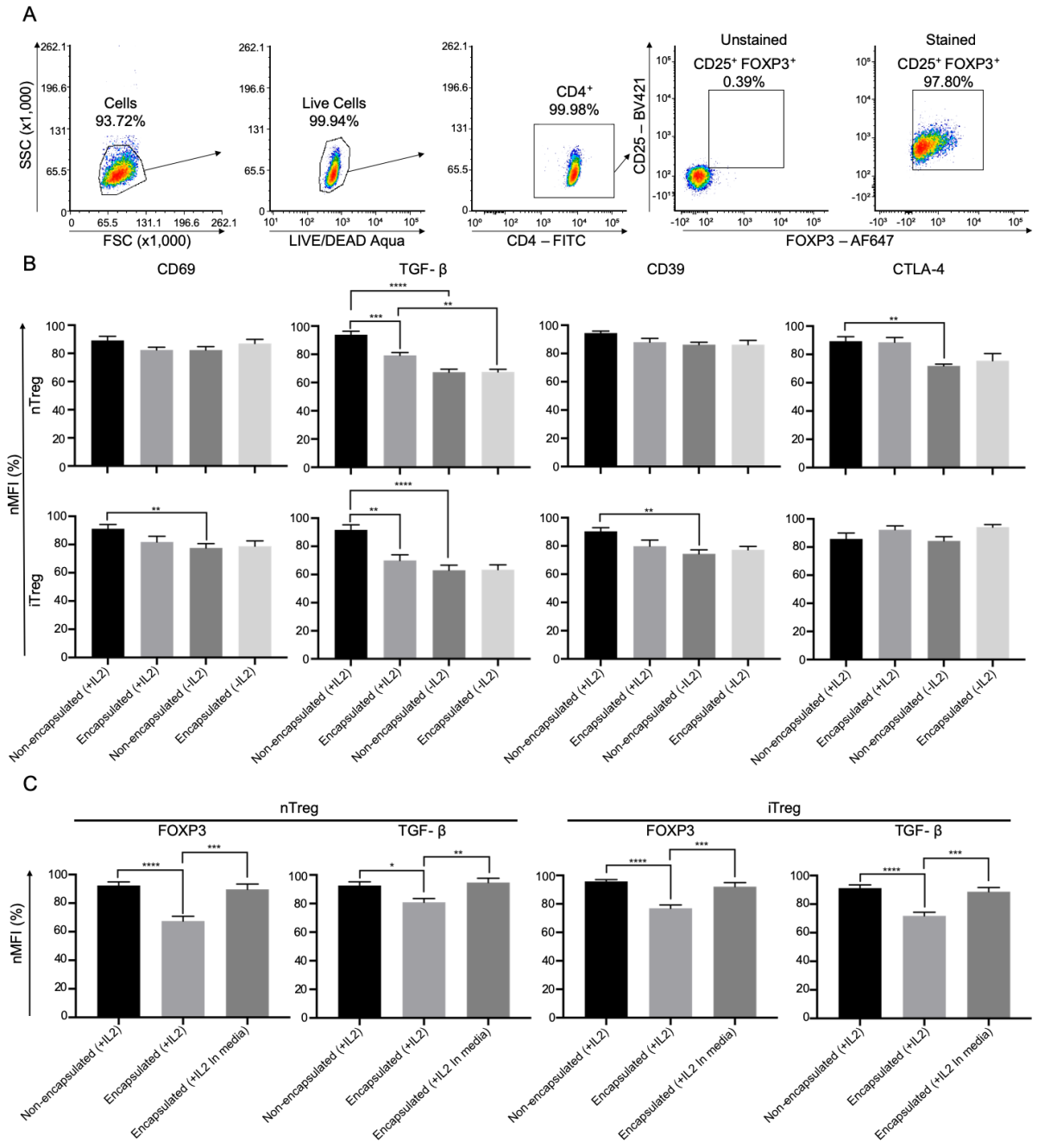


**Fig. 5.** Expression of Treg functionality markers upon encapsulation in alginate-gelMA hydrogel. (A) Gating strategy for $CD4^+$ $CD25^+$ $Foxp3^+$ cells using an unstained population. Mean fluorescence intensity (MFI) for CD69, TGF-β, CD39 and CTLA-4 were then measured from this $CD4^+$ $CD25^+$ $Foxp3^+$ population. MFI was normalized to the maximum raw value in each marker and experiment. (B) CD69, TGF-β, CD39 and CTLA-4 MFI in non-encapsulated and encapsulated nTregs and iTregs (±IL-2). (C) FOXP3 and TGF-β MFI of encapsulated nTregs and iTregs (+IL-2 in media). Data represented as mean ± SEM, n=3, statistical significance identified by One-way ANOVA with Tukey's multiple comparisons test *P<0.05, **0.01, ***0.001, ****0.0001.

## 3.4. Suppressor function of encapsulated Treg

Suppressive activities of non-encapsulated and encapsulated Tregs were assessed using CD154 suppression assays. CD154 is an activation marker transiently expressed during T-cell activation and can be measured in naïve $CD4^+$ T-cells (Teffectors) in the presence of Tregs to assess the suppressor

function of Tregs[32]. Tregs to Teffectors ratios of 1:1 to 1:8 were utilized. $DiOC_{18}(3)$ (3,30-dioctadecyloxacarbocyanine perchlorate) was used to differentiate Teffectors from Tregs in the flow cytometric analysis. Negative control ($DiOC_{18}(3)$ labelled and CD154 stained) Teffectors provided baseline unstimulated % $CD154^+$ to gate $CD154^+$ cells. Positive control ($DiOC_{18}(3)$ labelled, CD154 stained Teffectors stimulated with anti-CD3/CD28 beads) served as baseline stimulated $\%CD154^+$ to calculate % suppression (Fig. 6A). No significant differences in % suppression was shown between non-encapsulated and encapsulated Tregs at all ratios. In the absence of IL-2, Tregs displayed significant losses in their suppressor function compared with those in the presence of IL-2. At 1:1 ratio, both non-encapsulated and encapsulated groups displayed 10% (p=0.0115 and 0.0132) decreases in nTregs and 13% (p=0.0048 and 0.0038) decreases in iTregs. At 1:2 ratio, 8% (n.s; p=0.0771) and 10% (p=0.0324) decreases were shown in nTregs and 13% (p<0.0001) and 18% (p=0.0034) decreases were observed in iTregs (Fig. 6B).

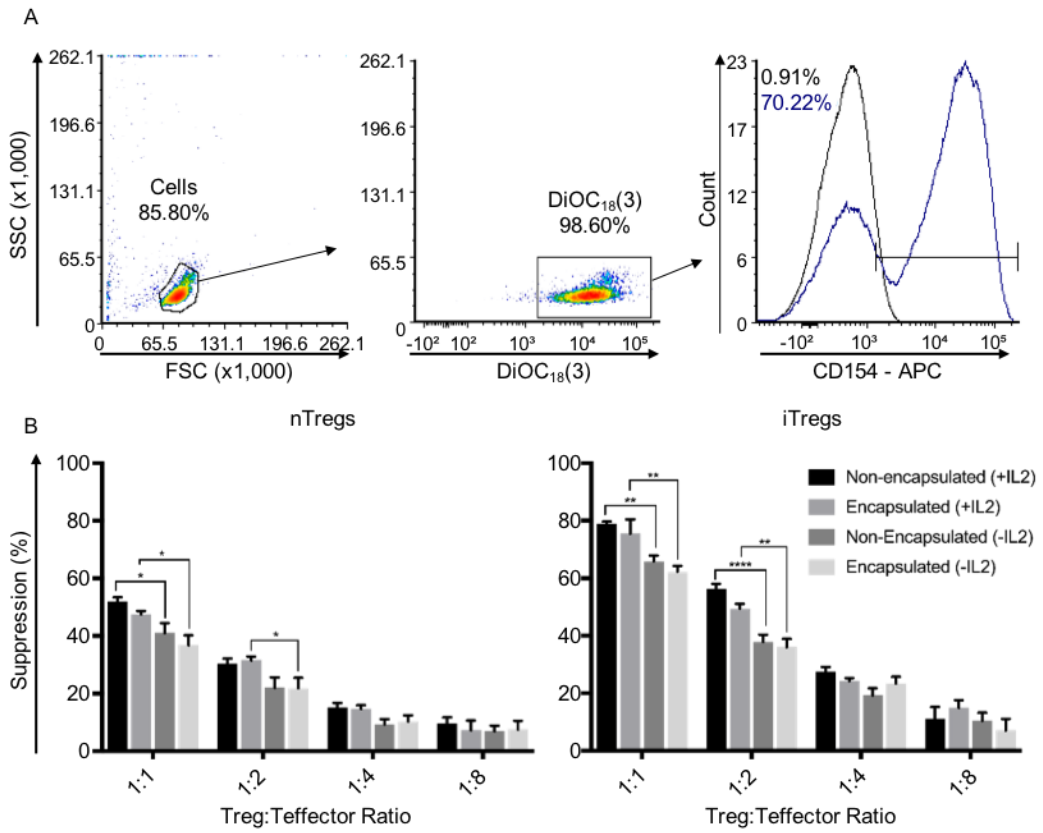


**Fig. 6.** Function of Tregs encapsulated in alginate-GelMA hydrogel. (A) Gating strategy to determine $\%CD154^+$ from $DiOC_{18}(3)^+$ cells. $DiOC_{18}(3)$ was used differentiate naïve T-cells (Teffectors) from Tregs. Unstained control was used to gate for $DiOC_{18}(3)^+$. Negative control (black; $DiOC_{18}(3)$-labelled and CD154-stained with no anti-CD3/CD28 beads) set baseline non-activated $\%CD154^+$. Positive control (indigo; DiOC18(3) and CD154 stained with anti-CD3/CD28 beads) provided baseline activated $\%CD154^+$ to calculate %suppression. Control wells contained no Tregs. (B) %suppression of non-encapsulated and encapsulated nTregs and iTregs (±IL-2) at various Treg:Teffector ratios (1:1 to 1:8). Data represented as mean ± SEM, n=3, statistical significance identified by Two-way ANOVA with Tukey's multiple comparisons test *P<0.05, **0.01, ***0.001, ****0.0001.

### 3.5. Migration capacity of encapsulated Tregs and CCL supplementation of the hydrogel

For successful localized immunosuppression, it is important that Tregs stay confined within the hydrogel structure, which can be facilitated by strong chemotactic signals. The chemotactic response profile of nTregs and iTregs to CCL1 was measured from 100 ng/mL to 10 μg/mL with 3-fold increments, to determine concentration dose response. Spontaneous migration with no chemokine was utilized to calculate migration index (MI). Maximal responses were observed at 10 μg/mL with migration index of 30 and 9 in nTregs and iTregs, respectively (Fig. 7A). 10 μg/mL of CCL1 was used to assess the migration capacity of non-encapsulated and encapsulated Tregs. Migration capacity of encapsulated Tregs was significantly reduced compared with non-encapsulated Tregs with 400-fold reduction ($p=0.0003$) for nTregs and 220-fold ($p<0.0001$) reduction for iTregs (Fig. 7B). In parallel, the Treg-recruitment capability of hydrogel discs supplemented with CCL1 was evaluated. CCL1-supplemented hydrogel demonstrated recruitment of Tregs with an MI of 5 in nTregs and 3 in iTregs. This was significantly lower than the 10 μg/mL of CCL1 in chemotaxis buffer which showed a MI of 43 with nTregs ($p<0.0001$) and 19 with iTregs ($p<0.0001$) (Fig. 7C). Moreover, CCL1 has been shown to enhance Treg function[33]. Therefore, CCL1-supplimented hydrogel was used to encapsulate Tregs and suppressive activities of encapsulated Tregs with and without CCL1 were measured. Interestingly, nTregs and iTregs showed completely opposite results. Suppressive activity of encapsulated nTregs was significantly higher in the presence of CCL1 with 12% ($p=0.0211$), 13% ($p=0.0125$) and 15% ($p=0.0365$) differences at 1:1, 1:2 and 1:8 ratios (1:4 ratio n.s with 12% difference; $p=0.1129$) while suppressive activity of iTregs was significantly lower in the presence of CCL1 with 8% ($p=0.0355$), 12% ($p=0.0385$), 16% ($p=0.0277$) and 18% ($p=0.0057$) differences at all ratios (Fig. 7D).

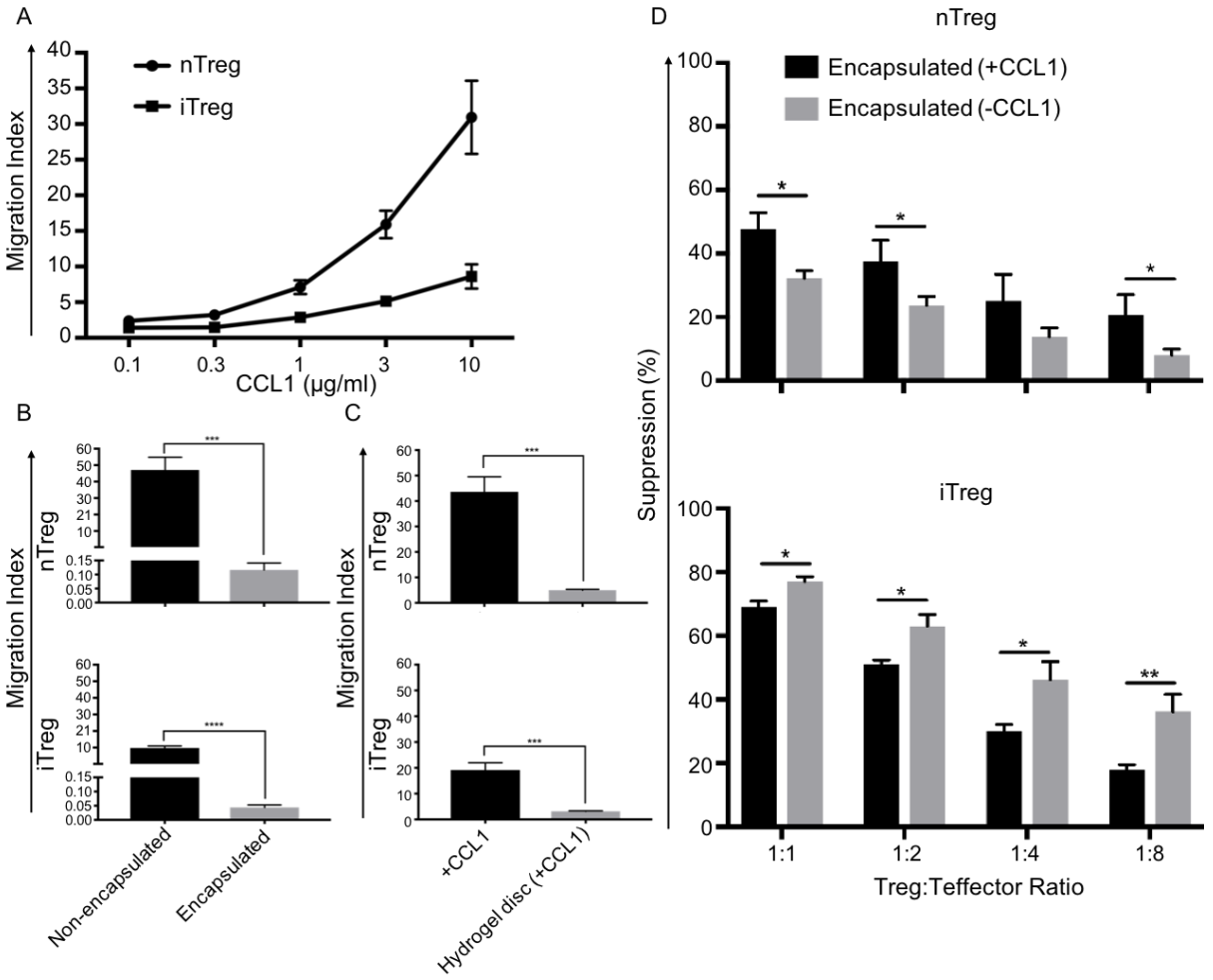


**Fig. 7.** Migration capacity of encapsulated Tregs and assessment of CCL-1-supplemented alginate-GelMA hydrogel. (A) Chemotactic response profile of nTregs and iTregs to CCL1 (100 ng/mL to 10 µg/mL). 10 µg/mL of CCL1 was used for subsequent experiments, either supplementing chemotaxis buffer or the hydrogel. (B) Migration capacity of non-encapsulated and encapsulated Tregs. (C) Treg recruitment capability of CCL-1-supplemented hydrogel and CCL-1-supplemeted buffer. (D) %suppression of encapsulated nTregs and iTregs (±CCL1). Data represented as mean ± SEM, n=3, statistical significance identified by paired two-tailed T-test *P<0.05, **0.01, ***0.001, ****0.0001.

To investigate which types of lymphocytes would be recruited from the human peripheral blood through CCL1-mediated chemotaxis, peripheral blood mononuclear cells (PBMCs) were isolated from whole blood for immunophenotyping. Particular interests were in $CD4^+$ T-cell subsets as most of $CCR8^+$ cells in the peripheral blood are $CD4^+$ memory T-cells[29]. PBMCs were stained for CD3, CD4, CD45RA, CD25, CD127, and CXCR3, CCR4, CCR6, CCR8 and CCR10 to compare proportions of $CD4^+$ T-cell subsets in the whole memory (inclusive of $CCR8^+$ and $CCR8^-$) $CD4^+$ T-cells with $CCR8^+$ memory $CD4^+$ T-cells. Within these two populations, memory Tregs (mTregs) and memory conventional T-cells (mTconvs) were gated based on their CD25 and CD127 expression.

mTconvs were then further divided into T-helper subsets using chemokine receptors (Fig. 8A). $CCR8^+$ memory $CD4^+$ T-cells showed significant enrichments of mTregs ($p=0.0006$), Th2 ($p=0.0036$) and Th22 cells ($p=0.0001$) compared to whole memory $CD4^+$ T-cells. Proportions of mTconvs ($p=0.0004$), Th1 ($p=0.0126$), Th1/17 ($p=0.0097$), Th17 ($p=0.0035$) and Th9 ($p<0.0001$) cells showed significant reduction (Fig. 8B). PBMCs were then utilized for the chemotaxis assay with CCL1. The proportions of mTregs and mTconvs migrated in response to CCL1 were comparable to $CCR8^+$ memory $CD4^+$ T-cells, with significant enrichment of mTregs ($p<0.0001$) and reduction of mTconvs ($p<0.0001$) compared to the whole memory $CD4^+$ T-cells (Fig. 8C). Percentages of $CCR8^+$ cells in each memory $CD4^+$ T-cell subsets were also measured (Fig. S4). Th22 cells had the highest expression of CCR8 followed by mTregs and Th2 cells at (53%, 28% and 28% respectively). Other subsets exhibited $\%CCR8^+$ below 10% (mTconvs at 10% and Th1, Th1/17 and Th17 at 7%) with Th9 cells being the least positive (2%) (Fig. 8D). Moreover, FOXP3 MFI of $CCR8^+$ mTregs and $CCR8^-$ mTregs was assessed (Fig. S5). $CCR8^+$ mTregs showed 1.5-fold higher FOXP3 MFI ($p=0.0062$) than $CCR8^-$ mTregs (Fig. 8E).

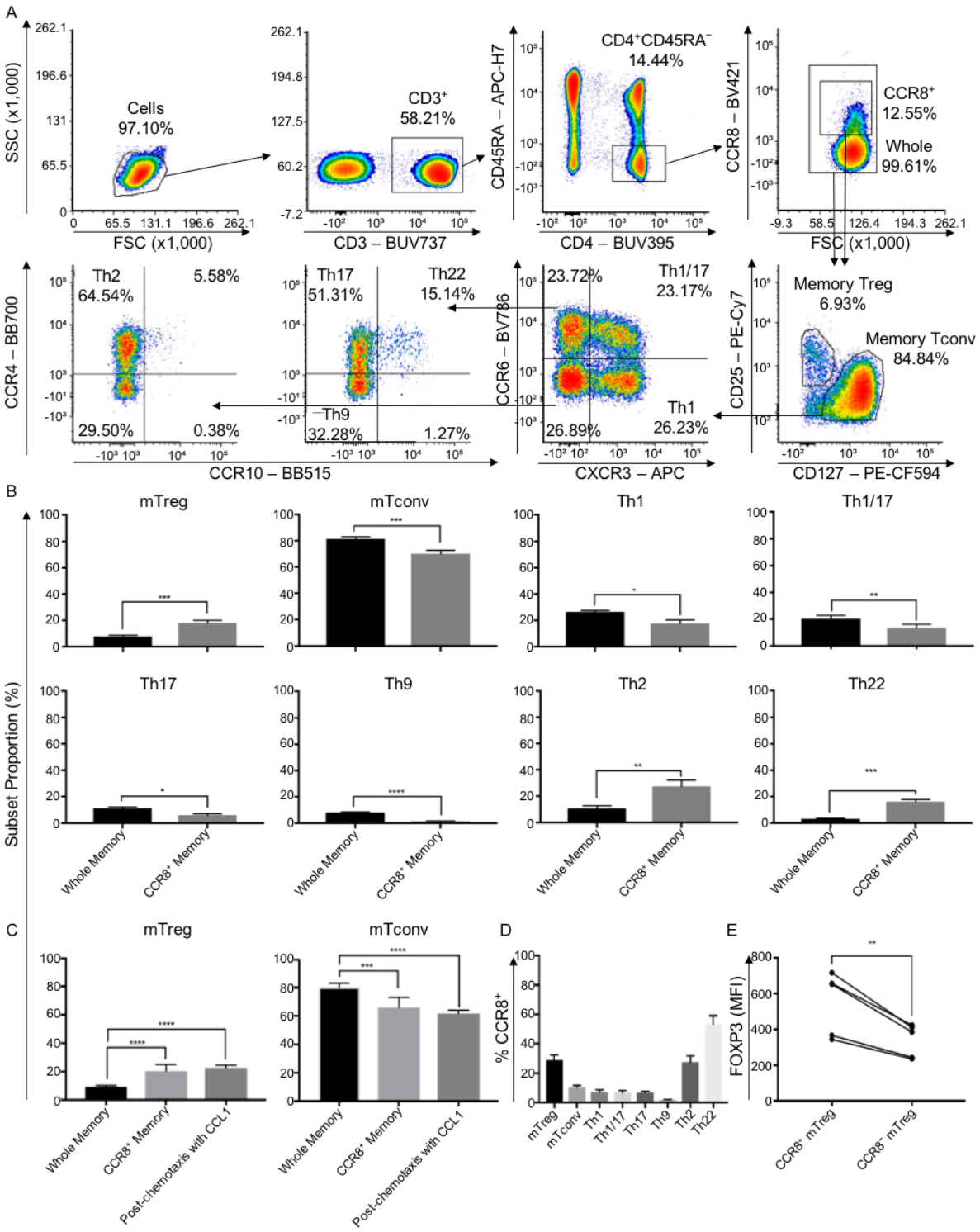


**Fig. 8.** Immunophenotyping of human peripheral blood CD4$^+$ memory T-cells. (A) Gating strategy for proportions of various CD4$^+$ T-cell subsets within whole memory (CD3$^+$ CD4$^+$ CD45RA$^-$) inclusive of both CCR8$^+$ and CCR8$^-$ and CCR8$^+$ memory T-cells from human whole blood PBMCs. CCR8$^+$ was gated using naïve CD4$^+$ T-cells (CD45RA$^+$) as a negative control. Memory Tregs (mTregs) and memory conventional T-cells (mTconvs) were defined as CD25$^+$ CD127$^-$ and CD25$^-$ CD127$^+$, respectively. mTconvs were divided into T-helper subsets using chemokine receptors: CXCR3$^+$ CCR6$^-$ Th1, CXCR3$^+$ CCR6$^+$ Th1/17, CXCR3$^-$, CXCR3$^-$ CCR6$^+$ CCR4$^+$ CCR10$^-$ Th17, CXCR3$^-$ CCR6$^+$ CCR4$^-$ CCR10$^-$ Th9, CCR6$^-$ CCR4$^+$ CCR10$^-$ Th2 and CXCR3$^-$ CCR6$^+$ CCR4$^+$ CCR10$^+$ Th22. (B) Proportions of T-cell subsets in whole memory and CCR8$^+$ memory populations. (C) Proportions of mTregs and mTconvs in PBMCs migrated in response to CCL1. (D) %CCR8$^+$ of T-cell subsets. (E) FOXP3 MFI of CCR8$^+$ and CCR8$^-$ mTregs. Data represented as mean ± SEM, n=6 for b-d and n=5 for e, statistical significance identified by paired two-tailed T-test *P<0.05, **0.01, ***0.001, ****0.0001.

## 4. Discussion

This is the first study to investigate encapsulation of human Tregs. Tregs are a crucial part of the human immune system, with their key role in the maintenance of immune tolerance and homeostasis. Through encapsulation, these intrinsic properties could be co-opted in a localized manner. In this study, we used 2%|7.5% w/v alginate-GelMA hydrogel to successfully encapsulate human nTregs and iTregs. The primary aim of this study was to demonstrate that Treg encapsulation caused no detrimental effects and thus have the capacity to provide local immune-protection to co-encapsulated cells. This hydrogel was recently formulated as a bioink for 3D-bioprinting of islets with supporting cells for its optimal macroscopic and rheological properties, its shear-thinning behavior, and its capacity to support cell survival. Tregs were "pseudo-printed" using encapsulation parameters that mimicked recently published islet 3D-bioprinting[25]. Our findings presented in this paper are applicable to the 3D-bioprinting setting, as demonstrated by highly viable 3D-bioprinted nTregs and iTregs (Fig. S6).

Encapsulated Tregs were shown to be viable, phenotypically stable and functional. Addition of IL-2 directly into the hydrogel protected Tregs from the encapsulation process, sustained viability during incubation, increased expression of CD25 and enhanced suppressive activity. The hydrogel was designed with high porosity to facilitate adequate nutrient and oxygen diffusion into the discs. Therefore, bioactive factors have the potential to diffuse out of the structure. As a result of this, Tregs encapsulated in IL-2-supplemented hydrogel displayed decreased viability at day 3 and reduced expression of FOXP3 and TGF-β compared with non-encapsulated Tregs cultured with IL-2, which was reversible upon addition of IL-2 directly to the media, instead of the hydrogel (Fig. 3-6). Given that the hydrogel discs (approx. 50 μL in volume) are cultured in 1 mL of IL-2-free media, the final concentration of IL-2, once equilibrium had been reached, would be 25 U/mL, which is much lower than the desired concentration of 500 U/mL. Moreover, as interaction of IL-2 with its receptor leads

to internalization of the complex[34], 25 U/mL of IL-2 may be rapidly sequestered by Tregs, as IL-2 induces high expression of CD25, the α chain of the high affinity IL-2 receptor[35]. IL-2 signaling also supports strong expression of FOXP3, reinforcing the Treg phenotype and lineage commitment[36,37]. This is important because Tregs are not able to produce IL-2 for autocrine signaling[1,38]. Thus, incorporation of an IL-2-eluting sustained-release system will be required to maintain IL-2 concentrations within the hydrogel. Additionally, given that IL-2 has extremely short half-life in serum and low-dose IL-2 therapy has demonstrated preferential expansion of Tregs, sustained-release of low-dose IL-2 may be more beneficial than sustained-release of high-dose IL-2[39,40].

The primary goal of Treg encapsulation is to serve as a localized cellular immunosuppression for co-encapsulated cell types such as islets. To achieve this, Tregs need to be able to remain in the vicinity of the co-encapsulated cells. To this end, encapsulation was shown to halt migration of Tregs out of the hydrogel structure in the presence of a potent chemotactic signal (Fig. 7B). Acute rejection episodes could be prevented by these Tregs, yet, they may not provide a long-term solution as *ex vivo* expanded Tregs are short-lived.[41,42] Utilization of a chemokine to recruit recipient Tregs could aid in the establishment of long-lasting recipient-driven tolerance. This is a common strategy employed by tumor cells. It has been shown that CCL1 is expressed in certain tumor cells, locally recruiting Tregs to generate an immunosuppressive milieu that abrogates the anti-tumor response mediated by effector $CD4^+$ and $CD8^+$ T-cells[43–45]. Indeed, CCL1-supplmented hydrogel demonstrated recruitment of Tregs. Treg-recruitment capability of CCL1-supplemented hydrogel was significantly lower than CCL1 in the chemotaxis buffer, again, due to the porous nature of the hydrogel. The final concentration of CCL-1 in the chemotaxis buffer (600 μL) would have been approximately 800 ng/mL once equilibrated, instead of 10 mg/mL. The migration indices shown in CCL-1-suplimented hydrogel discs were comparable with the 1 mg/mL of CCL1 in the buffer (Fig. 7A and 7C). In the

case of CCL1, the high porosity of the hydrogel facilitates the formation of chemokine gradients, and maintenance of this gradient through utilization of a CCL1-eluting sustained release system will maximize the recruitment capability. Furthermore, Tregs preferentially expressed CCR8 and were enriched in $CCR8^+$ and CCL1-recruited peripheral blood T-cells. Together, this suggests that the use of CCL1-supplemented hydrogel could provide a microenvironment enriched with recipient Tregs *in vivo*. Although, it is possible that the same chemokines may actively recruit other T helper cells to the site. Th2 and Th22 cells showed preferential expression of CCR8 and enrichment in $CCR8^+$ peripheral blood T-cells (Figure 8b-d). Despite previous studies regarding expression of CCR8 on Th2 cells[46], the use of CCL1 was justified as Th2 cells could assist with tolerization given their ability to inhibit rejection-causing Th1 responses[47]. Expression of CCR8 on Th22 cells had not been described to date. Moreover, the role of Th22 cells in transplantation is currently unknown[48]. It has been shown that $CCR8^+$ conventional skin T-cells are less effector-like, with decreased functionality compared with their $CCR8^-$ counterparts[49]. Thus, recruitment of $CCR8^+$ Th22 cells may not equate to a pro-inflammatory response, especially in an environment enriched with $CCR8^+$ Tregs which have greater FOXP3 expression than CCR8- Tregs (Fig. 8E), hence a greater suppressive capacity[33,50]. In addition, similar approaches have been demonstrated using CCL22[51] and CXCL12[52] with promising results, illustrating the potential of chemokine incorporation.

Two types of human Tregs, nTregs and iTregs, were compared in this study to determine which would be more suitable for encapsulation. While both types are defined as $CD4^+$ $CD25^+$ $FOXP^+$ T-cells, there are fundamental differences between them. Natural Tregs are generated during thymic development and pTregs are generated in the periphery *in vivo* or can be induced *in vitro* from conventional T-cells (iTregs). Induced Tregs were shown to be more sensitive to IL-2 than nTregs in terms of viability, CD25 expression and suppressive activity, which could be disadvantageous in an

IL-2-limited environment. iTregs displayed greater suppressive activity than nTregs, indicating that iTregs could suppress the recipient immune system more effectively[53]. Moreover, migration indices of nTregs in response to CCL1 was higher than iTregs. The migration index of nTregs in response to CXCL12, a ligand for pan-leukocyte chemokine receptor CXCR4[54], was also higher and there were no significant differences in CCR8 expression between nTregs and iTregs. This indicates that the differences in CCL1 migration index is due to iTregs being more motile in nature, rather than nTregs being more responsive to CCL1 (Fig. S7). CCL1 also had different effects on encapsulated nTregs and iTregs, enhancing nTreg suppressive activity while dampening iTreg suppressive activity. This may be due to CCR8 signaling causing iTregs to be less suppressive due to their origin of being differentiated from the conventional T-cell lineage[49]. Ultimately, while iTregs were found to be more suppressive than nTregs and possess a more relevant repertoire of antigen specificities for allogeneic transplantation[55], nTregs may be more suitable than iTregs due to their phenotypic stability. The methylation status of the FOXP3 promotor region and Treg-specific demethylation region (TSDR) determine the stability of the Treg phenotype. These regions in iTregs are incompletely demethylated, allowing iTregs to convert to a proinflammatory Th17 phenotype in a pro-inflammatory settings[56]. Thus, the utilization of iTregs for co-encapsulation with other cells may act as an immunological Trojan horse.

## 5. Conclusion

In this study, we demonstrated the potential of encapsulating human Tregs in alginate-GelMA hydrogel as a means to provide localized cellular immunosuppression to transplanted islets. IL-2 and CCL1, as Treg-specific bioactive factors, were investigated as supplements to the hydrogel. Encapsulated Tregs were viable, and phenotypically and functionally stable. Furthermore, encapsulation prevented migration of Tregs out of hydrogel structure. Addition of IL-2 and CCL1 to the hydrogel showed several benefits including the improvement of Treg viability, suppressive

phenotype and function, and the capacity to recruit additional Tregs. Due to the highly porous nature of the hydrogel, adding these factors directly into the hydrogel produced sup-optimal concentrations once the factors diffused into the surrounding media. Therefore, incorporation of a sustained-release system via recently developed polylactic-co-glycolic acid (PLGA)-based microspheres will be implemented for further improvement[57]. To further enhance Treg numbers, low-dose rapamycin could be added as an additional bioactive factor[58], utilizing recently developed rapamycin loaded porous silicon nanoparticles[59,60]. Moreover, peripheral blood $CCR8^{+}$ T-cells were highly enriched with Tregs, and CCL1 was shown to specifically induce chemotaxis of these cells, providing an insight into the cellular microenvironment in humans upon utilization of CCL-1-supplemented hydrogel. Lastly, while this study focused on the encapsulation of Tregs for future applications in islet transplantation through 3D-bioprinting, the findings could be applied to other types of cell therapies such as adrenocortical, thyroid and parathyroid cell transplantation[61–63].

**Acknowledgements**

The authors wish to acknowledge funding from the Australian Research Council (ARC) Centre of Excellence Scheme (CE140100012), The Hospital Research Foundation, Adelaide Australia, support of the Australian National Fabrication Facility (ANFF) – Materials Node and Australian Red Cross Blood Services for providing human buffy coat for Treg isolation. J.K acknowledges Dr Randall Grose of South Australian Health and Medical Research Institute for operating fluorescence activated cell sorter, Ms Ruth Williams from Adelaide Microscopy for help with TEM and Professor Shaun McColl and Dr Iain Comerford of Chemokine Biology Group for their help with transwell migration assay. G.G.W acknowledges the support of the ARC through an ARC Laureate Fellowship (FL110100196).

J.K designed and performed all experiments, analyzed data and wrote the manuscript. C.M.H. contributed to designing of experiments. C.M.H., G.B.P., S.O.S., N.G., Z.Y., X.L. and F.D.K helped with experiments; C.M.H. contributed to chemokine receptor phenotyping; G.B.P. contributed to CD154 suppression assay; S.O.S and F.D.K contributed to phenotyping of encapsulated Tregs; N.G., Z.Y. and X.L. contributed to hydrogel precursor synthesis. C.M.H., G.B.P., S.O.S., Z.Y., F.D.K., R.P.C., S.C.B, G.G.W. and P.T.H. edited the manuscript. S.O.S edited the figures. C.J.D., G.G.W. and P.T.H conceptualized the project and C.J.D., R.P.C., S.C.B., G.G.W., and P.T.H. supervised the study. G.G.W. and P.T.H. attained funding.

## Data availability

The raw/processed data required to reproduce these findings cannot be shared at this time due to technical or time limitations. The data will be made available upon request.

## References


[1] S. Sakaguchi, T. Yamaguchi, T. Nomura, M. Ono, Regulatory T Cells and Immune Tolerance, Cell. 133 (2008) 775–787. https://doi.org/10.1016/j.cell.2008.05.009.

[2] R. Gershon, K. Kondo, Infectious Immunological Tolerance, Immunology. 21 (1971) 903–914.

[3] S. Sakaguchi, N. Sakaguchi, M. Asano, M. Itoh, M. Toda, Immunologic Self-Tolerance is Maintained by Activated T cells Expressing IL-2 Receptor Alpha-Chains (CD25). Breakdown of a Single Mechanism of Self-Tolerance Causes Various Autoimmune Diseases, J. Immunol. 155 (1995) 1151–1164. https://doi.org/10.4049/jimmunol.164.8.4321.

[4] C. Baecher-Allan, J.A. Brown, G.J. Freeman, D.A. Hafler, CD4+CD25high Regulatory Cells in Human Peripheral Blood, J. Immunol. 167 (2001) 1245–1253. https://doi.org/10.1073/pnas.1103810108.

[5] S. Hori, T. Nomura, S. Sakaguchi, Control of regulatory T cell development by the transcription factor Foxp3., Science (80-. ). 299 (2003) 1057–1061. https://doi.org/10.1126/science.1079490.

[6] J.D. Fontenot, M.A. Gavin, A.Y. Rudensky, Foxp3 programs the development and function of CD4+CD25+ regulatory T cells, Nat.Immunol. 4 (2003) 330–336. https://doi.org/10.1038/ni904.

[7] W. Liu, A.L. Putnam, Z. Xu-Yu, G.L. Szot, M.R. Lee, S. Zhu, P.A. Gottlieb, P. Kapranov, T.R. Gingeras, B. Fazekas de St Groth, C. Clayberger, D.M. Soper, S.F. Ziegler, J.A. Bluestone, CD127 expression inversely correlates with FoxP3 and suppressive function of

human CD4+ T reg cells., J. Exp. Med. 203 (2006) 1701–11. https://doi.org/10.1084/jem.20060772.

[8] N. Seddiki, B. Santner-Nanan, J. Martinson, J. Zaunders, S. Sasson, A. Landay, M. Solomon, W. Selby, S.I. Alexander, R. Nanan, A. Kelleher, B. Fazekas de St Groth, Expression of interleukin (IL)-2 and IL-7 receptors discriminates between human regulatory and activated T cells., J. Exp. Med. 203 (2006) 1693–700. https://doi.org/10.1084/jem.20060468.

[9] B.D. Singer, L.S. King, F.R.D. Alessio, Regulatory T cells as immunotherapy, Front. Immunol. 5 (2014) 46. https://doi.org/10.3389/fimmu.2014.00046.

[10] M. Kanamori, H. Nakatsukasa, M. Okada, Q. Lu, A. Yoshimura, Induced Regulatory T Cells : Their Development , Stability , and Applications, Trends Immunol. 37 (2016) 803–811. https://doi.org/10.1016/j.it.2016.08.012.

[11] D.A.A. Vignali, L.W. Collison, C.J. Workman, How regulatory T cells work, Nat. Rev. Immunol. 8 (2008) 523–532. https://doi.org/10.1038/nri2343.

[12] Q. Tang, J.A. Bluestone, Regulatory T-Cell Therapy in Transplantation : Moving to the Clinic, Cold Spring Harb. Perspect. Med. 3 (2013) a015552. https://doi.org/10.1101/cshperspect.a015552.

[13] M. Romano, G. Fanelli, C.J. Albany, G. Giganti, G. Lombardi, Past, present, and future of regulatory T cell therapy in transplantation and autoimmunity, Front. Immunol. 10 (2019) 43. https://doi.org/10.3389/fimmu.2019.00043.

[14] C.B. Leitão, P. Cure, T. Tharvanji, D.A. Baidal, R. Alejandro, Current Challenges in Islet Transplantation, Curr. Diab. Rep. 8 (2008) 324–331. https://doi.org/10.1007/s11892-008-0057-3.

[15] N. Niemann, B. Sawitzki, Treg Therapy in Transplantation : How and When Will We Do It ?, Curr. Transplant. Reports. 2 (2015) 233–241. https://doi.org/10.1007/s40472-015-0066-5.

[16] A. Fuchs, M. Gliwinski, N. Grageda, R. Spiering, A.K. Abbas, S. Appel, R. Bacchetta, M. Battaglia, D. Berglund, B. Blazar, J.A. Bluestone, M. Bornhäuser, A. ten Brinke, T.M. Brusko, N. Cools, M.C. Cuturi, E. Geissler, N. Giannoukakis, K. Golab, D.A. Hafler, S.M. van Ham, J. Hester, K. Hippen, M. Di Ianni, N. Ilic, J. Isaacs, F. Issa, D. Iwaszkiewicz-Grzes, E. Jaeckel, I. Joosten, D. Klatzmann, H. Koenen, C. van Kooten, O. Korsgren, K. Kretschmer, M. Levings, N.M. Marek-Trzonkowska, M. Martinez-Llordella, D. Miljkovic, K.H.G. Mills, J.P. Miranda, C.A. Piccirillo, A.L. Putnam, T. Ritter, M.G. Roncarolo, S. Sakaguchi, S. Sánchez-Ramón, B. Sawitzki, L. Sofronic-Milosavljevic, M. Sykes, Q. Tang, M. Vives-Pi, H. Waldmann, P. Witkowski, K.J. Wood, S. Gregori, C.M.U. Hilkens, G. Lombardi, P. Lord, E.M. Martinez-Caceres, P. Trzonkowski, Minimum information about T regulatory cells: A step toward reproducibility and standardization, Front. Immunol. 8 (2018) 1844. https://doi.org/10.3389/fimmu.2017.01844.

[17] S. Todo, K. Yamashita, R. Goto, M. Zaitsu, A. Nagatsu, T. Oura, M. Watanabe, T. Aoyagi, T. Suzuki, T. Shimamura, T. Kamiyama, N. Sato, J. Sugita, K. Hatanaka, H. Bashuda, S. Habu, A.J. Demetris, K. Okumura, A Pilot Study of Operational Tolerance With a Regulatory T-Cell-Based Cell Therapy in Living Donor Liver Transplantation, Hepatology. 64 (2016) 632–643. https://doi.org/10.1002/hep.28459.

[18] S. Chandran, Q. Tang, M. Sarwal, Polyclonal Regulatory T Cell Therapy for Control of Inflammation in Kidney Transplants, Am. J. Transplant. 17 (2017) 2945–2954. https://doi.org/10.1111/ajt.14415.

[19] N. Safinia, G. Lombardi, Regulatory T cells : serious contenders in the promise for immunological tolerance in transplantation, Front. Immunol. 6 (2015) 438. https://doi.org/10.3389/fimmu.2015.00438.

[20] M. Romano, G. Fanelli, C.J. Albany, G. Giganti, G. Lombardi, Past, present, and future of regulatory T cell therapy in transplantation and autoimmunity, Front. Immunol. 10 (2019). https://doi.org/10.3389/fimmu.2019.00043.

[21] P.J.O. Connell, D.J. Holmes-Walker, D. Goodman, W.J. Hawthorne, T. Loudovaris, J.E. Gunton, H.E. Thomas, S.T. Grey, C.J. Drogemuller, G.M. Ward, D.J. Torpy, P.T. Coates, T.W. Kay, Multicenter Australian Trial of Islet Transplantation : Improving Accessibility and Outcomes, Am. J. Transplant. 13 (2013) 1850–1858. https://doi.org/10.1002/ajt.12250.

[22] D. Penko, D. Mohanasundaram, S. Sen, C. Drogemuller, C. Mee, C.S. Bonder, P.T.H. Coates, C.F. Jessup, Incorporation of endothelial progenitor cells into mosaic pseudoislets, Islets. 3 (2011) 73–79. https://doi.org/10.4161/isl.3.3.15392.

[23] D. Penko, D. Rojas-Canales, D. Mohanasundaram, H.S. Peiris, W.Y. Sun, C.J. Drogemuller, D.J. Keating, P.T.H. Coates, C.S. Bonder, C.F. Jessup, Endothelial progenitor cells enhance islet engraftment, influence beta cell function and modulate islet connexin 36 expression, Cell Transplant. 24 (2015) 37–48. https://doi.org/10.3727/096368913X673423.

[24] Z. Yue, X. Liu, P.T. Coates, G.G. Wallace, Advances in printing biomaterials and living cells, Curr. Opin. Organ Transplant. 21 (2016) 467–475. https://doi.org/10.1097/MOT.0000000000000346.

[25] X. Liu, S.-S.D. Carter, M.J. Renes, J. Kim, D.M. Rojas-Canales, D. Penko, C. Angus, S. Beirne, C.J. Drogemuller, Z. Yue, P.T. Coates, G.G. Wallace, Development of a Coaxial 3D Printing Platform for Biofabrication of Implantable Islet-Containing Constructs., Adv. Healthc. Mater. 8 (2019) 1801181. https://doi.org/10.1002/adhm.201801181.

[26] J. Kim, K. Kang, C.J. Drogemuller, G.G. Wallace, P.T. Coates, Bioprinting an Artificial Pancreas for Type 1 Diabetes, Curr. Diab. Rep. 19 (2019) 53. https://doi.org/10.1007/s11892-019-1166-x.

[27] F. Lim, A. Sun, Microencapsulated islets as bioartificial endocrine pancreas, Science (80-. ). 210 (1980) 908–910.

[28] T.Y. Wuest, J. Willette-Brown, S.K. Durum, A.A. Hurwitz, The influence of IL-2 family cytokines on activation and function of naturally occurring regulatory T cells, J. Leukoc. Biol. 84 (2008) 973–980. https://doi.org/10.1189/jlb.1107778.

[29] D. Soler, T.R. Chapman, L.R. Poisson, L. Wang, J. Cote-Sierra, M. Ryan, A. McDonald, S. Badola, E. Fedyk, A.J. Coyle, M.R. Hodge, R. Kolbeck, CCR8 Expression Identifies CD4 Memory T Cells Enriched for FOXP3+ Regulatory and Th2 Effector Lymphocytes, J. Immunol. 177 (2006) 6940–6951. https://doi.org/10.4049/jimmunol.177.10.6940.

[30] D. Loessner, C. Meinert, E. Kaemmerer, L.C. Martine, K. Yue, P.A. Levett, T.J. Klein, F.P.W. Melchels, A. Khademhosseini, D.W. Hutmacher, Functionalization , preparation and use of cell-laden gelatin methacryloyl – based hydrogels as modular tissue culture platforms, Nat. Protoc. 11 (2016) 727–746. https://doi.org/10.1038/nprot.2016.037.

[31] S.F. Ziegler, F. Ramsdell, M.R. Alderson, The activation antigen CD69, Stem Cells. 12 (1994) 456–465. https://doi.org/10.1002/stem.5530120502.

[32] D. Hill, N. Eastaff-Leung, S. Bresatz-Atkins, N. Warner, J. Ruitenberg, D. Krumbiegel, S. Pederson, N. McInnes, C.Y. Brown, T. Sadlon, S.C. Barry, Inhibition of activation induced CD154 on CD4+ CD25- cells: a valid surrogate for human Treg suppresor function, Immunol. Cell Biol. 90 (2012) 812–821. https://doi.org/10.1038/icb.2012.18.

[33] Y. Barsheshet, G. Wildbaum, E. Levy, A. Vitenshtein, C. Akinseye, J. Griggs, S.A. Lira, N. Karin, CCR8 $^{+}$ FOXp3 $^{+}$ T $_{reg}$ cells as master drivers of immune regulation, Proc. Natl. Acad. Sci. 114 (2017) 6086–6091. https://doi.org/10.1073/pnas.1621280114.

[34] A. Kumar, J.L. Moreau, M. Gibert, J. Theze, Internalization of interleukin 2 ( IL-2 ) by high affinity IL-2 receptors is required for the growth of IL-2-dependent T cell lines, J. Immunol. 139 (1987) 3680–3684.

[35] S. Létourneau, C. Krieg, G. Pantaleo, O. Boyman, IL-2- and CD25-dependent immunoregulatory mechanisms in the homeostasis of T-cell subsets, J. Allergy Clin. Immunol. 123 (2009) 758–762. https://doi.org/10.1016/j.jaci.2009.02.011.

[36] T.J. Sadlon, B.G. Wilkinson, S. Pederson, C.Y. Brown, S. Bresatz, T. Gargett, L. Melville, K. Peng, R.J.D. Andrea, G. Gary, G.J. Goodall, H. Zola, M. Frances, S.C. Barry, S. Bresatz, T. Gargett, E.L. Melville, K. Peng, Genome-Wide Identification of Human FOXP3 Target Genes in Natural Regulatory T Cells, J. Immunol. 185 (2010) 1071–1081. https://doi.org/10.4049/jimmunol.1000082.

[37] M. Beyer, Y. Thabet, R. Müller, T. Sadlon, S. Classen, K. Lahl, S. Basu, X. Zhou, S.L. Bailey-bucktrout, W. Krebs, E.A. Schönfeld, J. Böttcher, T. Golovina, C.T. Mayer, A. Hofmann, D. Sommer, S. Debey-pascher, E. Endl, A. Limmer, K.L. Hippen, B.R. Blazar, R. Balderas, T. Quast, A. Waha, G. Mayer, M. Famulok, P.A. Knolle, C. Wickenhauser, W. Kolanus, B. Schermer, J.A. Bluestone, S.C. Barry, T. Sparwasser, J.L. Riley, J.L. Schultze, Repression of the genome organizer SATB1 in regulatory T cells is required for suppressive function and inhibition of effector differentiation, Nat. Immunol. 12 (2011) 898–907. https://doi.org/10.1038/ni.2084.

[38] T. Chinen, A.K. Kannan, A.G. Levine, X. Fan, U. Klein, Y. Zheng, G. Gasteiger, Y. Feng, J.D. Fontenot, A.Y. Rudensky, An essential role for IL-2 receptor in regulatory T cell function Takatoshi, Nat. Immunol. 17 (2016) 1322–1333. https://doi.org/10.1038/ni.3540.

[39] J. Donohue, S. Rosenberg, The fate of interleukin-2 after in vivo administration, J. Immunol. 130 (1983) 2203–2208.

[40] J. Koreth, K. Matsuoka, H.T. Kim, S.M. McDonough, B. Bindra, E.P. Alyea, P. Armand, C. Cutler, V.T. Ho, N. Treister, D. Bienfang, S. Prasad, D. Tzachanis, R. Joyce, D. Avigan, J.H. Antin, J. Ritz, R.J. Soiffer, Interleukin-2 and Regulatory T Cells in Graft-versus-Host Disease, N. Engl. J. Med. 365 (2011) 2055–2066. https://doi.org/DOI: 10.1056/NEJMoa1108188.

[41] S. Gupta, T.B. Thornley, W. Gao, R. Larocca, L.A. Turka, V.K. Kuchroo, T.B. Strom, Allograft rejection is restrained by short-lived TIM-3+PD-1+Foxp3+ Tregs, J. Clin. Invest. 122 (2012) 2395–2404. https://doi.org/10.1172/JCI45138.

[42] S. Gupta, P. Samuels, S. Long, M. Tatum, J. Buckner, Ex Vivo Expanded Human Regulatory T Cells Are Potent Suppressors but May Be Short-Lived, Am. J. Transplant. 13 (2013).

[43] D.B. Hoelzinger, S.E. Smith, N. Mirza, A.L. Dominguez, S.Z. Manrique, J. Lustgarten, Blockade of CCL1 Inhibits T Regulatory Cell Suppressive Function Enhancing Tumor Immunity without Affecting T Effector Responses, J. Immunol. 184 (2010) 6833–6842. https://doi.org/10.4049/jimmunol.0904084.

[44] B. Kuehnemuth, I. Piseddu, G.M. Wiedemann, M. Lauseker, C. Kuhn, S. Hofmann, E. Schmoeckel, S. Endres, D. Mayr, U. Jeschke, D. Anz, CCL1 is a major regulatory T cell attracting factor in human breast cancer, BMC Cancer. 18 (2018) 1278. https://doi.org/10.1186/s12885-018-5117-8.

[45] E. Eruslanov, T. Stoffs, W.J. Kim, I. Daurkin, S.M. Gilbert, L.M. Su, J. Vieweg, Y. Daaka, S. Kusmartsev, Expansion of CCR8+ inflammatory myeloid cells in cancer patients with urothelial and renal carcinomas, Clin. Cancer Res. 19 (2013) 1670–1680. https://doi.org/10.1158/1078-0432.CCR-12-2091.

[46] A. Zingoni, H. Soto, J.A. Hedrick, A. Stoppacciaro, C.T. Storlazzi, F. Sinigaglia, D. D'Ambrosio, A. O'Garra, D. Robinson, M. Rocchi, A. Santoni, A. Zlotnik, M. Napolitano, The chemokine receptor CCR8 is preferentially expressed in Th2 but not Th1 cells., J. Immunol. 161 (1998) 547–51. https://doi.org/10.4049/jimmunol.179.3.1740.

[47] S.S. Tay, K.M. Plain, G.A. Bishop, Role of IL-4 and Th2 responses in allograft rejection and tolerance, Curr. Opin. Organ Transplant. 14 (2009) 16–22. https://doi.org/10.1097/MOT.0b013e32831ebdf5.

[48] Z. Liu, H. Fan, S. Jiang, CD4 + T-cell subsets in transplantation, Immunol. Rev. 252 (2013) 183–191. https://doi.org/10.1111/imr.12038.

[49] M.L. McCully, K. Ladell, R. Andrews, R.E. Jones, K.L. Miners, L. Roger, D.M. Baird, M.J. Cameron, Z.M. Jessop, I.S. Whitaker, E.L. Davies, D.A. Price, B. Moser, CCR8 Expression Defines Tissue-Resident Memory T Cells in Human Skin, J. Immunol. (2018) 1639–1649. https://doi.org/10.4049/jimmunol.1701377.

[50] S.K. Chauhan, D.R. Saban, H.K. Lee, R. Dana, Levels of Foxp3 in Regulatory T Cells Reflect Their Functional Status in Transplantation, J. Immunol. 182 (2009) 148–153. https://doi.org/10.4049/jimmunol.182.1.148.

[51] S. Jhunjhunwala, G. Raimondi, A.J. Glowacki, S.J. Hall, D. Maskarinec, S.H. Thorne, A.W. Thomson, Bioinspired Controlled Release of CCL22 Recruits Regulatory T Cells In Vivo, Adv. Mater. 24 (2012) 4735–4738. https://doi.org/10.1016/j.neuroimage.2013.08.045.The.

[52] D.A. Alagpulinsa, J.J.L. Cao, R.K. Driscoll, R.F. Sîrbulescu, M.F.E. Penson, M. Sremac, E.N. Engquist, T.A. Brauns, J.F. Markmann, D.A. Melton, M.C. Poznansky, Alginate-microencapsulation of human stem cell–derived β cells with CXCL12 prolongs their survival and function in immunocompetent mice without systemic immunosuppression, Am. J. Transplant. 19 (2019) 1930–1940. https://doi.org/10.1111/ajt.15308.

[53] H. Huang, Y. Ma, W. Dawicki, X. Zhang, J.R. Gordon, Comparison of Induced versus Natural Regulatory T Cells of the Same TCR Specificity for Induction of Tolerance to an Environmental Antigen, J. Immunol. 191 (2013) 1136–1143. https://doi.org/10.4049/jimmunol.1201899.

[54] J.W. Griffith, C.L. Sokol, A.D. Luster, Chemokines and Chemokine Receptors: Positioning Cells for Host Defense and Immunity, Annu. Rev. Immunol. 32 (2014) 659–702. https://doi.org/10.1146/annurev-immunol-032713-120145.

[55] E.G. Schmitt, C.B. Williams, Generation and function of induced regulatory T cells, Front. Immunol. 4 (2013) 152. https://doi.org/10.3389/fimmu.2013.00152.

[56] J.R. Ghali, M.A. Alikhan, S.R. Holdsworth, A.R. Kitching, Induced regulatory T cells are phenotypically unstable and do not protect mice from rapidly progressive glomerulonephritis, Immunology. 150 (2017) 100–114. https://doi.org/10.1111/imm.12671.

[57] F. Mehrpouya, Z. Yue, T. Romeo, R. Gorkin, R.M.I. Kapsa, S.E. Moulton, G.G. Wallace, A simple technique for development of fibres with programmable microsphere concentration gradients for local protein delivery, J. Mater. Chem. B. 7 (2019) 556–565. https://doi.org/10.1039/C8TB01504J.

[58] M. Battaglia, A. Stabilini, B. Migliavacca, J. Horejs-hoeck, T. Kaupper, M.-G. Roncarolo, Rapamycin Promotes Expansion of Functional CD4 + CD25 + FOXP3 + Regulatory T Cells of Both Healthy Subjects and Type 1 Diabetic Patients, J. Immunol. 177 (2006) 8338–8347. https://doi.org/10.4049/jimmunol.177.12.8338.

[59] S.O. Stead, S.J.P. McInnes, S. Kireta, P.D. Rose, S. Jesudason, D. Rojas-Canales, D. Warther, F. Cunin, J.O. Durand, C.J. Drogemuller, R.P. Carroll, P.T. Coates, N.H. Voelcker, Manipulating human dendritic cell phenotype and function with targeted porous silicon nanoparticles, Biomaterials. 155 (2018) 92–102. https://doi.org/10.1016/j.biomaterials.2017.11.017.

[60] S.O. Stead, S. Kireta, S.J.P. McInnes, F.D. Kette, K.N. Sivanathan, J. Kim, E.J. Cueto-Diaz, F. Cunin, J.O. Durand, C.J. Drogemuller, R.P. Carroll, N.H. Voelcker, P.T. Coates, Murine and Non-Human Primate Dendritic Cell Targeting Nanoparticles for in Vivo Generation of Regulatory T-Cells, ACS Nano. 12 (2018) 6637–6647. https://doi.org/10.1021/acsnano.8b01625.

[61] M. Balyura, E. Gelfgat, M. Ehrhart-Bornstein, B. Ludwig, Z. Gendler, U. Barkai, B. Zimerman, A. Rotem, N.L. Block, A. V. Schally, S.R. Bornstein, Transplantation of bovine

adrenocortical cells encapsulated in alginate, Proc. Natl. Acad. Sci. 112 (2015) 2527–2532. https://doi.org/10.1073/pnas.1500242112.

[62] Y. Yang, E.C. Opara, Y. Liu, A. Atala, W. Zhao, Microencapsulation of porcine thyroid cell organoids within a polymer microcapsule construct, Exp. Biol. Med. 242 (2017) 286–296. https://doi.org/10.1177/1535370216673746.

[63] L. Picariello, S. Benvenuti, R. Recenti, L. Formigli, A. Falchetti, A. Morelli, L. Masi, F. Tonelli, P. Cicchi, M.L. Brandi, Microencapsulation of human parathyroid cells: An “in Vitro” study, J. Surg. Res. 96 (2001) 81–89. https://doi.org/10.1006/jsre.2000.6054.

# Statement of Authorship

| | |
|---|---|
| Title of Paper | Generation of Stable Human Induced Regulatory T-cells |
| Publication Status | Under revision |
| Publication Details | Clinical and Translational Immunology<br>Impact factor 7.271 (2018) |

## Principal Author

| | | | |
|---|---|---|---|
| Name of Principal Author (Candidate) | Juewan Kim | | |
| Contribution to the Paper | Experiment design/ Conceptualisation of the project<br>Laboratory work<br>Data analysis<br>Manuscript writing/editing | | |
| Overall percentage (%) | 75 | | |
| Certification: | This paper reports on original research I conducted during the period of my Higher Degree by Research candidature and is not subject to any obligations or contractual agreements with a third party that would constrain its inclusion in this thesis. I am the primary author of this paper. | | |
| Signature | | Date | September 2019 |

## Co-Author Contributions

By signing the Statement of Authorship, each author certifies that:

i. the candidate's stated contribution to the publication is accurate (as detailed above);
ii. permission is granted for the candidate in include the publication in the thesis; and
iii. the sum of all co-author contributions is equal to 100% less the candidate's stated contribution.

| | | | |
|---|---|---|---|
| Name of Co-Author | Christopher M. Hope | | |
| Contribution to the Paper | Conceptualisation of the project<br>Assisted experimental design<br>Manuscript editing | | |
| Signature | | Date | September 2019 |

| | | | |
|---|---|---|---|
| Name of Co-Author | Jacqueline C. Scaffidi | | |
| Contribution to the Paper | Assisted with secondary expansion (Figure 7)<br>Assisted with Th17-polarising cytokine challenge – RT PCR (Figure 6)<br>Manuscript editing | | |
| Signature | | Date | September 2019 |

Please cut and paste additional co-author panels here as required.

| | | | |
|---|---|---|---|
| Name of Co-Author | Sebastian O. Stead | | |
| Contribution to the Paper | Assisted with time-course analysis (Figure 1)<br>Manuscript editing | | |
| Signature | | Date | September 2019 |

| | | | |
|---|---|---|---|
| Name of Co-Author | Griffith B. Perkins | | |
| Contribution to the Paper | Assisted with time-course analysis (Figure 1)<br>Manuscript editing | | |
| Signature | | Date | September 2019 |

| | | | |
|---|---|---|---|
| Name of Co-Author | Francis D. Kette | | |
| Contribution to the Paper | Assisted with cell culture<br>Manuscript editing | | |
| Signature | | Date | September 2019 |

| | | | |
|---|---|---|---|
| Name of Co-Author | Robert P. Carroll | | |
| Contribution to the Paper | Supervision of the study<br>Manuscript editing | | |
| Signature | | Date | September 2019 |

| | | | |
|---|---|---|---|
| Name of Co-Author | Simon C. Barry | | |
| Contribution to the Paper | Supervision of the study<br>Conceptualisation of the project<br>Manuscript editing | | |
| Signature | | Date | September 2019 |

| | | | |
|---|---|---|---|
| Name of Co-Author | P. Toby Coates | | |
| Contribution to the Paper | Supervision of the study<br>Conceptualisation of the project<br>Attained funding<br>Manuscript editing | | |
| Signature | | Date | September 2019 |

PUBLICATION 2

# Generation of Stable Human Induced Regulatory T-cells

**Generation of Stable Human Induced Regulatory T-cells**

Juewan Kim[1], Christopher M. Hope[2,6], Jacqueline C. Scaffidi[1], Sebastian O. Stead[3,4], Griffith B. Perkins[1], Francis D. Kette[3,4], Robert P. Carroll[4,5,7], Simon C. Barry[2,6,*], P. Toby Coates[4,5,*]

Affiliations:

1. The Department of Molecular & Cellular Biology, The School of Biological Sciences, The Faculty of Sciences, The University of Adelaide, Adelaide, South Australia
2. Department of Gastroenterology, Women's and Children's Hospital, Adelaide, South Australia
3. College of Medicine and Public Health, Discipline of Medicine, Flinders University, Bedford Park, South Australia
4. Discipline of Medicine, School of Medicine, The University of Adelaide, Adelaide, South Australia
5. Central Northern Adelaide Renal and Transplantation Service (CNARTS), The Royal Adelaide Hospital, Adelaide, South Australia
6. Molecular Immunology Group, Robinson Research Institute, School of Medicine, The University of Adelaide, Adelaide, South Australia
7. Division of Medical Sciences, University of South Australia, Adelaide, South Australia

*Co-responding authors. Email: toby.coates@sa.gov.au & simon.barry@adelaide.edu.au

Summary: Induced regulatory T-cells are an attractive alternative for adoptive transfer in an allogeneic transplant setting. Here, Kim et al. reports the generation of stable human induced regulatory T-cells with a differentiation method utilizing TGF-β, all-trans retinoic acid and low-dose rapamycin.

Regulatory T-cells are a vital sub-population of $CD4^+$ T-cells with major roles in immune tolerance and homeostasis. Treg-based immunotherapies have been extensively investigated, with a focus on adoptive transfer of *ex vivo*-expanded natural Tregs (nTregs). Induced Tregs (iTregs) provide an attractive alternative due to their diverse T-cell receptor repertoire and ease of generating ample cell numbers for clinical dosage. The challenge for therapeutic iTreg generation has been their instability. Here, we aim to optimize an iTreg-differentiation method for the generation of stable human iTregs. iTregs engineered with our optimized method are superior to iTregs generated with a commercial kit, with increased CD25 and FOXP3 expression, viability and rate of expansion. Furthermore, these iTregs show stability in the absence of IL-2, in the presence of Th17-polarizing cytokines, and upon re-stimulation without differentiation components. These iTregs are highly functional upon re-stimulation, displaying superior suppressive activities compared with nTregs. This work establishes a method to generate stable iTregs suitable for adoptive cell transfer.

## Introduction

Regulatory T-cells (Tregs) are a sup-population of $CD4^+$ T-cells with immune-suppressive and immune-modulatory properties. With such properties, Tregs form a vital part of immune homeostasis, providing tolerance to self and non-pathogenic foreign antigens, and down-regulating immune responses once pathogens are cleared in order to minimize tissue-damage (Sakaguchi et al., 2008). Currently, Tregs are defined by the surface phenotype $CD4^+$, $CD25^{hi}$ and $CD127^{lo}$, and expression of the master regulator of Treg-lineage, FOXP3 (Sakaguchi et al., 1995; Baecher-Allan et al., 2001; Hori et al., 2003; Fontenot et al., 2003; Liu et al., 2006; Seddiki et al., 2006). Within the $CD4^+$ $CD25^{hi}$ $CD127^-$ $FOXP3^+$ population, however, there are two main subgroups of Tregs: thymic-derived natural Tregs (nTregs) and periphery-induced peripheral Tregs (pTregs). nTreg generation occurs during thymic development from self-reactive $CD4^+$ T-cells, and accounts for 5-10% of circulating $CD4^+$ T-cells (Singer et al., 2014). Most self-reactive $CD4^+$ T-cells are negatively selected and deleted by apoptosis to establish central tolerance, however, some self-reactive $CD4^+$ T-cells with high affinity for self-antigens receive signals to differentiate into nTregs by the induction of FOXP3 expression (Bettini and Vignali, 2010). nTregs express a T-cell receptor (TCR) repertoire towards self-antigens and establish peripheral tolerance, suppressing self-reactive conventional T-cells that have escaped central tolerance and thus preventing autoimmunity (Pohar et al., 2018; Yadav et al., 2013). In contrast, peripheral naïve $CD4^+$ T cells, which account for 40-50% of circulating $CD4^+$ T cells in adults, can acquire FOXP3 expression upon activation, becoming pTregs. As pTregs are differentiated from conventional T-cells they express a TCR repertoire towards foreign antigens and play major roles establishing tolerance against microbiota, environmental and food allergens, and fetal alloantigens during pregnancy (Kanamori et al., 2016; Yadav et al., 2013). The induction of pTregs can be mimicked *in vitro* to generate induced Tregs (iTregs; Kanamori et al., 2016; Schmitt and Williams, 2013).

iTregs provide an attractive alternative for Treg-based immunotherapies in allogeneic transplantation. Currently, most Treg-based immunotherapies employ adoptive transfer of *ex vivo* expanded nTregs (Fuchs et al., 2018). To generate the required number of cells for clinical dosage, which requires up to 5 billion Tregs per patient, nTregs need to be *ex vivo* expanded for a prolonged period of time due their low frequency in peripheral blood (Romano et al., 2019; Safinia and Lombardi, 2015). Extended expansion could result in T-cell exhaustion, altering the functional/migratory ability of nTregs (Wherry, 2011). Thus, it would be beneficial to generate large

number of Tregs in a shorter time frame, by differentiating iTregs from naïve $CD4^+$ T-cells, which are at a significantly higher frequency in peripheral blood. The TCR repertoire of iTregs is potentially more relevant for allogeneic transplantation, as rejection of the donor tissue occurs in response to foreign antigens (Schmitt and Williams, 2013). In addition, the broader TCR repertoire of iTregs compared with nTregs has advantages in the generation of antigen-specific Tregs, potentially providing a more targeted therapy (Kanamori et al., 2016; Relland et al., 2012).

The pivotal point in the generation of iTregs has been the discovery of differentiation induction molecules converting naïve $CD4^+$ T-cells into pTregs. One particular environment in which pTregs are present in significant numbers is the gut (Russler-Germain et al., 2017; Luu et al., 2017). The gut mucosal environment contains TGF-β, all-trans retinoic acid (ATRA), and short chain fatty acids, such as butyrate, which have been shown to promote pTreg differentiation (Furusawa et al., 2013; Coombes et al., 2007). Additionally, manipulation of *ex vivo* iTreg generation has validated various molecules such as IL-2, rapamycin and progesterone as enhancer of pTreg differentiation (Schmitt and Williams, 2013). To date, different approaches using combinations of these molecules have been explored to generate human iTregs (Hippen et al., 2011; Schmidt et al., 2016, 2018; Zanin-Zhorov et al., 2017; Riquelme et al., 2018). While these approaches work, the issue of phenotypic instability of iTregs presents a major challenge upon re-stimulation, significantly limiting the use of iTregs for therapeutic applications.

Here, we optimized an iTreg differentiation method for the robust and reproducible production of iTregs with phenotypic and functional stability. Characteristics of iTregs, including expression of CD25 and FOXP3, viability, and growth were evaluated over time throughout expansion and after resting. The phenotypic stability of iTregs was assessed by resting in the absence of IL-2, measuring TSDR methylation status, challenging with Th17-polarizing cytokines, and re-stimulating without iTreg differentiation components. Furthermore, the *in vitro* suppressive function of iTregs was evaluated, and the functional stability of the iTregs was assessed upon re-stimulation.

## Results

### Characteristics of induced Tregs

Naïve $CD4^+$ T-cells were differentiated into iTregs over a 7-day culture period, followed by a 7-day rest in the presence of IL-2. During this time course, cells were periodically assessed for expression of Treg markers CD25 and FOXP3, as well as for viability and fold-expansion. iTregs were generated by an in-house optimized method (iTreg) or using a commercial kit (cTregs), and donor matched nTregs were expanded as Treg phenotype controls (Fig. 1 A). CD25 and FOXP3 expression was measured via flow cytometry and expressed as a percentage (%$CD25^+FOXP3^+$; gating was based on nTreg at ~85% $CD25^+FOXP3^+$) of the viable $CD4^+$ population, and as protein expression levels by MFI (MFI was normalized to the maximum value in each experiment as %; nMFI). Viability was evaluated concurrently using a dead cell discriminating dye (Fig. 1 B). On day 0, prior to induction and expansion, an nTreg baseline %$CD25^+FOXP3^+$ of 89% and a naïve $CD4^+$ T-cell baseline %$CD25^+FOXP3^+$ of 1.5% was shown with significant differences in MFI of CD25 and FOXP3 ($p<0.0001$ for all). After 1 day of culture, iTreg %$CD25^+FOXP3^+$ increased to 50% from the naïve CD4+ T-cell baseline, compared with 25% for cTregs ($p=0.0018$). By day 3, iTreg %$CD25^+FOXP3^+$ increased to 60% while cTregs reached 38% ($p=0.0041$). At day 5 and 7, iTregs were >85% $CD25^+FOXP3^+$ and cTregs were >75% $CD25^+FOXP3^+$. Upon resting, both iTregs and cTregs became >90% $CD25^+FOXP3^+$. The nTreg control culture maintained >85% $CD25^+FOXP3^+$ from day 1 to 14 (Fig. 1 C and Fig. S1 A). CD25 MFI of iTregs became equal to nTregs by day 5 ($p<0.0001$ on day 1 and 3), while CD25 MFI of cTregs became equal to nTregs by day 7 ($p<0.0001$ on day 1, 3 and 5). CD25 MFI of iTregs was significantly higher than cTregs on day 1, 3 and 5 ($p<0.0001$ for all). On day 10, CD25 MFI of iTregs and cTregs exceeded nTregs ($p<0.0001$ and $p=0.0012$, respectively). iTregs showed significantly higher CD25 MFI than cTregs ($p<0.0001$). Day 14, CD25 MFI of iTregs and cTregs remained higher than nTregs ($p<0.0001$ and $p=0.0013$, respectively), with no significant differences between iTregs and cTregs (Fig. 1 D and Fig. S1 B). FOXP3 MFI of both iTregs and cTregs equaled nTregs by day 5 ($p<0.0001$ for both day 1 and 3). On day 7, FOXP3 MFI of iTregs exceeded both nTregs and cTregs ($p=0.0027$ and $p<0.0001$, respectively). FOXP3 MFI of cTregs was lower than nTregs ($p<0.0091$). On day 10, FOXP3 MFI of iTregs was higher than nTregs ($p=0.0092$). Day 14 FOXP3 MFI of iTregs and nTregs were higher than cTregs ($p=0.0004$ and 0.0018, respectively; Fig, 1 E and Fig. S1 C). iTregs retained above 95% viability from day 0 to 14. cTreg and nTreg viability gradually decrease below 95% viability over days 1 to 14.

On day 7, cTregs showed 88% viability, significantly lower than iTregs with 98% viability (p=0.0007). Viability of cTregs decreased to 32% (p<0.0001 compared with iTregs and nTregs) on day 10. nTregs also displayed significantly lower viability (86%) than iTregs (p=0.0018). On day 14, the viability of cTregs further decreased to 22% (p<0.0001 compared with iTregs and nTregs). The viability of nTregs further reduced to 83% (p<0.0001 compared with iTregs; Fig. 1 F and Fig S1 D). All three types of Tregs showed similar cell growth rates throughout the induction/expansion. By day 7, iTregs, cTregs and nTregs showed 13, 11 and 12-fold cell growth, respectively. Upon resting at day 10, iTregs and nTregs continued to proliferate while cTregs showed no additional growth. iTregs and nTregs increased to 39 and 35-fold growth, significantly higher than cTregs which increased 11-fold (p=0.0001 and p=0.0007, respectively). On day 14, iTreg cell growth was at 43-fold, while nTregs displayed a decreased rate at 33-fold. cTregs also showing a decrease, at 8-fold. (p<0.0001 and p=0.0005 compared to iTregs and nTregs; Fig. 1 G and Fig S1 E).

### *In vitro* stability of induced Tregs

Stability of iTregs was evaluated initially by resting without IL-2 (Fig. 2 A), which plays a crucial role for maintenance of Treg phenotype (Sakaguchi et al., 2008). In the absence of IL-2, nTreg and iTreg remained >85% $CD25^{+}FOXP3^{+}$ with no significant differences compared with cells rested in the presence of IL-2. On the other hand, cTregs showed a significant reduction in $\%CD25^{+}FOXP3^{+}$ in the absence of IL-2 (p=0.0196). While all three Tregs showed no significant decreases in FOXP3 MFI in the absence of IL-2, CD25 MFI of all three Treg subtypes was significantly reduced in the absence of IL-2. iTregs displayed a 12% decrease (p=0.0009), nTregs a 11% decrease (p=0.0149), and cTregs a 46% decrease (p<0.0001; Fig. 2 A-C). Moreover, all three subtypes showed significant reductions in their viability in the absence of IL-2. The viability of iTregs decreased from 93% to 33%, nTregs decreased from 83% to 29%, and cTregs decreased from 37% to 2% (p<0.0001 for all; Fig. 2 E). The demethylation status of Treg-specific demethylation region (TSDR) is an important assay for stability of FOXP3 expression (Floess et al., 2007; Baron et al., 2007). Methylation levels of 11 CpG motifs in the TSDR were measured via targeted bisulfite pyrosequencing. DNA from iTregs and cTregs was collected at each timepoint throughout induction/expansion and resting, while DNA of nTregs was collected pre-expansion (day 0), at the end of expansion (day 7), and post-expansion (day 10; Fig. 3 A). iTreg and cTreg methylation was above 90% at each timepoint, while nTregs showed 42%, 57% and 62% methylation on days 0, 7 and 10, with

each CpG motifs showing various levels of methylation (Fig. 3, B and C and Table S1). cTregs were excluded from further investigations due to poor long-term viability.

It has previously been shown that iTregs can convert to pathogenic Th17 cells in a pro-inflammatory environment (Beres et al., 2011; Ghali et al., 2017). Therefore, the stability of iTregs was investigated by challenging them with Th17-polarizing cytokines IL-1β, IL-6, IL-21, IL-23 and TGF-β (Muranski and Restifo, 2013; Martinez et al., 2008). Due to the dual role of TGF-β for differentiation of both iTregs and Th17 cells (Tran, 2012), it was unclear whether inclusion of TGF-β would prevent or augment the effects of other Th17-polarizing cytokines on iTregs. Thus, two types of challenge media either excluding TGF-beta (1) or including TGF-beta (2) were used (Fig. 4 A). iTregs and nTregs remained >70% $CD25^{+}FOXP3^{+}$ in the presence of Th17-polarizing cytokines, with no significant differences compared with non-challenged Tregs. No significant differences were shown between with and without TGF-β (Fig. 4 B**)**. CD25 MFI of challenged iTregs and nTregs was significantly reduced compared with non-challenged Tregs (iTregs: p=0.0008 w/o TGF-β and p<0.0001 with TGF-β. nTregs: p=0.0146 w/o TGF-β and p<0.0001 with TGF-β). Inclusion of TGF-β was shown to further reduce CD25 MFI (p=0.0075 in iTregs, p=n/s in nTregs; Fig. 4 C). FOXP3 MFI of challenged iTregs and nTregs was also significantly decreased compared with non-challenged Tregs (iTregs: p=0.0316 w/o TGF-β and p=0.0118 with TGF-β. nTregs: p=0.0029 w/o TGF-β and p=0.0041 with TGF-β), with no significant differences with or without TGF-β (Fig. 4 D). Additionally, challenged iTregs and nTregs showed significantly lower viability compared with non-challenged Tregs (p<0.0001 for all). Although non-significant, inclusion of TGF-β reduced the viability of iTregs and nTregs by an additional 10%. Furthermore, expression of Th17 signature genes in challenged Tregs was evaluated via RT-qPCR (Fig. 5 A). *RORC, STAT3, IL17A* and *CCR6* were chosen to represent a Th17 transcriptional program, Th17-differentiation STAT pathway, Th17 signature cytokines, and Th17 signature chemokine receptor (Egwuagu, 2009; Castro et al., 2017). Expression of *RORC, STAT3* and *CCR6* was not upregulated in challenged iTregs and nTregs, with no significant differences compared with non-challenged Tregs. In the case of *IL17A*, nTregs showed significant upregulation upon challenge while iTregs did not (p=0.0273 w/o TGF-β and p=0.0006 with TGF-β; Fig. 5, B-E**)**. Baseline expression of *RORC* and *IL17A* were significantly higher in nTregs compared with iTregs (p=0.0176 and p=0.0233, respectively), while there were no differences in baseline expression of STAT3 and *CCR6* (Fig. S2).

Lastly, reduction of FOXP3 expression and suppressive activities has been observed in human iTregs upon re-stimulation without iTreg differentiation components (Rossetti et al., 2015). Thus, the stability of iTregs was assessed upon re-stimulation. Initially, the expression of CD25 and FOXP3 in iTregs re-stimulated without the components (referred to as "ss-iTregs"; single stimulated) was compared with iTregs re-stimulated with the components (referred to as "ds-iTregs"; double stimulated) and re-stimulated nTregs (Fig. 6 A). ss-iTregs remained >77% $CD25^{+}FOXP3^{+}$ with no significant difference compared with ds-iTregs and nTregs (Fig. 6 B). CD25 MFI of ss-iTregs was not significantly different between ds-iTregs and nTregs. ds-iTregs showed significantly higher CD25 MFI than nTreg ($p=0.0027$; Fig. 6 C). FOXP3 MFI of ss-iTregs was significantly lower than both ds-iTregs and nTregs ($p<0.0001$ for both; Fig. 6 D). Baseline *in vitro* suppressive activities of iTregs and nTregs prior to re-stimulation was evaluated, then the suppressive activities of ss-iTregs, ds-iTregs and nTregs were measured (Fig. 7 A**)**. T-cell suppression can be measured by using the expression of transient T-cell activation marker, CD154, in naïve $CD4^{+}$ T-cells (Teffectors) as a surrogate for T-cell proliferation (Hill et al., 2012; Fig. 7 B). Prior to re-stimulation, iTregs displayed significantly higher suppressive activities than nTregs at all ratios of Treg to Teffector ($p=0.0003$ at 1:1, $p=0.0356$ at 1:2, $p=0.0249$ at 1:4 and $p<0.0001$ at 1:8; Fig. 7 C). Upon re-stimulation, ss-iTregs retained their suppressive activity. The suppressive activity of ss-iTregs was higher than nTregs ($p=0.0310$ at 1:1, n.s at 1:2, $p=0.0275$ at 1:4 and n.s at 1:8) and lower than ds-iTregs (n.s at 1:1, $p<0.0001$ at 1:2, $p<0.0246$ at 1:4 and n.s at 1:8). ds-iTregs were significantly more suppressive than nTregs at all ratios ($p<0.0001$ for all; Fig. 7 D).

**Discussion**

In this study, we optimized an iTreg differentiation method utilizing TGF-β, ATRA, rapamycin, IL-2, and α-CD3/CD28 beads to differentiate and expand human iTregs from naïve $CD4^{+}$ T-cells. These molecules have previously been shown to induce or enhance iTreg generation. TGF-β secreted by $CD103^{+}$ intestinal dendritic cells (DCs) plays an essential role in the generation of pTregs in the gut by inducing binding of the transcription factors Smad2 and Smad3 to conserved non-coding DNA sequence 1 (CNS1) region of *FOXP3* locus (Kanamori et al., 2016; Schmitt and Williams, 2013), which is crucial for FOXP3 induction in pTregs but not in nTregs (Samstein et al., 2012). Additionally, ATRA secreted by $CD103^{+}$ intestinal DCs enhances binding of Smad3 to

CNS1 region through histone acetylation of Smad3 binding region, preventing Th17 polarization, also requiring TGF-β signaling (Kanamori et al., 2016; Schmitt and Williams, 2013; Oh and Li, 2013). Furthermore, the mTOR (mammalian target of rapamycin)-targeting drug, rapamycin, has been shown to stabilize FOXP3 expression (Zhang et al., 2013). Rapamycin also enhances purity of generated iTregs by selectively inhibiting the activation of conventional T-cells (Singer et al., 2014), as Tregs utilize an IL-2R-dependent STAT5 pathway for activation while conventional T-cells require the mTOR pathway for activation (Burchill et al., 2007; Delgoffe et al., 2009). Lastly, IL-2 promotes FOXP3 expression, Treg expansion, and inhibits Th17 polarization (Kryczek et al., 2007; Schmitt and Williams, 2013). The combination of TGF-β, ATRA, rapamycin, and IL-2 has previously been used to successfully generate iTregs with superior *in vitro* suppressive activities. However, these iTregs lost FOXP3 expression when rested in the absence of IL-2 and re-stimulation. The iTregs were then not able to prevent the onset of xenogeneic graft-versus-host-disease in a humanized mice model (Schmidt et al., 2016). Notably, inhibition of mTORC1, one of two distinct mTOR complexes, induces FOXP3 expression and promotes expansion (Chapman and Chi, 2014). Only 0.45 ng/mL of rapamycin is required to inhibit mTORC1 (Foster and Toschi, 2009), thus, we utilized low-dose rapamycin of 1 ng/mL, compared with 100 ng/mL traditionally seen in the literature (Schmidt et al., 2016, 2018), to minimize unwanted downstream signals induced by rapamycin at higher doses, such as the inhibition of glycolysis (Li et al., 2014), as glycolysis has been shown to be important for iTreg differentiation and function (De Rosa et al., 2015). It has been demonstrated that strong TCR stimulation stabilizes FOXP3 expression (Wakamatsu et al., 2018), and that superior stability is achieved with α-CD3/CD28 beads compared with plate-bound α-CD3 and soluble α-CD28 in murine iTregs (Gu et al., 2014). Hence, α-CD3/CD28 beads were used instead of plate-bound α-CD3 and soluble α-CD28 (Schmidt et al., 2016, 2018).

iTregs generated by the in-house optimized method ("iTregs") demonstrated superior expression of CD25 and FOXP3, viability, and fold expansion, compared with both nTregs and iTregs generated with a commercial kit ("cTregs"). iTregs became dual positive for CD25 and FOXP3 earlier than cTregs, and the expression level of CD25 in iTregs matched nTreg earlier than cTregs. Although the rate of increase in expression of FOXP3 was similar among iTregs and cTregs, this suggested higher stimulatory capacity of the in-house method compared with the commercial kit. Expression levels of CD25 in iTregs exceeded nTreg-levels. This high expression of

CD25 and FOXP3 was maintained throughout the 7-day resting period, while expression levels of CD25 and FOXP3 in nTregs and cTregs fluctuated, demonstrating phenotypic stability over long duration of resting. iTregs remained highly viable during expansion and resting while reduction in viability was observed in nTregs and cTregs. In particular, the viability of cTregs was significantly reduced upon resting. It was initially thought that cTregs were dying from exhaustion after extended expansion, as the commercial kit protocol specified 5-day expansion, however, cTregs rested after 5 days showed even lower viability (Fig. S3). This reduction in viability was due to significantly high percentages of apoptotic cells in cTregs (Fig. S4), however, it is unclear why these cells became apoptotic, as the contents of the commercial kit are not specified beyond the use of plate-bound α-CD3. The reduction in viability also affected the rate of expansion of the cTregs. iTregs, nTregs and cTregs showed similar initial expansion rates, while iTregs and nTregs continued to expand upon resting. As a result, the total cTreg cell number was not increased significantly, due to significant cell death. iTregs demonstrated the highest overall fold expansion, as they continued to proliferate after three days of resting, unlike nTregs. Together, these results suggested that the in-house optimized method for iTreg generation can produce significantly larger numbers of highly viable iTregs compared with conventional nTreg expansion methods, which is important given that the starting population for manufacturing iTregs, naïve $CD4^+$ T-cells, is 6-fold more frequent in human peripheral blood than nTregs (Fig. S5).

To provide a clinical benefit in the context of organ transplant it is important that iTregs remain stable in unfavorable conditions, such as the absence of IL-2. Given that Tregs cannot produce IL-2 for autocrine signaling, unlike conventional T-cells (Chinen et al., 2016), and IL-2 is crucial for survival of Tregs, maintenance of FOXP3 expression and reinforcement of Treg phenotype (Sadlon et al., 2010; Beyer et al., 2011), iTregs could lose FOXP3 expression (Schmidt et al., 2016) or convert back to conventional T-cells to produce autocrine IL-2 to survive. iTregs and nTregs remained dual positive for CD25 and FOXP3 upon resting without IL-2 while cTregs displayed a significant reduction. Expression levels of FOXP3 were not reduced, while expression of CD25 significantly decreased in all three Treg subtypes. This was expected as CD25 is the α chain of the high affinity IL-2 receptor complex (Létourneau et al., 2009). Expression of CD25 was more drastically reduced on cTregs compared with iTregs and nTregs, indicating that cTregs are more sensitive to IL-2. Moreover, significant cell death was observed in the absence of IL-2 in all three Treg subtypes. Currently,

demethylation of Treg-specific demethylation region (TSDR), the CpG-rich CNS2 region of *FOXP3* locus, is thought to be the hallmark of stable FOXP3 expression, thus stable Treg phenotype (Kanamori et al., 2016; Schreiber et al., 2014; Polansky et al., 2008). In humans, it has been shown that nTregs exhibit full demethylation of TSDR, while conventional T-cells and iTregs present partial methylation of TSDR (Baron et al., 2007). Even though iTregs demonstrated phenotype stability over extended periods of resting and in the absence of IL-2, demethylation of TSDR in iTregs was not observed throughout expansion and resting. cTregs also showed no demethylation of TSDR, and no differences were observed between iTregs and cTregs. Interestingly, pooled nTregs analyzed for methylation status only displayed partial demethylation, which suggested possible contamination by cells with non-demethylated TSDR, such as pTregs. As nTregs in this study were sorted based on their CD4, CD25 and CD127 expression, they contained both $CD45RA^+$ naïve Treg population and $CD45RA^-$ effector Treg population. Currently, there are no surface markers for distinguishing human nTregs and pTregs, and the exact proportions of circulating nTregs and pTregs in human peripheral blood are unknown (Szurek et al., 2015; Mohr et al., 2018). As such, the $CD45RA^-$ effector Treg population is heterogenous with both nTregs and pTregs, while $CD45RA^+$ naïve Treg population is thought to be predominantly nTregs (Mohr et al., 2018). Indeed, similar level of demethylation were observed in nTregs sorted with only CD25 expression (Schmidt et al., 2016). Thus, more complex gating strategies may need to be utilized to enhance the purity of nTreg expansion. Notably, it has been observed that $CD45RA^+$ Tregs show a higher degree of demethylation of the TSDR than $CD45RA^-$ Tregs (Baron et al., 2007). A sup-population of $CD45RA^-$ Tregs with intermediate expression of CD25, termed Fraction (Fr).III, display decreased demethylation (Cuadrado et al., 2018), supporting this notion. Furthermore, the degree of demethylation in nTregs decreased over the duration of expansion and resting, possibly indicating preferential expansion of pTregs or Fr.III Tregs over nTregs.

The tendency of iTregs to switch to a pro-inflammatory phenotype, such as Th17, in a pro-inflammatory microenvironment, needed to be assessed. This is because conversion of iTregs into pathogenic pro-inflammatory T cells *in vivo* is the major challenge to the use of iTregs for therapeutic purposes (Ghali et al., 2017; Dons et al., 2011; Beres et al., 2011). Despite their fully methylated TSDR, iTregs remained dual positive for CD25 and FOXP3 upon challenge with Th17-polarizing cytokines. Expression levels of CD25 and FOXP3

were significantly reduced, but these decreases were also observed in nTregs. Moreover, the viability of iTregs and nTregs was significantly reduced when challenged. While the decreases in expression level of CD25 and viability were most likely caused by the lack of IL-2 in the challenge media, the decreases in expression level of FOXP3 may have been due to IL-1β and IL-21, which have been shown to reduce FOXP3 expression (Li et al., 2010; Jandl et al., 2017). IL-2 was excluded from the challenge media due to its ability to limit Th17 polarization (Laurence et al., 2007), and IL-23 in the challenge media would have promoted survival and proliferation of Th17-converted iTregs (Fitch et al., 2007). Thus, these results demonstrated phenotypically stable iTregs in a pro-inflammatory environment. Interestingly, inclusion of TGF-β in the challenge media further decreased expression levels of CD25, especially in iTregs, and viability in both iTregs and nTregs. It has been shown that TGF-β without IL-2 signaling can promote cell death in T-cells (Travis and Sheppard, 2014), and IL-2 is essential for TGF-β-mediated induction of CD25 expression (Zheng et al., 2007). Moreover, upregulation of Th17 signature genes was not observed in iTregs, with relative expression of these genes being extremely low. Interestingly, although still extremely low compared to *RPL13A*, expression of *IL17A* was upregulated upon challenge in nTregs, which could have been due to higher baseline expression of *RORC* and *IL17A* in nTregs compared with iTregs. It has previously been shown that Tregs are divided into various subsets reflecting counterpart T-helper subsets (Duhen et al., 2012), and Tregs can be polarized to Th17-like Tregs, which express Th17 signature markers while retaining regulatory phenotype and function, under pro-inflammatory conditions (Jung et al., 2017; Kim et al., 2017). Thus, these results suggest that iTregs were not polarized into Th17-like Tregs in a Th17 differentiating environment, which could be a double-edged sword due to their expression of RORγt and Th17 cytokines (Jung et al., 2017), with perhaps more resistance to Th17-polarization than nTregs.

The efficacy of iTreg-based immunotherapies would rely on their ability to retain a regulatory phenotype and function upon reactivation within an *in vivo* environment. iTregs remained dual positive for CD25 and FOXP3 upon re-stimulation without iTreg differentiation components, which simulated *in vivo* reactivation. While the expression level of CD25 in these iTregs was lower than iTregs re-stimulated with differentiation components, it remained higher than nTregs. On the other hand, expression level of FOXP3 in these iTregs was significantly lower than both nTregs and iTregs re-stimulated with differentiation components. Furthermore, iTregs displayed

higher baseline suppressor function than nTregs prior to re-stimulation, and iTregs re-stimulated without differentiation components were still more suppressive than nTregs, despite having lower expression level of FOXP3. In contrast, iTregs re-stimulated with differentiation components were more suppressive than iTregs re-stimulated without differentiation components. It has been previously shown that expression levels of FOXP3 can be directly correlated with suppressive activity (Chauhan et al., 2009; Barsheshet et al., 2017), however, this indicated that FOXP3 cannot be a direct surrogate for suppressor function, particularly when comparing nTregs and iTregs. In this case, the suppressive activities of nTregs or iTregs re-stimulated with and without differentiation components, correlated with their expression levels of CD25 instead of FOXP3. This could, of course, be an over-simplified interpretation, as distinctive suppressive mechanisms are observed in nTregs and iTregs (Schmitt and Williams, 2013). Indeed, recent transcriptomic and proteomic profiling of iTregs generated by multiple differentiation protocols revealed iTreg-specific molecular pathways and molecules (Schmidt et al., 2018), even though these protocols were not able to generate stable iTregs. Thus, in-depth analysis of transcriptomes and proteomes may be required to see which factors and genes are attributing to discrepancies in the suppressor function of these Tregs. Nonetheless, these results corroborated functional stability as well as phenotypic stability of iTregs, even in an environment(s) which has previously resulted in loss of FOXP3 expression and loss of suppressive activities (Schmidt et al., 2016; Rossetti et al., 2015).

In summary, we demonstrated the generation of *in vitro* stable human iTregs with an in-house optimized method which utilized TGF-β, ATRA and low-dose rapamycin, providing an attractive alternative for manufacturing Treg-based immunotherapies. The in-house optimized method resulted in rapid generation of large number of iTregs that are superior to commercially generated iTregs. These iTregs were highly viable with strong CD25 and FOXP3 expression over resting periods. Their phenotypic stability was demonstrated in the absence of IL-2, in the presence of Th17-polarizing cytokines, and upon re-stimulation without TGF-β, ATRA and rapamycin. Furthermore, in the presence of Th17-polarizing cytokines, upregulation of Th17 signature genes was not observed in iTregs, while *IL17A* was upregulated in nTregs, further emphasizing the stability of iTregs. iTregs were also functionally stable upon re-stimulation without the components, and with higher suppressive activities than nTregs. Despite their phenotypic and functional stability, demethylation of TSDR was not shown for iTregs. While, TSDR demethylation has been thought to be a surrogate for Treg stability, there might be further factors

involved in stabilization of Treg phenotype. Indeed, it has been shown that demethylation of other Treg signature genes such as *TNFRSF18*, *CTLA-4*, *IKZF4* and *IL2RA*, dubbed as Treg-specific demethylation patterns ("TSDP"), is crucial for Treg development and stable FOXP3 expression, as well as TSDR demethylation (Ohkura et al., 2012). Moreover, the iTreg differentiation method could be modified to induce TSDR demethylation. Notably, in mice, hypoxia (Ma et al., 2018) and vitamin C (Sasidharan Nair et al., 2016; Someya et al., 2017) were shown to enhance expression and activity of TET (ten eleven translocation) enzymes, which facilitate demethylation of the TSDR. This differentiation protocol not only has the potential to generate robust suppressor cells, but it can be achieved with shorter culture times, which has a dramatic impact on the cost of manufacturing. While this work serves a proof of principle for generation of stable human iTregs, the stability, safety and effectiveness of this improved iTreg differentiation protocol requires validation in a preclinical transplant model such as pancreatic islet transplant model or graft-versus-host-disease (GVHD) model.

## Materials and Methods

### Cell isolation, induction and expansion

Human buffy coat (Australian Red Cross) was treated with a RosetteSep Human $CD4^+$ T-cell enrichment cocktail (STEMCELL Technologies) for 20 minutes on a platform mixer at 80 rpm. Treated buffy coat was diluted with PBS (+2% foetal calf serum (FCS), Bovogen) prior to isolation of $CD4^+$ T-cells by density-gradient centrifugation over Lymphoprep (STEMCELL Technologies). Enriched $CD4^+$ T-cells were surface-stained for CD4, CD25, CD127 and CD45RA. $CD4^+$ $CD25^+$ $CD127^-$ T cells (natural regulatory T-cells or nTregs) and $CD4^+$ $CD25^-$ $CD127^+$ $CD45RA^+$ T cells (naïve $CD4^+$ T-cells) were sorted by fluorescence-activated cell sorting (FACS; BD FACSAria Fusion, BD Biosciences). Sorted nTregs and naïve $CD4^+$ T-cells were rested overnight in a complete X-vivo medium at $1 \times 10^6$ cells/mL (cX-vivo: serum-free with gentamycin and phenol red, Lonza, supplemented with 2% HEPES, 1% L-glutamine and 5% human serum (Gibco, HyClone and Sigma-Aldrich, respectively) with 500 U/mL of IL-2 (Novartis Vaccines and Diagnostics). After overnight resting, nTregs were resuspended in an expansion medium consisting of cX-vivo and a 1:1 ratio of Human T-expander CD3/CD28 Dynabeads™ (Thermo Fisher Scientific) at $1 \times 10^6$ cells/mL. Naïve CD4+ T-cells were resuspended in either (1) an optimized iTreg differentiation medium composed of the expansion medium supplemented with 5 ng/mL of human TGF-β (eBioscience), 10 nM/mL of all-trans retinoic acid (Sigma-Aldrich) and 2 ng/mL rapamycin

(LC Laboratories) at $1 \times 10^6$ cells/mL (iTregs) or (2) a commercial iTreg differentiation kit medium at $1\text{-}2 \times 10^5$ cells/mL ("cTregs"). For the commercial kit (R&D Systems), manufacturer's protocol was followed with an exception regarding the culture time which was specified as 5 days. Expansion for nTregs, iTregs and cTregs were carried out for 7 days. For nTregs and iTregs, media was replenished on day 3 and 5 to keep the cell density at $1 \times 10^6$ cells/mL. For cTregs, media was not replenished as their starting densities were lower. On day 7, Tregs were washed three times with PBS (+2% FCS). After washing, expander beads were magnetically removed from nTregs and iTregs. Tregs were re-suspended in cX-Vivo with 500 U/mL of IL-2 at $2 \times 10^6$ cells/mL and rested up to 7 days. On day 10 (3 days of resting), media was replenished to keep the cell densities at $2 \times 10^6$ cells/mL.

**iTreg Stability Evaluation**

For evaluation of iTreg stability, iTregs were (1) rested in the absence of IL-2, (2) challenged with Th17-polarizing cytokines and (3) re-stimulated without iTreg differentiation components. For (1), Tregs were rested for 3 days with or without IL-2 in the media at $2 \times 10^6$ cells/mL after 7-day expansion. For (2), Tregs were challenged for 3 days with Th17-polarizing cytokines, IL-1β (10 ng/mL; Biolegend), IL-6 (10 ng/mL; Biolegend), IL-21 (10 ng/mL; Biolegend), IL-23 (10 ng/mL; Biolegend) and TGF-β (5 ng/mL; eBioscience), at $2 \times 10^6$ cells/mL. Two different media were prepared which contained (i) IL-1β, IL-6, IL-21 and IL-23 and (ii) IL-1β, IL-6, IL-21, IL-23 and TGF-β, respectively, after 7-day expansion. Tregs were rested with IL-2 as a control. For (3), Tregs were re-stimulated for 7 days at $1 \times 10^6$ cells/mL then rested with IL-2 for 3 days at $2 \times 10^6$ cells/mL, after initial 7-day expansion and 3-day resting. nTregs were re-stimulated using the same expansion media. iTregs were re-stimulated with or without iTreg differentiation components. For (2) and (3), cTregs were excluded.

**Flow Cytometric Analysis for CD25, FOXP3 and viability**

$1 \times 10^5$ cells were stained for viability and CD4 and CD25. Cells were fixed and permeabilized (Foxp3/ Transcription factor staining buffer set, eBioscience) then intracellularly stained for FOXP3. All samples were analyzed on a BD FACS Canto II flow cytometer (BD Biosciences), and the data analyzed with FCS Express 6 (De Novo Software).

**TSDR methylation assay**

Expander beads were magnetically removed from 2-3 × $10^5$ cells. Cells were spun down and all supernatants were discarded, leaving cell pellets. Cell pellets were stored at -80 ˚C until assay. Assay was conducted by EpigenDx using the assay ADS783-FS1 and ADS783-FS2 (Ensembl Transcript ID: ENST00000376207) which assessed the methylation status of 11 CpG sites in the TSDR region of *FOXP3* CNS2 by targeted bisulfite-pyrosequencing of genomic DNA isolated from the cell pellets. This region covered CpG sites -2376 (CpG#44), -2371 (CpG#43), -2330 (CpG#42), -2322 (CpG#41), -2312 (CpG#40), -2309 (CpG#39), -2303 (CpG#38), -2299 (CpG#37), -2291 (CpG#36), -2282 (CpG#35) and -2263 (CpG#34) relative to the FOXP3 ATG start codon. Internal low, medium, and high methylation controls were utilized.

**Reverse Transcription Quantitative Polymerase Chain Reaction**

5 × $10^5$ cells were pelleted, and supernatants removed. Cell pellets were lysed, and RNA was isolated using RNAqueous™ Total RNA Isolation Kit (ThermoFisher Scientific) as per manufacturer's protocol. Purified RNA was converted to cDNA using iScript Reverse Transcription Supermix (Bio-Rad) as per manufacturer's protocol. cDNA was then used for measurement of gene expression via quantitative polymerase chain reaction on a CFX Connect Real-Time PCR Detection System (Bio-Rad) using TaqMan™ Gene Expression Master Mix (ThermoFisher Scientific) and Taqman primers for *RORC* (Hs01076112_m1), *STAT3* (Hs00374280_m1), *IL17A* (Hs00174383_m1), *CCR6* (Hs01890706_s1) and *rpl13a* (Hs04194366_g1; Housekeeping gene; ThermoFisher Scientific for all), as per manufacture's protocol.

**CD154 suppression assay**

Human peripheral blood mononuclear cells (PBMCs) cells were isolated from a fresh buffy coat by density gradient centrifugation as described above. Naïve $CD4^+$ T-cells were isolated using EasySep™ Human Naïve CD4+ T Cell Isolation kit (STEMCELL Technologies). Naïve $CD4^+$ T-cells were labelled with 3,30-dioctadecyloxacarbocyanine perchlorate ($DiOC_{18}(3)$ (Thermo Fisher Scientific; a final concentration of 2 μg/mL) by incubation at 37 ˚C with 5% $CO_2$ for 45 minutes. 96-well round bottom plates were seeded with $DiOC_{18}(3)$-labelled naïve $CD4^+$ T-cells (5 × $10^4$ cells per well; "Teffector") and Tregs were added to the wells

at various ratios of Treg:Teffector (1:1, 1:2, 1:4 and 1:8). Human T-expander CD3/CD28 Dynabeads™ (bead:Teffector ratio of 1:4) and anti-CD154 antibody were added to each well. $DiOC_{18}(3)$-labelled naïve CD4+ T-cells with and without Tregs were used as positive and negative controls, respectively. The plate was incubated at 37 ˚C in 5% $CO_2$ for 7 hours then analyzed for expression of CD154 by flow cytometry (FACS Canto II). Percentage suppression was calculated as follows: 100 × [1 - (%$CD154^+$ in the experiment sample divided by %$CD154^+$ in the positive control)].

**Statistics**

Statistical significance ($p<0.05$) was analyzed using the GraphPad Prism 8. One-way ANOVA with Tukey's multiple comparisons test, Two-way ANOVA with Tukey's multiple comparisons test and paired two-tailed T-test were used to identify statistical significance. All replicates are biological replicates. All experiments utilized triplicates as technical replicates.

**Antibodies**

Antibody details are listed in the supplementary table 2.

**Flow Cytometric Analysis for Apoptosis**

$1 \times 10^5$ cells were stained for Annexin V. All samples were analyzed on a BD FACS Canto II flow cytometer and the data analyzed with FCS Express 6.

Acknowledgements

The authors wish to acknowledge funding from The Hospital Research Foundation, Adelaide Australia, support of Australian Red Cross Blood Services for providing human buffy coat for cell isolation. J.K acknowledges Dr Randall Grose of South Australian Health and Medical Research Institute for operating fluorescence activated cell sorter.

J.K designed and performed all experiments, analyzed data and wrote the manuscript. C.M.H. contributed to designing of experiments. J.C.S., S.O.S. and G.B.P. helped with experiments; J.C.S contributed to RT-PCR and re-stimulation experiment; S.O.S and G.B.P. contributed to time-course analysis assay. C.M.H., J.C.S., S.O.S., G.B.P., R.P.C., S.C.B. and P.T.H. edited the manuscript. S.O.S edited the figures. J.K., C.M.H., S.C.B. and P.T.H conceptualized the project and R.P.C., S.C.B., and P.T.H. supervised the study. P.T.H. attained funding.

**References**


Baecher-Allan, C., J.A. Brown, G.J. Freeman, and D.A. Hafler. 2001. CD4+CD25high Regulatory Cells in Human Peripheral Blood. *J. Immunol.* 167:1245–1253. doi:10.1073/pnas.1103810108.

Baron, U., S. Floess, G. Wieczorek, K. Baumann, A. Grützkau, J. Dong, A. Thiel, T.J. Boeld, P. Hoffmann, M. Edinger, I. Türbachova, A. Hamann, S. Olek, and J. Huehn. 2007. DNA demethylation in the human FOXP3 locus discriminates regulatory T cells from activated FOXP3 + conventional T cells. *Eur. J. Immunol.* 37:2378–2389. doi:10.1002/eji.200737594.

Barsheshet, Y., G. Wildbaum, E. Levy, A. Vitenshtein, C. Akinseye, J. Griggs, S.A. Lira, and N. Karin. 2017. CCR8 $^{+}$ FOXp3 $^{+}$ T $_{reg}$ cells as master drivers of immune regulation. *Proc. Natl. Acad. Sci.* 114:6086–6091. doi:10.1073/pnas.1621280114.

Beres, A., R. Komorowski, M. Mihara, and W. Drobyski. 2011. Induced Regulatory T Cells To Mitigate Graft. *Clin. Cancer Res.* 17:3969–3983. doi:10.1158/1078-0432.CCR-10-3347.INSTABILITY.

Bettini, M.L., and D.A.A. Vignali. 2010. Development of thymically derived natural regulatory T cells. *Ann. N. Y. Acad. Sci.* 1183:1–12. doi:10.1111/j.1749-6632.2009.05129.x.

Beyer, M., Y. Thabet, R. Müller, T. Sadlon, S. Classen, K. Lahl, S. Basu, X. Zhou, S.L. Bailey-bucktrout, W. Krebs, E.A. Schönfeld, J. Böttcher, T. Golovina, C.T. Mayer, A. Hofmann, D. Sommer, S. Debey-pascher, E. Endl, A. Limmer, K.L. Hippen, B.R. Blazar, R. Balderas, T. Quast, A. Waha, G. Mayer, M. Famulok, P.A. Knolle, C. Wickenhauser, W. Kolanus, B. Schermer, J.A. Bluestone, S.C. Barry, T. Sparwasser, J.L. Riley, and J.L. Schultze. 2011. Repression of the genome organizer SATB1 in regulatory T cells is required for suppressive function and inhibition of effector differentiation. *Nat. Immunol.* 12:898–907. doi:10.1038/ni.2084.

Burchill, M.A., J. Yang, C. Vogtenhuber, B.R. Blazar, and M.A. Farrar. 2007. IL-2 Receptor β-Dependent STAT5 Activation Is Required for the Development of Foxp3 + Regulatory T Cells . *J. Immunol.* 178:280–290. doi:10.4049/jimmunol.178.1.280.

Castro, G., X. Liu, K. Ngo, A. De Leon-Tabaldo, S. Zhao, R. Luna-Roman, J. Yu, T. Cao, R. Kuhn, P. Wilkinson, K. Herman, M.I. Nelen, J. Blevitt, X. Xue, A. Fourie, and W.P. Fung-Leung. 2017. RORγt and RORα signature genes in human Th17 cells. *PLoS One*. 12:1–22. doi:10.1371/journal.pone.0181868.

Chapman, N.M., and H. Chi. 2014. MTOR signaling, tregs and immune modulation. *Immunotherapy*. 6:1295–

1311. doi:10.2217/imt.14.84.

Chauhan, S.K., D.R. Saban, H.K. Lee, and R. Dana. 2009. Levels of Foxp3 in Regulatory T Cells Reflect Their Functional Status in Transplantation. *J. Immunol.* 182:148–153. doi:10.4049/jimmunol.182.1.148.

Chinen, T., A.K. Kannan, A.G. Levine, X. Fan, U. Klein, Y. Zheng, G. Gasteiger, Y. Feng, J.D. Fontenot, and A.Y. Rudensky. 2016. An essential role for IL-2 receptor in regulatory T cell function Takatoshi. *Nat. Immunol.* 17:1322–1333. doi:10.1038/ni.3540.

Coombes, J.L., K.R.R. Siddiqui, C. V. Arancibia-Cárcamo, J. Hall, C.M. Sun, Y. Belkaid, and F. Powrie. 2007. A functionally specialized population of mucosal CD103+ DCs induces Foxp3+ regulatory T cells via a TGF-β -and retinoic acid-dependent mechanism. *J. Exp. Med.* 204:1757–1764. doi:10.1084/jem.20070590.

Cuadrado, E., M. van den Biggelaar, S. de Kivit, Y. yen Chen, M. Slot, I. Doubal, A. Meijer, R.A.W. van Lier, J. Borst, and D. Amsen. 2018. Proteomic Analyses of Human Regulatory T Cells Reveal Adaptations in Signaling Pathways that Protect Cellular Identity. *Immunity*. 48:1046-1059.e6. doi:10.1016/j.immuni.2018.04.008.

Delgoffe, G.M., T.P. Kole, Y. Zheng, P.E. Zarek, K.L. Matthews, B. Xiao, P.F. Worley, S.C. Kozma, and J.D. Powell. 2009. The mTOR Kinase Differentially Regulates Effector and Regulatory T Cell Lineage Commitment. *Immunity*. 30:832–844. doi:10.1016/j.immuni.2009.04.014.

Dons, E.M., G. Raimondi, D.K.C. Cooper, and A.W. Thomson. 2011. Induced Regulatory T cells: Mechanisms of Conversion and Suppressive Potential. *Hum. Immunol.* 73:328–334. doi:10.1016/j.humimm.2011.12.011.

Duhen, T., R. Duhen, A. Lanzavecchia, F. Sallusto, and D.J. Campbell. 2012. Functionally distinct subsets of human FOXP3+ Treg cells that phenotypically mirror effector Th cells. *Blood*. 119:4430–4441. doi:10.1182/blood-2011-11-392324.The.

Egwuagu, C.E. 2009. STAT3 in CD4+ T helper cell differentiation and inflammatory diseases. *Cytokine*. 47:149–156. doi:10.1016/j.cyto.2009.07.003.

Fitch, E., E. Harper, I. Skorcheva, S.E. Kurtz, and A. Blauvelt. 2007. Pathophysiology of psoriasis: Recent advances on IL-23 and TH17 cytokines. *Curr. Rheumatol. Rep.* 9:461–467. doi:10.1007/s11926-007-0075-1.

Floess, S., J. Freyer, C. Siewert, U. Baron, S. Olek, J. Polansky, K. Schlawe, H.D. Chang, T. Bopp, E. Schmitt, S. Klein-Hessling, E. Serfling, A. Hamann, and J. Huehn. 2007. Epigenetic control of the foxp3 locus in regulatory T cells. *PLoS Biol.* 5:0169–0178. doi:10.1371/journal.pbio.0050038.

Fontenot, J.D., M.A. Gavin, and A.Y. Rudensky. 2003. Foxp3 programs the development and function of CD4+CD25+ regulatory T cells. *Nat.Immunol.* 4:330–336. doi:10.1038/ni904.

Foster, D.A., and A. Toschi. 2009. Targeting mTOR with rapamycin: One dose does not fit all. *Cell Cycle*. 8:1026–1029. doi:10.4161/cc.8.7.8044.

Fuchs, A., M. Gliwinski, N. Grageda, R. Spiering, A.K. Abbas, S. Appel, R. Bacchetta, M. Battaglia, D. Berglund, B. Blazar, J.A. Bluestone, M. Bornhäuser, A. ten Brinke, T.M. Brusko, N. Cools, M.C. Cuturi, E. Geissler, N. Giannoukakis, K. Golab, D.A. Hafler, S.M. van Ham, J. Hester, K. Hippen, M. Di Ianni, N. Ilic, J. Isaacs, F. Issa, D. Iwaszkiewicz-Grzes, E. Jaeckel, I. Joosten, D. Klatzmann, H. Koenen, C. van Kooten, O. Korsgren, K. Kretschmer, M. Levings, N.M. Marek-Trzonkowska, M. Martinez-Llordella, D. Miljkovic, K.H.G. Mills, J.P. Miranda, C.A. Piccirillo, A.L. Putnam, T. Ritter, M.G. Roncarolo, S. Sakaguchi, S. Sánchez-Ramón, B. Sawitzki, L. Sofronic-Milosavljevic, M. Sykes, Q. Tang, M. Vives-Pi, H. Waldmann, P. Witkowski, K.J. Wood, S. Gregori, C.M.U. Hilkens, G. Lombardi, P. Lord, E.M. Martinez-Caceres, and P. Trzonkowski. 2018. Minimum information about T regulatory cells: A step toward reproducibility and standardization. *Front. Immunol.* 8:1844. doi:10.3389/fimmu.2017.01844.

Furusawa, Y., Y. Obata, S. Fukuda, T.A. Endo, G. Nakato, D. Takahashi, Y. Nakanishi, C. Uetake, K. Kato, T. Kato, M. Takahashi, N.N. Fukuda, S. Murakami, E. Miyauchi, S. Hino, K. Atarashi, S. Onawa, Y. Fujimura, T. Lockett, J.M. Clarke, D.L. Topping, M. Tomita, S. Hori, O. Ohara, T. Morita, H. Koseki, J. Kikuchi, K. Honda, K. Hase, and H. Ohno. 2013. Commensal microbe-derived butyrate induces the differentiation of colonic regulatory T cells. *Nature*. 504:446–450. doi:10.1038/nature12721.

Ghali, J.R., M.A. Alikhan, S.R. Holdsworth, and A.R. Kitching. 2017. Induced regulatory T cells are phenotypically unstable and do not protect mice from rapidly progressive glomerulonephritis. *Immunology*. 150:100–114. doi:10.1111/imm.12671.

Gu, J., L. Lu, M. Chen, L. Xu, Q. Lan, Q. Li, Z. Liu, G. Chen, P. Wang, X. Wang, D. Brand, N. Olsen, and S.G. Zheng. 2014. TGF-β–Induced CD4 + Foxp3 + T Cells Attenuate Acute Graft-versus-Host Disease

by Suppressing Expansion and Killing of Effector CD8 + Cells . *J. Immunol.* 193:3388–3397. doi:10.4049/jimmunol.1400207.

Hill, D., N. Eastaff-Leung, S. Bresatz-Atkins, N. Warner, J. Ruitenberg, D. Krumbiegel, S. Pederson, N. McInnes, C.Y. Brown, T. Sadlon, and S.C. Barry. 2012. Inhibition of activation induced CD154 on CD4+ CD25- cells: a valid surrogate for human Treg suppresor function. *Immunol. Cell Biol.* 90:812–821. doi:10.1038/icb.2012.18.

Hippen, K.L., S.C. Merkel, D.K. Schirm, C. Nelson, N.C. Tennis, J.L. Riley, C.H. June, J.S. Miller, J.E. Wagner, and B.R. Blazar. 2011. Generation and large-scale expansion of human inducible regulatory T cells that suppress graft-versus-host disease. *Am. J. Transplant.* 11:1148–1157. doi:10.1111/j.1600-6143.2011.03558.x.

Hori, S., T. Nomura, and S. Sakaguchi. 2003. Control of regulatory T cell development by the transcription factor Foxp3. *Science.* 299:1057–1061. doi:10.1126/science.1079490.

Jandl, C., S.M. Liu, P.F. Cañete, J. Warren, W.E. Hughes, A. Vogelzang, K. Webster, M.E. Craig, G. Uzel, A. Dent, P. Stepensky, B. Keller, K. Warnatz, J. Sprent, and C. King. 2017. IL-21 restricts T follicular regulatory T cell proliferation through Bcl-6 mediated inhibition of responsiveness to IL-2. *Nat. Commun.* 8. doi:10.1038/ncomms14647.

Jung, M.K., J.-E. Kwak, and E.-C. Shin. 2017. IL-17A-Producing Foxp3 + Regulatory T Cells and Human Diseases . *Immune Netw.* 17:276. doi:10.4110/in.2017.17.5.276.

Kanamori, M., H. Nakatsukasa, M. Okada, Q. Lu, and A. Yoshimura. 2016. Induced Regulatory T Cells : Their Development , Stability , and Applications. *Trends Immunol.* 37:803–811. doi:10.1016/j.it.2016.08.012.

Kim, B.S., H. Lu, K. Ichiyama, X. Chen, Y.B. Zhang, N.A. Mistry, K. Tanaka, Y. hee Lee, R. Nurieva, L. Zhang, X. Yang, Y. Chung, W. Jin, S.H. Chang, and C. Dong. 2017. Generation of RORγt + Antigen-Specific T Regulatory 17 Cells from Foxp3 + Precursors in Autoimmunity. *Cell Rep.* 21:195–207. doi:10.1016/j.celrep.2017.09.021.

Kryczek, I., S. Wei, L. Vatan, J. Escara-Wilke, W. Szeliga, E.T. Keller, and W. Zou. 2007. Cutting Edge: Opposite Effects of IL-1 and IL-2 on the Regulation of IL-17 + T Cell Pool IL-1 Subverts IL-2-Mediated Suppression . *J. Immunol.* 179:1423–1426. doi:10.4049/jimmunol.179.3.1423.

Laurence, A., C.M. Tato, T.S. Davidson, Y. Kanno, Z. Chen, Z. Yao, R.B.B. Blank, F. Meylan, R. Siegel, L. Hennighausen, E.M. Shevach, and J.J.J. O'Shea. 2007. Interleukin-2 Signaling via STAT5 Constrains T Helper 17 Cell Generation. *Immunity*. 26:371–381. doi:10.1016/j.immuni.2007.02.009.

Létourneau, S., C. Krieg, G. Pantaleo, and O. Boyman. 2009. IL-2- and CD25-dependent immunoregulatory mechanisms in the homeostasis of T-cell subsets. *J. Allergy Clin. Immunol.* 123:758–762. doi:10.1016/j.jaci.2009.02.011.

Li, J., S.G. Kim, and J. Blenis. 2014. Rapamycin: One drug, many effects. *Cell Metab.* 19:373–379. doi:10.1016/j.cmet.2014.01.001.

Li, L., J. Kim, and V.A. Boussiotis. 2010. IL-1β–Mediated Signals Preferentially Drive Conversion of Regulatory T Cells but Not Conventional T Cells into IL-17–Producing Cells. *J. Immunol.* 185:4148–4153. doi:10.4049/jimmunol.1001536.

Liu, W., A.L. Putnam, Z. Xu-Yu, G.L. Szot, M.R. Lee, S. Zhu, P.A. Gottlieb, P. Kapranov, T.R. Gingeras, B. Fazekas de St Groth, C. Clayberger, D.M. Soper, S.F. Ziegler, and J.A. Bluestone. 2006. CD127 expression inversely correlates with FoxP3 and suppressive function of human CD4+ T reg cells. *J. Exp. Med.* 203:1701–11. doi:10.1084/jem.20060772.

Luu, M., U. Steinhoff, and A. Visekruna. 2017. Functional heterogeneity of gut-resident regulatory T cells. *Clin. Transl. Immunol.* 6:e156. doi:10.1038/cti.2017.39.

Ma, H., W. Gao, X. Sun, and W. Wang. 2018. STAT5 and TET2 cooperate to regulate FOXP3-TSDR demethylation in CD4+ T cells of patients with colorectal cancer. *J. Immunol. Res.* 2018. doi:10.1155/2018/6985031.

Martinez, G.J., R.I. Nurieva, X.O. Yang, and C. Dong. 2008. Regulation and function of proinflammatory TH17 cells. *Ann. N. Y. Acad. Sci.* 1143:188–211. doi:10.1196/annals.1443.021.

Mohr, A., R. Malhotra, G. Mayer, G. Gorochov, and M. Miyara. 2018. Human FOXP3+ T regulatory cell heterogeneity. *Clin. Transl. Immunol.* 7:1–11. doi:10.1002/cti2.1005.

Muranski, P., and N.P. Restifo. 2013. Essentials of Th17 cell commitment and plasticity. *Blood*. 121:2402–2414. doi:10.1182/blood-2012-09-378653.

Oh, S.A., and M.O. Li. 2013. TGF-β: Guardian of T Cell Function. *J. Immunol.* 191:3973–3979. doi:10.4049/jimmunol.1301843.

Ohkura, N., M. Hamaguchi, H. Morikawa, K. Sugimura, A. Tanaka, Y. Ito, M. Osaki, Y. Tanaka, R. Yamashita, N. Nakano, J. Huehn, H.J. Fehling, T. Sparwasser, K. Nakai, and S. Sakaguchi. 2012. T Cell Receptor Stimulation-Induced Epigenetic Changes and Foxp3 Expression Are Independent and Complementary Events Required for Treg Cell Development. *Immunity*. 37:785–799. doi:10.1016/j.immuni.2012.09.010.

Pohar, J., Q. Simon, and S. Fillatreau. 2018. Antigen-specificity in the thymic development and peripheral activity of CD4+FOXP3+ T regulatory cells. *Front. Immunol.* 9:1701. doi:10.3389/fimmu.2018.01701.

Polansky, J.K., K. Kretschmer, J. Freyer, S. Floess, A. Garbe, U. Baron, S. Olek, A. Hamann, H. von Boehmer, and J. Huehn. 2008. DNA methylation controls Foxp3 gene expression. *Eur. J. Immunol.* 38:1654–1663. doi:10.1002/eji.200838105.

Relland, L.M., J.B. Williams, G.N. Relland, D. Haribhai, J. Ziegelbauer, M. Yassai, J. Gorski, and C.B. Williams. 2012. The TCR Repertoires of Regulatory and Conventional T Cells Specific for the Same Foreign Antigen Are Distinct. *J. Immunol.* 189:3566–3574. doi:10.4049/jimmunol.1102646.

Riquelme, P., J. Haarer, A. Kammler, L. Walter, S. Tomiuk, N. Ahrens, A.K. Wege, I. Goecze, D. Zecher, B. Banas, R. Spang, F. Fändrich, M.B. Lutz, B. Sawitzki, H.J. Schlitt, J. Ochando, E.K. Geissler, and J.A. Hutchinson. 2018. TIGIT + iTregs elicited by human regulatory macrophages control T cell immunity. *Nat. Commun.* 9:1–18. doi:10.1038/s41467-018-05167-8.

Romano, M., G. Fanelli, C.J. Albany, G. Giganti, and G. Lombardi. 2019. Past, present, and future of regulatory T cell therapy in transplantation and autoimmunity. *Front. Immunol.* 10:43. doi:10.3389/fimmu.2019.00043.

De Rosa, V., M. Galgani, A. Porcellini, A. Colamatteo, M. Santopaolo, C. Zuchegna, A. Romano, S. De Simone, C. Procaccini, C. La Rocca, P.B. Carrieri, G.T. Maniscalco, M. Salvetti, M.C. Buscarinu, A. Franzese, E. Mozzillo, A. La Cava, and G. Matarese. 2015. Glycolysis controls the induction of human regulatory T cells by modulating the expression of FOXP3 exon 2 splicing variants. *Nat. Immunol.* 16:1174–1184. doi:10.1038/ni.3269.

Rossetti, M., R. Spreafico, S. Saidin, C. Chua, M. Moshref, J.Y. Leong, Y.K. Tan, J. Thumboo, J. van Loosdregt, and S. Albani. 2015. Ex Vivo–Expanded but Not In Vitro–Induced Human Regulatory T Cells Are Candidates for Cell Therapy in Autoimmune Diseases Thanks to Stable Demethylation of the

FOXP3 Regulatory T Cell–Specific Demethylated Region. *J. Immunol.* 194:113–124. doi:10.4049/jimmunol.1401145.

Russler-Germain, E. V., S. Rengarajan, and C.S. Hsieh. 2017. Antigen-specific regulatory T-cell responses to intestinal microbiota. *Mucosal Immunol.* 10:1375–1386. doi:10.1038/mi.2017.65.

Sadlon, T.J., B.G. Wilkinson, S. Pederson, C.Y. Brown, S. Bresatz, T. Gargett, L. Melville, K. Peng, R.J.D. Andrea, G. Gary, G.J. Goodall, H. Zola, M. Frances, S.C. Barry, S. Bresatz, T. Gargett, E.L. Melville, and K. Peng. 2010. Genome-Wide Identification of Human FOXP3 Target Genes in Natural Regulatory T Cells. *J. Immunol.* 185:1071–1081. doi:10.4049/jimmunol.1000082.

Safinia, N., and G. Lombardi. 2015. Regulatory T cells : serious contenders in the promise for immunological tolerance in transplantation. *Front. Immunol.* 6:438. doi:10.3389/fimmu.2015.00438.

Sakaguchi, S., N. Sakaguchi, M. Asano, M. Itoh, and M. Toda. 1995. Immunologic Self-Tolerance is Maintained by Activated T cells Expressing IL-2 Receptor Alpha-Chains (CD25). Breakdown of a Single Mechanism of Self-Tolerance Causes Various Autoimmune Diseases. *J. Immunol.* 155:1151–1164. doi:10.4049/jimmunol.164.8.4321.

Sakaguchi, S., T. Yamaguchi, T. Nomura, and M. Ono. 2008. Regulatory T Cells and Immune Tolerance. *Cell*. 133:775–787. doi:10.1016/j.cell.2008.05.009.

Samstein, R., S. Josefowicz, A. Arvey, P. Treuting, and A.Y. Rudensky. 2012. Extrathymic generation of regulatory T cells in placental mammals mitigates maternal-fetal conflict. *Cell*. 150:29–38. doi:10.1016/j.cell.2012.05.031.

Sasidharan Nair, V., M.H. Song, and K.I. Oh. 2016. Vitamin C Facilitates Demethylation of the Foxp3 Enhancer in a Tet-Dependent Manner . *J. Immunol.* 196:2119–2131. doi:10.4049/jimmunol.1502352.

Schmidt, A., M. Eriksson, M.M. Shang, H. Weyd, and J. Tegnér. 2016. Comparative analysis of protocols to induce human CD4+Foxp3+ regulatory T cells by combinations of IL-2, TGF-beta, retinoic acid, rapamycin and butyrate. *PLoS One*. 11:1–31. doi:10.1371/journal.pone.0148474.

Schmidt, A., F. Marabita, N.A. Kiani, C.C. Gross, H.J. Johansson, S. Éliás, S. Rautio, M. Eriksson, S.J. Fernandes, G. Silberberg, U. Ullah, U. Bhatia, H. Lähdesmäki, J. Lehtiö, D. Gomez-Cabrero, H. Wiendl, R. Lahesmaa, and J. Tegnér. 2018. Time-resolved transcriptome and proteome landscape of human regulatory T cell (Treg) differentiation reveals novel regulators of FOXP3. *BMC Biol.* 16:1–36.

doi:10.1186/s12915-018-0518-3.

Schmitt, E.G., and C.B. Williams. 2013. Generation and function of induced regulatory T cells. *Front. Immunol.* 4:152. doi:10.3389/fimmu.2013.00152.

Schreiber, L., B. Pietzsch, S. Floess, C. Farah, L. Jänsch, I. Schmitz, and J. Huehn. 2014. The Treg-specific demethylated region stabilizes Foxp3 expression independently of NF-κB signaling. *PLoS One*. 9:e88318. doi:10.1371/journal.pone.0088318.

Seddiki, N., B. Santner-Nanan, J. Martinson, J. Zaunders, S. Sasson, A. Landay, M. Solomon, W. Selby, S.I. Alexander, R. Nanan, A. Kelleher, and B. Fazekas de St Groth. 2006. Expression of interleukin (IL)-2 and IL-7 receptors discriminates between human regulatory and activated T cells. *J. Exp. Med.* 203:1693–700. doi:10.1084/jem.20060468.

Singer, B.D., L.S. King, and F.R.D. Alessio. 2014. Regulatory T cells as immunotherapy. *Front. Immunol.* 5:46. doi:10.3389/fimmu.2014.00046.

Someya, K., H. Nakatsukasa, M. Ito, T. Kondo, K. ichi Tateda, T. Akanuma, I. Koya, T. Sanosaka, J. Kohyama, Y. ichi Tsukada, T. Takamura-Enya, and A. Yoshimura. 2017. Improvement of Foxp3 stability through CNS2 demethylation by TET enzyme induction and activation. *Int. Immunol.* 29:365–375. doi:10.1093/intimm/dxx049.

Szurek, E., A. Cebula, L. Wojciech, M. Pietrzak, G. Rempala, P. Kisielow, and L. Ignatowicz. 2015. Differences in expression level of Helios and neuropilin-1 do not distinguish thymus-derived from extrathymically-induced CD4+Foxp3+ regulatory T cells. *PLoS One*. 10:1–16. doi:10.1371/journal.pone.0141161.

Tran, D.Q. 2012. TGF-β: The sword, the wand, and the shield of FOXP3 + regulatory T cells. *J. Mol. Cell Biol.* 4:29–37. doi:10.1093/jmcb/mjr033.

Travis, M.A., and D. Sheppard. 2014. TGF-β Activation and Function in Immunity. *Annu. Rev. Immunol.* 32:51–82. doi:10.1146/annurev-immunol-032713-120257.

Wakamatsu, E., H. Omori, A. Kawano, S. Ogawa, and R. Abe. 2018. Strong TCR stimulation promotes the stabilization of Foxp3 expression in regulatory T cells induced in vitro through increasing the demethylation of Foxp3 CNS2. *Biochem. Biophys. Res. Commun.* 503:2597–2602. doi:10.1016/j.bbrc.2018.07.021.

Wherry, E.J. 2011. T cell exhaustion. *Nat. Immunol.* 12:492–499. doi:10.1038/ni.2035.

Yadav, M., S. Stephan, and J.A. Bluestone. 2013. Peripherally induced Tregs-role in immune homeostasis and autoimmunity. *Front. Immunol.* 4:232. doi:10.3389/fimmu.2013.00232.

Zanin-Zhorov, A., S. Kumari, K.L. Hippen, S.C. Merkel, M.L. MacMillan, B.R. Blazar, and M.L. Dustin. 2017. Human in vitro-induced regulatory T cells display Dlgh1dependent and PKC-θ restrained suppressive activity. *Sci. Rep.* 7:1–8. doi:10.1038/s41598-017-04053-5.

Zhang, P., S.-K. Tey, M. Koyama, R.D. Kuns, S.D. Olver, K.E. Lineburg, M. Lor, B.E. Teal, N.C. Raffelt, J. Raju, L. Leveque, K.A. Markey, A. Varelias, A.D. Clouston, S.W. Lane, K.P.A. MacDonald, and G.R. Hill. 2013. Induced Regulatory T Cells Promote Tolerance When Stabilized by Rapamycin and IL-2 In Vivo. *J. Immunol.* 191:5291–5303. doi:10.4049/jimmunol.1301181.

Zheng, S.G., J. Wang, P. Wang, J.D. Gray, and D.A. Horwitz. 2007. IL-2 Is Essential for TGF-β to Convert Naive CD4 + CD25 − Cells to CD25 + Foxp3 + Regulatory T Cells and for Expansion of These Cells . *J. Immunol.* 178:2018–2027. doi:10.4049/jimmunol.178.4.2018.

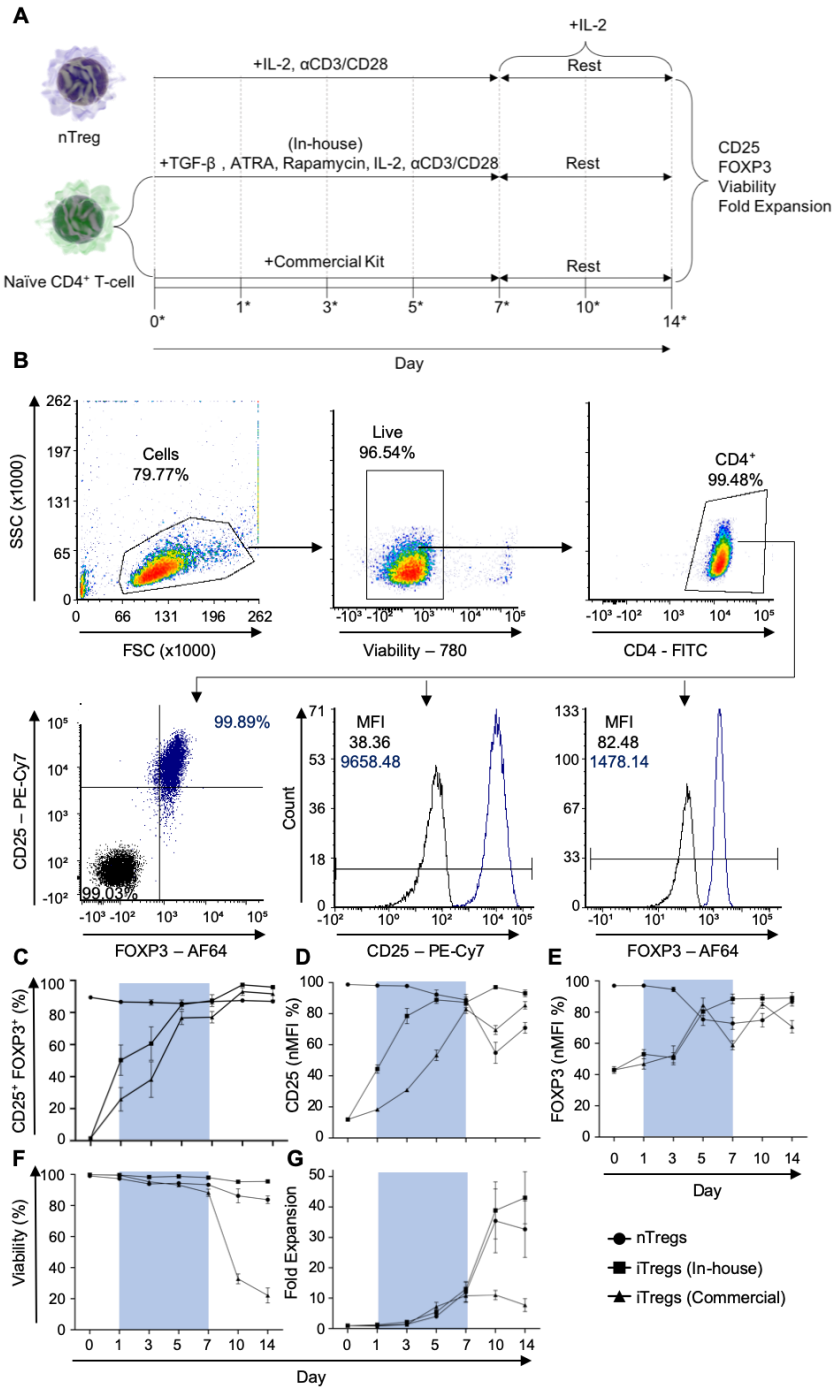


Figure 1. **Time-course analysis of iTreg characteristics. (A)** Schematic for experimental design. nTregs were expanded with αCD3/CD28 beads and IL-2. iTregs were differentiated from naïve CD4⁺ T-cells using the in-house optimized method and a commercial kit. iTregs (In-house) was expanded with αCD3/CD28 beads and IL-2. The commercial kit included components for expansion. Following 7-day expansion, cells were rested up to 7 days with IL-2. Cells were analyzed on daypecified with asterisks. Expression of CD25 and FOXP3, viability and fold expansion were analyzed. MFI of CD25 and FOXP3 normalized to the maximum raw value in each experiment. **(B)** Gating strategy to determine viability, %CD25⁺FOXP3⁺ and MFI of CD25 and FOXP3 (unstained nTreg: black; stained nTreg: indigo). Viability was measured from lymphocyte population while %CD25⁺FOXP3⁺ and MFI of CD25 and FOXP3 were measured from viable CD4⁺ population. MFI was normalized to the maximum raw value in each marker and experiment. Fold expansion was calculated by tracking cell counts at each timepoints. Time-course analysis for **(C)** %CD25⁺FOXP3⁺, **(D)** CD25 MFI, **(E)** FOXP3 MFI, **(F)** Viability and **(G)** Fold expansion. Blue-shaded area indicates expansion. Data represented as mean ± SEM, n=3.

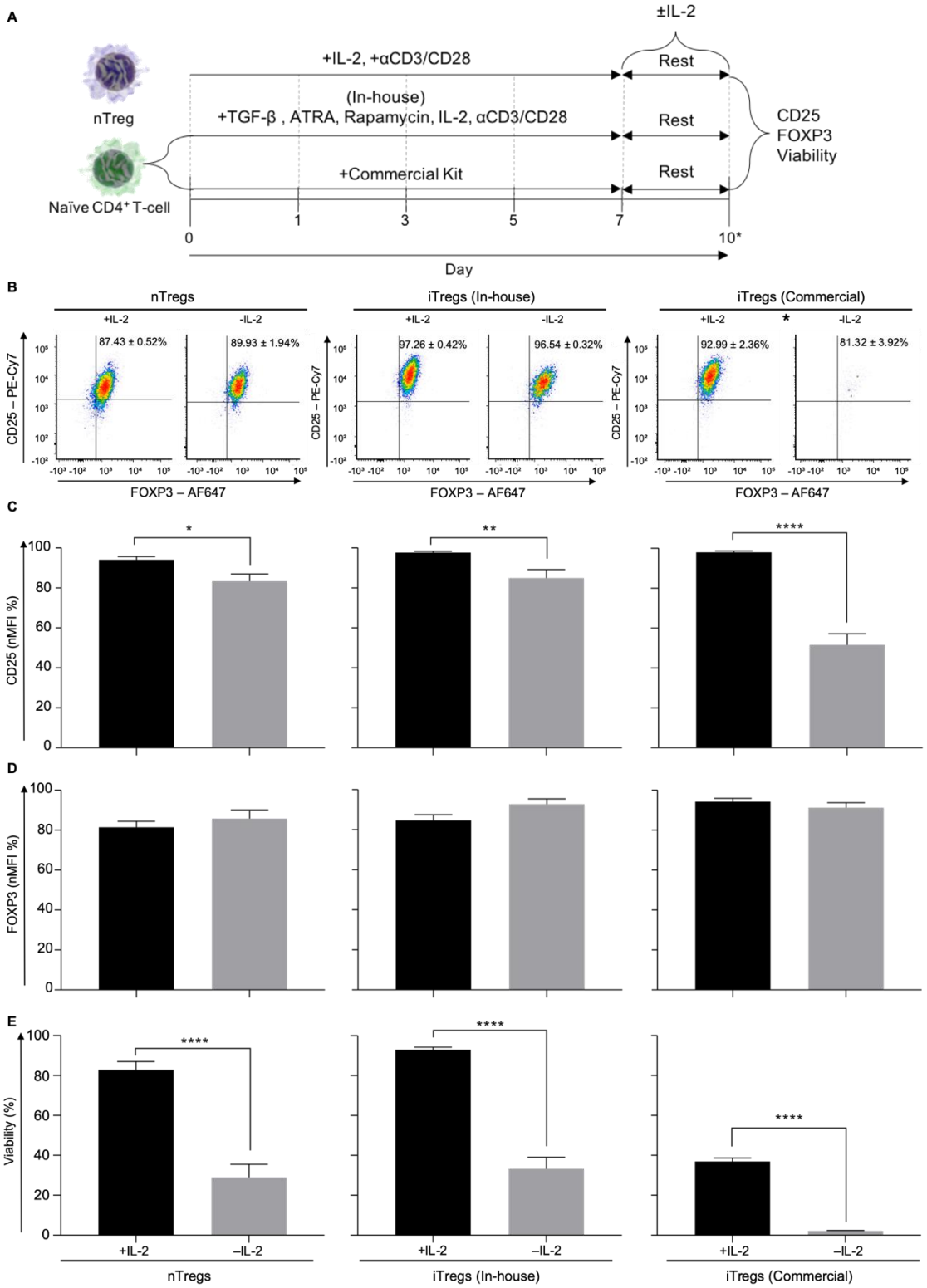


Figure 2. **Stability of iTregs in the absence of IL-2. (A)** Schematic for experimental design. Following 7-day expansion, cells were rested for 3 days with or without IL-2. Cells were analyzed at the end-point of the experiment (day 10) specific by an asterisk. Expression of CD25 and FOXP3 and viability were analyzed. MFI of CD25 and FOXP3 normalized to the maximum raw value in each experiment. **(B)** %CD25$^{+}$FOXP3$^{+}$, **(C)** CD25 MFI, **(D)** FOXP3 MFI and **(E)** Viability of nTregs, iTregs (In-house) and iTregs (Commercial) rested with or without IL-2. Data represented as mean ± SEM, n=3. Statistical significance identified by unpaired two-tailed T-test *P<0.05, **0.01, ***0.001, ****0.0001.

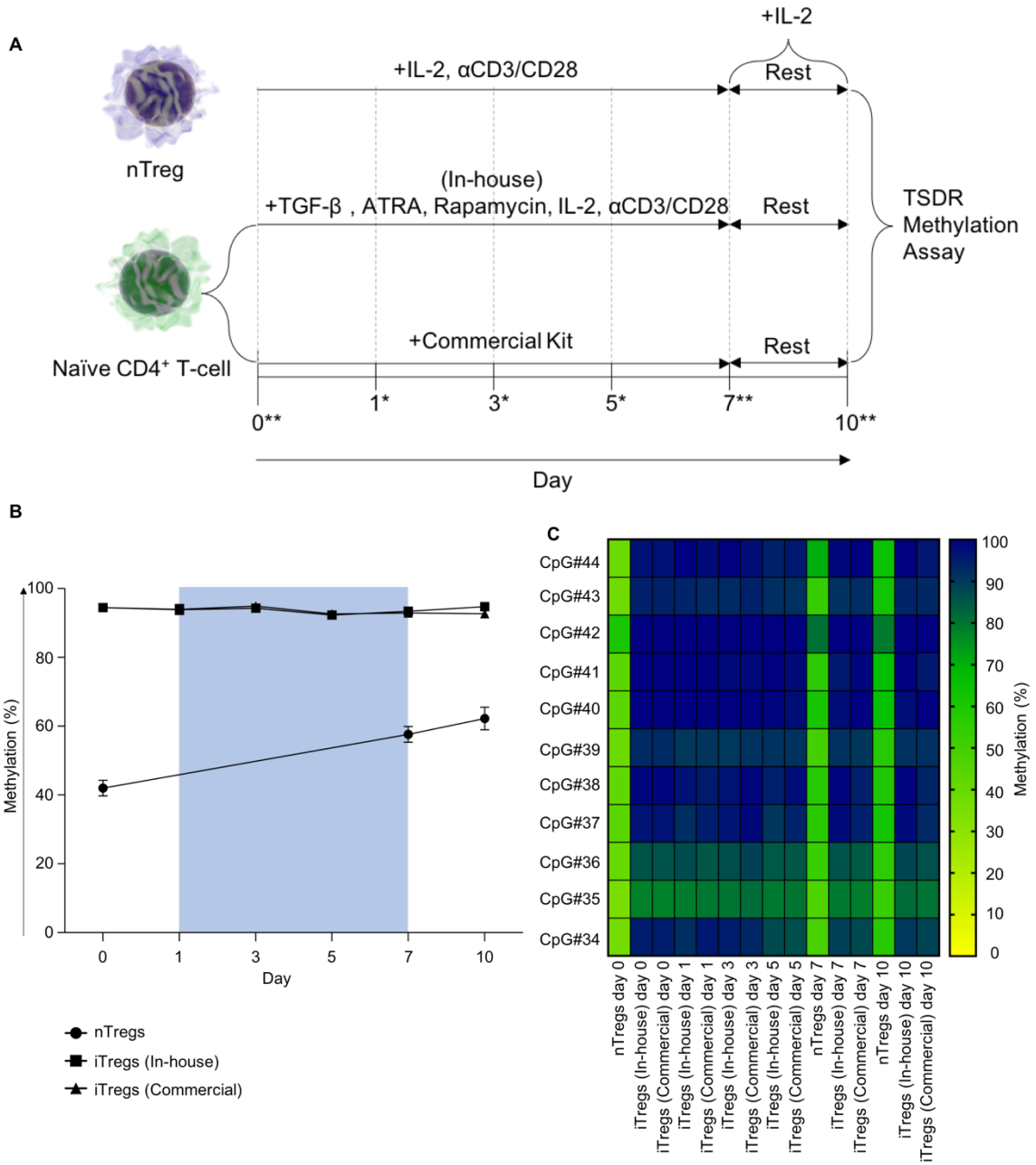


Figure 3. **TSDR methylation status of iTregs. (A)** Schematic representing experimental design. DNA of cells were harvested at timepoints specified by asterisks. Two asterisks indicate timepoints where DNA of Tregs was also harvested. Methylation levels of 11 CpG locations from TSDR in FOXP*3* CNS2 were measured by bisulfite pyrosequencing. **(B)** Time-course analysis of TSDR methylation status in nTregs, iTregs (In-house) and iTregs (Commercial). Methylation level of 11 CpG locations was averaged. Blue-shaded area indicates expansion. **(C)** Methylation levels of individual CpG locations in nTregs, iTregs (In-house) and iTregs (Commercial) at various timepoints. Data represented as mean ± SEM, n=3.

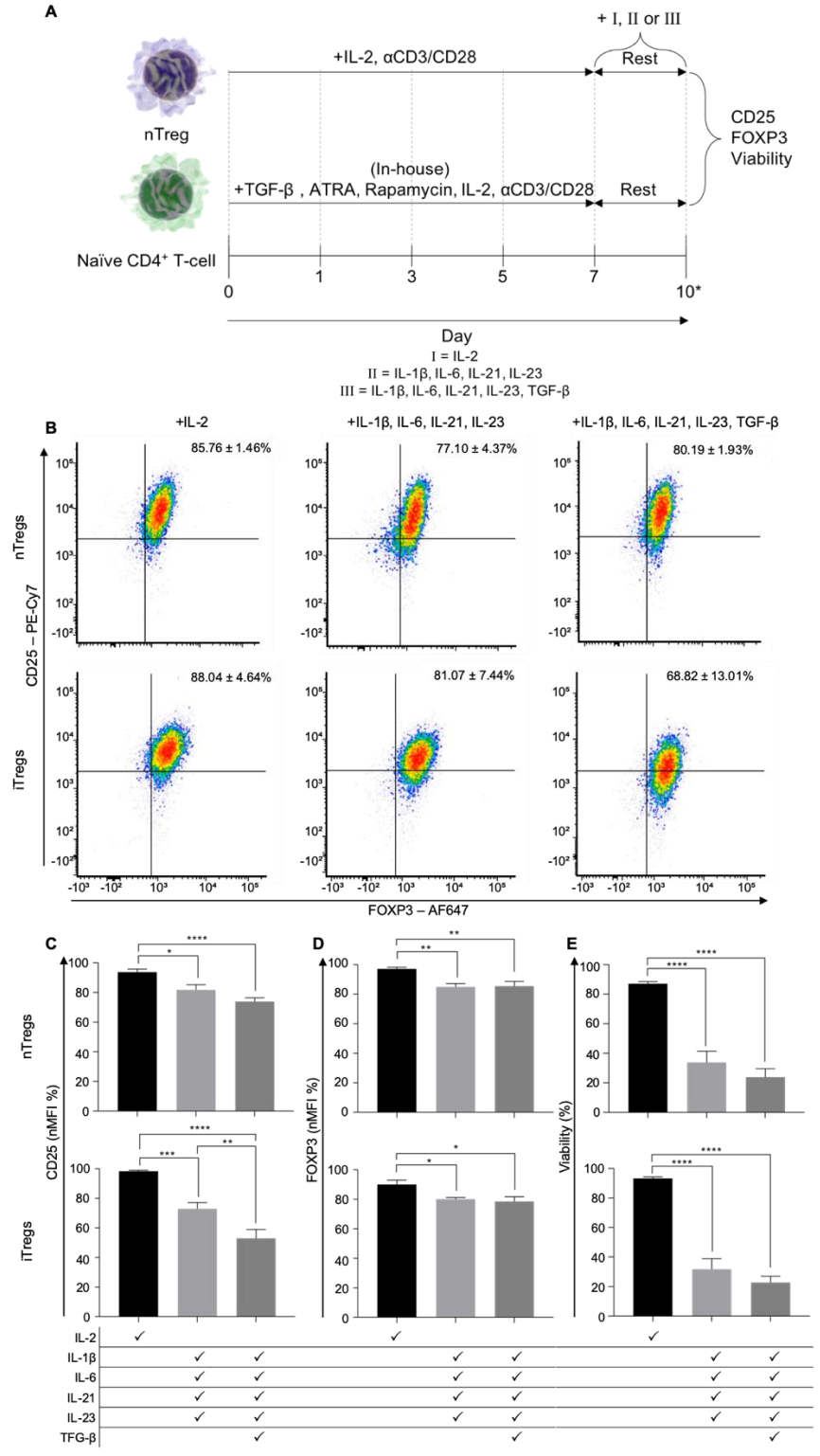


Figure 4. **Stability of iTregs in the presence of Th17-polarizing cytokines. (A)** Schematic for experimental design. Following 7-day expansion, cells were rested with (I) IL-2 or challenged with (II) IL-1β, IL-6, IL-21, IL-23 or (III) IL-1β, IL-6, IL-21, IL-23, TGF-β, for 3 days. Cells were analyzed at the end-point of the experiment (day 10) specified by an asterisk. Expression of CD25 and FOXP3 was analyzed. MFI of CD25 and FOXP3 normalized to the maximum raw value in each experiment. **(B)** %CD25$^{+}$FOXP3$^{+}$, **(C)** CD25 MFI, **(D)** FOXP3 MFI and **(E)** Viability of nTregs and iTregs (In-house) rested with (I) IL-2 or challenged with (II) IL1β, IL-6, IL-21, IL-23 or (III) IL1β, IL-6, IL-21, IL-23, TGF-β. Data represented as mean ± SEM, n=3. Statistical significance identified by One-way ANOVA with Tukey's multiple comparisons test *P<0.05, **0.01, ***0.001, ****0.0001.

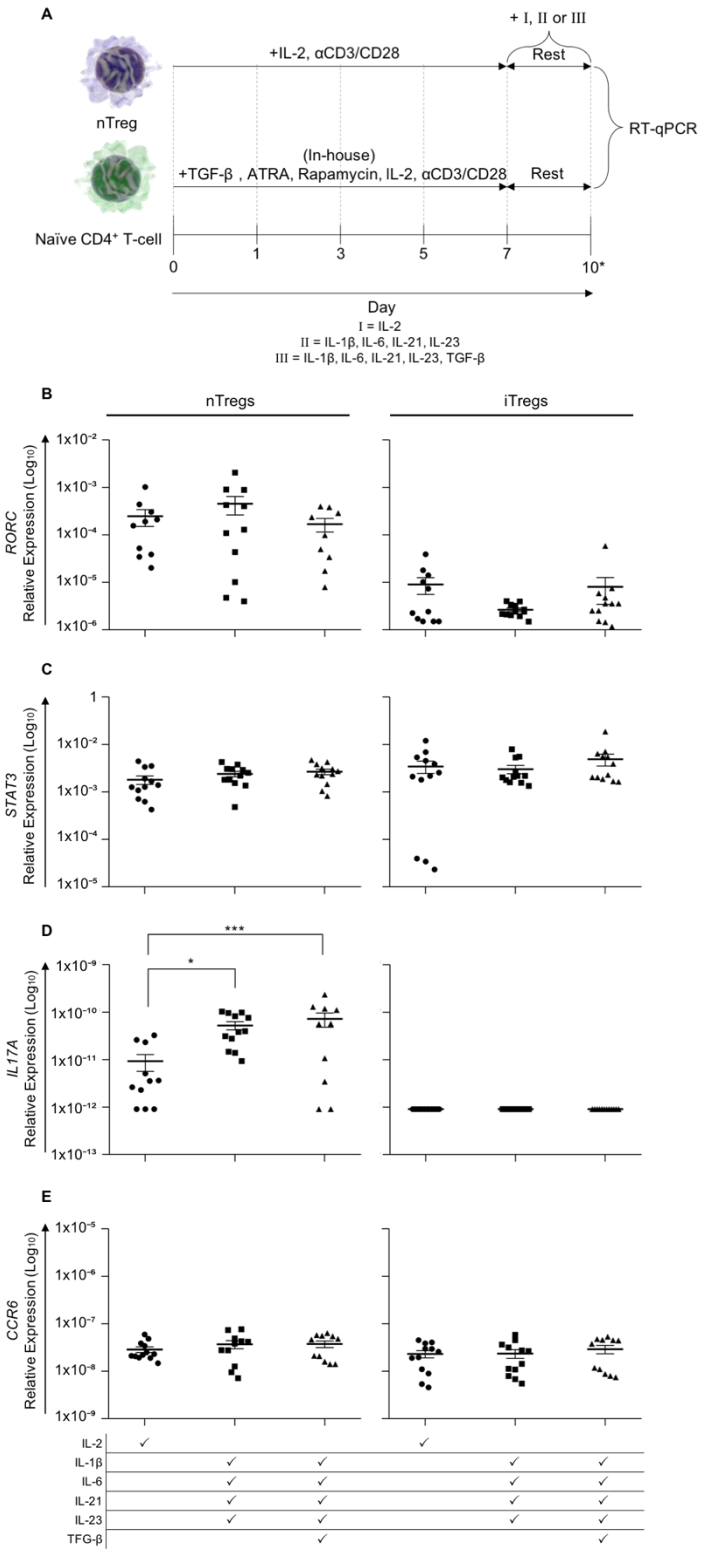


Figure 5. **Expression of Th17 signature genes in iTregs challenged with Th17-polarizing cytokines. (A)** Schematic for experimental design. Following 7-day expansion, cells were rested with (I) IL-2 or challenged with (II) IL-1β, IL-6, IL-21, IL-23 or (III) IL-1β, IL-6, IL-21, IL-23, TGF-β, for 3 days. RNA was harvested at the end-point of the experiment (day 10) specified by an asterisk. Expression of *RORC*, *STAT3*, *IL17A*, *CCR6* was measured via RT-qPCR. *rpl13a* was utilized as a housekeeping gene to calculate fold change in expression. Expression of **(B)** *RORC*, **(C)** *STAT3*, **(D)** *IL17A* and **(E)** *CCR6* in nTregs and iTregs (In-house) rested with (I) IL-2 or challenged with (II) IL1β, IL-6, IL-21, IL-23 or (III) IL1β, IL-6, IL-21, IL-23, TGF-β. Data represented as mean ± SEM, n=4. Statistical significance identified by One-way ANOVA with Tukey's multiple comparisons test *P<0.05, **0.01, ***0.001, ****0.0001.

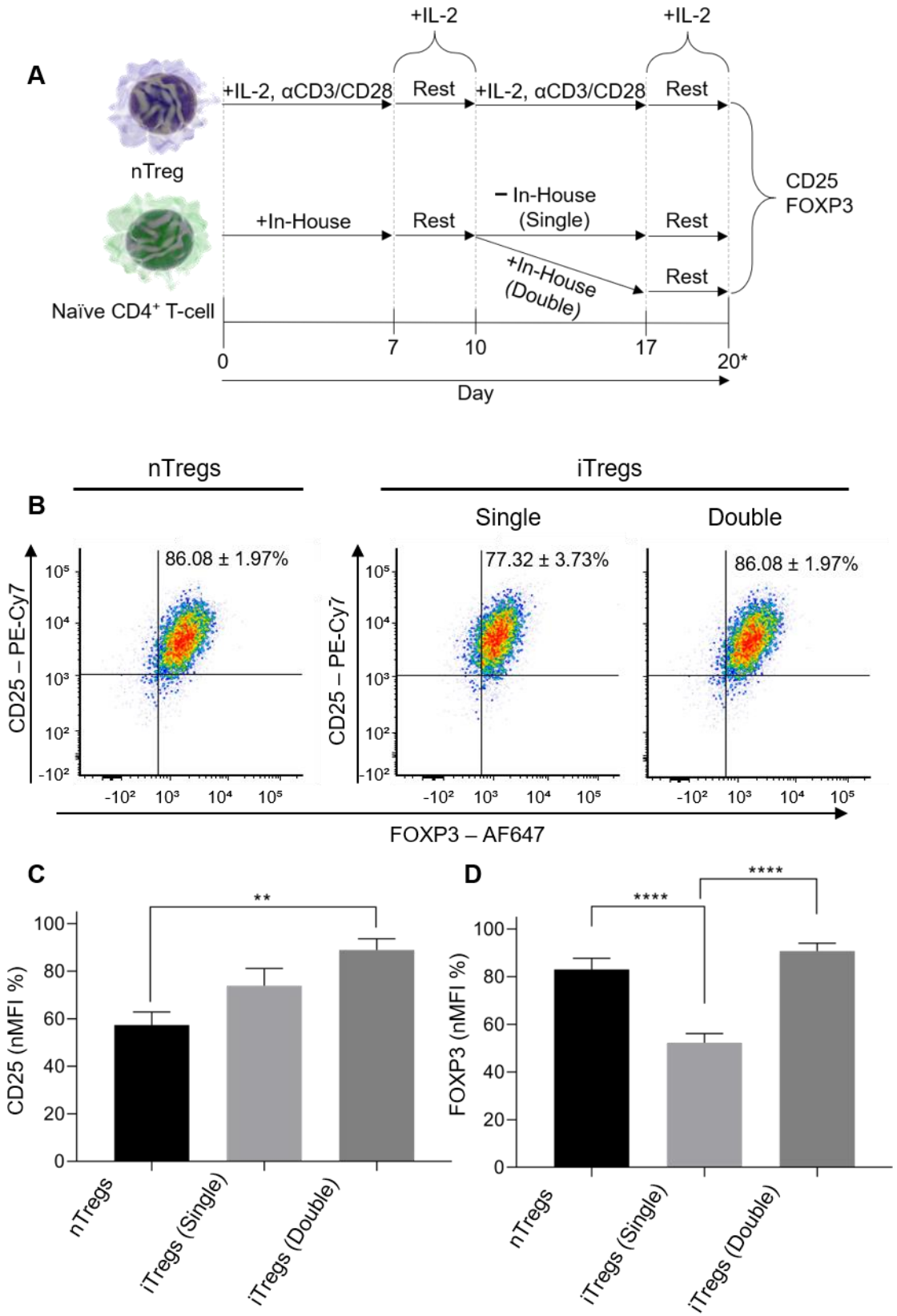


Figure 6. **Stability of iTregs upon re-stimulation without iTreg differentiation components. (A)** Schematic for experimental design. Following 7-day expansion and 3-day resting, cells were re-stimulated for 7 days then rested with IL-2 for 3 days. nTregs were re-stimulated with αCD3/CD28 beads and IL-2. iTregs (In-house) were re-stimulated either with iTreg differentiation components (double stimulated; "Double") or without iTreg differentiation components (single stimulated; "Single"). Cells were analyzed at the end-point of the experiment (day 20) specified by an asterisk. Expression of CD25 and FOXP3 was analyzed. MFI of CD25 and FOXP3 normalized to the maximum raw value in each experiment. **(B)** %CD25$^{+}$FOXP3$^{+}$, **(C)** CD25 MFI and **(D)** FOXP3 MFI of re-stimulated nTregs and iTregs (In-house) re-stimulated with or without iTreg differentiation components. Data represented as mean ± SEM, n=3. Statistical significance identified by One-way ANOVA with Tukey's multiple comparisons test *P<0.05, **0.01, ***0.001, ****0.0001.

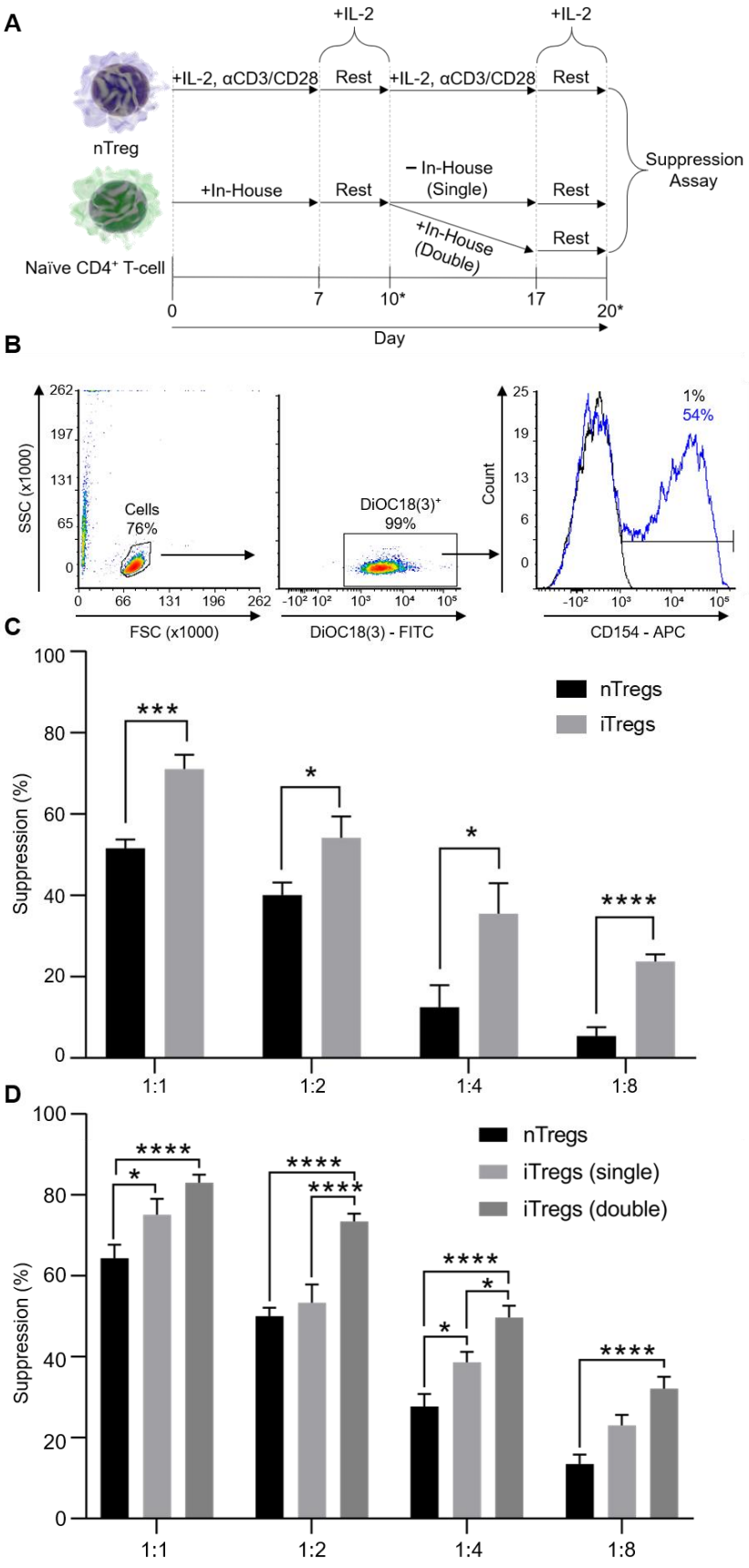


Figure 7. **Suppressive function of iTregs upon re-stimulation without iTreg differentiation components. (A)** Schematic for experimental design. Following 7-day expansion and 3-day resting, cells were re-stimulated for 7 days then rested with IL-2 for 3 days. nTregs were re-stimulated with αCD3/CD28 beads and IL-2. iTregs (In-house) were re-stimulated either with iTreg differentiation components (double stimulated; "Double") or without iTreg differentiation components (single stimulated; "Single"). Base-line suppressive activities of nTregs and iTregs were analyzed after initial expansion and resting (day 10) then suppressive activities of re-stimulated cells were analyzed at the end-point of the experiment (day 20). These timepoints are specified with asterisks. CD154 suppression assay was utilized to measure suppressive activities. **(B)** Gating strategy to determine %CD154$^{+}$ from DiOC$_{18}$(3)$^{+}$ cells. DiOC$_{18}$(3) was used differentiate naïve T-cells (Teffectors) from Tregs. Unstained control was used to gate for DiOC$_{18}$(3)$^{+}$. Negative control (black; DiOC$_{18}$(3)-labelled and CD154-stained with no anti-CD3/CD28 beads) set baseline non-activated %CD154$^{+}$. Positive control (blue; DiOC$_{18}$(3) and CD154 stained with anti-CD3/CD28 beads) provided baseline activated %CD154$^{+}$ to calculate %suppression. Control wells contained no Tregs. **(C)** Base-line %suppression of nTregs and iTregs. **(D)** %suppression of re-stimulated nTregs and iTregs (In-house) re-stimulated with or without iTreg differentiation components. Data represented as mean ± SEM, n=3. Statistical significance identified by unpaired two-tailed T-test (C) and Two-way ANOVA with Tukey's multiple comparisons test (D) *P<0.05, **0.01, ***0.001, ****0.0001.

# CONCLUSION

In conclusion, we have been the first to show successful encapsulated of human Tregs, using parameters that mimicked 3D-bioprinting. We demonstrated the minimal impact encapsulation has on Treg viability, phenotype and function while also confining Tregs in the hydrogel structure, preventing cell migration. We further demonstrated the positive impacts of hydrogel supplementation with IL-2 and CCL1. IL-2 improved encapsulated Treg viability, phenotype and function while CCL1 showed the capability of recruiting Treg-rich populations from peripheral blood, further augmenting the immunosuppressive milieu of the transplantation site. In this study, we encapsulated human Tregs subtypes, nTregs and iTregs, to evaluate the suitability of each type for encapsulation therapies. iTregs proved to be more suppressive than nTregs, indicating they may provide increased transplanted islet protection. Previously, phenotype instability and tendencies to convert into pathologic Th17 cells under pro-inflammatory environments, such as the site of allogeneic transplantation, have limited the use of iTregs for therapeutic applications. Thus, we optimized an iTreg differentiation protocol for the generation of stable human iTregs, utilizing TGF-β, ATRA and low-dose rapamycin. Our optimized method resulted in rapid generation of large number of iTregs with superior viability and phenotype compared to a commercially available kit. The stability of iTregs were demonstrated in environments previously shown to cause loss of FOXP3 expression, such as the absence of IL-2, the presence of Th17-polarising cytokines and upon re-stimulation without the differentiation components. Although our Tregs maintained methylated TSDR, iTregs displayed higher resistance to Th17-polarising cytokines than nTregs, with no upregulation of Th17 signature genes. iTregs remained highly suppressive upon re-stimulation, demonstrating their superiority to nTregs. The studies performed here provide a promising alternative utilizing 3D-bioprinting technology and human iTregs, tackling inherent challenges of conventional islet transplantation. Future experiments should evaluate the *in vitro* and *in vivo* immunomodulatory function of Tregs co-printed with islets. Furthermore, *in vivo* assessment of iTregs should be carried out to further confirm their stability, which may potentially shift the current paradigm of Treg stability by demonstrating that demethylation of TSDR is not required for stable expression FOXP3.

## *References*


1. Gregory JM, Moore DJ. Type 1 Diabetes Mellitus [Internet]. Pediatr. Rev. 2013. Doi:10.1016/B978-1-4377-1604-7.00561-3.

2. Ogurtsova K, da Rocha Fernandes JD, Huang Y, Linnenkamp U, Guariguata L, Cho NH, et al. IDF Diabetes Atlas: Global estimates for the prevalence of diabetes for 2015 and 2040. Diabetes Res Clin Pract. Elsevier B.V.; 2017;128:40–50. Doi:10.1016/j.diabres.2017.03.024.

3. Diabetes DOF. Diagnosis and classification of diabetes mellitus. Diabetes Care. 2013;36:67–74. Doi:10.2337/dc13-S067.

4. Forouhi NG, Wareham NJ. Epidemiology of diabetes. Medicine (Baltimore). 2014;42:698–702. Doi:10.1383/medc.2006.34.2.57.

5. Pathiraja V, Kuehlich JP, Campbell PD, Krishnamurthy B, Loudovaris T, Coates PTH, et al. Proinsulin-specific, HLA-DQ8, and HLA-DQ8-transdimer-restricted CD4+ T cells infiltrate islets in type 1 diabetes. Diabetes. 2015;64:172–82. Doi:10.2337/db14-0858.

6. Rezania A, Bruin JE, Arora P, Rubin A, Batushansky I, Asadi A, et al. Reversal of diabetes with insulin-producing cells derived in vitro from human pluripotent stem cells. Nat Biotechnol. 2014;32:1121–33. Doi:10.1038/nbt.3033.

7. Prabakar KR, Domínguez-Bendala J, Damaris Molano R, Pileggi A, Villate S, Ricordi C, et al. Generation of Glucose-Responsive, Insulin-Producing Cells from Human Umbilical Cord Blood-Derived Mesenchymal Stem Cells. Cell Transplant. 2012;21:1321–39. Doi:10.3727/096368911X612530.

8. Agarwal A, Brayman KL. Update on islet cell transplantation for type 1 diabetes. Semin Intervent Radiol. 2012;29:90–8. Doi:10.1055/s-0032-1312569.

9. Robertson RP, Davis C, Larsen J, Stratta R, Sutherland DER, American Diabetes Association. Pancreas and islet transplantation in type 1 diabetes. Diabetes Care. 2006;29:935. Doi:10.2337/diacare.29.04.06.dc06-9908.

10. Chan C, Chim TM, Leung K, Tong C, Wong T, Leung GK. Simultaneous pancreas and kidney transplantation as the standard surgical treatment for diabetes mellitus patients with end-stage renal disease. Hong Kong Med J. 2016; Doi:10.12809/hkmj154613.

11. Troppmann C. Complications after pancreas transplantation. Curr Opin Organ Transpl. 2010;15:112–8. Doi:10.1097/MOT.0b013e3283355349.

12. Vardanyan M, Parkin E, Gruessner C, Rilo HLR. Pancreas vs . islet transplantation : a call on the future. Curr Opin Organ Transplant. 2010;15:124–30. Doi:10.1097/MOT.0b013e32833553f8.

13. Robertson RP. Islet Transplantation as a Treatment for Diabetes — A Work in Progress. N Engl J Med. 2004;350:694–705. Doi:10.1056/NEJMra032425.

14. Connell PJO, Holmes-Walker DJ, Goodman D, Hawthorne WJ, Loudovaris T, Gunton JE, et al. Multicenter Australian Trial of Islet Transplantation : Improving Accessibility and Outcomes. Am J Transplant. 2013;13:1850–8. Doi:10.1002/ajt.12250.

15. Ichii H, Ricordi C. Current status of Islet Cell transplantation. J Hepatobiliary Pancreat Surg. 2013;16:101–12. Doi:10.1007/s00534-008-0021-2.Current.

16. Lacy PE, Walker MM, Fink CJ, Louis S. Perifusion of Isolated Rat Islets in Vitro Participation of the Microtubular System in the Biphasic Release of Insulin. Diabetes. 1972;21:987–98. Doi:10.2337/diab.21.10.987.

17. Najarian JS, Sutherland DER, Baumgartner D, Burke B, Rynasiewicz JJ, Matas AJ, et al. Total or near total pancreatectomy and islet autotransplantation for treatment of chronic pancreatitis.pdf. Ann Surg. 1980;192:526–42. Doi:0003-4932/80/1000/0526.

18. Robertson RP, Lanz KJ, Sutherland DER, Kendall DM. Prevention of Diabetes for up to 13 Years by Autoislet Transplantation after Pancreatectomy for Chronic Pancreatitis. Diabetes. 2001;50:48–50. Doi:10.2337/diabetes.50.1.47.

19. Shapiro AMJ, Lakey JRT, Ryan EA, Korbutt GS, Toth E, Warnock GL, et al. Islet Transplantation in Seven Patients with Type 1 Diabetes Mellitus Using a Glucocoricoid-Free Imunosuppressive Regimen. N Engl J Med. 2000;343:230–8. Doi:10.1056/NEJM200007273430401.

20. Ryan EA, Paty BW, Senior PA, Bigam D, Alfadhli E, Kneteman NM, et al. Five-Year Follow-Up After Clinical Islet Transplantation. Diabetes. 2005;54:2060–9. Doi:diabetes.54.7.2060.

21. Leitão CB, Cure P, Tharvanji T, Baidal DA, Alejandro R. Current Challenges in Islet Transplantation. Curr Diab Rep. 2008;8:324–31. Doi:10.1007/s11892-008-0057-3.

22. Rheinheimer J, Bauer AC, Silveiro SP, Estivalet AAF, Bouças AP, Rosa AR, et al. Human pancreatic islet transplantation: an update and description of the establishment of a pancreatic islet isolation laboratory. Arch Endocrinol Metab. 2015;59:161–70. Doi:10.1590/2359-3997000000030.

23. Lacy PE, Kostianovsky M. Method for the isolation of intact islets of Langerhans from the rat pancreas. Diabetes. 1967;16:35–9. Doi:10.2337/diab.16.1.35.

24. Carlsson PO, Palm F, Andersson A, Liss P. Markedly decreased oxygen tension in transplanted rat pancreatic islets irrespective of the implantation site. Diabetes. 2001;50:489–95. Doi:10.2337/diabetes.50.3.489.

25. Bennet W, Sundberg B, Groth CG, Brendel MD, Brandhorst D, Brandhorst H, et al. Incompatibility between human blood and isolated islets of langerhans: A finding with implications for clinical intraportal islet transplantation? Diabetes. 1999;48:1907–14. Doi:10.2337/diabetes.48.10.1907.

26. Moberg L, Johansson H, Lukinius A, Berne C, Foss A, Källen R, et al. Production of tissue factor by pancreatic islet cells as a trigger of detrimental thrombotic reactions in clinical islet transplantation. Lancet. 360:2039–45. Doi:10.1016/S0140-6736(02)12020-4.

27. Van Der Windt DJ, Bottino R, Casu A, Campanile N, Cooper DKC. Rapid loss of intraportally transplanted islets: An overview of pathophysiology and preventive strategies. Xenotransplantation. 2007;14:288–97. Doi:10.1111/j.1399-3089.2007.00419.x.

28. Cantarelli E, Piemonti L. Alternative transplantation sites for pancreatic islet grafts. Curr Diab Rep. 2011;11:364–74. Doi:10.1007/s11892-011-0216-9.

29. Bennet W, Groth CG, Larsson R, Nilsson B, Korsgren O. Isolated human islets trigger an instant blood mediated inflammatory reaction: implications for intraportal islet transplantation as a treatment for patients with type 1 diabetes. Ups J Med Sci. 2000;105:125–33. Doi:10.1517/03009734000000059.

30. Golshayan D, Pascual M. Tolerance-inducing Immunosuppressive Strategies in Clinical Transplantation. Drugs. 2008;68:2113–30. Doi:10.1016/S0140-6736(98)07493-5.

31. Game DS, Lechler RI. Pathways of allorecognition: Implications for transplantation tolerance. Transpl Immunol. 2002;10:101–8. Doi:10.1016/S0966-3274(02)00055-2.

32. Caballero A, Fernandez N, Lavado R, Bravo MJ, Miranda JM, Alonso A. Tolerogenic response: Allorecognition pathways. Transpl Immunol. 2006;17:3–6. Doi:10.1016/j.trim.2006.09.034.

33. Afzali B, Lechler RI, Hernandez-Fuentes MP. Allorecognition and the alloresponse: Clinical implications. Tissue Antigens. 2007;69:545–56. Doi:10.1111/j.1399-0039.2007.00834.x.

34. Schwartz RE, Dameshek W. Drug-induced immunological tolerance. Nature. 1959;183:1682–3.

35. Hitchings G, Elion G. Chemical immunosuppression of the immune response. Pharmacol Rev. 1963;15:365–405.

36. Murray J, Merrill J, Harrison J, Wilson R, Dammin G. Prolonged survival of human-kidney homografts by immunosuppressive drug therapy. N Engl J Med. 1963;268:1315–23.

37. Kahan B. Cycolsporine. N Engl J Med. 1989;321:1725–38.

38. Calne R, Collier D, Lim S. Rapamycin in immunosuppression in organ allografting. Lancet. 1989;2:227.

39. Sawada S, Suzuki G, Kawase Y, Takaku F. Novel immunosuppressive agent, FK506: in vitro effects on the cloned T cell activation. J Immunol. 1987;139:1797–803.

40. Margolis RN, Holup JJ, Selawry HP. Effects of intratesticular islet transplantation on hepatic glycogen metabolism in the rat. Diabetes Res Clin Pract. 2:291–9. Doi:10.1016/S0168-8227(86)80006-7.

41. Ar'Rajab A, Dawidson IJ, Harris RB, Sentementes JT. Immune privilege of the testis for islet xenotransplantation (rat to mouse). Cell Transplant. 3:493–8. Doi:10.1177/096368979400300606.

42. Kemp CB, Knight MJ, Scharp DW, Ballinger WF, Lacy PE. Effect of transplantation site on the results of pancreatic islet isografts in diabetic rats. Diabetologia. 1973;9:486–91. Doi:10.1007/BF00461694.

43. Melzi R, Sanvito F, Mercalli A, Andralojc K, Bonifacio E, Piemonti L. Intrahepatic islet transplant in the mouse: functional and morphological characterization. Cell Transplant. 2008;17:1361–70. Doi:10.3727/096368908787648146.

44. Desai T, Shea LD. Advances in islet encapsulation technologies. Nat Rev Drug Discov. 2017;16:338–50. Doi:10.1038/nrd.2016.232.

45. Sakata N, Aoki T, Yoshimatsu G, Tsuchiya H, Hata T, Katayose Y, et al. Strategy for clinical setting in intramuscular and subcutaneous islet transplantation. Diabetes Metab Res Rev. 2014;30:1–10. Doi:10.1002/dmrr.

46. Mao G, Chen G, Bai H, Song T, Wang Y. The reversal of hyperglycaemia in diabetic mice using PLGA scaffolds seeded with islet-like cells derived from human embryonic stem cells. Biomaterials. 2009;30:1706–14. Doi:10.1016/j.biomaterials.2008.12.030.

47. Nicodemus GD, Bryant SJ. Cell Encapsulation in Biodegradable Hydrogels for Tissue Engineering Applications. Tissue Eng Part B Rev. 2008;14:149–65. Doi:10.1089/ten.teb.2007.0332.

48. Lee K, Mooney D. Alginate : properties and biomedical applications. Prog Polym Sci. 2012;37:106–26. Doi:10.1016/j.progpolymsci.2011.06.003.Alginate.

49. Sakata N, Sumi S, Yoshimatsu G, Goto M, Egawa S, Unno M. Encapsulated islets transplantation: Past, present and future. World J Gastrointest Pathophysiol. 2012;3:19–26. Doi:10.4291/wjgp.v3.i1.19.

50. Vériter S, Mergen J, Goebbels R-M, Aouassar N, Grégoire C, Jordan B, et al. In vivo selection of biocompatible alginates for islet encapsulation and subcutaneous transplantation. Tissue Eng Part A. 2010;16:1503–13. Doi:10.1089/ten.TEA.2009.0286.

51. Lum ZP, Tai IT, Krestow M, Norton J, Vacek I, Sun AM. Prolonged reversal of diabetic state in NOD mice by xenografts of microencapsulated rat islets. Diabetes. 1991;40:1511–6. Doi:10.2337/diab.40.11.1511.

52. Cui W, Barr G, Faucher KM, Sun X-L, Safley SA, Weber CJ, et al. A membrane-mimetic barrier for islet encapsulation. Transplant Proc. 2004;36:1206–8. Doi:10.1016/j.transproceed.2004.04.059.

53. Lamb M, Storrs R, Li S, Liang O, Laugenour K, Dorian R, et al. Function and viability of human islets encapsulated in alginate sheets: In vitro and in vivo culture. Transplant Proc. 2011;43:3265–6. Doi:10.1016/j.transproceed.2011.10.028.

54. Zhi ZL, Kerby A, King AJF, Jones PM, Pickup JC. Nano-scale encapsulation enhances allograft survival and function of islets transplanted in a mouse model of diabetes. Diabetologia. 2012;55:1081–90. Doi:10.1007/s00125-011-2431-y.

55. Ma M, Chiu A, Sahay G, Doloff JC, Dholakia N, Thakrar R, et al. Core-Shell Hydrogel Microcapsules for Improved Islets Encapsulation. Adv Healthc Mater. 2013;2:667–72. Doi:10.1002/adhm.201200341.

56. Hobbs HA, Kendall WF, Darrabie M, Opara EC. Prevention of morphological changes in alginate microcapsules for islet xenotransplantation. J Investig Med. 2001;49:572–5. Doi:10.2310/6650.2001.33722.

57. De Vos P, Hillebrands JL, De Haan BJ, Strubbe JH, Van Schilfgaarde R. Efficacy of a prevascularized expanded polytetrafluoroethylene solid support system as a transplantation site for pancreatic islets. Transplantation. 1997;63:824–30. Doi:10.1097/00007890-199703270-00006.

58. Dufour JM, Rajotte R V, Zimmerman M, Rezania A, Kin T, Dixon DE, et al. Development of an ectopic site for islet transplantation, using biodegradable scaffolds. Tissue Eng. 11:1323–31. Doi:10.1089/ten.2005.11.1323.

59. Wang RN, Rosenberg L. Maintenance of beta-cell function and survival following islet isolation requires re-establishment of the islet-matrix relationship. J Endocrinol. 1999;163:181–90. Doi:10.1677/joe.0.1630181.

60. Gibly RF, Zhang X, Graham ML, Hering BJ, Kaufman DB, Lowe WL, et al. Extrahepatic islet transplantation with microporous polymer scaffolds in syngeneic mouse and allogeneic porcine models. Biomaterials. 2011;32:9677–84. Doi:10.1016/j.biomaterials.2011.08.084.

61. Berman DM, O'Neil JJ, Coffey LCK, Chaffanjon PCJ, Kenyon NM, Ruiz P, et al. Long-term survival of nonhuman primate islets implanted in an omental pouch on a biodegradable scaffold. Am J Transplant. 2009;9:91–104. Doi:10.1111/j.1600-6143.2008.02489.x.

62. Blomeier H, Zhang X, Rives C, Brissova M, Hughes E, Baker M, et al. Polymer scaffolds as synthetic microenvironments for extrahepatic islet transplantation. Transplantation. 2006;82:452–9. Doi:10.1097/01.tp.0000231708.19937.21.

63. Murphy S V, Atala A. 3D bioprinting of tissues and organs. Nat Biotechnol. 2014;32:773–85. Doi:10.1038/nbt.2958.

64. Schubert C, van Langeveld MC, Donoso LA. Innovations in 3D printing: a 3D overview from optics to organs. Br J Ophthalmol. 2014;98:159–61. Doi:10.1136/bjophthalmol-2013-304446.

65. Ozbolat IT, Chen H, Yu Y. Development of 'Multi-arm Bioprinter' for hybrid biofabrication of tissue engineering constructs. Robot Comput Integr Manuf. 2014;30:295–304. Doi:10.1016/j.rcim.2013.10.005.

66. Kolesky DB, Truby RL, Gladman AS, Busbee TA, Homan KA, Lewis JA. 3D Bioprinting of Vascularized, Heterogeneous Cell-Laden Tissue Constructs. Adv Mater. 2014;26:3124–30. Doi:10.1002/adma.201305506.

67. Poldervaart MT, Gremmels H, van Deventer K, Fledderus JO, Oner FC, Verhaar MC, et al. Prolonged presence of VEGF promotes vascularization in 3D bioprinted scaffolds with defined architecture. J Control Release. 2014;184:58–66. Doi:10.1016/j.jconrel.2014.04.007.

68. Yue Z, Liu X, Coates PT, Wallace GG. Advances in printing biomaterials and living cells. Curr Opin Organ Transplant. 2016;21:467–75. Doi:10.1097/MOT.0000000000000346.

69. Mandrycky C, Wang Z, Kim K, Kim DH. 3D bioprinting for engineering complex tissues. Biotechnol Adv. Elsevier Inc.; 2016;34:422–34. Doi:10.1016/j.biotechadv.2015.12.011.

70. Di Bella C, Duchi S, O'Connell CD, Blanchard R, Augustine C, Yue Z, et al. In situ handheld three-dimensional bioprinting for cartilage regeneration. J Tissue Eng Regen Med. 2018;12:611–21. Doi:10.1002/term.2476.

71. Kesti M, Eberhardt C, Pagliccia G, Kenkel D, Grande D, Boss A, et al. Bioprinting Complex Cartilaginous Structures with Clinically Compliant Biomaterials. Adv Funct Mater. 2015;25:7406–17. Doi:10.1002/adfm.201503423.

72. Lee JW, Choi Y-J, Yong W-J, Pati F, Shim J-H, Kang KS, et al. Development of a 3D cell printed construct considering angiogenesis for liver tissue engineering Development of a 3D cell printed construct considering angiogenesis for liver tissue engineering. Biofabrication. 2016;8:015007. Doi:10.1088/1758-5090/7/2/025009.

73. Gu Q, Tomaskovic-crook E, Lozano R, Chen Y, Kapsa RM, Zhou Q, et al. Functional 3D Neural Mini-Tissues from Printed Gel-Based Bioink and Human Neural Stem Cells. Adv Healthc Mater. 2016;5:1429–38. Doi:10.1002/adhm.201600095.

74. Marchioli G, Van Gurp L, Van Krieken PP, Stamatialis D, Engelse M, Van Blitterswijk CA, et al. Fabrication of three-dimensional bioplotted hydrogel scaffolds for islets of Langerhans transplantation. Biofabrication. 2015;7. Doi:10.1088/1758-5090/7/2/025009.

75. Duin S, Schütz K, Ahlfeld T, Lehmann S, Lode A, Ludwig B, et al. 3D Bioprinting of Functional Islets of Langerhans in an Alginate / Methylcellulose Hydrogel Blend. Adv Healthc Mater. 2019;1801631:1–14. Doi:10.1002/adhm.201801631.

76. Penko D, Mohanasundaram D, Sen S, Drogemuller C, Mee C, Bonder CS, et al. Incorporation of endothelial progenitor cells into mosaic pseudoislets. Islets. 2011;3:73–9. Doi:10.4161/isl.3.3.15392.

77. Liu X, Carter S-SD, Renes MJ, Kim J, Rojas-Canales DM, Penko D, et al. Development of a Coaxial 3D Printing Platform for Biofabrication of Implantable Islet-Containing Constructs. Adv Healthc Mater. 2019;8:1801181. Doi:10.1002/adhm.201801181.

78. Bluestone J. Mechanisms of Tolerance. Immunol Rev. 2011;241:5–19. Doi:10.1002/9781118416426.ch12.

79. Walker LSK, Abbas AK. THE ENEMY WITHIN: KEEPING SELF-REACTIVE T CELLS AT BAY IN THE PERIPHERY. Nat Rev Immunol. 2002;2:11. Doi:10.1038/nri701.

80. Gershon R, Kondo K. Infectious Immunological Tolerance. Immunology. 1971;21:903–14.

81. Sakaguchi S, Takahashi T, Nishizuka Y. Study on Cellular Events in Post-Thymectomy Autoimmune OOphoritis in Mice. J Exp Med. 1982;156:1577–86.

82. Sakaguchi S, Fukuma K, Kuribayashi K, Masuda T. Organ-Specific Autoimmune Diseases Induced in Mice by Elimination of T Cell Subset. J Exp Med. 1985;161:72–87.

83. Sakaguchi S, Sakaguchi N, Asano M, Itoh M, Toda M. Immunologic Self-Tolerance is Maintained by Activated T cells Expressing IL-2 Receptor Alpha-Chains (CD25). Breakdown of a Single Mechanism of Self-Tolerance Causes Various Autoimmune Diseases. J Immunol. 1995;155:1151–64. Doi:10.4049/jimmunol.164.8.4321.

84. Baecher-Allan C, Brown JA, Freeman GJ, Hafler DA. CD4+CD25high Regulatory Cells in Human Peripheral Blood. J Immunol. 2001;167:1245–53. Doi:10.1073/pnas.1103810108.

85. Jonuleit H, Schmitt E, Stassen M, Tuettenberg A, Knop J, Enk AH. Identification and Functional Characterization of Human Cd4 $^{+}$ Cd25 $^{+}$ T Cells with Regulatory Properties Isolated from Peripheral Blood. J Exp Med. 2001;193:1285–94. Doi:10.1084/jem.193.11.1285.

86. Levings MK, Sangregorio R, Roncarolo MG. Human cd25(+)cd4(+) t regulatory cells suppress naive and memory T cell proliferation and can be expanded in vitro without loss of function. J Diabetes Res. 2001;193:1295–302.

87. Dieckmann D, Plottner H, Berchtold S, Berger T, Schuler G. Ex vivo isolation and characterization of CD4(+)CD25(+) T cells with regulatory properties from human blood. J Exp Med. 2001;193:1303–10. Doi:10.1084/jem.193.11.1303.

88. Hori S, Nomura T, Sakaguchi S. Control of regulatory T cell development by the transcription factor Foxp3. Science (80- ). 2003;299:1057–61. Doi:10.1126/science.1079490.

89. Fontenot JD, Gavin MA, Rudensky AY. Foxp3 programs the development and function of CD4+CD25+ regulatory T cells. NatImmunol. 2003;4:330–6. Doi:10.1038/ni904.

90. Khattri R, Cox T, Yasayko SA, Ramsdell F. An essential role for Scurfin in CD4+CD25+ T regulatory cells. NatImmunol. 2003;4:337–42. Doi:10.1038/ni909.

91. Liu W, Putnam AL, Xu-Yu Z, Szot GL, Lee MR, Zhu S, et al. CD127 expression inversely correlates with FoxP3 and suppressive function of human CD4+ T reg cells. J Exp Med. 2006;203:1701–11. Doi:10.1084/jem.20060772.

92. Seddiki N, Santner-Nanan B, Martinson J, Zaunders J, Sasson S, Landay A, et al. Expression of interleukin (IL)-2 and IL-7 receptors discriminates between human regulatory and activated T cells. J Exp Med. 2006;203:1693–700. Doi:10.1084/jem.20060468.

93. Xing Y, Hogquist KA. T-Cell Tolerance : Central and Peripheral. Cold Spring Harb Perspect Biol. 2012;1–16.

94. Sakaguchi S, Miyara M, Costantino CM, Hafler D a. FOXP3+ regulatory T cells in the human immune system. Nat Rev Immunol. 2010;10:490–500. Doi:10.1038/nri2785.

95. Lin X, Chen M, Liu Y, Guo Z, He X, Brand D, et al. Advances in distinguishing natural from induced Foxp3 + regulatory T cells. Int J Clin Exp Pathol. 2013;6:116–23.

96. Singer BD, King LS, Alessio FRD. Regulatory T cells as immunotherapy. Front Immunol. 2014;5:46. Doi:10.3389/fimmu.2014.00046.

97. Kanamori M, Nakatsukasa H, Okada M, Lu Q, Yoshimura A. Induced Regulatory T Cells : Their Development , Stability , and Applications. Trends Immunol. Elsevier Ltd; 2016;37:803–11. Doi:10.1016/j.it.2016.08.012.

98. Sakaguchi S, Yamaguchi T, Nomura T, Ono M. Regulatory T Cells and Immune Tolerance. Cell. 2008;133:775–87. Doi:10.1016/j.cell.2008.05.009.

99. Vignali DAA, Collison LW, Workman CJ. How regulatory T cells work. Nat Rev Immunol. 2008;8:523–32. Doi:10.1038/nri2343.

100. Bennett CL, Christie J, Ramsdell F, Brunkow ME, Ferguson PJ, Whitesell L, et al. The immune dysregulation, polyendocrinopathy, enteropathy, X-linked syndrome (IPEX) is caused by mutations of FOXP3. Nat Genet. 2001;27:20–1. Doi:10.1038/83713.

101. Tang Q, Bluestone JA. Regulatory T-Cell Therapy in Transplantation : Moving to the Clinic. Cold Spring Harb Perspect Med. 2013;3:a015552. Doi:10.1101/cshperspect.a015552.

102. Cunningham EC, Sharland AF, Alex Bishop G. Liver transplant tolerance and its application to the clinic: Can we exploit the high dose effect? Clin Dev Immunol. 2013;2013. Doi:10.1155/2013/419692.

103. Cippà PE, Fehr T. Spontaneous tolerance in kidney transplantation - An instructive, but very rare paradigm. Transpl Int. 2011;24:534–5. Doi:10.1111/j.1432-2277.2011.01260.x.

104. Orlando G, Hematti P, Stratta R, Burke G, Di Cocco P, Pisani F, et al. Clinical Operational Tolerance After Renal Transplantation. Ann Surg. 2010;252:915–28. Doi:10.1038/nbt.3121.ChIP-nexus.

105. Li W, Kuhr CS, Zheng XX, Carper K, Thomson AW, Reyes JD, et al. New insights into mechanisms of spontaneous liver transplant tolerance: The role of Foxp3-expressing CD25+CD4+ regulatory T cells. Am J Transplant. 2008;8:1639–51. Doi:10.1111/j.1600-6143.2008.02300.x.

106. Heidt S, Wood KJ. Biomarkers of Operational Tolerance in Solid Organ Transplantation. Expert Opin Med Diagn. 2012;6:281–93. Doi:10.1517/17530059.2012.680019.BIOMARKERS.

107. Niemann N, Sawitzki B. Treg Therapy in Transplantation : How and When Will We Do It ? Curr Transplant Reports. 2015;2:233–41. Doi:10.1007/s40472-015-0066-5.

108. Kendal AR, Waldmann H. Infectious tolerance: Therapeutic potential. Curr Opin Immunol. Elsevier Ltd; 2010;22:560–5. Doi:10.1016/j.coi.2010.08.002.

109. Andersson J, Tran DQ, Pesu M, Davidson TS, Ramsey H, O'Shea JJ, et al. CD4+ FoxP3+ regulatory T cells confer infectious tolerance in a TGF-beta-dependent manner. J Exp Med. 2008;205:1975–81. Doi:10.1084/jem.20080308.

110. Suntharalingam G, Perry M, Ward S, Brett S, Castello-Cortes A, Brunner M, et al. Cytokine Storm in a Phase 1 Trial of the Anti-CD28 Monoclonal Antibody TGN1412. N Engl J Med. 2006;1018–28.

111. Riley JL, June CH, Blazar BR. Human T Regulatory Cells as Therapeutic Agents: Take a Billion or So of These and Call Me in the Morning. Immunity. 2010;30:656–65. Doi:10.1016/j.immuni.2009.04.006.Human.

112. McMurchy AN, Bushell A, Levings MK, Wood KJ. Moving to tolerance: Clinical application of T regulatory cells. Semin Immunol. 2011;23:304–13. Doi:10.1016/j.smim.2011.04.001.

113. Fuchs A, Gliwinski M, Grageda N, Spiering R, Abbas AK, Appel S, et al. Minimum information about T regulatory cells: A step toward reproducibility and standardization. Front Immunol. 2018;8:1844. Doi:10.3389/fimmu.2017.01844.

114. Brunstein CG, Miller JS, Cao Q, Mckenna DH, Hippen KL, Curtsinger J, et al. Infusion of ex vivo expanded T regulatory cells in adults transplanted with umbilical cord blood : safety profile and detection

kinetics Infusion of ex vivo expanded T regulatory cells in adults transplanted with umbilical cord blood : safety profile and. Blood. 2013;117:1061–70. Doi:10.1182/blood-2010-07-293795.

115. Hanash AM, Levy RB. Donor CD4+CD25+ T cells promote engraftment and tolerance following MHC-mismatched hematopoietic cell transplantation. Blood. 2005;105:1828–36. Doi:10.1182/blood-2004-08-3213.Supported.

116. Joffre O, Gorsse N, Romagnoli P, Hudrisier D, Meerwijk JPM Van. Induction of antigen-speci c tolerance to bone marrow allografts with CD4. Blood. 2004;103:4216–21. Doi:10.1182/blood-2004-01-0005.Supported.

117. Nadig SN, Wieckiewicz J, Wu DC, Warnecke G, Zhang W, Luo S, et al. In vivo prevention of transplant arteriosclerosis by ex vivo-expanded human regulatory T cells. Nat Med. 2010;16:809–13. Doi:10.1038/nm.2154.

118. Issa F, Hester J, Goto R, Nadig S, Goodacre TE. Ex vivo-expanded human regulatory T cells prevent the rejection of skin allografts in a humanised mouse model. Transplantation. 2010;90:1321–7. Doi:10.1097/TP.0b013e3181ff8772.Ex.

119. Xiao F, Ma L, Zhao M, Huang G, Mirenda V, Dorling A, et al. Ex vivo expanded human regulatory T cells delay islet allograft rejection via inhibiting islet-derived monocyte chemoattractant protein-1 production in CD34+ stem cells-reconstituted NOD-scid IL2rgnull mice. PLoS One. 2014;9:1–12. Doi:10.1371/journal.pone.0090387.

120. Wu DC, Hester J, Nadig SN, Zhang W, Trzonkowski P, Gray D, et al. Ex vivo expanded human regulatory T cells can prolong survival of a human islet allograft in a humanized mouse model. Transplantation. 2013;96:707–16. Doi:10.1097/TP.0b013e31829fa271.

121. Todo S, Yamashita K, Goto R, Zaitsu M, Nagatsu A, Oura T, et al. A Pilot Study of Operational Tolerance With a Regulatory T-Cell-Based Cell Therapy in Living Donor Liver Transplantation. Hepatology. 2016;64:632–43. Doi:10.1002/hep.28459.

122. Chandran S, Tang Q, Sarwal M. Polyclonal Regulatory T Cell Therapy for Control of Inflammation in Kidney Transplants. Am J Transplant. 2017;17:2945–54. Doi:10.1111/ajt.14415.

123. Safinia N, Grageda N, Scottà C, Thirkell S, Fry LJ, Vaikunthanathan T, et al. Cell therapy in organ transplantation: Our experience on the clinical translation of regulatory T cells. Front Immunol. 2018;9:354. Doi:10.3389/fimmu.2018.00354.

124. Romano M, Fanelli G, Albany CJ, Giganti G, Lombardi G. Past, present, and future of regulatory T cell therapy in transplantation and autoimmunity. Front Immunol. 2019;10:43. Doi:10.3389/fimmu.2019.00043.

125. Kasow KA, Chen X, Knowles J, Wichlan D, Handgretinger R, Riberdy JM. Human CD4 + CD25 + Regulatory T Cells Share Equally Complex and Comparable Repertoires with CD4 + CD25 − Counterparts . J Immunol. 2004;172:6123–8. Doi:10.4049/jimmunol.172.10.6123.

126. Fazilleau N, Bachelez H, Gougeon M-L, Viguier M. Cutting Edge: Size and Diversity of CD4 + CD25 high Foxp3 + Regulatory T Cell Repertoire in Humans: Evidence for Similarities and Partial Overlapping with CD4 + CD25 − T Cells . J Immunol. 2007;179:3412–6. Doi:10.4049/jimmunol.179.6.3412.

127. Wong J, Obst R, Correia-Neves M, Losyev G, Mathis D, Benoist C. Adaptation of TCR Repertoires to Self-Peptides in Regulatory and Nonregulatory CD4 + T Cells . J Immunol. 2007;178:7032–41. Doi:10.4049/jimmunol.178.11.7032.

128. Andersson J, Tran DQ, Pesu M, Davidson TS, Ramsey H, O'Shea JJ, et al. CD4+ FoxP3+ regulatory T cells confer infectious tolerance in a TGF-beta-dependent manner. J Exp Med. 2008;205:1975–81. Doi:10.1084/jem.20080308.

129. Hsieh CS, Zheng Y, Liang Y, Fontenot JD, Rudensky AY. An intersection between the self-reactive regulatory and nonregulatory T cell receptor repertoires. Nat Immunol. 2006;7:401–10. Doi:10.1038/ni1318.

130. Wing JB, Sakaguchi S. TCR diversity and Treg cells, sometimes more is more. Eur J Immunol. 2011;41:3097–100. Doi:10.1002/eji.201142115.

131. Schmitt EG, Williams CB. Generation and function of induced regulatory T cells. Front Immunol. 2013;4:152. Doi:10.3389/fimmu.2013.00152.

132. Ghali JR, Alikhan MA, Holdsworth SR, Kitching AR. Induced regulatory T cells are phenotypically unstable and do not protect mice from rapidly progressive glomerulonephritis. Immunology. 2017;150:100–14. Doi:10.1111/imm.12671.

133. Boyman O, Sprent J. The role of interleukin - 2 during homeostasis and activation of the immune system. Nat Rev Immunol. 2012;12:180–90. Doi:10.1038/nri3156.

134. Chinen T, Kannan AK, Levine AG, Fan X, Klein U, Zheng Y, et al. An essential role for IL-2 receptor in regulatory T cell function Takatoshi. Nat Immunol. 2016;17:1322–33. Doi:10.1038/ni.3540.

135. Létourneau S, Krieg C, Pantaleo G, Boyman O. IL-2- and CD25-dependent immunoregulatory mechanisms in the homeostasis of T-cell subsets. J Allergy Clin Immunol. 2009;123:758–62. Doi:10.1016/j.jaci.2009.02.011.

136. Sadlon TJ, Wilkinson BG, Pederson S, Brown CY, Bresatz S, Gargett T, et al. Genome-Wide Identification of Human FOXP3 Target Genes in Natural Regulatory T Cells. J Immunol. 2010;185:1071–81. Doi:10.4049/jimmunol.1000082.

137. Beyer M, Thabet Y, Müller R, Sadlon T, Classen S, Lahl K, et al. Repression of the genome organizer SATB1 in regulatory T cells is required for suppressive function and inhibition of effector differentiation. Nat Immunol. 2011;12:898–907. Doi:10.1038/ni.2084.

138. Kryczek I, Wei S, Vatan L, Escara-Wilke J, Szeliga W, Keller ET, et al. Cutting Edge: Opposite Effects of IL-1 and IL-2 on the Regulation of IL-17 + T Cell Pool IL-1 Subverts IL-2-Mediated Suppression . J Immunol. 2007;179:1423–6. Doi:10.4049/jimmunol.179.3.1423.

139. Whitehouse G, Gray E, Mastoridis S, Merritt E, Kodela E, Yang JHM. IL-2 therapy restores regulatory T-cell dysfunction induced by calcineurin inhibitors. 2017;114:7083–8. Doi:10.1073/pnas.1620835114.

140. Shevach EM. Application of IL-2 therapy to target T regulatory cell function. Trends Immunol. 2013;33:626–32. Doi:10.1016/j.it.2012.07.007.

141. Zorn E, Nelson EA, Mohseni M, Porcheray F, Kim H, Litsa D, et al. IL-2 regulates FOXP3 expression in human CD4+ CD25+ regulatory T cells through a STAT-dependent mechanism and induces the expansion of these cells in vivo. Blood. 2006;108:1571–80. Doi:10.1182/blood-2006-02-004747.

142. Koreth J, Matsuoka K, Kim HT, McDonough SM, Bindra B, Alyea EP, et al. Interleukin-2 and Regulatory T Cells in Graft-versus-Host Disease. N Engl J Med. 2011;365:2055–66. Doi:DOI: 10.1056/NEJMoa1108188.

143. Matsuoka K, Koreth J, Kim HT, Bascug OG, Kawano Y, Murase K, et al. Low-dose interleukin-2 therapy restores regulatory T cell homeostasis in patients with chronic graft-versus-host disease. Sci Transl Med. 2013;5. Doi:10.1126/scitranslmed.3005265.

144. Koreth J, Kim HT, Jones KT, Lange PB, Reynolds CG, Chammas MJ, et al. Efficacy , durability , and response predictors of low-dose interleukin-2 therapy for chronic graft-versus-host disease. Blood. 2016;128:130–8. Doi:10.1182/blood-2016-02-702852.

145. Griffith JW, Sokol CL, Luster AD. Chemokines and Chemokine Receptors: Positioning Cells for Host Defense and Immunity. Annu Rev Immunol. 2014;32:659–702. Doi:10.1146/annurev-immunol-032713-120145.

146. Soler D, Chapman TR, Poisson LR, Wang L, Cote-Sierra J, Ryan M, et al. CCR8 Expression Identifies CD4 Memory T Cells Enriched for FOXP3+ Regulatory and Th2 Effector Lymphocytes. J Immunol. 2006;177:6940–51. Doi:10.4049/jimmunol.177.10.6940.

147. Hoelzinger DB, Smith SE, Mirza N, Dominguez AL, Manrique SZ, Lustgarten J. Blockade of CCL1 Inhibits T Regulatory Cell Suppressive Function Enhancing Tumor Immunity without Affecting T Effector Responses. J Immunol. 2010;184:6833–42. Doi:10.4049/jimmunol.0904084.

148. Kuehnemuth B, Piseddu I, Wiedemann GM, Lauseker M, Kuhn C, Hofmann S, et al. CCL1 is a major regulatory T cell attracting factor in human breast cancer. BMC Cancer. BMC Cancer; 2018;18:1278. Doi:10.1186/s12885-018-5117-8.

149. Eruslanov E, Stoffs T, Kim WJ, Daurkin I, Gilbert SM, Su LM, et al. Expansion of CCR8+ inflammatory myeloid cells in cancer patients with urothelial and renal carcinomas. Clin Cancer Res. 2013;19:1670–80. Doi:10.1158/1078-0432.CCR-12-2091.

150. Barsheshet Y, Wildbaum G, Levy E, Vitenshtein A, Akinseye C, Griggs J, et al. CCR8 $^{+}$ FOXp3 $^{+}$ T $_{reg}$ cells as master drivers of immune regulation. Proc Natl Acad Sci. 2017;114:6086–91. Doi:10.1073/pnas.1621280114.

151. Tay SS, Plain KM, Bishop GA. Role of IL-4 and Th2 responses in allograft rejection and tolerance. Curr Opin Organ Transplant. 2009;14:16–22. Doi:10.1097/MOT.0b013e32831ebdf5.

152. Tran DQ. TGF-β: The sword, the wand, and the shield of FOXP3 + regulatory T cells. J Mol Cell Biol. 2012;4:29–37. Doi:10.1093/jmcb/mjr033.

153. Chen WJ, Jin W, Hardegen N, Lei KJ, Li L, Marinos N, et al. Conversion of Peripheral CD4 + CD25 - Naive T Cells to CD4 + CD25 + Regulatory T Cells by TGF-β Induction of Transcription Factor Foxp3. J Exp Med. 2003;198:1875–86. Doi:10.1084/jem.20030152.

154. Samstein R, Josefowicz S, Arvey A, Treuting P, Rudensky AY. Extrathymic generation of regulatory T cells in placental mammals mitigates maternal-fetal conflict. Cell. 2012;150:29–38. Doi:10.1016/j.cell.2012.05.031.

155. Bono MR, Tejon G, Flores-Santibañez F, Fernandez D, Rosemblatt M, Sauma D. Retinoic acid as a modulator of T cell immunity. Nutrients. 2016;8:1–15. Doi:10.3390/nu8060349.

156. Oh SA, Li MO. TGF-β: Guardian of T Cell Function. J Immunol. 2013;191:3973–9. Doi:10.4049/jimmunol.1301843.

157. Zhou X, Kong N, Wang J, Fan H, Zou H, Horwitz D, et al. Cutting Edge: All- Trans Retinoic Acid Sustains the Stability and Function of Natural Regulatory T Cells in an Inflammatory Milieu . J Immunol. 2010;185:2675–9. Doi:10.4049/jimmunol.1000598.

158. Lu L, Lan Q, Li Z, Zhou X, Gu J, Li Q, et al. Critical role of all-trans retinoic acid in stabilizing human natural regulatory T cells under inflammatory conditions. Proc Natl Acad Sci U S A. 2014;111. Doi:10.1073/pnas.1408780111.

159. Conway TF, Hammer L, Furtado S, Mathiowitz E, Nicoletti F, Mangano K, et al. Oral delivery of particulate transforming growth factor beta 1 and all-trans retinoic acid reduces gut inflammation in murine models of inflammatory bowel disease. J Crohn's Colitis. 2015;9:647–58. Doi:10.1093/ecco-jcc/jjv089.

160. Kudelski A, Sehgal SN. RAPAMYCIN (AY-22,989), A New Antifungal Antibiotic Taxonomy of the Producing Streptomycete and Isolation of the Active Principle. J Antibiot (Tokyo). 1975;22:989–95.

161. Zoncu R, Efeyan A, Sabatini DM. MTOR: From growth signal integration to cancer, diabetes and ageing. Nat Rev Mol Cell Biol. Nature Publishing Group; 2011;12:21–35. Doi:10.1038/nrm3025.

162. Li J, Kim SG, Blenis J. Rapamycin: One drug, many effects. Cell Metab. Elsevier Inc.; 2014;19:373–9. Doi:10.1016/j.cmet.2014.01.001.

163. Dumont FJ, Su Q. Mechanism of action of the immunosuppressant rapamycin. Life Sci. 1995;58:373–95. Doi:10.1016/0024-3205(95)02233-3.

164. Gonzalez J, Harris T, Childs G, Prystowsky MB. Rapamycin blocks IL-2-driven T cell cycle progression while preserving T cell survival. Blood Cells, Mol Dis. 2001;27:572–85. Doi:10.1006/bcmd.2001.0420.

165. Augustine JJ, Bodziak KA, Hricik DE. Use of sirolimus in solid organ transplantation. Drugs. 2007;67:369–91. Doi:10.2165/00003495-200767030-00004.

166. Battaglia M, Stabilini A, Migliavacca B, Horejs-hoeck J, Kaupper T, Cd CD, et al. Rapamycin Promotes Expansion of Functional CD4 + CD25 + FOXP3 + Regulatory T Cells of Both Healthy Subjects and Type 1 Diabetic Patients. J Immunol. 2006;177:8338–47. Doi:10.4049/jimmunol.177.12.8338.

167. Burchill MA, Yang J, Vogtenhuber C, Blazar BR, Farrar MA. IL-2 Receptor β-Dependent STAT5 Activation Is Required for the Development of Foxp3 + Regulatory T Cells . J Immunol. 2007;178:280–90. Doi:10.4049/jimmunol.178.1.280.

168. Delgoffe GM, Kole TP, Zheng Y, Zarek PE, Matthews KL, Xiao B, et al. The mTOR Kinase Differentially Regulates Effector and Regulatory T Cell Lineage Commitment. Immunity. Elsevier Ltd; 2009;30:832–44. Doi:10.1016/j.immuni.2009.04.014.

169. Rossetti M, Spreafico R, Saidin S, Chua C, Moshref M, Leong JY, et al. Ex Vivo–Expanded but Not In Vitro–Induced Human Regulatory T Cells Are Candidates for Cell Therapy in Autoimmune Diseases Thanks to Stable Demethylation of the FOXP3 Regulatory T Cell–Specific Demethylated Region. J Immunol. 2015;194:113–24. Doi:10.4049/jimmunol.1401145.

170. Zhang P, Tey S-K, Koyama M, Kuns RD, Olver SD, Lineburg KE, et al. Induced Regulatory T Cells Promote Tolerance When Stabilized by Rapamycin and IL-2 In Vivo. J Immunol. 2013;191:5291–303. Doi:10.4049/jimmunol.1301181.

SUPPLEMENTARY INFORMATION 1

# Encapsulation of Human Natural and Induced Regulatory T-cells in IL-2 and CCL1 Supplemented Alginate-GelMA Hydrogel for 3D-Bioprinting

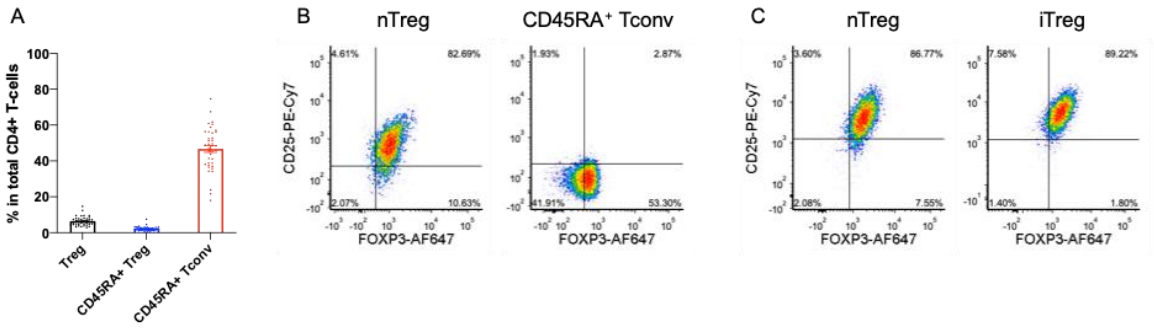


**Fig. S1.** (A) Percentage of nTregs, CD45RA$^+$ nTregs and CD45RA$^+$ Tconv in total CD4$^+$ T-cells, mean ± SEM, n=33. (B) CD25 and FOXP3 staining of nTregs and CD45RA$^+$ Tconv post-sorting. (C) CD25 and FOXP3 staining of nTregs and iTregs after .

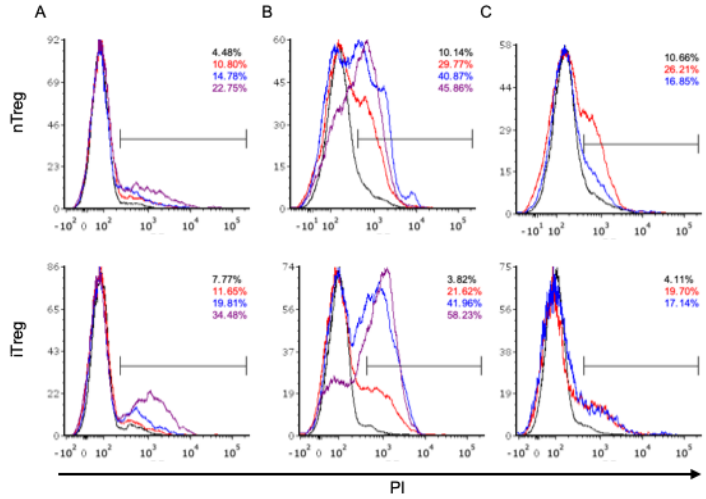


**Fig. S2.** Representative flow cytometry plots for viability assessment (A) day 1, (B) day 3 and (C) day 3 with additional condition of encapsulated with IL-2 in media. For (A) and (B), black: non-encapsulated with IL-2, red: encapsulated with IL-2, blue: non-encapsulated without IL-2 and purple: encapsulated without IL-2. For (C), black: non-encapsulated with IL-2, red: encapsulated with IL-2 and blue: encapsulated with IL-2 in media.

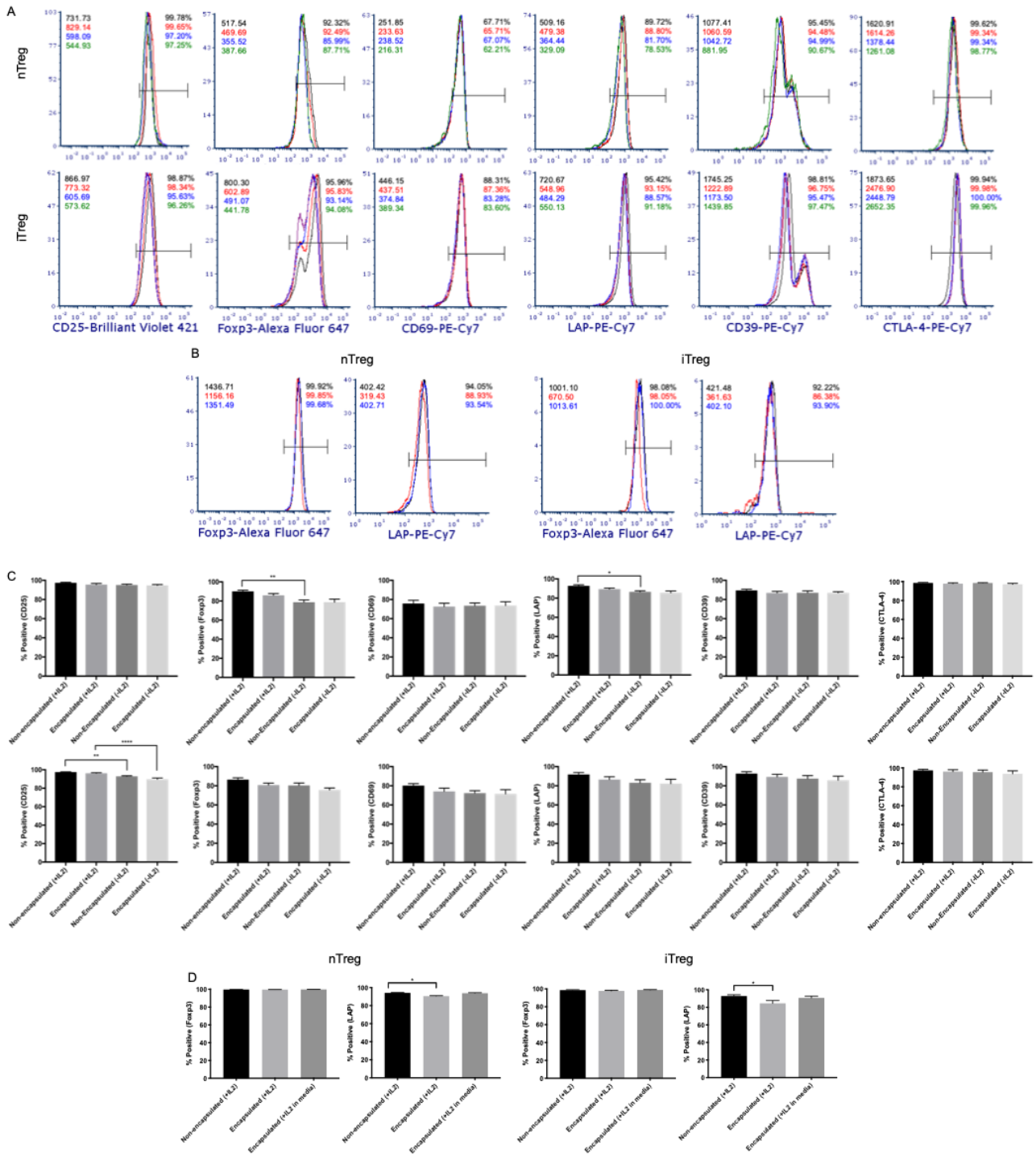


**Fig. S3.** (A, B) Representative flow cytometry plots for phenotype and functionality assessment. For (A) black: non-encapsulated with IL-2, red: encapsulated with IL-2, blue: non-encapsulated without IL-2 and green: encapsulated without IL-2. For (B), black: non-encapsulated with IL-2, red: encapsulated with IL-2 and blue: encapsulated with IL-2 in media. (C, D) Percentage positive of each markers used in phenotype and functionality assessment.

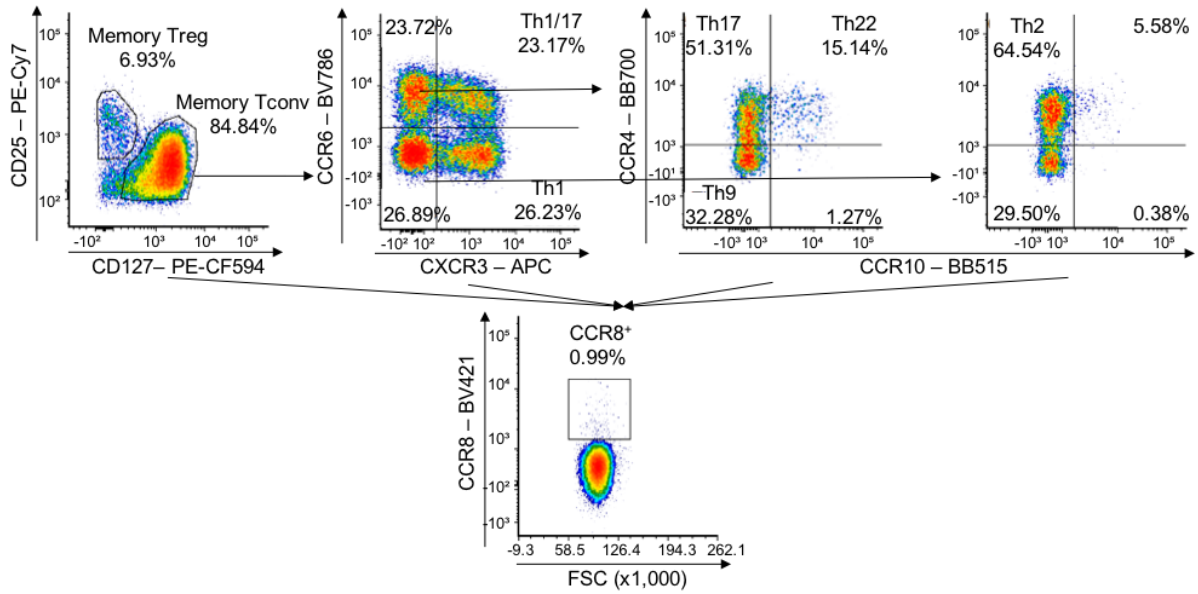


**Fig. S4.** Gating strategy for Figure 8D. %CCR8$^+$ was gated using naïve CD4$^+$ T-cells (CD45RA$^+$) as a negative control then %CCR8$^+$ of various T-cell subsets were measured.

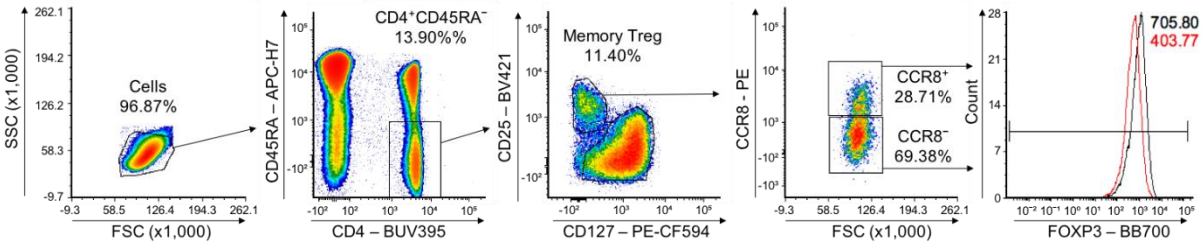


**Fig. S5.** Gating strategy for Figure 8E. CCR8$^+$ and CCR8$^-$ memory Tregs were gated then their Foxp3 MFI were measured (black: CCR8$^+$ and red: CCR8$^-$).

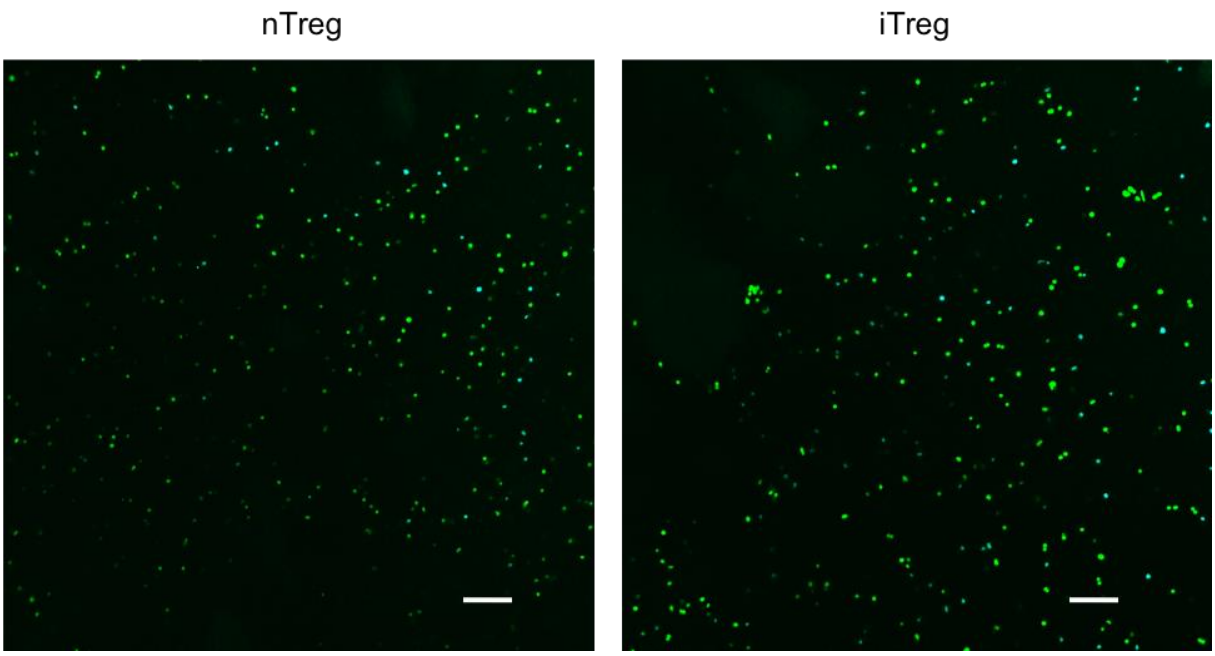


**Fig. S6.** Viability of 3D-bioprinted nTregs and iTregs. Confocal laser scanning microscope images of 3D-Bioprinted nTregs and iTregs. Calcein AM was used to stain live cells (green) and DAPI was used to stain dead cells (light blue). Scale bars represent 100 µm at 10× magnification.

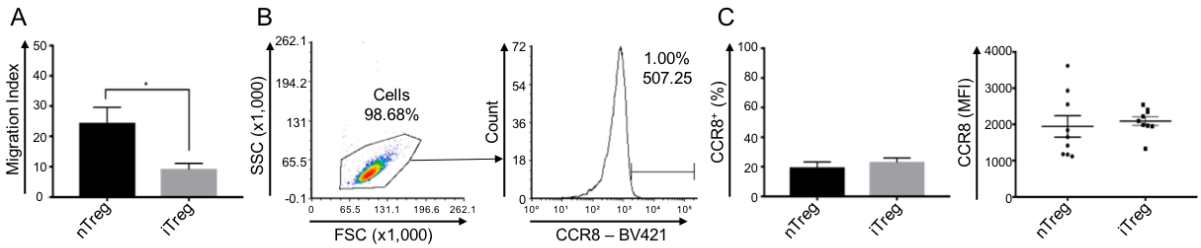


**Fig. S7.** Migration indices of nTregs and iTregs for CXCL12 and CCR8 expression of nTregs and iTregs. (A) Migration indices of nTregs and iTregs for CXCL12. CXCL12 was used as a positive control for CCL1 chemotactic response experiment. (B) Gating strategy for %CCR8$^+$ and CCR8 MFI in nTreg and iTreg. (C) %CCR$^+$ and CCR8 MFI of nTregs and iTregs. Data represented as mean ± SEM, n=3, statistical significance identified by paired two-tailed T-test *P<0.05, **0.01, ***0.001, ****0.0001

**Table S1.** Antibody panels

| Antibody | Clone | Flurochrome | Company |
|---|---|---|---|
| **Treg sorting/purity check** | | | |
| CD4 | SK3 | APC-H7 | BD |
| CD25 | M-A251 | PE-Cy7 | BD |
| CD127 | HIL-7R-M21 | FITC | BD |
| CD45RA | HI100 | PE | BD |
| FOXP3 | 259D/C7 | AF647 | BD |
| **Treg phenotype/functionality** | | | |
| CD4 | OKT4 | FITC | eBioscience |
| CD25 | BC96 | BV421 | Biolegend |
| FOXP3 | 259D/C7 | AF647 | BD |
| CD69 | L78 | PE-Cy7 | BD |
| TGF-β | FNLAP | PE-Cy7 | eBioscience |
| CD39 | eBioA1 | PE-Cy7 | eBioscience |
| CTLA-4 | L3D10 | PE-Cy7 | Biolegend |
| LIVE/DEAD Stain | - | V500 | ThermoFisher Scientific |
| **CD154 suppression assay** | | | |
| CD154 | 89-76 | APC | BD |
| **Immunophenotyping panel** | | | |
| CD3 | UCTH1 | BUV737 | BD |
| CD4 | SK3 | BUV395 | BD |
| CD25 | M-A251 | PE-Cy7 | BD |
| CD45RA | HI100 | APC-H7 | BD |
| CD127 | HIL-7R-M21 | PE-CF594 | BD |
| CXCR3 | 1C6 | APC | BD |
| CCR4 | 1G1 | BB700 | BD |
| CCR6 | 11A9 | BV786 | BD |
| CCR8 | 433H | BV421 | BD |
| CCR10 | 1B5 | BB515 | BD |
| **CCR8 FOXP3 panel** | | | |
| CD4 | SK3 | BUV395 | BD |
| CD45RA | HI100 | APC-H7 | BD |
| CD127 | HIL-7R-M21 | PE-CF594 | BD |
| FOXP3 | 236A/E7 | BB700 | BD |
| CD25 | M-A251 | BV421 | BD |
| CCR8 | L263G8 | PE | Biolegend |

Abbreviations: CD, cluster of differentiation; FOXP3, forkhead box P3; TGF-β, transforming growth factor beta; CTLA-4, cytotoxic t-lymphocyte-associated protein 4; CXCR; CXC chemokine receptor, CCR; C-C chemokine receptor

SUPPLEMENTARY INFORMATION 2

# Generation of Stable Human Induced Regulatory T-cells

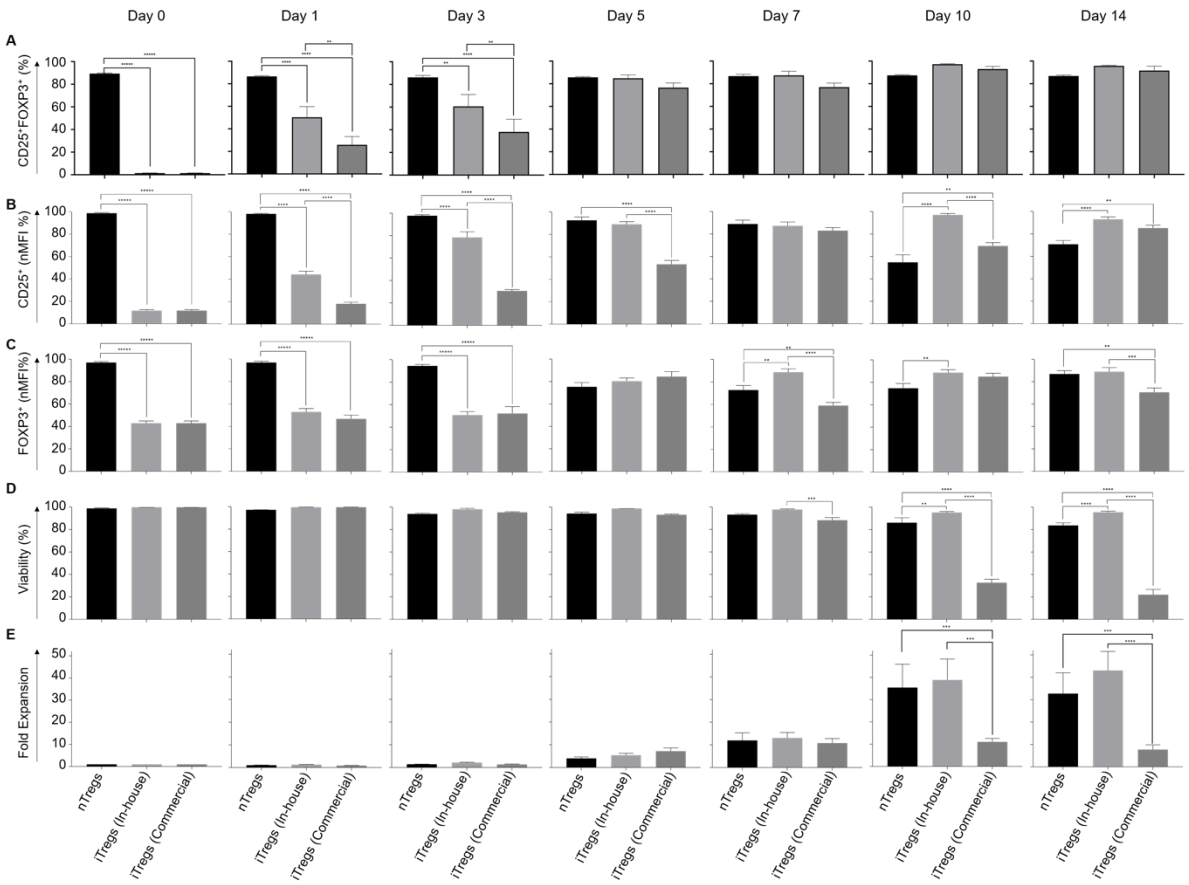


**Figure S1.** Induvial timepoints from Figure 1. A) %CD25$^+$FOXP3$^+$, B) CD25 MFI, C) FOXP3 MFI, D) Viability and E) Fold expansion of nTregs, iTregs (In-house) and iTregs (Commercial) at individual timepoints. Data represented as mean ± SEM, n=3. Statistical significance identified by One-way ANOVA with Tukey's multiple comparisons test *P<0.05, **0.01, ***0.001, ****0.0001.

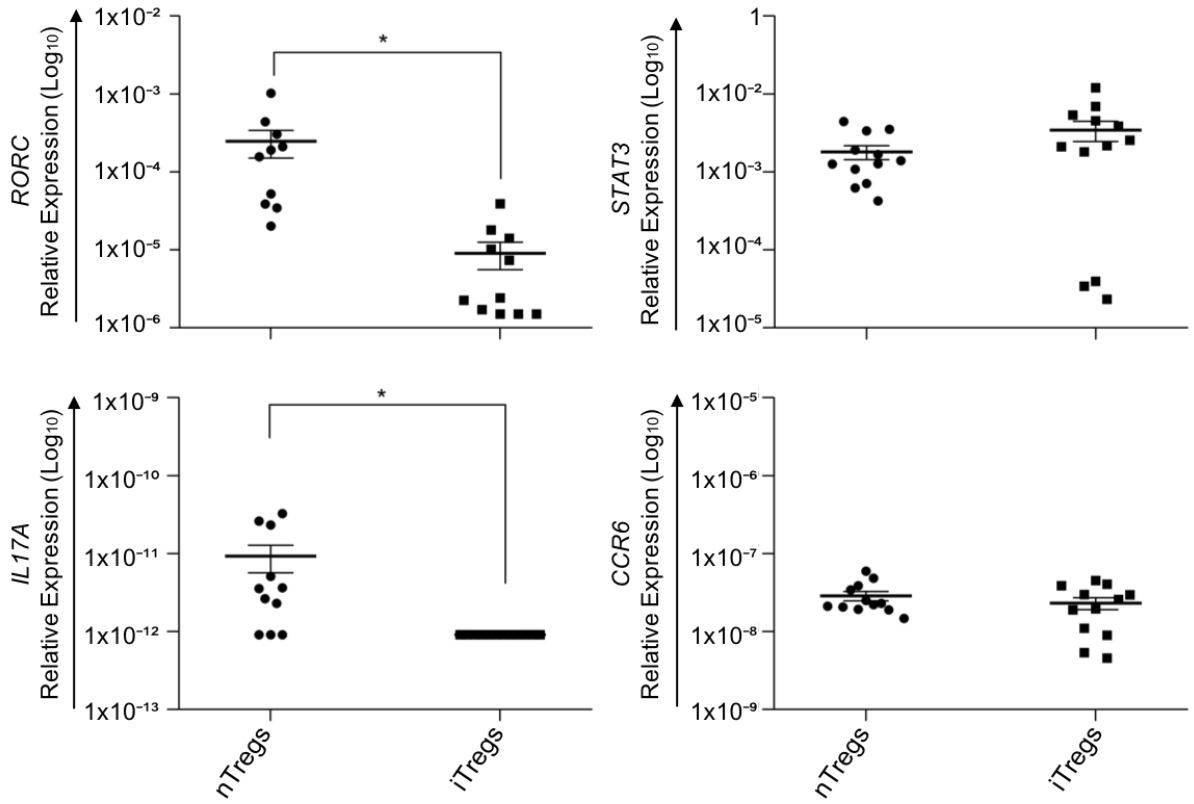


**Figure S2.** Baseline expression of Th17 signature genes, *RORC, STAT3, IL17A* and *CCR6* in nTregs and iTregs. Data represented as mean ± SEM, n=4. Statistical significance identified by unpaired two-tailed T-test *P<0.05, **0.01, ***0.001, ****0.0001.

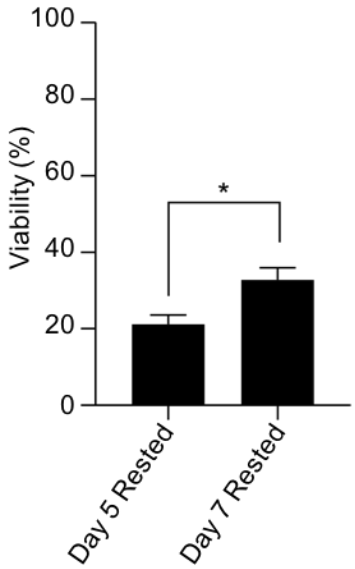


**Figure S3.** Viability of day 5 rested iTregs (Commercial) and day 7 rested iTregs (Commercial). Data represented as mean ± SEM, n=3. Statistical significance identified by unpaired two-tailed T-test *P<0.05, **0.01, ***0.001, ****0.0001

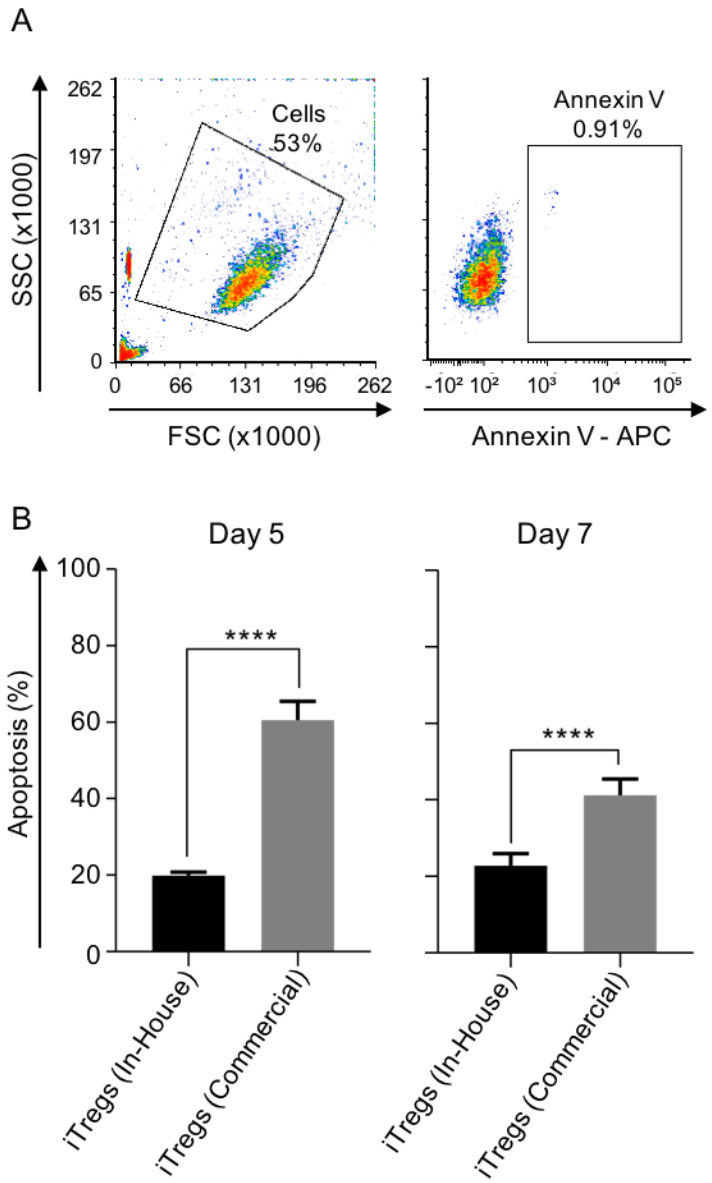


**Figure S4.** Percentage of apoptotic iTregs (In-house) and iTregs (Commercial). Annexin V was used to stain for apoptotic cells A) Gating strategy to determine %Annexin $V^+$ from lymphocyte population. B) Percentage of apoptotic iTregs (In-house) and iTregs (Commercial) on day 5 and day 7 of expansion. Data represented as mean ± SEM, n=3. Statistical significance identified by unpaired two-tailed T-test *P<0.05, **0.01, ***0.001, ****0.0001

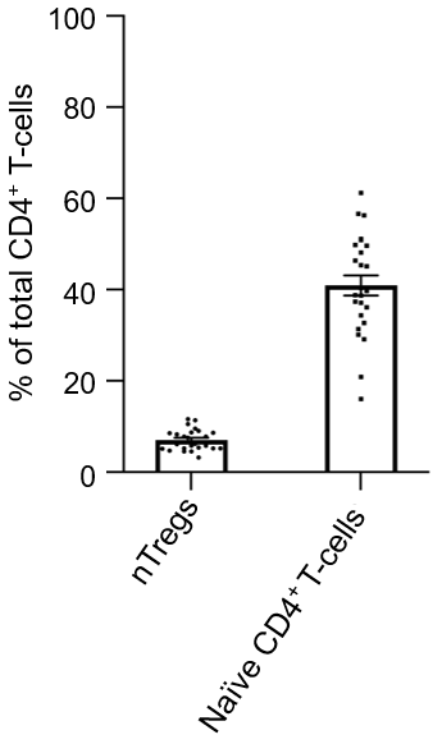


**Figure S5.** Percentage of nTregs and naïve $CD4^+$ T-cells in total peripheral $CD4^+$ T-cells. Data represented as mean ± SEM, n=25. Technical replicates were not used.

**Table S1.** Individual timepoint TSDR methylation values at each CpG locations.

| | | #44 | #43 | #42 | #41 | #40 | #39 | #38 | #37 | #36 | #35 | #34 |
|---|---|---|---|---|---|---|---|---|---|---|---|---|
| nTregs D0 | Mean | 39.23 | 37.77 | 60.77 | 43.23 | 43.47 | 39.03 | 42.07 | 43.87 | 40.7 | 35.3 | 36.67 |
| | SEM | 6.04 | 7.49 | 10.09 | 8.92 | 7.95 | 7.75 | 8.91 | 8.02 | 7.82 | 7.23 | 7.74 |
| iTregs (In-house) D0 | Mean | 97.10 | 94.30 | 100.00 | 100.00 | 100.00 | 92.77 | 99.23 | 96.83 | 85.87 | 78.10 | 95.10 |
| | SEM | 1.70 | 0.95 | 0.00 | 0.00 | 0.00 | 0.22 | 0.43 | 1.24 | 0.75 | 0.89 | 1.02 |
| iTregs (Commercial) D0 | Mean | 97.10 | 94.30 | 100.00 | 100.00 | 100.00 | 92.77 | 99.23 | 96.83 | 85.87 | 78.10 | 95.10 |
| | SEM | 1.70 | 0.95 | 0.00 | 0.00 | 0.00 | 0.22 | 0.43 | 1.24 | 0.75 | 0.89 | 1.02 |
| iTregs (In-house) D1 | Mean | 100.00 | 94.10 | 100.00 | 100.00 | 100.00 | 90.60 | 97.00 | 92.40 | 87.20 | 79.10 | 92.35 |
| | SEM | 0.00 | 0.00 | 0.00 | 0.00 | 0.00 | 0.50 | 1.80 | 0.10 | 2.00 | 4.10 | 3.65 |
| iTregs (Commercial) D1 | Mean | 98.00 | 93.00 | 100.00 | 100.00 | 100.00 | 91.15 | 95.35 | 95.05 | 85.40 | 79.90 | 95.95 |
| | SEM | 2.00 | 0.90 | 0.00 | 0.00 | 0.00 | 0.15 | 2.95 | 3.35 | 0.70 | 0.30 | 4.05 |
| iTregs (In-house) D3 | Mean | 100.00 | 92.87 | 100.00 | 98.40 | 100.00 | 90.67 | 96.83 | 96.60 | 86.73 | 80.43 | 95.03 |
| | SEM | 0.00 | 1.32 | 0.00 | 1.60 | 0.00 | 0.15 | 2.27 | 1.00 | 0.57 | 0.22 | 1.67 |
| iTregs (Commercial) D3 | Mean | 97.70 | 94.37 | 100.00 | 98.47 | 100.00 | 91.43 | 99.27 | 98.70 | 89.00 | 81.73 | 93.37 |
| | SEM | 0.97 | 1.07 | 0.00 | 0.93 | 0.00 | 0.55 | 0.73 | 0.85 | 1.04 | 0.82 | 2.42 |
| iTregs (In-house) D5 | Mean | 94.40 | 92.27 | 100.00 | 100.00 | 99.23 | 91.47 | 94.93 | 90.80 | 84.87 | 79.60 | 87.53 |
| | SEM | 2.82 | 1.10 | 0.00 | 0.00 | 0.77 | 0.58 | 1.48 | 0.32 | 0.52 | 0.15 | 1.39 |
| iTregs (Commercial) D5 | Mean | 95.87 | 91.80 | 100.00 | 98.00 | 97.70 | 91.50 | 97.73 | 93.97 | 85.27 | 80.23 | 86.73 |
| | SEM | 0.32 | 1.48 | 0.00 | 1.29 | 1.46 | 0.31 | 0.38 | 0.52 | 0.94 | 0.67 | 0.49 |
| nTregs D7 | Mean | 70.73 | 53.57 | 80.93 | 56.17 | 61.43 | 49.60 | 57.23 | 57.00 | 52.40 | 46.60 | 48.57 |
| | SEM | 9.66 | 4.14 | 8.17 | 7.25 | 6.64 | 4.07 | 5.45 | 4.26 | 5.24 | 4.84 | 6.07 |
| iTregs (In-house) D7 | Mean | 98.77 | 91.60 | 100.00 | 95.83 | 97.97 | 91.90 | 99.03 | 98.13 | 85.87 | 79.60 | 89.17 |
| | SEM | 0.62 | 1.65 | 0.00 | 1.71 | 1.05 | 1.01 | 0.61 | 0.80 | 0.77 | 0.90 | 0.79 |
| iTregs (Commercial) D7 | Mean | 100.00 | 92.30 | 100.00 | 99.10 | 100.00 | 90.73 | 94.53 | 94.77 | 84.67 | 78.70 | 87.53 |
| | SEM | 0.00 | 2.15 | 0.00 | 0.90 | 0.00 | 0.58 | 1.18 | 1.44 | 0.67 | 0.55 | 1.34 |
| nTregs D7 | Mean | 64.70 | 63.30 | 79.15 | 67.00 | 66.05 | 57.75 | 59.45 | 62.45 | 55.50 | 52.40 | 57.00 |
| | SEM | 10.50 | 11.80 | 15.95 | 15.90 | 15.15 | 13.35 | 12.75 | 11.65 | 11.80 | 12.00 | 13.00 |
| iTregs (In-house) D10 | Mean | 100.00 | 93.87 | 100.00 | 100.00 | 97.90 | 91.83 | 99.30 | 98.40 | 88.20 | 81.90 | 90.70 |
| | SEM | 0.00 | 0.95 | 0.00 | 0.00 | 1.31 | 0.68 | 0.36 | 1.10 | 2.07 | 0.95 | 1.04 |
| iTregs (Commercial) D10 | Mean | 96.13 | 93.17 | 100.00 | 95.67 | 100.00 | 91.93 | 93.87 | 93.03 | 86.50 | 80.33 | 88.70 |
| | SEM | 1.90 | 1.26 | 0.00 | 0.18 | 0.00 | 0.72 | 0.70 | 0.57 | 1.18 | 1.27 | 1.16 |

**Table S2.** Antibody panels

| Antibody | Clone | Flurochrome | Company |
|---|---|---|---|
| **Treg sorting** | | | |
| CD4 | SK3 | APC-H7 | BD |
| CD25 | M-A251 | PE-Cy7 | BD |
| CD127 | HIL-7R-M21 | FITC | BD |
| CD45RA | HI100 | PE | BD |
| **Treg phenotype** | | | |
| CD4 | OKT4 | FITC | BD |
| CD25 | M-A251 | PE-Cy7 | BD |
| FOXP3 | 259D/C7 | AF647 | BD |
| Fixable Viability Stain | - | 780 | BD |
| **CD154 suppression assay** | | | |
| CD154 | 89-76 | APC | BD |
| **Apoptosis staining** | | | |
| Annexin V | - | APC | BD |

Abbreviations: CD, cluster of differentiation; FOXP3, forkhead box P3

# APPENDIX

Current Diabetes Reports (2019) 19: 53
https://doi.org/10.1007/s11892-019-1166-x

IMMUNOLOGY, TRANSPLANTATION, AND REGENERATIVE MEDICINE (L PIEMONTI AND V SORDI, SECTION EDITORS)

# Bioprinting an Artificial Pancreas for Type 1 Diabetes

Juewan Kim[1] · Kyungwon Kang[2] · Christopher J. Drogemuller[2,3] · Gordon G. Wallace[4] · P. Toby Coates[2,3]

Published online: 4 July 2019


## Abstract

**Purpose of Review** Pancreatic islet cell transplantation is currently the only curative cell therapy for type 1 diabetes mellitus. However, its potential to treat many more patients is limited by several challenges. The emergence of 3D bioprinting technology from recent advances in 3D printing, biomaterials, and cell biology has provided the means to overcome these challenges.

**Recent Findings** 3D bioprinting allows for the precise fabrication of complex 3D architectures containing spatially distributed cells, biomaterials (bioink), and bioactive factors. Different strategies to capitalize on this ability have been investigated for the 3D bioprinting of pancreatic islets. In particular, with co-axial bioprinting technology, the co-printability of islets with supporting cells such as endothelial progenitor cells and regulatory T cells, which have been shown to accelerate revascularization of islets and improve the outcome of various transplantations, respectively, has been achieved.

**Summary** 3D bioprinting of islets for generation of an artificial pancreas is a newly emerging field of study with a vast potential to improve islet transplantation.

**Keywords** 3D bioprinting · Pancreatic islet transplantation · Regulatory T cell therapy · Endothelial progenitor cell therapy · Type 1 diabetes

## Introduction

Diabetes mellitus (DM) is a chronic disorder characterized by hyperglycemia due to failing of glucose metabolism, which causes long-term complications in multiple organs including retinopathy, nephropathy, neuropathy, and vasculopathy [1]. DM is a serious global public health problem, causing significant cost to both the health care system and the global economy. Globally, DM is the eighth leading cause of death causing over 1.5 million deaths directly, and 1.5 million indirectly through hyperglycemia-associated illness such as cardiovascular diseases. In 2014, there were an estimated 422 million adults with diabetes worldwide with the global prevalence of 8.5% and it is predicted to increase to 592 million within 20 years [2].

Type 1 diabetes mellitus (T1DM), also known as juvenile diabetes, accounts for 5–10% of the population with diabetes [3]. Symptoms of T1DM include polyuria, polydipsia, polyphagia, weight loss, blurry vision, and extreme fatigue. T1DM may occur at virtually any age but is most common in children

This article is part of the Topical Collection on *Immunology, Transplantation, and Regenerative Medicine*

✉ P. Toby Coates
toby.coates@sa.gov.au

Juewan Kim
juewan.kim@adelaide.edu.au

Kyungwon Kang
dannykang9847@gmail.com

Christopher J. Drogemuller
chris.drogemuller@sa.gov.au

Gordon G. Wallace
gwallace@uow.edu.au

[1] Department of Molecular & Cellular Biology, School of Biological Sciences, The University of Adelaide, Adelaide, South Australia 5005, Australia

[2] Discipline of Medicine, School of Medicine, The University of Adelaide, Adelaide, South Australia 5000, Australia

[3] Central Northern Adelaide Renal and Transplantation Service (CNARTS), The Royal Adelaide Hospital, Adelaide, South Australia 5000, Australia

[4] Intelligent Polymer Research Institute, ARC Centre of Excellence for Electromaterial Science, University of Wollongong, Wollongong, New South Wales 2522, Australia

and young adults and occurs as a consequence of an autoimmune destruction of the insulin-producing β cells of the islets of Langerhans in the pancreas, leading to absolute insulin deficiency [1, 2]. The autoimmune destruction is caused by islet-specific T cell response [4] by various autoantibodies such as autoantibodies to insulin [1, 3]. Recent studies suggest T1DM is triggered by environmental factors such as exposure to pathogens or environmental antigens in individuals who are genetically predisposed to diabetes by particular genes such as the HLA genes, which contribute to 50% of the genetic susceptibility to T1DM [2, 3].

Currently, patients with T1DM are treated with daily exogenous insulin administration [5, 6]. However, despite advances in medicine, there has not yet been a development of an insulin therapy that can mimic the physiological rhythms or a mechanical replacement for pancreatic β cells. An intensive monitoring of blood glucose level accompanied by exogenous insulin therapy via insulin injection or pump represents the current state of treatments for T1DM. Although these treatments are able to delay the progression of diabetic complications including neuropathy and retinopathy, it is not sufficient to prevent these complications [7]. The replacement of β cell function through whole pancreas transplantation is presently the only permanent alternative for re-establishing endogenous insulin secretion in patients with T1DM [8].

## Current Approaches for β Cell Replacement

Pancreas transplantation is reserved and performed in patients with T1DM and advanced or end-stage renal disease. As a result, over three-quarters of the whole pancreas is transplanted in conjunction with kidney transplantation as either simultaneous kidney-pancreas transplantation or alternatively pancreas after kidney transplantation [9]. Furthermore, the surgical procedure is associated with significant mortality risk, accompanied with clinically significant complications such as pancreatitis, bleeding, re-occurrence of autoimmunity, and rejection post-transplantation, which motivates the urgent need for the search of an alternative therapy [10].

A logical alternative to whole organ transplantation is to transplant the cells that have been destroyed. Pancreatic islet transplantation is a minimally invasive approach where purified allogeneic donor islets, isolated from deceased organ donor pancreata, are currently percutaneously infused into recipient liver through the portal vein [11–13]. This procedure has lower risk compared with pancreas transplantation, as major surgery is not required and a differing immunosuppression regimen is employed. A cellular approach was first tried unsuccessfully in man in 1894 using fragmented sheep pancreas in a subject with diabetes [12, 14]. The successful application of islet transplantation as a treatment for diabetes was not realized for many decades until reversal of diabetes was initially observed in rodents and in a patient with chronic pancreatitis who underwent pancreatectomy followed by islet autotransplantation [15–17]. Following these findings, intensive research has been conducted in the field of islet transplantation. In 2000, the Edmonton immunosuppression protocol, which utilized a corticosteroid-free immunosuppression regimen and multiple islet infusions from different donors, was established [18]. An insulin independence rate of 100% was achieved in seven patients following 1 year of islet transplantation and partial graft function was observed in most of the seven patients after 5 years [18, 19] which represented a significant improvement from the success rate of 10% prior to the protocol [12, 20, 21]. Critically long-term insulin independence has been difficult to achieve, and most patients require at least two infusions to achieve insulin independence [19]. Islet transplantation has been adopted as a treatment option for T1DM in a number of countries and has proved an attractive method of β cell replacement [21].

Despite the significant progress in islet transplantation procedures, numerous obstacles remain that currently limit its clinical application [8, 22]. The current clinical standard of care involves the infusion of islets into the patient liver via the portal vein where islets encounter a sub-optimal non-pancreatic environment: high glucose concentration, lower oxygen tension, and higher level of toxins [23]. Moreover, infusion of islets via the hepatic portal vein triggers an innate immune reaction upon contact with blood, known as the instant blood-mediated inflammatory reaction [24]. The hypoxic islets secrete chemokines and express tissue factors, which activates a thrombotic reaction [25]. Platelets are attracted to the islet surface, recruiting leukocytes and macrophages to infiltrate and destroy the islet cells [24, 26]. Together, these factors kill up to 70% of transplanted islets in the first 48 h [27, 28] and consequentially islets from up to three donor pancreata are required for clinical benefit, limiting the availability of the transplantation. Additionally, the obligatory use of immunosuppressive regimen is another major challenge of islet transplantation. Immunosuppressive drugs used for islet transplantation are associated with many side effects including risks of infection, higher rate of malignancy, β cell toxicity, and organ toxicity, significantly decreasing the individual's quality of life [20].

## Alternative Transplantation Site

Many studies in recent years have explored alternative sites for islet transplantation with the following key characteristics: (a) sufficient space for islet engraftment; (b) close proximity to vascular network to provide optimal oxygen tension, sensing, and release of insulin; (c) allow real-time communication between cellular graft and the circulation; and (d) offer minimal inflammatory potential to support long-term graft survival. A

few sites with immunological privileges such as the testis or thymus have been tested in small animals; however, to date, they remained clinically irrelevant due to limited space for islet engraftment [29, 30]. Among many sites explored, the skin site received attention as it offers a readily accessible site via a minimally invasive surgical procedure. The only drawback is that unlike the liver or kidney capsule, dermal poor vascularization limits the integration and functionality of engrafted islets [31]. The pancreas, the native home of islets, has also been explored as a site of islet transplantation. However, it is not considered for a transplantation site due to the metabolic complications such as pancreatitis (potentially induced after embolization) and limited vascular supply. At this point in time, for clinical islet transplantation, intra-portal infusion remains the gold standard [32].

As no suitable alternative transplantation site in the human body has been found, one option to explore is the fabrication of an artificial transplantation site. The recent advancements in bio-engineering technology now enable constructing of such sites. Hydrogels are a multi-component system comprised of a tri-dimensional network of polymer chains with absorbed water filling the space between the macromolecules, within which various biomaterials may be incorporated to mimic tissue-like properties. To date, various types of naturally derived polymers (e.g., alginate, collagen, gelatin, fibrin, and fibronectin) and synthetic polymers (e.g., poly (lactic-co-glycolic acid), polysulfone, poly (lactic acid), poly (vinyl alcohol)) have been evaluated [33]. Among all, alginate-based hydrogels have been the most extensively investigated polymers for their utility with pancreatic islets to treat T1DM. Alginate is a naturally occurring anionic polymer typically obtained from brown seaweed. It is bio-inert, and naturally hydrophilic, thus allowing covalent functionalization via interaction with extracellular matrix proteins, peptides, and growth factors [34, 35].

The main approach of incorporating such technology in islet transplantation is via islet encapsulation. Pancreatic islets are embedded within a hydrogel, and this "mini organ" holds pores which allow bidirectional diffusion of small molecules such as insulin (~ 6 kDa), nutrients, and glucose, and at the same time, protects islets from immune attack by restricting the access of immune cells or antibodies (~ 150–900 kDa) [36]. Numerous small animal models have demonstrated that islet encapsulation is able to improve glucose homeostasis for a short term, but no permanent restoration of euglycemia was observed [37–41]. Several challenges are suggested to limit this biomedical approach to advance into clinical settings. One challenge arises as physical irregularities from fabricating hydrogel result in an incomplete coverage of the islets within the capsules. This may trigger a pericapsular fibrotic overgrowth (PFO) which blocks the diffusion of nutrients and oxygen, resulting in islet necrosis [42, 43]. Even the successfully encapsulated islets suffer from hypoxia due to the restricting hydrogel permeability and increased distance from the surrounding blood vessels reduces the availability of oxygen by diffusion. This introduces a challenge in scaling up into a large animal model or clinically relevant dose of islets. Moreover, encapsulation prevents immediate revascularization post-transplantation, subjecting the islets to further hypoxic stress. As hypoxia hampers the function and responsiveness of islets to glucose, even a larger number of islets are needed to restore normoglycemia.

## 3D Bioprinting

One approach to address hypoxia involves "seeding" of islets onto degradable 3D scaffold structures [44]. Scaffolds are made of similar biopolymers to mimic the pancreatic microenvironment. The construct provides increased surface area to volume ratio compared with the hydrogel capsules, and even allows for vascular ingrowth, thereby providing increased oxygen and nutrient supply [45]. Upon slow degradation of the scaffold, the extracellular matrix proteins are deposited by surrounding tissues and engrafted islets, gradually rebuilding the suitable environment required for islet survival [46]. Even though immune isolation is not achieved through this method, the scaffolds can prevent direct contact of embedded islets to circulating immune cells to reduce the inflammatory response until the scaffolds eventually degrades [24]. The efficacy of such device has been demonstrated in animal studies [47–49]. Moreover, utilization of 3D bioprinting technology with higher accuracy could provide highly controlled seeding of islets, thereby minimizing the onset of PFO arising with conventional techniques.

The concept of 3D printing was first introduced in 1986 by Charles W. Hull and has become increasingly prominent over the past decades [50]. 3D printing technology allows printing of a 3D structure, typically through stacking successive thin layers in a layer-by-layer fashion. Advances in engineering technology have now opened up the possibility of using 3D printing to "print" spatially controlled biomaterial structures with embedded bioactive factors and cells into a functional tissue construct [51]. Such automated printing allows for the precise control of architecture, pore interconnectivity, and a high degree of reproducibility necessary for commercial clinical application and regulation. Furthermore, bioprinting allows the deposition of a wide array of cell types and bioactive factors in a precise order to simulate native tissue environment and support cell survival [52–54].

The current varieties of 3D bioprinting techniques include extrusion printing, inkjet printing, laser-assisted bioprinting, and stereolithography bioprinting [55]. Among these, extrusion bioprinting has been most extensively investigated for the generation of artificial tissue constructs such as cartilages [56, 57], liver [58], and neural tissues [59], with its ability to print

various biomaterials at high cell density [60]. Extrusion bioprinting has been utilized for the generation of artificial pancreata. A rat β cell line, mouse and human islets were successfully printed into a predefined 3D scaffold using alginate-based bioinks and the subsequent cell viability and morphology were found to be unaffected [61••]. Furthermore, rat islets were printed into macroporous 3D constructs using an alginate/methylcellulose bioink. These printed rat islets retained their viability, morphology, and function, for up to 7 days in culture [62••].

Beyond the modification of the bioinks to support islet cells, bioprinting also enables the co-transplantation of islets with supporting cells that could enhance islet survival [63]. Recently, our group developed a 3D bioprinter equipped with a co-axial extruder nozzle and two separate ink chambers [64••]. Different bioinks tailored with cell type–specific bioactive molecules can be utilized in each chamber, allowing co-printing of islets with supporting cells. These geometries have the advantage that more delicate components can be strategically placed within the core with a surrounding protective layer, referred to as the shell. The use of a co-axial structure has been shown to significantly improve islet encapsulation by minimizing material volume per islet and reducing the risk of PFO [42]. Co-axially printed mouse islets and endothelial progenitor cells (EPCs) demonstrated high viability using recently formulated alginate-gelatin methacryloyl bioink [64••]. Together, co-axial 3D bioprinting has the potential to enable the embedding of clinically relevant doses of islets with support for islet survival, including supporting cells and bioactive factors.

## Supporting Cells

### Endothelial Progenitor Cells

The islet of Langerhans is densely vascularized with fenestrated endothelium, and this feature is crucial for β cells to readily sense the blood glucose and secrete insulin into the systemic circulation [65]. Endothelial cells are also crucial for promoting islet function through upregulating insulin transcription via either cell-to-cell contact mechanism or secretion of humoral factors [66]. However, islets are removed from the vasculature during isolation and remain avascular for up to several days post-transplantation [67]. As native islets are physiologically adapted to receiving a rich supply of oxygen (the islet mass in the pancreas comprises 1% of the cells but receives 10% of the blood supply), prolonged hypoxia is detrimental to islet viability and function. The hypoxia induced by isolation triggers activation of NF-kB and inducible nitric oxide synthase, leading to the production of cytotoxic nitric oxide [68, 69]. The consequence of free radical production is decreased insulin production, macrophage cell infiltration, and islet apoptosis. Moreover, islets exposed to hypoxia pre-transplantation display dysregulated glucose responsiveness and elevated basal insulin secretion, due to the upregulation of hypoxic response genes which can continue post-transplantation, resulting in poor glycemic control [70]. Normally, the revascularization occurs 2–4 days post-transplantation and takes over 2 weeks to complete [71]. The eventual vascular density and oxygen tension in transplanted engraftments are less than 50% as compared with the native pancreatic islets [72]. This highlights the crucial need for a mechanism to improve revascularization to restore full function of engrafted islets.

One approach to achieving such acceleration is to directly use pro-angiogenic cells such as EPCs. EPCs are a heterogeneous group of stem cells derived from the bone marrow that are recruited to the site of hypoxia. EPCs promote vascularization by recruiting and differentiating other cell types, or by differentiating themselves into endothelial cells, the building blocks of the endothelial lining of blood vessels [73, 74]. Furthermore, the crosstalk between intra-islet endothelial cells and islets enhances expression and secretion of insulin and islet survival [75]. These properties of EPCs were shown to be beneficial when EPCs were co-transplanted with islets in several studies. Co-transplantation of human umbilical cord–derived EPCs with porcine islets in diabetic nude mice significantly accelerated the revascularization in the first 2 weeks, compared with islet transplantation alone, and increased expression of pro-angiogenic factor, vascular endothelial growth factor-A (VEGF-A), in islets [76]. Co-transplantation of rat bone marrow–derived EPCs with rat islets in diabetic rats demonstrated long-lasting normoglycemia [77]. Moreover, co-transplantation of mouse bone marrow–derived EPCs with mouse islets in diabetic mice improved the cure rate and glucose control with higher final β cell mass [78•].

### Regulatory T Cells

Upon transplantation, recipient T cells recognize alloantigens of the allograft, which activate recipient T cells to induce inflammation at the site of the allograft, as part of the alloresponse [79]. Alloresponse results in acute graft rejection as well as chronic graft dysfunction, and as such the use of immunosuppressive drugs is necessitated to prevent the commencement of alloresponse. However, as aforementioned, immunosuppressants are associated with deleterious side effects; there is a need for novel immunotherapies to achieve immunosuppression-free transplantation. Regulatory T cells (Tregs) are a promising candidate for this.

Tregs are a sub-population of T cells that specialize in immune regulation and suppression. Tregs are defined as $CD4^+$ $FOXP3^+$ $CD25^{hi}$ $CD127^-$ T cells with two main types of Tregs. Natural Tregs (nTregs) arise from highly self-reactive T cells in the thymus during T cell development and establishment of central tolerance [80]. nTregs are characterized by

complete demethylation of the *FOXP3* promoter, which results in stable expression of FOXP3 and a suppressive phenotype [81]. On the other hand, peripheral or induced Tregs are generated from naïve CD4+ T cells in the periphery or in vitro upon stimulation with transforming growth factor beta (TGF-β) and retinoic acid. The *FOXP3* promoter of induced Tregs is only partially demethylated leading to their functional instability. Treg-mediated suppression is the main mechanism of peripheral tolerance. Tregs play many roles in the immune system including downregulation of immune responses once pathogens have been cleared, maintaining tolerance to self, gut microbiota, new chemicals, environmental and food antigens, and the fetus in cases of pregnancy. Treg-mediated suppression targets a broad spectrum of immune cells such as other T cell subsets, B cells, antigen-presenting cells, and natural killer cells [82]. Suppression is achieved via several circumstance-dependent mechanisms, including inhibitory cytokines, cytolysis, metabolic disruption, and modulation of dendritic cells [83].

Since the first organ transplantation clinical trials, spontaneous graft tolerance (the acceptance of allograft without immunosuppressive regimen) has been observed, mostly in liver transplant recipients [84–86]. The exact factors underlying this phenomenon have not yet been fully identified; however, it has been shown that Tregs play a major role in spontaneous graft tolerance in mice liver allograft models [87, 88] and there is elevation of Treg proportion in spontaneously tolerant patients [89]. Thus, various approaches to utilize their natural abilities have been extensively investigated. In particular, adoptive transfer of ex vivo expanded Tregs has a number of advantages including greater control over the expansion/generation of Tregs, the possibility of functional and phenotypical analysis prior to delivery, and finer control of dosage and delivery time [90, 91]. This has proved promising in murine islet transplantation models [92, 93] and in clinical trials for kidney [94•] and liver [95•] transplantation.

## Bioactive Factors

### Insulin-Like Growth Factor-2

Insulin-like growth factor-2 is a potent growth factor highly expressed in islets during fetal development with much less activity in post-natal life [96, 97]. The fetal overexpression of IGF-II can enlarge individual organs, and the whole body size of a new born murine, in a dose-dependent manner [98]. Notably, the expression pattern of IGF-II in pre-natal period coincides with the pancreatic mass growth, suggesting its role in proliferation or survival of β cells [99, 100]. In vitro, IGF-II showed increased DNA replication in β cell lines, and IGF-II survival effect on transplanted islets has been observed in animal models [101–103]. Together, it is suggested that IGF-II plays a dual beneficial role on β cells as a survival and mitogenic factor. In addition, IGF-II pre-incubation or viral transfection-induced overexpression of IGF-II can effectively improve islet survival against cytokine exposure and islet engraftment [104]. As such, incorporation of IGF-II could protect islets from hypoxia and cytokine-driven cell deaths until revascularization is established.

### Vascular Endothelial Growth Factor

VEGF is a family of pro-angiogenic proteins which includes VEGF-A, VEGF-B, VEGF-C, VEGF-D, VEGF-E, VEGF-F, and PIGF (placental growth factor) in human. Among these, VEGF-A plays a crucial role in vasculogenesis during embryogenesis as well as angiogenesis in post-natal life [105]. Furthermore, VEGF-A is required for formation of a dense network of fenestrated blood vessels around islets [106]. These properties give VEGF-A the therapeutic potential to induce neovascularization in islet transplantation. VEGF-A containing alginate scaffolds were demonstrated to prevascularize murine intramuscular space prior to islet transplantation and to improve islet survival after transplantation [107]. In addition, 3D ring-shaped polycaprolactone scaffolds functionalized with VEGF-A were able to induce vascularization and improve function of encapsulated islets embedded in the polycaprolactone scaffolds, compared with free-floating islets [108•]. Thus, incorporation of VEGF-A in conjunction with EPCs could accelerate revascularization of the islets.

### Interleukin-2

IL-2 is a T cell stimulatory cytokine, largely produced by $CD4^+$ T helper cells. IL-2 signaling is crucial for activation and clonal expansion T cells [109]. While $CD4^+$ T helper cells can produce IL-2 for autocrine signaling upon T cell receptor stimulation, Treg cells cannot and thus are reliant on IL-2 produced by other cells [110, 111]. IL-2 is crucial for Treg function as well as their survival. Tregs highly express CD25, the α-chain of the high-affinity IL-2 receptor complex [112] and the interaction of IL-2 and CD25 induces high expression of FOXP3 thereby reinforcing Treg phenotype and function [113, 114]. Moreover, with high expression of CD25, Tregs can respond to low concentrations of IL-2 and bind to IL-2 with high affinity [115], which can lead to sequestration of IL-2 from effector T cells, depriving them of survival signal [83]. Administration of exogenous IL-2 in autoimmunity and organ transplantation has been investigated to augment Treg numbers and function [116]. Particularly, low-dose IL-2 therapy has shown promising results in hematopoietic stem cell transplantation graft-versus-host disease, selectively increasing Treg numbers [117–120]. Thus, incorporation of IL-2 may enhance survival and function of printed Tregs and create a Treg-rich microenvironment around the 3D bioprinted scaffold.

## Conclusion

Pancreatic islet transplantation is a promising curative cell therapy for T1DM. The field is limited by human cadaveric islet cell sources at present, but newer cell sources such as embryonic stem cell or xenogeneic cell sources are in the pipeline. The current procedure of islet infusion into liver may not be optimal for these newer cell sources, and so alternative transplant strategies such as 3D bioprinting may provide new strategies. Modifications of the bioinks with local immunosuppression and bioactive factors to support the cells are new directions for the field. The recent 3D bioprinting technology, especially with the development of the co-axial bioprinter, thus has potential to change the current pancreatic islet transplantation paradigm. The possibility of co-printing islets with supporting cells and bioactive factors potentiates direct improvement of engraftment condition, and thus survival and function of transplanted islets. Incorporation of EPCs may accelerate revascularization of islets to support their function, and the incorporation of Tregs could provide localized immune protection to islets. Bioactive factors such IGF-II, VEGF, and IL-2 could enhance the survival and function of printed cells to maximize the efficacy of the graft. Together, extra-hepatic islet transplantation without the use of immunosuppression might be clinically achieved by utilizing 3D bioprinting technology.

### Compliance with Ethical Standards

**Conflict of Interest** The authors declare that they have no conflict of interest.

**Human and Animal Rights and Informed Consent** This article does not contain any studies with human or animal subjects performed by any of the authors.

## References

Papers of particular interest, published recently, have been highlighted as:
- • Of importance
- •• Of major importance


1. Gregory JM, Moore DJ. Type 1 diabetes mellitus. Pediatr Rev 2013. https://doi.org/10.1016/B978-1-4377-1604-7.00561-3.
2. Forouhi NG, Wareham NJ. Epidemiology of diabetes. Medicine (Baltimore). 2014;42:698–702. https://doi.org/10.1383/medc.2006.34.2.57.
3. Diabetes DOF. Diagnosis and classification of diabetes mellitus. Diabetes Care. 2013;36:67–74. https://doi.org/10.2337/dc13-S067.
4. Pathiraja V, Kuehlich JP, Campbell PD, Krishnamurthy B, Loudovaris T, Coates PTH, et al. Proinsulin-specific, HLA-DQ8, and HLA-DQ8-transdimer-restricted CD4+ T cells infiltrate islets in type 1 diabetes. Diabetes. 2015;64:172–82. https://doi.org/10.2337/db14-0858.
5. Rezania A, Bruin JE, Arora P, Rubin A, Batushansky I, Asadi A, et al. Reversal of diabetes with insulin-producing cells derived in vitro from human pluripotent stem cells. Nat Biotechnol. 2014;32:1121–33. https://doi.org/10.1038/nbt.3033.
6. Prabakar KR, Domínguez-Bendala J, Damaris Molano R, Pileggi A, Villate S, Ricordi C, et al. Generation of glucose-responsive, insulin-producing cells from human umbilical cord blood-derived mesenchymal stem cells. Cell Transplant. 2012;21:1321–39. https://doi.org/10.3727/096368911X612530.
7. Agarwal A, Brayman KL. Update on islet cell transplantation for type 1 diabetes. Semin Interv Radiol. 2012;29:90–8. https://doi.org/10.1055/s-0032-1312569.
8. Robertson RP, Davis C, Larsen J, Stratta R, Sutherland DER, American Diabetes Association. Pancreas and islet transplantation in type 1 diabetes. Diabetes Care. 2006;29:935. https://doi.org/10.2337/diacare.29.04.06.dc06-9908.
9. Chan C, Chim TM, Leung K, Tong C, Wong T, Leung GK. Simultaneous pancreas and kidney transplantation as the standard surgical treatment for diabetes mellitus patients with end-stage renal disease. Hong Kong Med J. 2016;22(1):62–9. https://doi.org/10.12809/hkmj154613.
10. Troppmann C. Complications after pancreas transplantation. Curr Opin Organ Transpl. 2010;15:112–8. https://doi.org/10.1097/MOT.0b013e3283355349.
11. Vardanyan M, Parkin E, Gruessner C, Rilo HLR. Pancreas vs. islet transplantation: a call on the future. Curr Opin Organ Transplant. 2010;15:124–30. https://doi.org/10.1097/MOT.0b013e32833553f8.
12. Robertson RP. Islet transplantation as a treatment for diabetes — a work in progress. N Engl J Med. 2004;350:694–705. https://doi.org/10.1056/NEJMra032425.
13. Connell PJO, Holmes-Walker DJ, Goodman D, Hawthorne WJ, Loudovaris T, Gunton JE, et al. Multicenter Australian trial of islet transplantation: improving accessibility and outcomes. Am J Transplant. 2013;13:1850–8. https://doi.org/10.1002/ajt.12250.
14. Ichii H, Ricordi C. Current status of islet cell transplantation. J Hepato-Biliary-Pancreat Surg. 2013;16:101–12. https://doi.org/10.1007/s00534-008-0021-2.Current.
15. Lacy PE, Walker MM, Fink CJ, Louis S. Perifusion of isolated rat islets in vitro participation of the microtubular system in the biphasic release of insulin. Diabetes. 1972;21:987–98. https://doi.org/10.2337/diab.21.10.987.
16. Najarian JS, Sutherland DER, Baumgartner D, Burke B, Rynasiewicz JJ, Matas AJ, et al. Total or near total pancreatectomy and islet autotransplantation for treatment of chronic pancreatitis.pdf. Ann Surg. 1980;192:526–42.
17. Robertson RP, Lanz KJ, Sutherland DER, Kendall DM. Prevention of diabetes for up to 13 years by autoislet transplantation after pancreatectomy for chronic pancreatitis. Diabetes. 2001;50:48–50. https://doi.org/10.2337/diabetes.50.1.47.
18. Shapiro AMJ, Lakey JRT, Ryan EA, Korbutt GS, Toth E, Warnock GL, et al. Islet transplantation in seven patients with type 1 diabetes mellitus using a glucocoricoid-free imunosuppressive regimen. N Engl J Med. 2000;343:230–8. https://doi.org/10.1056/NEJM200007273430401.
19. Ryan EA, Paty BW, Senior PA, Bigam D, Alfadhli E, Kneteman NM, et al. Five-year follow-up after clinical islet transplantation. Diabetes. 2005;54:2060–9.
20. Leitão CB, Cure P, Tharvanji T, Baidal DA, Alejandro R. Current challenges in islet transplantation. Curr Diab Rep. 2008;8:324–31. https://doi.org/10.1007/s11892-008-0057-3.
21. Rheinheimer J, Bauer AC, Silveiro SP, Estivalet AAF, Bouças AP, Rosa AR, et al. Human pancreatic islet transplantation: an update and description of the establishment of a pancreatic islet isolation

laboratory. Arch Endocrinol Metab. 2015;59:161–70. https://doi.org/10.1590/2359-3997000000030.
22. Lacy PE, Kostianovsky M. Method for the isolation of intact islets of Langerhans from the rat pancreas. Diabetes. 1967;16:35–9. https://doi.org/10.2337/diab.16.1.35.
23. Carlsson PO, Palm F, Andersson A, Liss P. Markedly decreased oxygen tension in transplanted rat pancreatic islets irrespective of the implantation site. Diabetes. 2001;50:489–95. https://doi.org/10.2337/diabetes.50.3.489.
24. Bennet W, Sundberg B, Groth CG, Brendel MD, Brandhorst D, Brandhorst H, et al. Incompatibility between human blood and isolated islets of Langerhans: a finding with implications for clinical intraportal islet transplantation? Diabetes. 1999;48:1907–14. https://doi.org/10.2337/diabetes.48.10.1907.
25. Moberg L, Johansson H, Lukinius A, Berne C, Foss A, Källen R, et al. Production of tissue factor by pancreatic islet cells as a trigger of detrimental thrombotic reactions in clinical islet transplantation. Lancet. 2002;360:2039–45. https://doi.org/10.1016/S0140-6736(02)12020-4.
26. Van Der Windt DJ, Bottino R, Casu A, Campanile N, Cooper DKC. Rapid loss of intraportally transplanted islets: an overview of pathophysiology and preventive strategies. Xenotransplantation. 2007;14:288–97. https://doi.org/10.1111/j.1399-3089.2007.00419.x.
27. Cantarelli E, Piemonti L. Alternative transplantation sites for pancreatic islet grafts. Curr Diab Rep. 2011;11:364–74. https://doi.org/10.1007/s11892-011-0216-9.
28. Bennet W, Groth CG, Larsson R, Nilsson B, Korsgren O. Isolated human islets trigger an instant blood mediated inflammatory reaction: implications for intraportal islet transplantation as a treatment for patients with type 1 diabetes. Ups J Med Sci. 2000;105:125–33. https://doi.org/10.1517/03009734000000059.
29. Margolis RN, Holup JJ, Selawry HP. Effects of intratesticular islet transplantation on hepatic glycogen metabolism in the rat. Diabetes Res Clin Pract. 1986;2:291–9. https://doi.org/10.1016/S0168-8227(86)80006-7.
30. Ar'Rajab A, Dawidson IJ, Harris RB, Sentementes JT. Immune privilege of the testis for islet xenotransplantation (rat to mouse). Cell Transplant. 2017;3:493–8. https://doi.org/10.1177/096368979400300606.
31. Kemp CB, Knight MJ, Scharp DW, Ballinger WF, Lacy PE. Effect of transplantation site on the results of pancreatic islet isografts in diabetic rats. Diabetologia. 1973;9:486–91. https://doi.org/10.1007/BF00461694.
32. Melzi R, Sanvito F, Mercalli A, Andralojc K, Bonifacio E, Piemonti L. Intrahepatic islet transplant in the mouse: functional and morphological characterization. Cell Transplant. 2008;17:1361–70. https://doi.org/10.3727/096368908787648146.
33. Mao G, Chen G, Bai H, Song T, Wang Y. The reversal of hyperglycaemia in diabetic mice using PLGA scaffolds seeded with islet-like cells derived from human embryonic stem cells. Biomaterials. 2009;30:1706–14. https://doi.org/10.1016/j.biomaterials.2008.12.030.
34. De Vos P, Hamel AF, Tatarkiewicz K. Considerations for successful transplantation of encapsulated pancreatic islets. Diabetologia. 2002;45:159–73. https://doi.org/10.1007/s00125-001-0729-x.
35. Mallett AG, Korbutt GS. Alginate modification improves long-term survival and function of transplanted encapsulated islets. Tissue Eng Part A. 2009;15:1301–9. https://doi.org/10.1089/ten.tea.2008.0118.
36. Desai T, Shea LD. Advances in islet encapsulation technologies. Nat Rev Drug Discov. 2017;16:338–50. https://doi.org/10.1038/nrd.2016.232.
37. Vériter S, Mergen J, Goebbels R-M, Aouassar N, Grégoire C, Jordan B, et al. In vivo selection of biocompatible alginates for islet encapsulation and subcutaneous transplantation. Tissue Eng Part A. 2010;16:1503–13. https://doi.org/10.1089/ten.TEA.2009.0286.
38. Lum ZP, Tai IT, Krestow M, Norton J, Vacek I, Sun AM. Prolonged reversal of diabetic state in NOD mice by xenografts of microencapsulated rat islets. Diabetes. 1991;40:1511–6. https://doi.org/10.2337/diab.40.11.1511.
39. Cui W, Barr G, Faucher KM, Sun X-L, Safley SA, Weber CJ, et al. A membrane-mimetic barrier for islet encapsulation. Transplant Proc. 2004;36:1206–8. https://doi.org/10.1016/j.transproceed.2004.04.059.
40. Lamb M, Storrs R, Li S, Liang O, Laugenour K, Dorian R, et al. Function and viability of human islets encapsulated in alginate sheets: in vitro and in vivo culture. Transplant Proc. 2011;43:3265–6. https://doi.org/10.1016/j.transproceed.2011.10.028.
41. Zhi ZL, Kerby A, King AJF, Jones PM, Pickup JC. Nano-scale encapsulation enhances allograft survival and function of islets transplanted in a mouse model of diabetes. Diabetologia. 2012;55:1081–90. https://doi.org/10.1007/s00125-011-2431-y.
42. Ma M, Chiu A, Sahay G, Doloff JC, Dholakia N, Thakrar R, et al. Core-shell hydrogel microcapsules for improved islets encapsulation. Adv Healthc Mater. 2013;2:667–72. https://doi.org/10.1002/adhm.201200341.
43. Hobbs HA, Kendall WF, Darrabie M, Opara EC. Prevention of morphological changes in alginate microcapsules for islet xenotransplantation. J Investig Med. 2001;49:572–5. https://doi.org/10.2310/6650.2001.33722.
44. De Vos P, Hillebrands JL, De Haan BJ, Strubbe JH, Van Schilfgaarde R. Efficacy of a prevascularized expanded polytetrafluoroethylene solid support system as a transplantation site for pancreatic islets. Transplantation. 1997;63:824–30. https://doi.org/10.1097/00007890-199703270-00006.
45. Dufour JM, Rajotte RV, Zimmerman M, Rezania A, Kin T, Dixon DE, et al. Development of an ectopic site for islet transplantation, using biodegradable scaffolds. Tissue Eng. 2005;11:1323–31. https://doi.org/10.1089/ten.2005.11.1323.
46. Wang RN, Rosenberg L. Maintenance of beta-cell function and survival following islet isolation requires re-establishment of the islet-matrix relationship. J Endocrinol. 1999;163:181–90. https://doi.org/10.1677/joe.0.1630181.
47. Gibly RF, Zhang X, Graham ML, Hering BJ, Kaufman DB, Lowe WL, et al. Extrahepatic islet transplantation with microporous polymer scaffolds in syngeneic mouse and allogeneic porcine models. Biomaterials. 2011;32:9677–84. https://doi.org/10.1016/j.biomaterials.2011.08.084.
48. Berman DM, O'Neil JJ, Coffey LCK, Chaffanjon PCJ, Kenyon NM, Ruiz P, et al. Long-term survival of nonhuman primate islets implanted in an omental pouch on a biodegradable scaffold. Am J Transplant. 2009;9:91–104. https://doi.org/10.1111/j.1600-6143.2008.02489.x.
49. Blomeier H, Zhang X, Rives C, Brissova M, Hughes E, Baker M, et al. Polymer scaffolds as synthetic microenvironments for extrahepatic islet transplantation. Transplantation. 2006;82:452–9. https://doi.org/10.1097/01.tp.0000231708.19937.21.
50. Murphy SV, Atala A. 3D bioprinting of tissues and organs. Nat Biotechnol. 2014;32:773–85. https://doi.org/10.1038/nbt.2958.
51. Schubert C, van Langeveld MC, Donoso LA. Innovations in 3D printing: a 3D overview from optics to organs. Br J Ophthalmol. 2014;98:159–61. https://doi.org/10.1136/bjophthalmol-2013-304446.
52. Ozbolat IT, Chen H, Yu Y. Development of 'multi-arm bioprinter' for hybrid biofabrication of tissue engineering constructs. Robot Comput Integr Manuf. 2014;30:295–304. https://doi.org/10.1016/j.rcim.2013.10.005.
53. Kolesky DB, Truby RL, Gladman AS, Busbee TA, Homan KA, Lewis JA. 3D bioprinting of vascularized, heterogeneous cell-

laden tissue constructs. Adv Mater. 2014;26:3124–30. https://doi.org/10.1002/adma.201305506.

54. Poldervaart MT, Gremmels H, van Deventer K, Fledderus JO, Oner FC, Verhaar MC, et al. Prolonged presence of VEGF promotes vascularization in 3D bioprinted scaffolds with defined architecture. J Control Release. 2014;184:58–66. https://doi.org/10.1016/j.jconrel.2014.04.007.
55. Yue Z, Liu X, Coates PT, Wallace GG. Advances in printing biomaterials and living cells. Curr Opin Organ Transplant. 2016;21:467–75. https://doi.org/10.1097/MOT.0000000000000346.
56. Di Bella C, Duchi S, O'Connell CD, Blanchard R, Augustine C, Yue Z, et al. In situ handheld three-dimensional bioprinting for cartilage regeneration. J Tissue Eng Regen Med. 2018;12:611–21. https://doi.org/10.1002/term.2476.
57. Kesti M, Eberhardt C, Pagliccia G, Kenkel D, Grande D, Boss A, et al. Bioprinting complex cartilaginous structures with clinically compliant biomaterials. Adv Funct Mater. 2015;25:7406–17. https://doi.org/10.1002/adfm.201503423.
58. Lee JW, Choi Y-J, Yong W-J, Pati F, Shim J-H, Kang KS, et al. Development of a 3D cell printed construct considering angiogenesis for liver tissue engineering. Biofabrication. 2016;8:015007. https://doi.org/10.1088/1758-5090/7/2/025009.
59. Gu Q, Tomaskovic-crook E, Lozano R, Chen Y, Kapsa RM, Zhou Q, et al. Functional 3D neural mini-tissues from printed gel-based bioink and human neural stem cells. Adv Healthc Mater. 2016;5:1429–38. https://doi.org/10.1002/adhm.201600095.
60. Derakhshanfar S, Mbeleck R, Xu K, Zhang X, Zhong W, Xing M. 3D bioprinting for biomedical devices and tissue engineering: a review of recent trends and advances. Bioact Mater Elsevier Ltd. 2018;3:144–56. https://doi.org/10.1016/j.bioactmat.2017.11.008.
61.•• Marchioli G, Van Gurp L, Van Krieken PP, Stamatialis D, Engelse M, Van Blitterswijk CA, et al. Fabrication of three-dimensional bioplotted hydrogel scaffolds for islets of Langerhans transplantation. Biofabrication. 2015;7:025009. https://doi.org/10.1088/1758-5090/7/2/025009 **3D bioprinting technology was used to print pancreatic islets using alginate-based bioinks. 3D bioprinted human islets were highly viable and morphologically sound.**
62.•• Duin S, Schütz K, Ahlfeld T, Lehmann S, Lode A, Ludwig B, et al. 3D bioprinting of functional islets of Langerhans in an alginate/methylcellulose hydrogel blend. Adv Healthc Mater. 2019;1801631:1–14. https://doi.org/10.1002/adhm.201801631 **3D bioprinting technology was used to print rat islets using an alginate/methylcellulose bioink with minimal impact on islet viability, morphology, and function.**
63. Penko D, Mohanasundaram D, Sen S, Mee C, Bonder CS, Coates PTH, et al. Incorporation of endothelial progenitor cells into mosaic pseudoislets. Islets. 2011;3:73–9. https://doi.org/10.4161/isl.3.3.15392.
64.•• Liu X, Carter SSD, Renes MJ, Kim J, Rojas-Canales DM, Penko D, et al. Development of a coaxial 3D printing platform for biofabrication of implantable islet-containing constructs. Adv Healthc Mater. 2019;8(7):e1801181. https://doi.org/10.1002/adhm.201801181 A **co-axial bioprinter was developed in-house and alginate-gelatin methacryloyl bioink was formulated, for co-printing of islets with supporting cells such as endothelial progenitor cells and regulatory T cells. Co-printed mouse islets and endothelial progenitor cells were highly viable.**
65. Lifson N, Lassa CV, Dixit PK. Relation between blood flow and morphology in islet organ of rat pancreas. Am J Phys. 1985;249:E43–8. https://doi.org/10.1152/ajpendo.1985.249.1.E43.
66. Johansson A, Lau J, Sandberg M, Borg LAH, Magnusson PU, Carlsson P-O. Endothelial cell signalling supports pancreatic beta cell function in the rat. Diabetologia. 2009;52:2385–94. https://doi.org/10.1007/s00125-009-1485-6.
67. Davalli AM, Scaglia L, Zangen DH, Hollister J, Bonner-Weir S, Weir GC. Vulnerability of islets in the immediate posttransplantation period. Dynamic changes in structure and function. Diabetes. 1996;45:1161–7. https://doi.org/10.2337/diabetes.45.9.1161.
68. de Groot M, Schuurs T, Fekken S, Leuvenink H, van Schilfgaarde R, Keizer J. Response of encapsulated rat pancreatic islets to hypoxia. Cell Transplant. 2003;12:867–75. https://doi.org/10.3727/000000003771000219.
69. Campbell PD, Weinberg A, Chee J, Mariana L, Ayala R, Hawthorne WJ, et al. Expression of pro- and antiapoptotic molecules of the Bcl-2 family in human islets postisolation. Cell Transplant. 2012;21:49–60. https://doi.org/10.3727/096368911X566262.
70. Cantley J, Walters SN, Jung M, Weinberg A, Cowley MJ, Whitworth PT, et al. A preexistent hypoxic gene signature predicts impaired islet graft function and glucose homeostasis. Cell Transplant. 2013;22:2147–59. https://doi.org/10.3727/096368912X658728.
71. Vajkoczy P, Menger MD, Simpson E, Messmer K. Angiogenesis and vascularization of murine pancreatic islet isografts. Transplantation. 1995;60:123–7. https://doi.org/10.1097/00007890-199507000-00002.
72. Mattsson G, Jansson L, Carlsson P-O. Decreased vascular density in mouse pancreatic islets after transplantation. Diabetes. 2002;51:1362–6. https://doi.org/10.2337/diabetes.51.5.1362.
73. Cho H-J, Lee N, Lee JY, Choi YJ, Ii M, Wecker A, et al. Role of host tissues for sustained humoral effects after endothelial progenitor cell transplantation into the ischemic heart. J Exp Med. 2007;204:3257–69. https://doi.org/10.1084/jem.20070166.
74. Rafii S, Lyden D. Therapeutic stem and progenitor cell transplantation for organ vascularization and regeneration. Nat Med. 2003;9:702–12. https://doi.org/10.1038/nm0603-702.
75. Peiris HS, Bonder CS, Coates PT, Keating DJ, Jessup CF. The b-cell/EC axis: how do islet cells talk to each other? Diabetes Care. 2014;63:3–11. https://doi.org/10.2337/db13-0617.
76. Kang S, Park HS, Jo A, Hong SH, Lee HN, Lee YY, et al. Endothelial progenitor cell cotransplantation enhances islet engraftment by rapid revascularization. Diabetes. 2012;61:866–76. https://doi.org/10.2337/db10-1492.
77. Quaranta P, Antonini S, Spiga S, Mazzanti B, Curcio M, Mulas G, et al. Co-transplantation of endothelial progenitor cells and pancreatic islets to induce long-lasting normoglycemia in streptozotocin-treated diabetic rats. PLoS One. 2014;9:1–13. https://doi.org/10.1371/journal.pone.0094783.
78.• Penko D, Rojas-Canales D, Mohanasundaram D, Peiris HS, Sun WY, Drogemuller CJ, et al. Endothelial progenitor cells enhance islet engraftment, influence beta cell function and modulate islet connexin 36 expression. Cell Transplant. 2015;24:37–48. https://doi.org/10.3727/096368913X673423 **Co-transplantation of endothelial progenitor cells with pancreatic islets enhanced islet engraftment by improving the cure rate and the glucose control.**
79. Golshayan D, Pascual M. Tolerance-inducing immunosuppressive strategies in clinical transplantation. Drugs. 2008;68:2113–30. https://doi.org/10.1016/S0140-6736(98)07493-5.
80. Xing Y, Hogquist KA. T-cell tolerance: central and peripheral. Cold Spring Harb Perspect Biol 2012;1–16.
81. Sakaguchi S, Miyara M, Costantino CM, Hafler DA. FOXP3+ regulatory T cells in the human immune system. Nat Rev Immunol. 2010;10:490–500. https://doi.org/10.1038/nri2785.
82. Tang Q, Bluestone JA. Regulatory T-cell therapy in transplantation: moving to the clinic. Cold Spring Harb Perspect Med. 2013;3:1–15. https://doi.org/10.1101/cshperspect.a015552.

83. Vignali DAA, Collison LW, Workman CJ. How regulatory T cells work. Nat Rev Immunol. 2008;8:523–32. https://doi.org/10.1038/nri2343.
84. Cunningham EC, Sharland AF, Alex Bishop G. Liver transplant tolerance and its application to the clinic: can we exploit the high dose effect? Clin Dev Immunol. 2013;2013:1–9. https://doi.org/10.1155/2013/419692.
85. Cippà PE, Fehr T. Spontaneous tolerance in kidney transplantation - an instructive, but very rare paradigm. Transpl Int. 2011;24:534–5. https://doi.org/10.1111/j.1432-2277.2011.01260.x.
86. Orlando G, Hematti P, Stratta R, Burke G, Di Cocco P, Pisani F, et al. Clinical operational tolerance after renal transplantation. Ann Surg. 2010;252:915–28. https://doi.org/10.1038/nbt.3121.ChIP-nexus.
87. Li W, Kuhr CS, Zheng XX, Carper K, Thomson AW, Reyes JD, et al. New insights into mechanisms of spontaneous liver transplant tolerance: the role of Foxp3-expressing CD25+CD4+ regulatory T cells. Am J Transplant. 2008;8:1639–51. https://doi.org/10.1111/j.1600-6143.2008.02300.x.
88. Heidt S, Wood KJ. Biomarkers of operational tolerance in solid organ transplantation. Expert Opin Med Diagn. 2012;6:281–93. https://doi.org/10.1517/17530059.2012.680019.BIOMARKERS.
89. Niemann N, Sawitzki B. Treg therapy in transplantation: how and when will we do it ? Curr Transplant Reports. 2015;2:233–41. https://doi.org/10.1007/s40472-015-0066-5.
90. Riley JL, June CH, Blazar BR. Human T regulatory cells as therapeutic agents: take a billion or so of these and call me in the morning. Immunity. 2010;30:656–65. https://doi.org/10.1016/j.immuni.2009.04.006.Human.
91. McMurchy AN, Bushell A, Levings MK, Wood KJ. Moving to tolerance: clinical application of T regulatory cells. Semin Immunol. 2011;23:304–13. https://doi.org/10.1016/j.smim.2011.04.001.
92. Xiao F, Ma L, Zhao M, Huang G, Mirenda V, Dorling A, et al. Ex vivo expanded human regulatory T cells delay islet allograft rejection via inhibiting islet-derived monocyte chemoattractant protein-1 production in CD34+ stem cells-reconstituted NOD-scid IL2rgnull mice. PLoS One. 2014;9:1–12. https://doi.org/10.1371/journal.pone.0090387.
93. Wu DC, Hester J, Nadig SN, Zhang W, Trzonkowski P, Gray D, et al. Ex vivo expanded human regulatory T cells can prolong survival of a human islet allograft in a humanized mouse model. Transplantation. 2013;96:707–16. https://doi.org/10.1097/TP.0b013e31829fa271.
94.• Chandran S, Tang Q, Sarwal M, Polyclonal Regulatory T. Cell therapy for control of inflammation in kidney transplants. Am J Transplant. 2017;17:2945–54. https://doi.org/10.1111/ajt.14415 **Infusion of ex vivo expanded regulatory T cells was well tolerated with no adverse effects in kidney transplant recipients.**
95.• Todo S, Yamashita K, Goto R, Zaitsu M, Nagatsu A, Oura T, et al. A pilot study of operational tolerance with a regulatory T-cell-based cell therapy in living donor liver transplantation. Hepatology. 2016;64:632–43. https://doi.org/10.1002/hep.28459 **Infusion of ex vivo expanded regulatory T cells was well tolerated with no adverse effects in liver transplant recipients. Seven patients have been maintaining normal graft function without the use of immunosuppressive drugs for more than 16 months.**
96. Ackermann AM, Gannon M. Molecular regulation of pancreatic beta-cell mass development, maintenance, and expansion. J Mol Endocrinol. 2007;38:193–206. https://doi.org/10.1677/JME-06-0053.
97. Hughes A, Rojas-canales D, Drogemuller C. IGF2: an endocrine hormone to improve islet transplant survival. J Endocrinol. 2014;221:R41–8. https://doi.org/10.1530/JOE-13-0557.
98. Reik W, Sun F-L, Dean WL, Kelsey G, Allen ND. Transactivation of Igf2 in a mouse model of Beckwith-Wiedemann syndrome. Nature. 1997;389:809–15. https://doi.org/10.1038/39797.
99. Petrik J, Arany E, McDonald TJ, Hill DJ. Apoptosis in the pancreatic islet cells of the neonatal rat is associated with a reduced expression of insulin-like growth factor II that may act as a survival factor. Endocrinology. 1998;139:2994–3004. https://doi.org/10.1210/endo.139.6.6042.
100. Hill DJ, Strutt B, Arany E, Zaina S, Coukell S, Graham CF. Increased and persistent circulating insulin-like growth factor II in neonatal transgenic mice suppresses developmental apoptosis in the pancreatic islets. Endocrinology. 2000;141:1151–7. https://doi.org/10.1210/endo.141.3.7354.
101. Hogg J, Han VK, Clemmons DR, Hill DJ. Interactions of nutrients, insulin-like growth factors (IGFs) and IGF-binding proteins in the regulation of DNA synthesis by isolated fetal rat islets of Langerhans. J Endocrinol. 1993;138:401–12. https://doi.org/10.1677/joe.0.1380401.
102. Robitaille R, Dusseault J, Henley N, Rosenberg L, Hallé J-P. Insulin-like growth factor II allows prolonged blood glucose normalization with a reduced islet cell mass transplantation. Endocrinology. 2003;144:3037–45. https://doi.org/10.1210/en.2002-0185.
103. Petrik J, Reusens B, Arany E, Remacle C, Coelho C, Hoet JJ, et al. A low protein diet alters the balance of islet cell replication and apoptosis in the fetal and neonatal rat and is associated with a reduced pancreatic expression of insulin-like growth factor-II. Endocrinology. 1999;140:4861–73. https://doi.org/10.1210/endo.140.10.7042.
104. Hughes A, Mohanasundaram D, Kireta S, Jessup CF, Drogemuller CJ, Coates PTH. Insulin-like growth factor-II (IGF-II) prevents proinflammatory cytokine-induced apoptosis and significantly improves islet survival after transplantation. Transp J. 2013;95:671–8. https://doi.org/10.1097/TP.0b013e31827fa453.
105. Shibuya M. Vascular endothelial growth factor (VEGF) and its receptor (VEGFR) signaling in angiogenesis: a crucial target for anti- and pro-angiogenic therapies. Genes and Cancer. 2011;2:1097–105. https://doi.org/10.1177/1947601911423031.
106. Lammert E, Gu G, Mclaughlin M, Brown D, Brekken R, Murtaugh LC, et al. Role of VEGF-A in vascularization of pancreatic islets. Curr Biol. 2003;13:1070–4. https://doi.org/10.1016/S0960-9822(03)00378-6.
107. Witkowski P, Sondermeijer H, Hardy MA, Woodland DC, Lee K, Bhagat G, et al. Islet grafting and imaging in a bioengineered intramuscular space. Transplantation. 2009;88:1065–74. https://doi.org/10.1097/TP.0b013e3181ba2e87.
108.• Marchioli G, Di Luca A, De Koning E, Engelse M, Van Blitterswijk CA, Karperien M, et al. Hybrid polycaprolactone/alginate scaffolds functionalized with VEGF to promote de novo vessel formation for the transplantation of islets of Langerhans. Adv Healthc Mater. 2016;5:1606–16. https://doi.org/10.1002/adhm.201600058 **Polycaprolactone scaffold functionalized with VEGF promoted vascularization and improved function of encapsulated islets embedded within the polycaprolactone scaffold.**
109. Boyman O, Sprent J. The role of interleukin - 2 during homeostasis and activation of the immune system. Nat Rev Immunol. 2012;12:180–90. https://doi.org/10.1038/nri3156.
110. Sakaguchi S, Takahashi T, Nishizuka Y. Study on cellular events in post-thymectomy autoimmune oophoritis in mice. J Exp Med. 1982;156:1577–86.
111. Chinen T, Kannan AK, Levine AG, Fan X, Klein U, Zheng Y, et al. An essential role for IL-2 receptor in regulatory T cell function Takatoshi. Nat Immunol. 2016;17:1322–33. https://doi.org/10.1038/ni.3540.

112. Létourneau S, Krieg C, Pantaleo G, Boyman O. IL-2- and CD25-dependent immunoregulatory mechanisms in the homeostasis of T-cell subsets. J Allergy Clin Immunol. 2009;123:758–62. https://doi.org/10.1016/j.jaci.2009.02.011.
113. Sadlon TJ, Wilkinson BG, Pederson S, Brown CY, Bresatz S, Gargett T, et al. Genome-wide identification of human FOXP3 target genes in natural regulatory T cells. J Immunol. 2010;185:1071–81. https://doi.org/10.4049/jimmunol.1000082.
114. Beyer M, Thabet Y, Müller R, Sadlon T, Classen S, Lahl K, et al. Repression of the genome organizer SATB1 in regulatory T cells is required for suppressive function and inhibition of effector differentiation. Nat Immunol. 2011;12:898–907. https://doi.org/10.1038/ni.2084.
115. Whitehouse G, Gray E, Mastoridis S, Merritt E, Kodela E, Yang JHM. IL-2 therapy restores regulatory T-cell dysfunction induced by calcineurin inhibitors. Proc Natl Acad Sci USA. 2017;114:7083–8. https://doi.org/10.1073/pnas.1620835114.
116. Shevach EM. Application of IL-2 therapy to target T regulatory cell function. Trends Immunol. 2013;33:626–32. https://doi.org/10.1016/j.it.2012.07.007.
117. Zorn E, Nelson EA, Mohseni M, Porcheray F, Kim H, Litsa D, et al. IL-2 regulates FOXP3 expression in human CD4+ CD25+ regulatory T cells through a STAT-dependent mechanism and induces the expansion of these cells in vivo. Blood. 2006;108:1571–80. https://doi.org/10.1182/blood-2006-02-004747.
118. Koreth J, Matsuoka K, Kim HT, McDonough SM, Bindra B, Alyea EP, et al. Interleukin-2 and regulatory T cells in graft-versus-host disease. N Engl J Med. 2011;365:2055–66. https://doi.org/10.1056/NEJMoa1108188.
119. Matsuoka K, Koreth J, Kim HT, Bascug OG, Kawano Y, Murase K, et al. Low-dose interleukin-2 therapy restores regulatory T cell homeostasis in patients with chronic graft-versus-host disease. Sci Transl Med. 2013;5:179ra43. https://doi.org/10.1126/scitranslmed.3005265.
120. Koreth J, Kim HT, Jones KT, Lange PB, Reynolds CG, Chammas MJ, et al. Efficacy , durability , and response predictors of low-dose interleukin-2 therapy for chronic graft-versus-host disease. Blood. 2016;128:130–8. https://doi.org/10.1182/blood-2016-02-702852.

ADVANCED FUNCTIONAL MATERIALS
www.afm-journal.de



# Encapsulation of Human Natural and Induced Regulatory T-Cells in IL-2 and CCL1 Supplemented Alginate-GelMA Hydrogel for 3D Bioprinting

*Juewan Kim, Christopher M. Hope, Narangerel Gantumur, Griffith B. Perkins, Sebastian O. Stead, Zhilian Yue, Xiao Liu, Ane U. Asua, Francis D. Kette, Daniella Penko, Christopher J. Drogemuller, Robert P. Carroll, Simon C. Barry, Gordon G. Wallace,* and Patrick Toby Coates**

**Regulatory T-cells (Tregs) are important modulators of the immune system through their intrinsic suppressive functions. Systemic adoptive transfer of ex vivo expanded Tregs has been extensively investigated for allogeneic transplantation. Due to the time-consuming and costly expansion protocols of Tregs, more targeted approaches could be beneficial. The encapsulation of human natural and induced Tregs for localized immunosuppression is described for the first time. Tregs encapsulated in alginate-gelatin methacryloyl hydrogel remain viable, phenotypically stable, functional, and confined in the structure. Supplementation of the hydrogel with the Treg-specific bioactive factors interleukin-2 and chemokine ligand 1 improves Treg viability, suppressive phenotype, and function, and attracts to the structure CCR8$^+$ T-cells enriched with anti-inflammatory subpopulations, including Tregs, from human peripheral blood. Furthermore, these findings are applicable to 3D bioprinting. Co-axial printing of murine pancreatic islets with human natural and induced Tregs protects the islets from xenoresponse upon co-culture with human peripheral blood mononuclear cells. This establishes the co-encapsulation of Tregs by co-axial 3D bioprinting as a valid option for providing local immune protection to allogeneic cellular transplants such as pancreatic islets.**

## 1. Introduction

Regulatory T-cells (Tregs) constitute a vital CD4$^+$ T-cell subpopulation specialized in immune suppression and regulation.[1] Tregs were initially reported in 1970 as suppressor T-cells, a subset of T-cells with the ability to abrogate the proinflammatory immune responses.[2] Since then, intensive investigations led to the discoveries of Treg-defining surface markers, CD4$^+$, CD25$^{hi}$, and CD127$^-$, and the master transcriptional regulator of Treg-lineage, FOXP3.[3–8] To date, two main subgroups of natural Tregs (nTregs) exhibit the CD4$^+$ CD25$^{hi}$ CD127$^-$ FOXP3$^+$ profile: thymic-derived natural Tregs (tTregs), which stably express FOXP3, and CD4$^+$ T cells that acquire FOXP3 expression in the periphery, called pTregs. pTregs generated in vitro are known as induced Tregs (iTregs).[9,10]

J. Kim, G. B. Perkins
Department of Molecular and Cellular Biology
School of Biological Sciences
The University of Adelaide
Adelaide, South Australia 5005, Australia

Dr. C. M. Hope, Prof. S. C. Barry
Department of Gastroenterology
Women's and Children's Hospital
Adelaide, South Australia 5006, Australia

N. Gantumur, Dr. Z. Yue, Dr. X. Liu, A. U. Asua, Prof. G. G. Wallace
Intelligent Polymer Research Institute
ARC Centre of Excellence for Electromaterial Science
University of Wollongong
Wollongong, New South Wales 2522, Australia
E-mail: gwallace@uow.edu.au

The ORCID identification number(s) for the author(s) of this article can be found under https://doi.org/10.1002/adfm.202000544.

**DOI: 10.1002/adfm.202000544**

Dr. S. O. Stead, F. D. Kette, C. J. Drogemuller, Dr. R. P. Carroll, Prof. P. T. Coates
Discipline of Medicine
School of Medicine
The University of Adelaide
Adelaide, South Australia 5000, Australia
E-mail: toby.coates@sa.gov.au

Dr. S. O. Stead, F. D. Kette
College of Medicine and Public Health
Discipline of Medicine
Flinders University
Bedford Park, South Australia 5042, Australia

D. Penko, C. J. Drogemuller, Dr. R. P. Carroll, Prof. P. T. Coates
Central Northern Adelaide Renal and Transplantation Service (CNARTS)
The Royal Adelaide Hospital
Adelaide, South Australia 5000, Australia

Prof. S. C. Barry
Molecular Immunology Group
Robinson Research Institute
School of Medicine
The University of Adelaide
Adelaide, South Australia 5005, Australia

 

Tregs are a crucial component of immunological tolerance and homeostasis, playing many roles in the immune system, including establishing tolerance to self and selected foreign antigens, and regulating the duration of immune responses to minimize self-damage.[1] Tregs mediate suppression via the secretion of anti-inflammatory cytokines, cytolysis of target cells, metabolic disruption, and modulation of dendritic cells.[11] Treg-mediated suppression, thus, targets a broad range of immune cells including other T-cell subsets, B cells, antigen presenting cells, and natural killer cells.[12] With such versatility in modes and targets of action, immunotherapies utilizing Tregs have been extensively investigated for the treatment of autoimmunity and allogeneic transplantation.[13]

In particular, Treg-therapy could establish allograft tolerance in transplant recipients, overcoming challenges associated with the requirement for life-long systemic immunosuppression to prevent allograft rejection, such as an increased risk of infection, malignancy, and organ toxicity.[14] Furthermore, spontaneous allogeneic organ tolerance, a phenomenon in which transplant recipients accept the allografts without the use of immunosuppressive regimen, has been observed in liver transplant recipients with elevated Treg levels.[15] Currently, most clinical trials of Treg-therapies utilize systemic adoptive transfer of ex vivo expanded Tregs.[16] While this method has shown promising results in clinical trials,[17,18] ex vivo expansion of Tregs requires extremely time-consuming and costly protocols to generate appropriate numbers of cells for clinically significant results, due to the low frequency of Tregs in human peripheral blood.[13,19] Thus, it would be advantageous to employ more targeted approaches requiring less Tregs, such as hydrogel encapsulation to provide localized immunosuppression.

Pancreatic islet transplantation is currently the only curative cell therapy for type 1 diabetes mellitus. Islet transplantation is unique, compared to solid organ transplantation, as it involves the isolation and purification of islets from a donor pancreas, which are then infused into the recipient liver via the hepatic portal vein.[20] Due to such characteristics, it is possible to co-transplant islets with other cell types beneficial to their survival.[21,22] As rejection by the immune system remains a major hurdle, co-encapsulation of islets with Tregs could be of great benefit. This could be achieved via 3D bioprinting using a recently developed customized co-axial bioprinter, equipped with dual bioink chambers, to generate a scaffold containing a core of islets surrounded by a shell of Tregs, providing localized immune protection.[23–25]

Here, we encapsulated human nTregs and iTregs in an alginate-gelatin methacryloyl (GelMA) hydrogel, a bioink that we recently developed for co-axial bioprinting of islets with supporting cells.[24] While islets have been routinely encapsulated since 1980,[26] Tregs have never previously been encapsulated. Therefore, this study investigated the impact of encapsulation on human nTregs and iTregs. Furthermore, the hydrogel was supplemented with Treg-specific bioactive factors, interleukin-2 (IL-2) and chemokine ligand 1 (CCL1), to enhance the encapsulation of Tregs. IL-2 is a T-cell stimulatory cytokine that is crucial for Treg survival and function.[27] The effect of IL-2 on the encapsulated Tregs was evaluated. CCL1 is a ligand for chemokine receptor 8 (CCR8) that is preferentially expressed on Tregs.[28] The capability of CCL1 to recruit additional Tregs to the hydrogel structure was examined, as well as the composition of the lymphocyte population that would actively be recruited from human peripheral blood. Lastly, utilizing an alginate-GelMA based bioink, murine islets were co-axially printed with human nTregs and iTregs, and then co-cultured with human peripheral blood mononuclear cells (PBMCs) to investigate the immune-protective ability of printed Tregs.

## 2. Results

### 2.1. Preparation of Alginate-GelMA Hydrogel Precursor and Treg Encapsulation

Alginate-GelMA hydrogel precursor was generated by the addition of GelMA to an alginate solution. GelMA was prepared from porcine gelatin by the addition of methacrylic anhydride (**Figure 1**a). The degree of functionalization (DoF) was measured by a ninhydrin assay quantifying absorbance at 570 nm. The concentration of unfunctionalized gelatin remaining in the GelMA was interpolated from gelatin standards ranging from 0 to 100 mg $mL^{-1}$, confirming successful methacryloyl functionalization with a DoF of 82 ± 5%. The hydrogel precursor was then used to encapsulate Tregs via photo and chemical crosslinking (Figure 1b). Successful encapsulation was demonstrated by transmission electron microscopy (TEM) (Figure 1c). In some experiments, Tregs were recovered via enzymatic dissolution of the hydrogel discs using TrypLE, which targets peptide bonds on the C-termini of lysine and arginine of GelMA.

### 2.2. Viability of Encapsulated Tregs

The viability of encapsulated or control nonencapsulated Tregs at days 1 and 3 was evaluated by measuring dye exclusion, expressed as % propidium $iodide^+$ (**Figure 2**a). On day 1, encapsulated Treg viability was significantly reduced in both nTregs and iTregs (8% and 10%; $P = 0.0034$ and $P = 0.0038$, respectively) in the absence of IL-2, while there was no significant decrease in viability upon encapsulation in the presence of IL-2. Nonencapsulated and encapsulated Tregs without IL-2 displayed significantly lower viability than those with IL-2, a 9% ($P = 0.0012$) and 12% ($P < 0.0001$) decrease in nTregs and 16% ($P < 0.0001$) and 23% ($P < 0.0001$) decrease in iTregs, respectively. At day 3, viability of nonencapsulated and encapsulated Tregs without IL-2 decreased by 23% and 41% in nTregs and 29% and 40% in iTregs ($P < 0.0001$), compared with those IL-2. The viability of encapsulated Tregs with IL-2 was significantly lower than nonencapsulated Tregs with IL-2 (18% decreases in both nTregs and iTregs, $P = 0.0001$ and 0.0042, respectively; Figure 2b). These decreases were reversed by supplementing the media with IL-2 ("encapsulated with IL-2 in media") instead of the hydrogel. The viability of encapsulated Tregs with IL-2 in the media displayed no significant differences from nonencapsulated Tregs with IL-2 (Figure 2c).

### 2.3. Phenotype of Encapsulated Tregs

Tregs are classically defined as $CD4^+$ $CD25^+$ $FOXP3^+$ cells. Expression of CD25 and FOXP3 was measured as mean

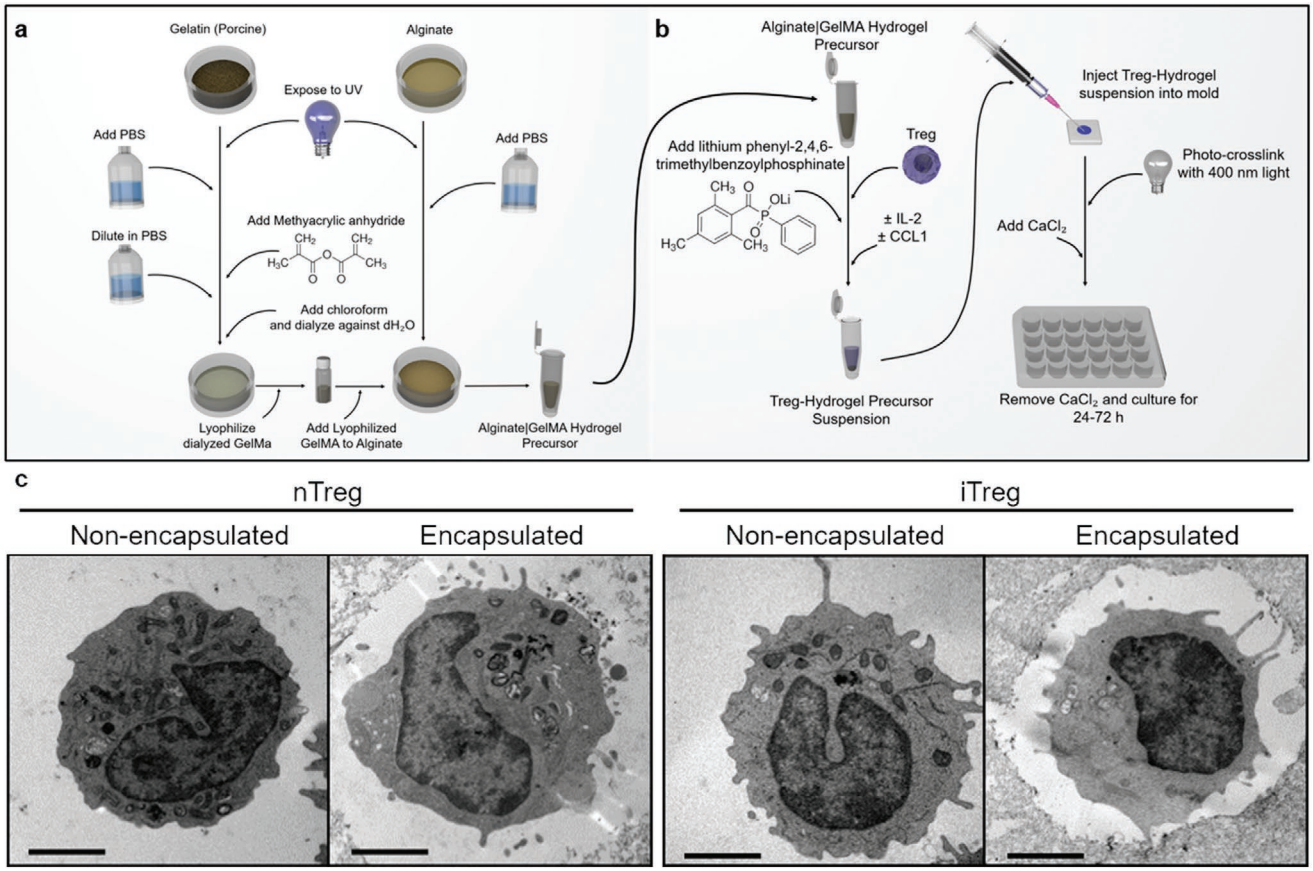


**Figure 1.** a) Schematics for preparation of alginate-GelMA hydrogel precursor and b) Treg encapsulation. c) Transmission electron microscope images of nonencapsulated and encapsulated nTregs and iTregs. Best represented images from $n = 3$. Scale bar represents 2 µm at 11 500 × magnification.

fluorescence intensity (MFI) in viable CD4+ populations (**Figure 3**a). Analysis showed no significant differences in the MFI of CD25 expression between nonencapsulated and encapsulated Tregs. CD25 MFI of nonencapsulated and Tregs encapsulated with IL-2 were higher than Tregs without IL-2 for nTregs (nonencapsulated: $P = 0.0305$) and iTregs ($P < 0.0001$). Tregs encapsulated with IL-2 showed significantly lower FOXP3 MFI than nonencapsulated Tregs cultured with IL-2 ($P = 0.0006$ for nTregs and $P < 0.0001$ for iTregs). This was in contrast to Tregs encapsulated without IL-2, which showed no significant decrease in FOXP3 MFI compared with nonencapsulated Tregs cultured without IL-2. Moreover, FOXP3 MFI of nonencapsulated and encapsulated Tregs without IL-2 was significantly reduced compared with those with IL-2 in both nTregs ($P < 0.0001$ and $P = 0.0069$) and iTregs ($P < 0.0001$ and $P = 0.0001$; Figure 3b). Treg functional markers CD69 (activation marker), transforming growth factor beta (TGF-$\beta$; inhibitory cytokine), CD39 (metabolic disruption), and cytotoxic T-lymphocyte-associated protein 4 (CTLA-4; dendritic cell modulation), which are surrogates for activation status and suppressive functionality,[11,29] were also assessed (**Figure 4**a). There were no significant differences in CD69, CD39, and CLTA-4 MFI between nonencapsulated and encapsulated Tregs. Nonencapsulated Tregs without IL-2 showed significantly lower CD69 ($P = 0.0472$) and CD39 ($P = 0.0062$) MFI in iTregs and CTLA-4 ($P = 0.0062$) MFI in nTregs while there were significant differences between encapsulated Tregs with and without IL-2. TGF-$\beta$ expression mimicked that of FOXP3, showing significant differences between nonencapsulated and encapsulated Tregs with IL-2 ($P = 0.0001$ in nTregs and $P = 0.0011$ in iTregs) and between nonencapsulated and encapsulated Tregs with and without IL-2 ($P < 0.0001$ and $P = 0.0023$ in nTregs and $P < 0.0001$ in iTregs; encapsulated Tregs showed n.s in iTregs; Figure 4b). Again, upon supplementation of the media with IL-2, FOXP3, and TGF-$\beta$ MFI expression was equivalent to nonencapsulated Tregs, showing significantly higher MFI (FOXP3: $P < 0.0001$ in both nTregs and iTregs. TGF-$\beta$: $P = 0.0044$ in nTregs and $P = 0.0003$ in iTregs) than encapsulated Tregs with IL-2 (Figure 4c).

### 2.4. Suppressor Function of Encapsulated Treg

Suppressive activities of nonencapsulated and encapsulated Tregs were assessed using CD154 suppression assays. CD154 is an activation marker transiently expressed during T-cell activation and can be measured in naïve $CD4^+$ T-cells (Teffectors) in the presence of Tregs to assess the suppressor function of Tregs.[30] Tregs to Teffectors ratios of 1:1 to 1:8 were utilized. $DiOC_{18}(3)$ (3,30-dioctadecyloxacarbocyanine perchlorate) was used to differentiate Teffectors from Tregs in the flow cytometric analysis. Negative control ($DiOC_{18}(3)$ labeled and CD154

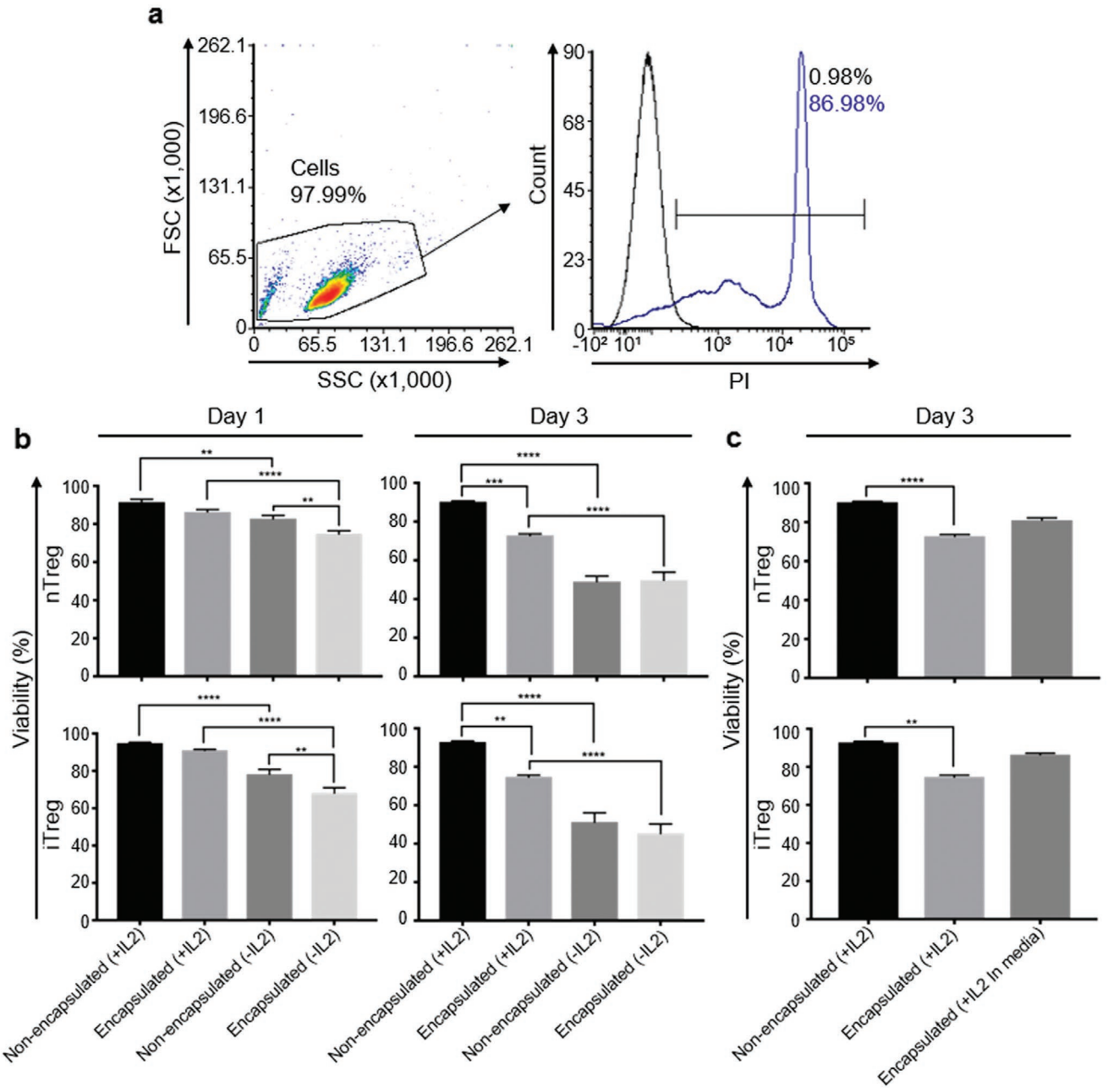


**Figure 2.** Viability of Tregs encapsulated in alginate-GelMA hydrogel at days 1 and 3. a) Gating strategy to determine the percentage of dead cells. Propidium iodide (PI) was used to stain dead cells (black line: unstained control; Indigo line: positive dead control). b) Viability at days 1 and 3 for both nTregs and iTregs. Nonencapsulated Tregs were cultured in either IL-2-supplemented media "nonencapsulated (+IL-2)" or IL-2-free media "non-encapsulated (-IL-2)". Encapsulated Tregs were made with either IL-2-supplemented hydrogel "encapsulated (+IL-2)" or IL-2-free hydrogel "encapsulated (-IL-2)" and then cultured in IL-2-free media. c) Day 3 viability of encapsulated Tregs upon supplementation of the media with IL-2 instead of the hydrogel "encapsulated (+IL2 in media)". Data represented as mean ± SEM, $n = 3$, statistical significance identified by One-Way ANOVA with Tukey's multiple comparisons test: $^{*}P < 0.05$, $^{**}P < 0.01$, $^{***}P < 0.001$, and $^{****}P < 0.0001$.

stained) Teffectors provided baseline unstimulated % $CD154^+$ to gate $CD154^+$ cells. Positive control ($DiOC_{18}(3)$ labeled, CD154 stained Teffectors stimulated with anti-CD3/CD28 beads) served as baseline stimulated %$CD154^+$ to calculate % suppression (**Figure 5**a). No significant differences in % suppression were shown between nonencapsulated and encapsulated Tregs at all ratios. In the absence of IL-2, Tregs displayed significant losses in their suppressor function compared with those in the presence of IL-2. At 1:1 ratio, both nonencapsulated and encapsulated groups displayed 10% ($P = 0.0115$ and 0.0132) decreases in nTregs and 13% ($P = 0.0048$ and 0.0038) decreases in iTregs. At 1:2 ratio, 8% (n.s; $P = 0.0771$) and 10% ($P = 0.0324$) decreases were shown in nTregs and 13% ($P < 0.0001$) and 18% ($P = 0.0034$) decreases were observed in iTregs (Figure 5b).

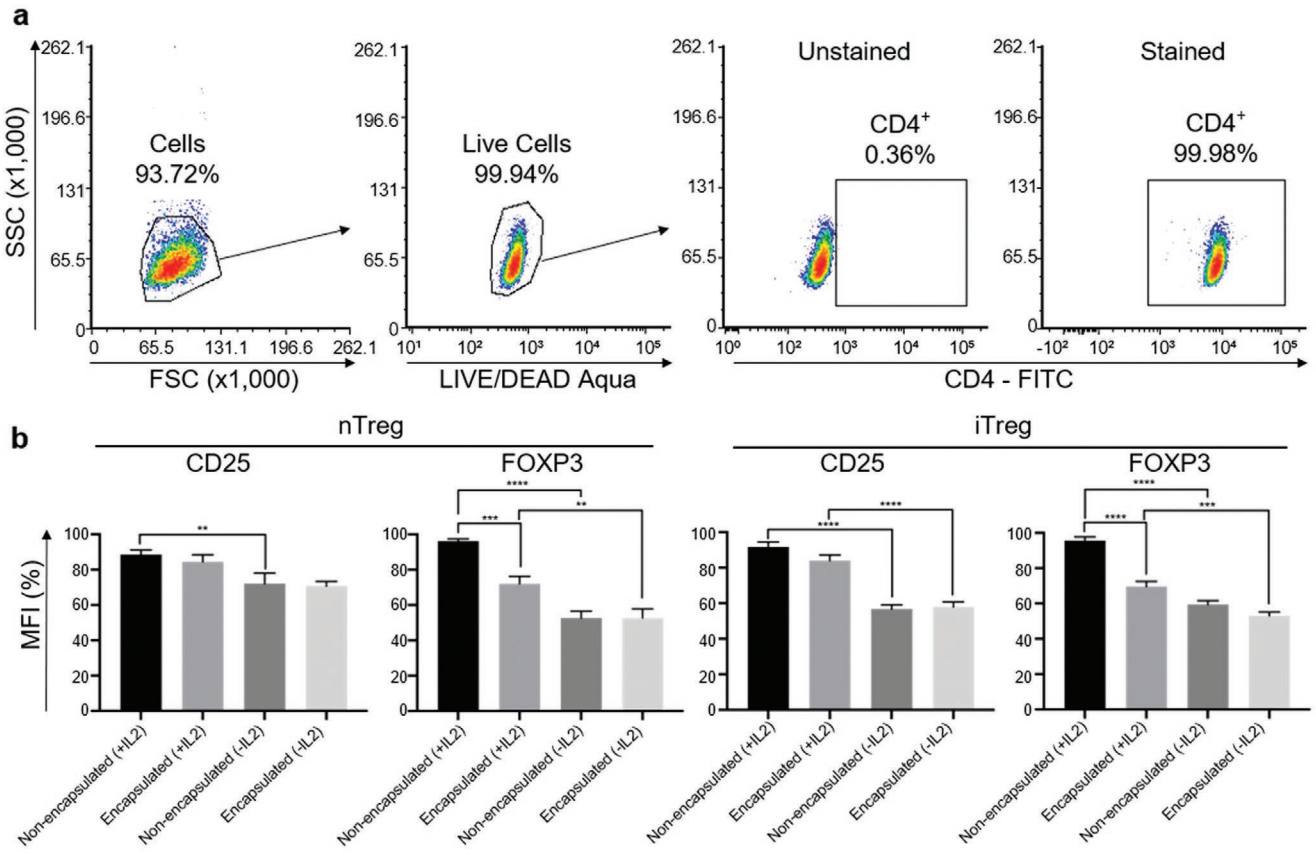


**Figure 3.** Expression of Treg phenotype markers upon encapsulation in alginate-GelMA hydrogel. a) Gating strategy for $CD4^+$ cells using an unstained population. Mean fluorescence intensity (MFI) for CD25 and FOXP3 was measured from this $CD4^+$ population. MFI was normalized to the maximum raw value in each marker and experiment. b) CD25 and FOXP3 MFI in nonencapsulated and encapsulated nTregs and iTregs (±IL-2). Data represented as mean ± SEM, $n = 3$, statistical significance identified by One-Way ANOVA with Tukey's multiple comparisons test: $^*P < 0.05$, $^{**}P < 0.01$, $^{***}P < 0.001$, and $^{****}P < 0.0001$.

### 2.5. Migration Capacity of Encapsulated Tregs and CCL Supplementation of the Hydrogel

For successful localized immunosuppression, it is important that Tregs stay confined within the hydrogel structure, which can be facilitated by strong chemotactic signals. The chemotactic response profile of nTregs and iTregs to CCL1 was measured from 100 ng $mL^{-1}$ to 10 µg $mL^{-1}$ with threefold increment, to determine concentration dose response. Spontaneous migration with no chemokine was utilized to calculate migration index (MI). Maximal responses were observed at 10 µg $mL^{-1}$ with migration index of 30 and 9 in nTregs and iTregs, respectively (**Figure 6**a). 10 µg $mL^{-1}$ of CCL1 was used to assess the migration capacity of nonencapsulated and encapsulated Tregs. Migration capacity of encapsulated Tregs was significantly reduced compared with nonencapsulated Tregs with 400-fold reduction ($P = 0.0003$) for nTregs and 220-fold ($P < 0.0001$) reduction for iTregs (Figure 6b). In parallel, the Treg-recruitment capability of hydrogel discs supplemented with CCL1 was evaluated. CCL1-supplemented hydrogel demonstrated recruitment of Tregs with an MI of 5 in nTregs and that of 3 in iTregs. This was significantly lower than the 10 µg $mL^{-1}$ of CCL1 in chemotaxis buffer, which showed an MI of 43 with nTregs ($P < 0.0001$) and that of 19 with iTregs ($P < 0.0001$) (Figure 6c). Moreover, CCL1 has been shown to enhance Treg function.[31] Therefore, CCL1-supplimented hydrogel was used to encapsulate Tregs and suppressive activities of encapsulated Tregs with and without CCL1 were measured. Interestingly, nTregs and iTregs showed completely opposite results. Suppressive activity of encapsulated nTregs was significantly higher in the presence of CCL1 with 12% ($P = 0.0211$), 13% ($P = 0.0125$), and 15% ($P = 0.0365$) differences at 1:1, 1:2, and 1:8 ratios (1:4 ratio n.s with 12% difference; $P = 0.1129$) while suppressive activity of iTregs was significantly lower in the presence of CCL1 with 8% ($P = 0.0355$), 12% ($P = 0.0385$), 16% ($P = 0.0277$), and 18% ($P = 0.0057$) differences at all ratios (Figure 6d).

To investigate which types of lymphocytes would be recruited from the human peripheral blood through CCL1-mediated chemotaxis, PBMCs were isolated from whole blood for immunophenotyping. Particular interests were in $CD4^+$ T-cell subsets as most of the $CCR8^+$ cells in the peripheral blood are $CD4^+$ memory T-cells.[28] PBMCs were stained for CD3, CD4, CD45RA, CD25, and CD127 and CXCR3, CCR4, CCR6, CCR8, and CCR10 to compare proportions of $CD4^+$ T-cell subsets in the whole memory (inclusive of $CCR8^+$ and $CCR8^-$) $CD4^+$ T-cells with $CCR8^+$ memory $CD4^+$ T-cells. Within these two populations, memory Tregs (mTregs) and memory conventional T-cells (mTconvs) were gated based on their CD25 and CD127 expression. mTconvs

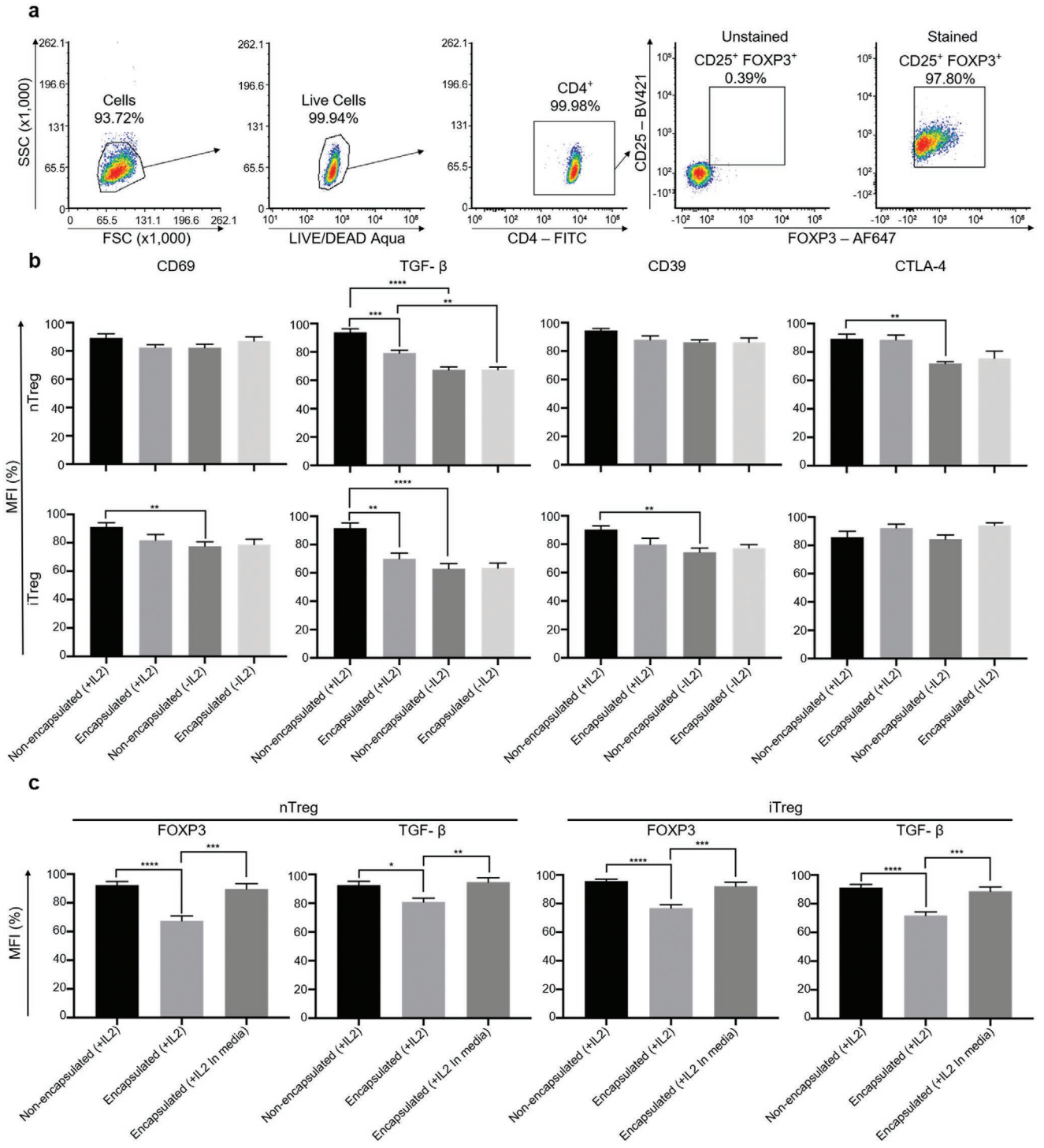


**Figure 4.** Expression of Treg functionality markers upon encapsulation in alginate-GelMA hydrogel. a) Gating strategy for $CD4^+$ $CD25^+$ $Foxp3^+$ cells using an unstained population. Mean fluorescence intensity (MFI) for CD69, TGF-$\beta$, CD39, and CTLA-4 was then measured from this $CD4^+$ $CD25^+$ $Foxp3^+$ population. MFI was normalized to the maximum raw value in each marker and experiment. b) CD69, TGF-$\beta$, CD39, and CTLA-4 MFI in nonencapsulated and encapsulated nTregs and iTregs (±IL-2). c) FOXP3 and TGF-$\beta$ MFI of encapsulated nTregs and iTregs (+IL-2 in media). Data represented as mean ± SEM, $n = 3$, statistical significance identified by One-Way ANOVA with Tukey's multiple comparisons test: $^*P < 0.05$, $^{**}P < 0.01$, $^{***}P < 0.001$, and $^{****}P < 0.0001$.

were then further divided into T-helper subsets using chemokine receptors (**Figure 7**a). $CCR8^+$ memory $CD4^+$ T-cells showed significant enrichments of mTregs ($P = 0.0006$), Th2 ($P = 0.0036$), and Th22 cells ($P = 0.0001$) compared to whole memory $CD4^+$ T-cells. Proportions of mTconvs ($P = 0.0004$), Th1 ($P = 0.0126$), Th1/17 ($P = 0.0097$), Th17 ($P = 0.0035$), and Th9 ($P < 0.0001$)

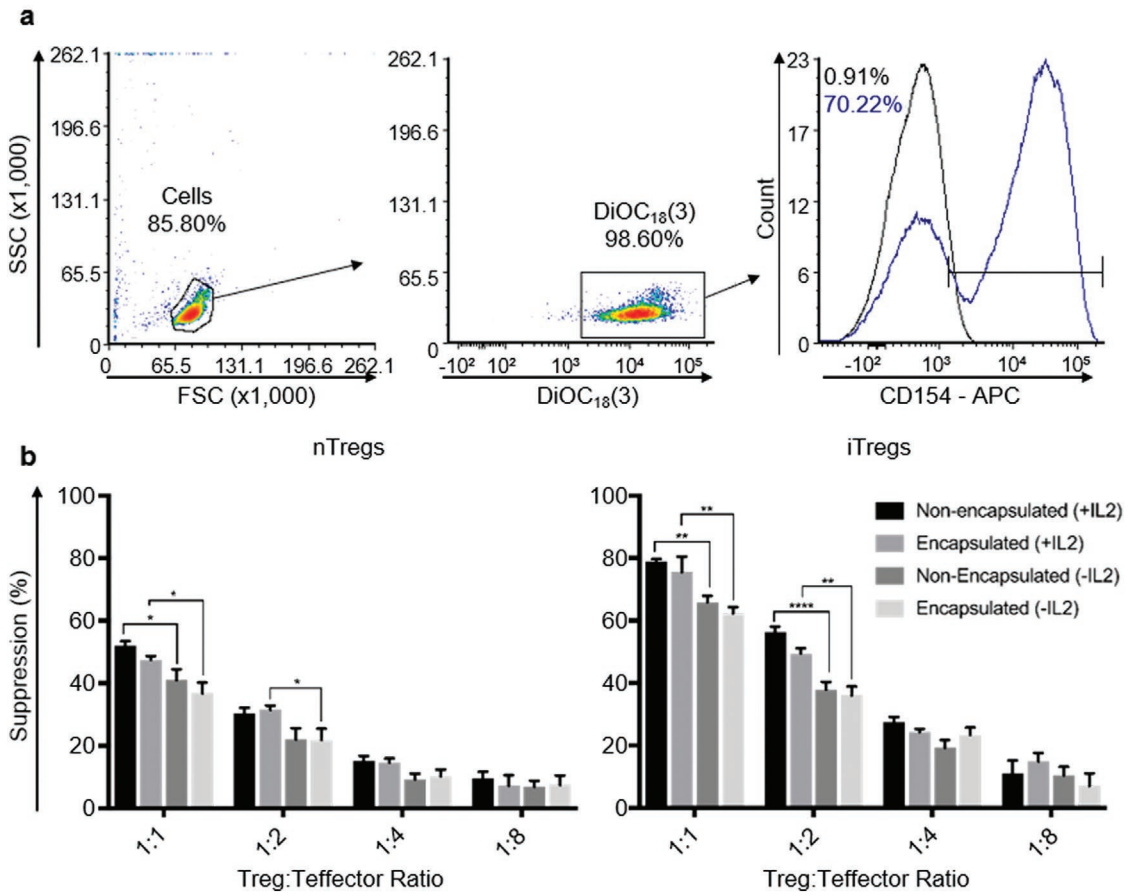


**Figure 5.** Function of Tregs encapsulated in alginate-GelMA hydrogel. a) Gating strategy to determine %CD154$^+$ from DiOC$_{18}$(3)$^+$ cells. DiOC$_{18}$(3) was used to differentiate naïve T-cells (Teffectors) from Tregs. Unstained control was used to gate for DiOC$_{18}$(3)$^+$. Negative control (black; DiOC$_{18}$(3) labeled and CD154 stained with no anti-CD3/CD28 beads) set baseline nonactivated %CD154$^+$. Positive control (indigo; DiOC18(3) and CD154 stained with anti-CD3/CD28 beads) provided baseline activated %CD154$^+$ to calculate %suppression. Control wells contained no Tregs. b) %suppression of nonencapsulated and encapsulated nTregs and iTregs (±IL-2) at various Treg:Teffector ratios (1:1 to 1:8). Data represented as mean ± SEM, $n = 3$, statistical significance identified by Two-Way ANOVA with Tukey's multiple comparisons test: *$P < 0.05$, **$P < 0.01$, ***$P < 0.001$, and ****$P < 0.0001$.

cells showed significant reduction (Figure 7b). PBMCs were then utilized for the chemotaxis assay with CCL1. The proportions of mTregs and mTconvs migrated in response to CCL1 were comparable to CCR8$^+$ memory CD4$^+$ T-cells, with significant enrichment of mTregs ($P < 0.0001$) and reduction of mTconvs ($P < 0.0001$) compared to the whole memory CD4$^+$ T-cells (Figure 7c). Percentages of CCR8$^+$ cells in each memory CD4$^+$ T-cell subsets were also measured (Figure S1, Supporting Information). Th22 cells had the highest expression of CCR8 followed by mTregs and Th2 cells at (53%, 28%, and 28%, respectively). Other subsets exhibited %CCR8$^+$ below 10% (mTconvs at 10% and Th1, Th1/17, and Th17 at 7%) with Th9 cells being the least positive (2%) (Figure 7d). Moreover, FOXP3 MFI of CCR8$^+$ mTregs and CCR8$^-$ mTregs was assessed (Figure S2, Supporting Information). CCR8$^+$ mTregs showed 1.5-fold higher FOXP3 MFI ($P = 0.0062$) than CCR8$^-$ mTregs (Figure 7e).

### 2.6. Co-Axial Bioprinting of Pancreatic Islets with Tregs

The alginate-GelMA hydrogel precursor (bioink) is not printable at temperatures higher than 15 °C as it loses its gel-like characteristics.[24] An increase in gelatin concentration has been shown to enhance the storage moduli of hydrogels,[32] and the addition of unmodified gelatin can act as a thickening agent to increase printability at room temperature.[33] Thus, gelatin was added to alginate-GelMA bioink at 2.5%–5% w/v. The preliminary printability was assessed by evaluating the ability to form continuous filament and by observing filament morphology.[34] Upon extrusion, alginate-GelMA bioink formed liquid droplets while alginate-GelMA-gelatin bioinks formed filaments. The 2|7.5|5% w/v alginate-GelMA-gelatin showed the longest continuous filament (≈3.5 cm; **Figure 8**a). In addition, upon multilayer printing ranging from two to ten layers, alginate-GelMA-gelatin bioinks retained scaffold structures. As gelatin concentration increased, the filaments in the scaffolds displayed over-gelation (Figure 8b). Over-"gelled" bioink is not optimal in extrusion-based bioprinting due to nonuniformity in fiber deposition leading to undesirable scaffold morphology and stability.[35] High cell density has been shown to decrease the viscosity of the bioink;[36] thus, 2|7.5|3.5% w/v alginate-GelMA-gelatin bioink with slight over-gelation was further characterized by rheology measurements. Upon oscillation temperature

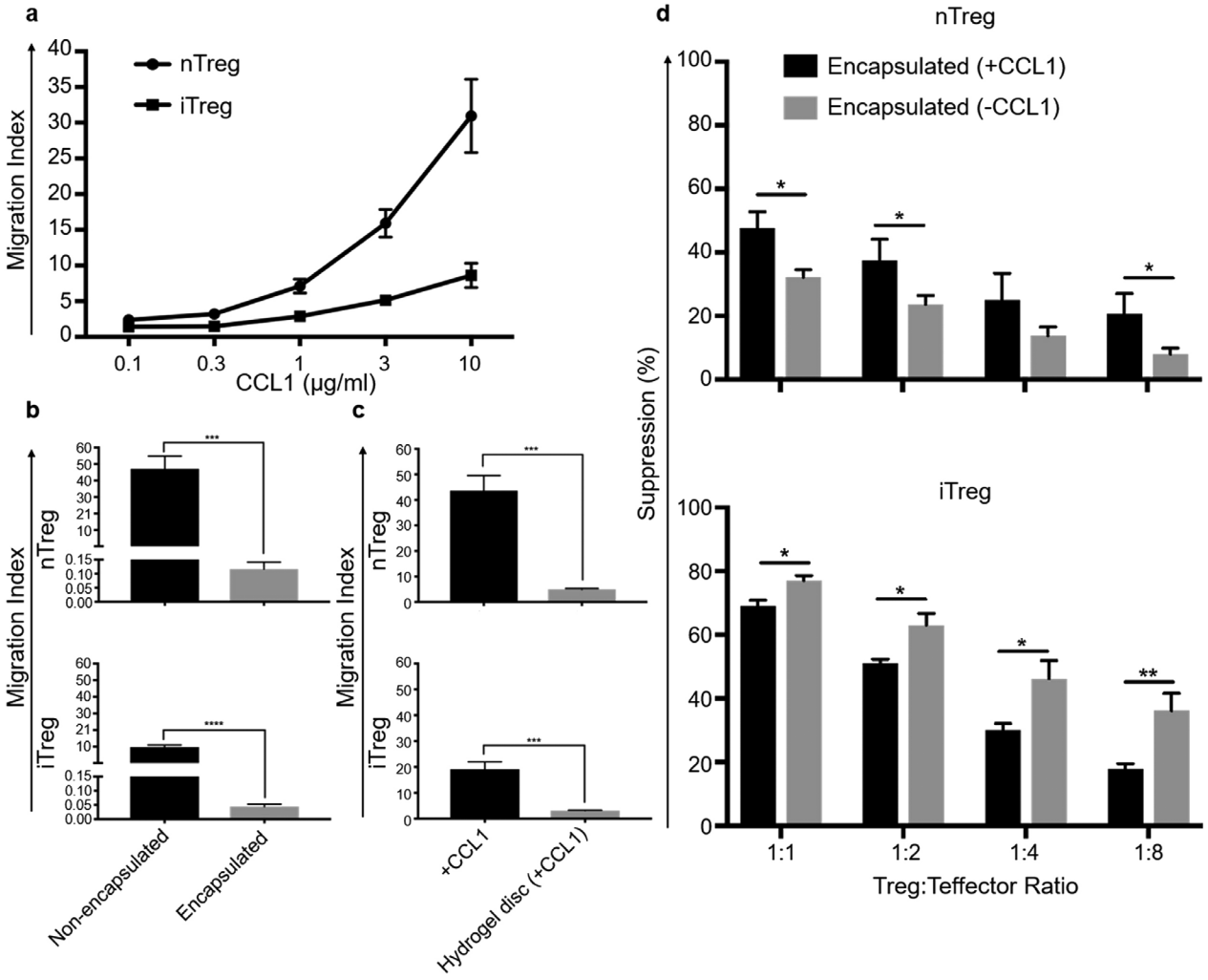


**Figure 6.** Migration capacity of encapsulated Tregs and assessment of CCL-1-supplemented alginate-GelMA hydrogel. a) Chemotactic response profile of nTregs and iTregs to CCL1 (100 ng $mL^{-1}$ to 10 μg $mL^{-1}$). 10 μg $mL^{-1}$ of CCL1 was used for subsequent experiments, either supplementing chemotaxis buffer or the hydrogel. b) Migration capacity of nonencapsulated and encapsulated Tregs. c) Treg recruitment capability of CCL-1-supplemented hydrogel and CCL-1-supplemeted buffer. d) %suppression of encapsulated nTregs and iTregs (±CCL1). Data represented as mean ± SEM, $n = 3$, statistical significance identified by paired two-tailed *T*-test: $^{*}P < 0.05$, $^{**}P < 0.01$, $^{***}P < 0.001$, and $^{****}P < 0.0001$.

sweep, alginate-GelMA-gelatin bioink showed higher storage moduli (G′) than alginate-GelMA bioink across the temperature range. The storage moduli of alginate-GelMA-gelatin bioink reached ≈4 kPa at 5 °C while alginate-GelMA bioink reached ≈0.4 kPa. Furthermore, gelation point (G′ and G″ intersects) of alginate-GelMA-gelatin bioink occurred at ≈21 °C while it occurred at ≈14 °C for alginate-GelMA bioink (Figure 8c). Upon rotational viscosity test at 22.5 °C, both alginate-GelMA and alginate-GelMA-gelatin bioinks displayed decreases in viscosity as shear rate increased (Figure 8d). Furthermore, at shear rate of 1 $s^{-1}$ alginate-GelMA-gelatin bioink showed significantly higher viscosity of ≈134 Pa s compared with alginate-GelMa bioink with viscosity of ≈1.5 Pa s ($P = 0.0005$; Figure S3, Supporting Information).

To demonstrate the applicability of Treg encapsulation to a 3D bioprinting setting and the immune-protective efficacy of Treg co-axial printing, murine islets were co-axially printed alone or with human nTregs or iTregs using further refined alginate-GelMA-gelatin bioink and then co-cultured with human PBMCs. The viability of printed murine islets was assessed up to 5 d post-printing through live/dead staining using fluorescein diacetate (FDA; live cell dye) and propidium iodide (PI; dead cell dye). On days 1, 3 and 5, without human PBMCs in the culture, most of the islets printed alone were $FDA^{+}$ indicating high viability. In contrast, with human PBMCs in the culture, islets printed alone were $PI^{+}$ indicating extremely low viability and substantial cell death, while islets printed with nTregs or iTregs were $FDA^{+}$ indicating high viability (**Figure 9**). The viability of the nTregs and iTregs in the hydrogel was also evaluated. On day 1, most nTregs and iTregs were viable when printed alone (Figure S4, Supporting Information; calcein AM and DAPI staining) or with islets (Figure S5, Supporting Information). On day 5, nTregs remained largely viable with mostly $FDA^{+}$ cells, while iTregs showed considerable cell death with many $PI^{+}$ cells.

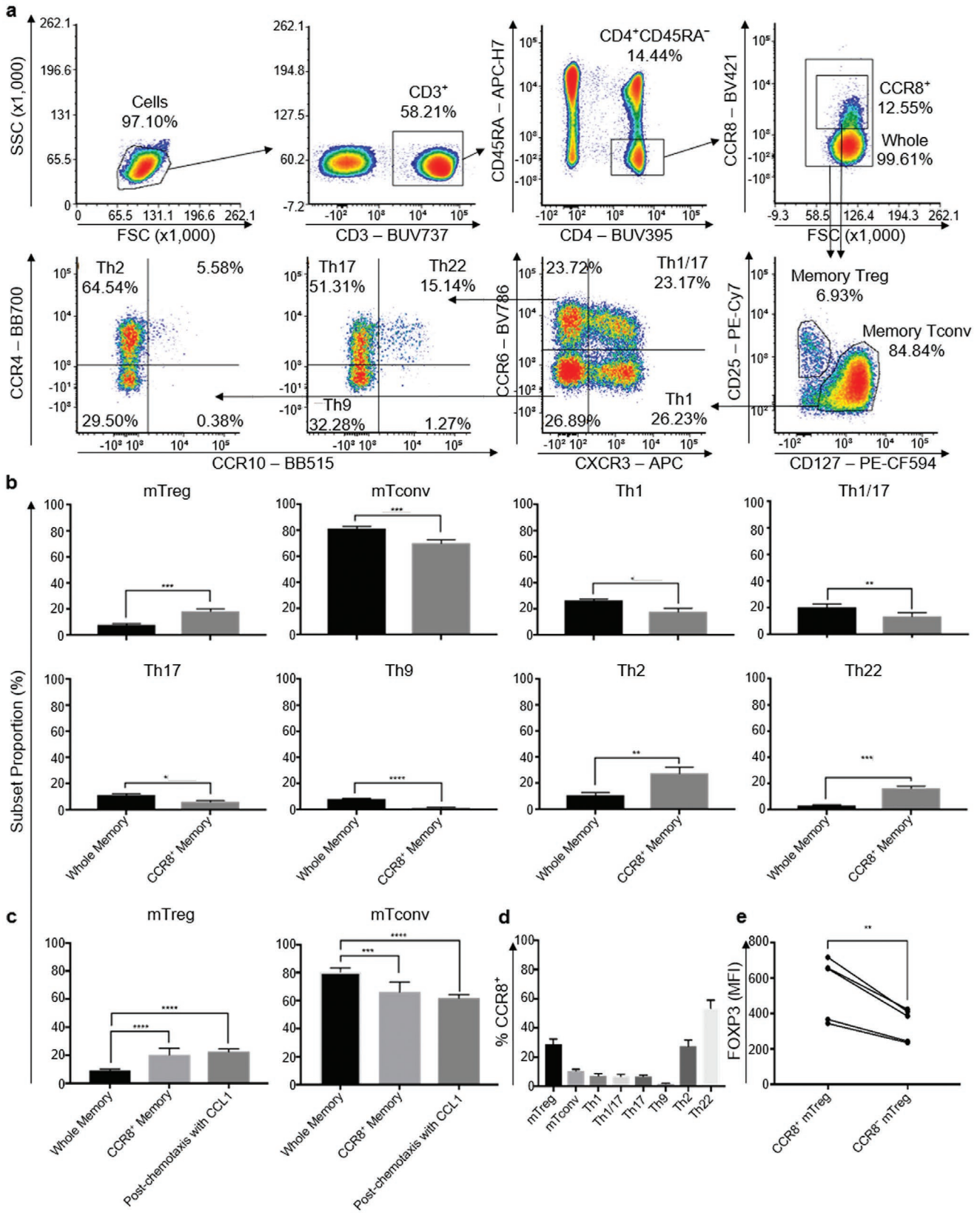


**Figure 7.** Immunophenotyping of human peripheral blood CD4+ memory T-cells. a) Gating strategy for proportions of various CD4+ T-cell subsets within whole memory (CD3+ CD4+ CD45RA−) inclusive of both CCR8+ and CCR8− and CCR8+ memory T-cells from human whole blood PBMCs. CCR8+ was gated using naïve CD4+ T-cells (CD45RA+) as a negative control. Memory Tregs (mTregs) and memory conventional T-cells (mTconvs) were defined

## 3. Discussion

This is the first study to investigate encapsulation of human Tregs for applications in 3D bioprinting. Tregs are a crucial part of the human immune system, with their key role in the maintenance of immune tolerance and homeostasis. Through encapsulation, these intrinsic properties could be co-opted in a localized manner. In this study, we used 2%|7.5% w/v alginate-GelMA hydrogel to successfully encapsulate human nTregs and iTregs. The primary aim of this study was to demonstrate that Treg encapsulation caused no detrimental effects and thus has the capacity to provide local immune protection to co-encapsulated cells. Indeed, encapsulated Tregs were shown to be viable, phenotypically stable and functional. Addition of IL-2 directly into the hydrogel protected Tregs from the damage during the encapsulation process, sustained viability during incubation, increased expression of CD25, and enhanced suppressive activity. The hydrogel was designed with high porosity to facilitate adequate nutrient and oxygen diffusion into the discs. Therefore, bioactive factors have the potential to diffuse out of the structure. As a result of this, Tregs encapsulated in IL-2-supplemented hydrogel displayed decreased viability at day 3 and reduced expression of FOXP3 and TGF-$\beta$ compared with nonencapsulated Tregs cultured with IL-2, which was reversible upon addition of IL-2 directly to the media, instead of the hydrogel (Figures 2–5). Given that the hydrogel discs (≈50 µL in volume) are cultured in 1 mL of IL-2-free media, the final concentration of IL-2, once equilibrium had been reached, would be 25 U mL$^{-1}$, which is much lower than the desired concentration of 500 U mL$^{-1}$. Moreover, as interaction of IL-2 with its receptor leads to internalization of the complex,[37] 25 U mL$^{-1}$ of IL-2 may be rapidly sequestered by Tregs, as IL-2 induces high expression of CD25, the $\alpha$ chain of the high affinity IL-2 receptor.[38] IL-2 signaling also supports strong expression of FOXP3, reinforcing the Treg phenotype and lineage commitment.[39,40] This is important because Tregs are not able to produce IL-2 for autocrine signaling.[1,41] Thus, incorporation of an IL-2-eluting sustained-release system will be required to maintain high concentration of IL-2 within the hydrogel.

The primary goal of Treg encapsulation is to serve as a localized cellular immunosuppression for co-encapsulated cell types such as islets. To achieve this, Tregs need to be able to remain in the vicinity of the co-encapsulated cells. To this end, encapsulation was shown to halt migration of Tregs out of the hydrogel structure in the presence of a potent chemotactic signal (Figure 6b). Acute rejection episodes could be prevented by these Tregs, yet, they may not provide a long-term solution as ex vivo expanded Tregs are short-lived.[42,43] Utilization of a chemokine to recruit recipient Tregs could aid in the establishment of long-lasting recipient-driven tolerance. This is a common strategy employed by tumor cells. It has been shown that CCL1 is expressed in certain tumor cells, locally recruiting Tregs to generate an immunosuppressive milieu that abrogates the anti-tumor response mediated by effector CD4$^+$ and CD8$^+$ T-cells.[44–46] Therefore, we mimicked this strategy, and CCL1-supplmented hydrogel demonstrated recruitment of Tregs. Treg-recruitment capability of CCL1-supplemented hydrogel was significantly lower than CCL1 in the chemotaxis buffer, again, due to the porous nature of the hydrogel. The final concentration of CCL-1 in the chemotaxis buffer (600 µL) would have been ≈800 ng mL$^{-1}$ once equilibrated, instead of 10 mg mL$^{-1}$. The migration indices shown in CCL-1-suplimented hydrogel discs were comparable with the 1 mg mL$^{-1}$ of CCL1 in the buffer (Figure 6a,c). In the case of CCL1, the high porosity of the hydrogel facilitates the formation of chemokine gradients, and maintenance of this gradient through utilization of a CCL1-eluting sustained release system will maximize the recruitment capability. Furthermore, Tregs preferentially expressed CCR8 and were enriched in CCR8$^+$ and CCL1-recruited peripheral blood T-cells. Taken together, this suggests that the use of CCL1-supplemented hydrogel could provide a microenvironment enriched with recipient Tregs in vivo. Although, it is possible that the same chemokines may actively recruit other T helper cells to the site. Th2 and Th22 cells showed preferential expression of CCR8 and enrichment in CCR8$^+$ peripheral blood T-cells (Figure 7b–d). Despite previous studies regarding expression of CCR8 on Th2 cells,[47] the use of CCL1 was justified as Th2 cells could assist with tolerization given their ability to inhibit rejection-causing Th1 responses.[48] Expression of CCR8 on Th22 cells had not been described to date. Moreover, the role of Th22 cells in transplantation is currently unknown.[49] It has been shown that CCR8$^+$ conventional skin T-cells are less effector-like, with decreased functionality compared with their CCR8$^-$ counterparts.[50] Thus, recruitment of CCR8$^+$ Th22 cells may not equate to a proinflammatory response, especially in an environment enriched with CCR8$^+$ Tregs that have greater FOXP3 expression than CCR8$^-$ Tregs (Figure 7e), hence a greater suppressive capacity.[31,51] In addition, similar approaches have been demonstrated using CCL22[52] and CXCL12[53] with promising results, illustrating the potential of chemokine incorporation.

For translation of these findings into the clinic it is crucial to demonstrate that Tregs can be bioprinted and protect co-printed cells from proinflammatory responses that would normally mediate rejection in vivo. The alginate-GelMA hydrogel was formulated as a bioink for 3D bioprinting of islets with supporting cells for its optimal macroscopic properties and its capacity to support cell survival; however, it only showed ideal rheological properties below 15 °C.[24] Given the lack of temperature control module in the customized co-axial bioprinter, the bioink formulation needed to be further refined to increase the printability at room temperate. Indeed, addition of 3.5% w/v gelatin to 2%|7.5% w/v alginate-GelMA

as CD25$^+$ CD127$^-$ and CD25$^-$ CD127$^+$, respectively. mTconvs were divided into T-helper subsets using chemokine receptors: CXCR3$^+$ CCR6$^-$ Th1, CXCR3$^+$ CCR6$^+$ Th1/17, CXCR3$^-$, CXCR3$^-$ CCR6$^+$ CCR4$^+$ CCR10$^-$ Th17, CXCR3$^-$ CCR6$^+$ CCR4$^-$ CCR10$^-$ Th9, CCR6$^-$ CCR4$^+$ CCR10$^-$ Th2, and CXCR3$^-$ CCR6$^+$ CCR4$^+$ CCR10$^+$ Th22. b) Proportions of T-cell subsets in whole memory and CCR8$^+$ memory populations. c) Proportions of mTregs and Tconvs in PBMCs migrated in response to CCL1. d) %CCR8$^+$ of T-cell subsets. e) FOXP3 MFI of CCR8$^+$ and CCR8$^-$ mTregs. Data represented as mean ± SEM, $n = 6$ for (b) and (d) and $n = 5$ for (e), statistical significance identified by paired two-tailed *T*-test: *$P < 0.05$, **$P < 0.01$, ***$P < 0.001$, and ****$P < 0.0001$.

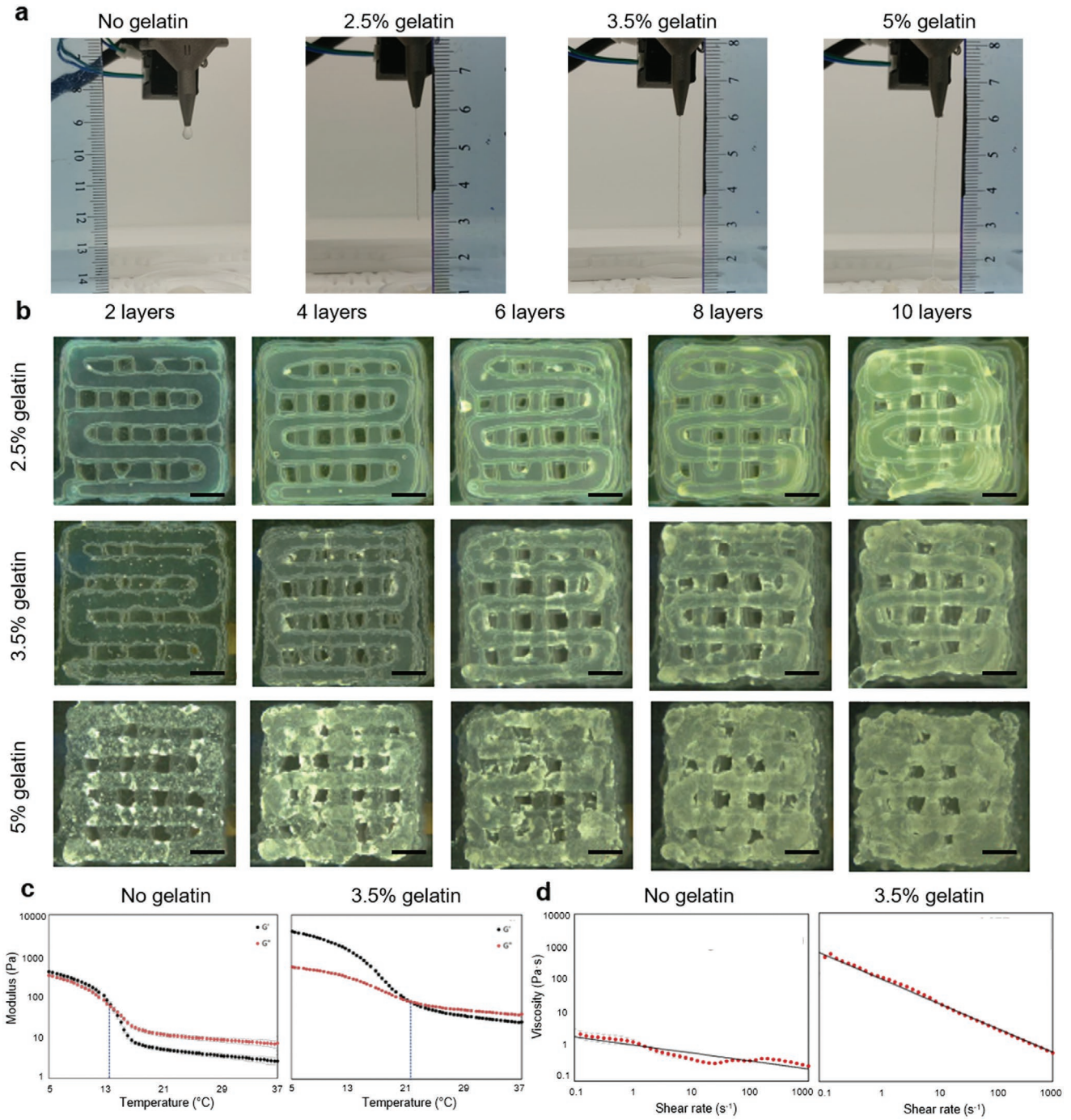


**Figure 8.** Addition of gelatin to alginate-GelMA hydrogel precursor (bioink). Gelatin was added to 2%|7.5% alginate-GelMA bioink at 2.5%, 3.5%, and 5% w/v. Printability of these bioinks at room temperature was assessed macroscopically and rheologically. a) Extrusion of bioinks with no gelatin, 2.5%, 3.5%, and 5% w/v gelatin were recorded and the frames with the longest continuous filaments were utilized. b) Images of multilayered scaffolds printed using bioinks with 2.5%, 3.5%, and 5% w/v gelatin. Scale bars represent 2 mm at 11 × magnification. c) Oscillatory temperature sweep of bioinks with no gelatin and 3.5% w/v gelatin between 5 and 37 °C. The blue dotted line indicates gelation point. d) Rotational viscosity test of bioinks with no gelatin and 3.5% w/v gelatin as a function of shear rate between 0.1 and 1000 $s^{-1}$. Best represented images from $n = 3$ for (a) and (b). Data represented as mean ± SD, $n = 3$ for (c) and (d).

bioink enabled the bioink to form continuous filaments and retain structure upon multilayer printing at room temperature, with higher gelation point and higher viscosity at any given shear rate than alginate-GelMA bioink (Figure 8). Using further refined alginate-GelMA-gelatin bioink, we successfully bioprinted murine islets in a co-axial manner with an empty shell, nTregs or iTregs. To simulate infiltration of leukocytes into the site of engraftment in vivo, we developed a

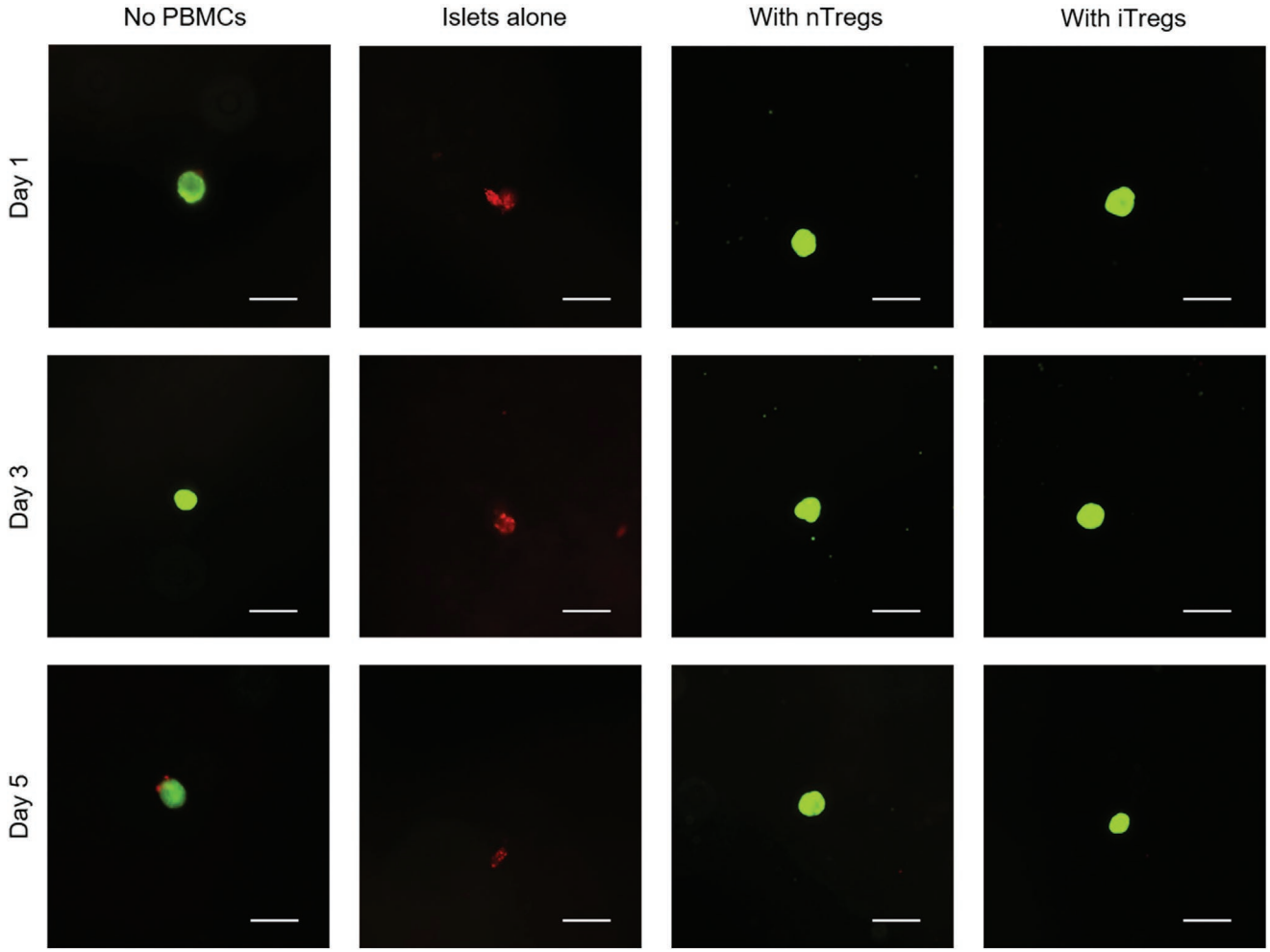


**Figure 9.** Viability of murine islets co-axially printed with human Tregs. Murine islets were printed alone or with nTregs or with iTregs using alginate-GelMA-gelatin bioink and then co-cultured with human PBMCs up to 5 d. No PBMC control was utilized for baseline islet viability. Viability was assessed on days 1, 3, and 5 through fluorescent microscopy using fluorescein diacetate (FDA; green) and propidium iodide (PI; red) to stain live cells and dead cells, respectively. Best represented images from $n = 3$. Scale bars represent 200 µm at 10 × magnification.

co-culture system using murine islets, human Tregs, and human PBMCs. In this co-culture system, without Tregs, murine islets were destroyed by day 1, with substantial cell death and disturbed morphology compared with murine islets cultured without human PBMCs. Given that we utilized murine islets with human PBMCs, this was expected as the xenoresponse is characterized as hyperacute and aggressive with substantial infiltration of leukocytes within the first 24 h.[54–56] On the other hand, when printed with either human nTregs or iTregs, murine islets remained highly viable up to day 5 (Figure 9). This proof of principle demonstrated that co-printing of murine islets with human Tregs can protect the islets from xenorejection. While the encapsulation experiment was confined to suppression of $CD4^+$ T-cells by encapsulated Tregs, this also showcased the ability of Treg to suppress various types of leukocyte in PBMCs including $CD4^+$ T-cells, $CD8^+$ T-cells, B cells, natural killer cells, monocytes, and dendritic cells.[57] Moreover, some of the printed nTregs and iTregs survived up to day 5 in this co-culture system without the addition of exogenous IL-2 to the bioink or the media (Figures S4 and S5, Supporting Information). This contrasts with previous data which showed that, in the absence of IL-2, encapsulated nTregs and iTregs undergo a significant reduction in viability by day 3. This may be due to the presence of IL-2 produced by $CD4^+$ T-cells, $CD8^+$ T-cells, and dendritic cells upon activation by murine islet antigen,[58] and sequestered by printed Tregs. Although this does not negate the requirement of IL-2-eluting sustained release system, potentially lower concentrations of IL-2 may be required.

Two types of human Tregs, nTregs and iTregs, were compared in this study to determine which would be more suitable for encapsulation. While both types are defined as $CD4^+$ $CD25^+$ $FOXP^+$ T-cells, there are fundamental differences between them. Natural Tregs consists of tTregs generated during thymic development and pTregs generated in the periphery in vivo while iTregs are differentiated in vitro from conventional T-cells. Encapsulated iTregs were shown to be more sensitive to IL-2 than nTregs in terms of viability, CD25 expression and suppressive activity, which could be disadvantageous in an IL-2-limited environment. Aligning with this, more cell death

was observed with printed iTregs than nTregs in the xenogeneic co-culture system. iTregs displayed greater suppressive activity than nTregs, indicating that iTregs could suppress the recipient immune system more effectively.[59] Moreover, migration indices of nTregs in response to CCL1 was higher than iTregs. The migration index of nTregs in response to CXCL12, a ligand for pan-leukocyte chemokine receptor CXCR4,[60] was also higher and there were no significant differences in CCR8 expression between nTregs and iTregs. This indicates that the differences in CCL1 migration index are due to iTregs being more motile in nature, rather than nTregs being more responsive to CCL1 (Figure S6, Supporting Information). CCL1 also had different effects on encapsulated nTregs and iTregs, enhancing nTreg suppressive activity while dampening iTreg suppressive activity. This may be due to CCR8 signaling causing iTregs to be less suppressive due to their origin of being differentiated from the conventional T-cell lineage.[50] Ultimately, while iTregs were found to be more suppressive than nTregs and possess a more relevant repertoire of antigen specificities for allogeneic transplantation,[61] nTregs may be more suitable than iTregs due to their phenotypic stability. The methylation status of the FOXP3 promotor region and Treg-specific demethylation region determine the stability of the Treg phenotype. These regions in iTregs are not demethylated, allowing iTregs to convert to a proinflammatory Th17 phenotype in a proinflammatory setting.[62] Thus, the utilization of iTregs for co-encapsulation with other cells may act as an immunological Trojan horse.

## 4. Conclusion

In this study, we demonstrated the potential of encapsulating human Tregs in alginate-GelMA hydrogel to provide localized cellular immunosuppression to transplanted islets. IL-2 and CCL1, as Treg-specific bioactive factors, were investigated as supplements to the hydrogel. Encapsulated Tregs were viable, and phenotypically and functionally stable. Furthermore, encapsulation prevented migration of Tregs out of hydrogel structure. Addition of IL-2 and CCL1 to the hydrogel showed several benefits including 1) improvement of Treg viability, 2) enhanced suppressive phenotype and function, and 3) capacity to recruit additional Tregs. Due to the highly porous nature of the hydrogel, adding these factors directly into the hydrogel produced sup-optimal concentrations once the factors diffused into the surrounding media. Therefore, incorporation of a sustained-release system via recently developed polylactic-co-glycolic acid-based microspheres will be implemented for additional improvement.[63] To further enhance Treg numbers, low-dose rapamycin could be added as an additional bioactive factor,[64] utilizing recently developed rapamycin-loaded porous silicon nanoparticles.[65,66] Moreover, peripheral blood CCR8$^+$ T-cells were highly enriched with Tregs, and CCL1-supplemented hydrogel was shown to specifically induce chemotaxis of these cells, providing an insight into the cellular microenvironment in humans upon utilization of CCL-1-supplemented hydrogel. Lastly, the findings from Treg encapsulation translated into the 3D bioprinting system as bioprinted Tregs were viable and functional, and protected co-printed murine islets from xenoresponse mediated by human PBMCs. While this study focused on the encapsulation and 3D bioprinting of Tregs for applications in islet transplantation, the findings could be applied to other types of cell therapies such as adrenocortical, thyroid, and parathyroid cell transplantation.[67–69]

## 5. Experimental Section

*Preparation of Alginate-GelMA Hydrogel Precursor*: Gelatin (porcine skin, type A, gel strength ≈175 g Bloom, Sigma-Aldrich) was dissolved in phosphate buffered saline (PBS; 10% w/v) for 1 h at 50 °C. Methacrylic anhydride (Sigma-Aldrich) was added to the 10% w/v gelatin solution in a drop-wise manner with stirring (final concentration of 7.4% v/v). The reaction continued for 3 h and then terminated by diluting the solution four times with PBS. 1% v/v of chloroform was added, and the mixture was dialyzed against distilled water for 7 d at 40 °C (cellulose membrane, molecular weight cutoff: ≈12 kDa). The dialyzed GelMA solution was lyophilized to white porous foam (stored at −20 °C until further use). The above process was undertaken under sterile conditions. The DoF of GelMA was measured by a ninhydrin assay as described by Loessner et al.[70] Alginate (medium viscosity, Sigma-Aldrich) was sterilized by UV for 20 min and then dissolved in PBS (2% w/v) for 2 d at 37 °C. GelMA was added to the alginate solution at a concentration of 7.5% w/v, resulting in 2%|7.5% w/v alginate-GelMA. The alginate-GelMA hydrogel precursor was incubated at 37 °C with occasional shaking until a homogenous formulation was formed.

*Cell Isolation and In Vitro Expansion*: Human buffy coat (Australian Red Cross) was treated with a RosetteSep Human CD4+ T cell enrichment cocktail (STEMCELL Technologies) for 20 min on a platform mixer at 80 rpm. Treated buffy coat was diluted with PBS (+2% fetal calf serum (FCS), Bovogen) prior to isolation of CD4$^+$ T cells by density-gradient centrifugation over Lymphoprep (STEMCELL Technologies). Enriched CD4$^+$ T cells were surface-stained for CD4, CD25, CD127, and CD45RA. CD4$^+$ CD25$^+$ CD127$^-$ T cells (natural regulatory T cells or nTregs) and CD4$^+$ CD25$^-$ CD127$^+$ CD45RA$^+$ T cells (naïve CD4$^+$ T-cells) were sorted by fluorescence-activated cell sorting (FACS; BD FACSAria Fusion, BD Biosciences). Sorted nTregs and naïve CD4$^+$ T-cells were rested overnight in a complete X-vivo 15 medium (cX-vivo: serum-free with gentamycin and phenol red, Lonza, supplemented with 2% HEPES, 1% L-glutamine and 5% human serum (Gibco, HyClone, and Sigma-Aldrich, respectively)) with 500 U mL$^{-1}$ of IL-2 (Novartis Vaccines and Diagnostics). nTregs were cultured in an expansion medium consisting of cX-vivo and a 1:1 ratio of Human T-expander CD3/CD28 Dynabeads (Thermo Fisher Scientific). Naïve CD4+ T-cells were cultured in an induction medium composed of the expansion medium supplemented with 5 ng mL$^{-1}$ of human TGF-$\beta$ (eBioscience), 10 1 × 10$^{-9}$ M mL$^{-1}$ of all-trans retinoic acid (Sigma-Aldrich), and 2 1 × 10$^{-9}$ M mL$^{-1}$ rapamycin (LC Laboratories) for the generation of induced regulatory T cells (iTregs). nTreg expansion and iTreg generation were verified by expression of CD4, CD25, and FOXP3 (Foxp3/transcription factor staining buffer set, eBioscience). Following expansion, the expander beads were removed and Tregs were rested in cX-vivo (+500 U mL$^{-1}$ of IL-2) for 2 d prior to use.

*Encapsulation of Tregs*: Rested Tregs were mixed well with 2%|7.5% w/v alginate-GelMA hydrogel precursor at 2 × 10$^6$ cells mL$^{-1}$, and then lithium phenyl-2,4,6-trimethylbenzoylphosphinate (LAP, Tocris Bioscience; a final concentration of 0.06% w/v) was added. For some experiments, IL-2 (500 U mL$^{-1}$) or CCL1 (10 µg mL$^{-1}$) was directly added to the above cell suspension. The hydrogel precursor-cell suspension was injected into a disc-mold (8 mm diameter with 1 mm height; ≈50 µL in volume per disc) using a drawing-up needle (BD Biosciences), which was then photo crosslinked at 400 nm (Omnicure LX505, Excelitas) for 1 min and then further crosslinked in 2% w/v $CaCl_2$ (BDH) solution for 10 min. The cell-laden discs were cultured in cX-vivo medium (no IL-2) for 24 or 72 h at 37 °C with 5% $CO_2$ prior to downstream assays. Nonencapsulated Tregs were prepared by suspending Tregs at

$2 \times 10^6$ cells $mL^{-1}$ in cX-vivo medium (+ 500 U $mL^{-1}$ of IL-2). Some discs made with IL-2-free 2%|7.5% w/v alginate-GelMa were cultured in cX-vivo medium (+ 500U $mL^{-1}$ of IL-2); these were dubbed "Encapsulated (+IL-2 in media)". For viability, phenotype, functionality, and CD154 suppression assay, the encapsulated Tregs were recovered by digesting the hydrogel constructs in TrypLE Express (Thermo Fisher Scientific) for 10 min at 37 °C and then washed twice with PBS (nonencapsulated Tregs were treated the same way).

*Transmission Electron Microscopy*: Encapsulated Tregs and nonencapsulated controls were fixed overnight in electron microscopy fixative (4% paraformaldehyde/1.25% glutaraldehyde in PBS, + 4% sucrose, pH 7.2). Fixed samples were washed in washing buffer (PBS + 4% sucrose) for 5 min and then stained with 2% $OsO_4$ solution for 1 h. Stained samples were dehydrated through a series of washes (two washes in 70% ethanol for 15 min each, two washes in 90% ethanol for 15 min each, three washes in 100% ethanol for 15 min each and then one wash in propylene oxide for 15 min). Dehydrated samples underwent resin infiltration (50% propylene oxide 50% epoxy resin for 1 h, two washes in 100% resin for 1 h each and then 100% resin overnight). After overnight incubation, samples were embedded in fresh 100% resin and then polymerized at 70 °C for at least 24 h. Sections were cut from the polymerized samples and analyzed by FEI Tecnai G2 Spirit Biotwin TEM at 100 kV after appropriate staining.

*Viability, Treg Phenotype, and Treg Functionality Assay*: Unstained control and compensation controls were used when required. For assessment of viability, a positive dead control was prepared by three cycles of rapid freeze-thaw (at −80 °C and 37 °C, respectively). For viability, PI (50 μg $mL^{-1}$; Thermo Fisher Scientific) was added to the samples to a final concentration of 2.5 μg $mL^{-1}$. For Treg phenotype and functionality, recovered cells were stained for viability and then surface-stained for CD4 and CD25 before being fixed, permeabilized, and intracellularly stained for FOXP3. Stained cells were divided into four groups: the first group was stained for CD69, the second for TGF-$\beta$, the third for CD39, and the fourth for CTLA-4. All samples were analyzed on a BD FACS Canto II flow cytometer (BD Biosciences), and the data analyzed with FCS Express 6 (De Novo Software).

*CD154 Suppression Assay*: Human PBMCs cells were isolated from a fresh buffy coat by density gradient centrifugation as described above. Naïve $CD4^+$ T-cells were isolated using EasySep Human Naïve CD4+ T Cell Isolation kit (STEMCELL Technologies). Naïve $CD4^+$ T-cells were labeled with $DiOC_{18}(3)$ (Thermo Fisher Scientific; a final concentration of 2 μg $mL^{-1}$) by incubation at 37 °C with 5% $CO_2$ for 45 min. 96-well round bottom plates were seeded with $DiOC_{18}(3)$-labeled naïve $CD4^+$ T-cells ($5 \times 10^4$ cells per well; "Teffector") and Tregs were added to the wells at various ratios of Treg:Teffector (1:1, 1:2, 1:4, and 1:8). Human T-expander CD3/CD28 Dynabeads (bead:Teffector ratio of 1:4) and anti-CD154 antibody were added to each well. $DiOC_{18}(3)$-labeled naïve CD4+ T-cells with and without Tregs were used as positive and negative controls, respectively. The plate was incubated at 37 °C with 5% $CO_2$ for 7 h and then analyzed for expression of CD154 by flow cytometry (FACS Canto II). Percentage suppression was calculated as follows: 100 × [1 − (%$CD154^+$ in the experiment sample divided by %$CD154^+$ in the positive control)].

*Whole Blood Chemokine Receptor Phenotyping*: Human PBMCs were isolated from a fresh whole blood by density gradient centrifugation, as above. PBMCs were stained for CD3, CD4, CD45RA, CD25, CD127, CXCR3, CCR4, CCR6, CCR8, and CCR10 and then analyzed on BD FACSymphony (BD Biosciences). Additionally, PBMCs were stained for CD4, CD45RA, CD25, CD127, CCR8, and FOXP3 for assessment of FOXP3 expression by $CCR8^+$ and $CCR8^-$ Tregs.

*Chemotaxis Assay*: Chemotaxis assays were performed with either 96-well or 24-well transwell plates with 5 μm polycarbonate membranes (Corning). All chemokines and cells were resuspended in a chemotaxis buffer composed of RPMI 1640 medium (Gibco) with 0.5% w/v bovine serum albumin (Sigma-Aldrich) and 2.5% HEPES. 96-well plates employed 150 μL in the lower chamber and 50 μL in the upper chamber. 24-well plates employed 600 μL in the lower chamber and 100 μL in the upper chamber. To generate a migration response profile for CCL1 (96-well), various concentrations of CCL1 ranging from 100 ng $mL^{-1}$ to 10 μg $mL^{-1}$ (threefold increments) were placed in the lower chambers, and Tregs ($2 \times 10^6$ cells $mL^{-1}$) were placed in the upper chambers. CXCL12 (30 ng $mL^{-1}$) was utilized as a positive control. For assessment of encapsulated Treg migration (24-well), 10 μg $mL^{-1}$ of CCL1 was placed in the lower chamber and encapsulated ($2 \times 10^6$ cells $mL^{-1}$) and nonencapsulated ($1 \times 10^6$ cells $mL^{-1}$) Tregs were placed in the upper chamber. For assessment of CCL1 addition to the hydrogel (24-well), CCL-1-added hydrogel disc (no cells) and 10 μg $mL^{-1}$ of CCL1 were placed in the lower chamber and Tregs ($2 \times 10^6$ cells $mL^{-1}$) were placed in the upper chamber. For all transwell migration assays, a spontaneous migration control with no chemokine in the lower chamber was included. The plates were incubated for 3 h at 37 °C with 5% $CO_2$, and then migrated cells in the lower chamber were analyzed by flow cytometry (BD LSRFortessa for the 96-well setup and BD FACS Canto II for the 24-well setup; BD Biosciences) using counting beads (CountBright Absolute Counting Beads; Thermo Fisher Scientific). Migration index was calculated as follows: the number of cells in the experimental sample per 1000 beads divided by the number of cells in the spontaneous migration control per 1000 beads. For immune phenotyping post-chemotaxis with CCL1, human PBMCs ($2 \times 10^6$ cells $mL^{-1}$) were placed in the upper chambers with 10 μg $mL^{-1}$ of CCL1 in the lower chamber (24-well). After 3 h incubation, cells in the lower chamber were stained as described in whole blood chemokine receptor phenotyping.

*Preparation of Alginate-GelMA-Gelatin Bioink*: Gelatin was sterilized by UV for 20 min and then added to 2%|7.5% w/v alginate-GelMA hydrogel precursor (bioink) at 2.5%, 3.5%, and 5% w/v. Resulting bioink formulations were incubated at 37 °C with occasional shaking until homogenous formulations were formed.

*Printability Test*: Alginate-GelMA bioink and alginate-GelMA-gelatin bioinks with 2.5%, 3.5%, and 5% gelatin concentrations were incubated at room temperature and then extruded using a customized co-axial printer.[24] Extrusion of each bioink was recorded to measure length of extruded filament from the nozzle, prior to the break point. Additionally, multilayered scaffolds ranging from two to ten layers were printed using the co-axial printer for each bioink to observe filament morphology. Images of the scaffolds were taken using Leica M205 C microscope (Leica Microsystems).

*Rheology Measurement*: Oscillation temperature sweeps and viscosity tests were performed with TA instruments AR-G2 controlled-stress rheometer equipped with 2° 20 mm stainless steel geometry (New Castle, DE) for 2%|7.5% w/v alginate-GelMA bioink and 2%|7.5%|3.5% w/v alginate-GelMA-gelatin bioink. The temperature sweep was performed within the range of 5–37 °C with a ramp of 1.5 °C $min^{-1}$. The storage moduli (G′) and loss moduli (G″) were recorded. The viscosity was tested as a function of shear rate ranging from 0.1 to 1000 $s^{-1}$ at 22.5 °C. All the measurements were performed at oscillation frequency of 1 Hz and 0.1% strain. Prior to rheological tests, bioinks were incubated at 37 °C for 30 min and then loaded into prewarmed plates. The hydrogel precursor and bioink were equilibrated for 5 min to remove their thermos-history at given temperature. A trap was also equipped on each test to reduce dehydration. The gap between the geometry plates was set at 52 μm and ≈750 μL sample was loaded each time.

*Murine Islet Isolation*: This procedure was approved by the Animal Ethics Committee of the University of Adelaide (Ethics number M-2018-123) and conformed to the guidelines established by the Australian Code of Practice for the Care and Use of Animals for Scientific Purposes. Murine islets were isolated from 7 to 8 week old male C57BL/6 mice (University of Adelaide Laboratory Animal Services). 3 mL cold M199 medium (Sigma-Aldrich) containing Liberase T-Flex Research Grade (collagenase I/II blend at 0.227 mg $mL^{-1}$ and thermolysin at 0.0136 mg $mL^{-1}$; Roche) was injected into the pancreatic duct in situ to inflate the pancreas. Upon full inflation, the pancreas was harvested and then digested at 37 °C for 11 min. Digested pancreatic acinar tissue was homogenized through 425 μm test sieve (Endecotts). Islets were purified from homogenized pancreatic tissue by density-gradient centrifugation over Lymphoprep. Purified islets were counted and then rested overnight in complete RPMI 1640 medium (Gibco), supplemented with 10%

FCS, 1% L-glutamine, and 1% penicillin-streptomycin (Gibco), on nonadherent 6-well plates.

*Co-Axial Printing of Murine Islets with Human Tregs*: The customized co-axial printer was placed into a PC2 biosafety cabinet and then sterilized with 70% ethanol followed by UV for 20 min. Co-axial nozzle and tweezers were sterilized as well. Murine islets and human nTregs and iTregs were washed with printing culture medium (X-vivo 15 supplemented with 5% FCS, 1% L-glutamine, and 2% HEPES) three times and then resuspended in 2%|7.5%|3.5% alginate-GelMA-gelatin bioink (prewarmed at 37 °C at 300 islets $mL^{-1}$ and $2 \times 10^6$ cells $mL^{-1}$). LAP was added to islet-containing, nTreg-containing, iTreg-containing, and empty bioinks at 0.06% w/v. Each bioink was loaded into 3 mL Luer-Lock syringe (Hapool) and then locked with Luer-Lock caps to maintain sterility. Bioink loaded syringes were cooled on ice for 10 min and then incubated at room temperature for 10 min. Islet-containing bioink was placed into the core compartment and other bioinks were placed into the shell compartment nonsimultaneously. Islet-laden structures, islet-nTreg-laden structures, and islet-iTreg-laden structures were printed as two layers of 10 mm × 10 mm × 6 mm with 2.5 mm fiber spacing at core:shell ratio of 0.5:0.5. Each structure consisted of ≈100 µL of core bioink and 100 µL of shell bioink. Printed structures were crosslinked as described above. After washing twice in PBS, printed structures were placed in 1 mL of printing culture medium on 24-well plates. Human PBMCs were isolated as above and $2 \times 10^5$ human PBMCs (Treg:PBMC ratio of 1:1) were added to each well, except for no PBMC controls (islet-laden structures with no PBMCs). Printed structures and PBMCs were co-cultured up to 5 d at 37 °C with 5% $CO_2$.

*Fluorescence Microscopy*: Printed structures were washed three times with PBS to remove human PBMCs. Printed structures were placed in 400 µL of PBS. Printed structures were stained with FDA (Thermo Fisher Scientific) and PI at final concentrations of $500 \times 10^{-6}$ M and 5 µg $mL^{-1}$, respectively, for 10 min at room temperature in the dark. Printed structures were washed in PBS and imaged with Olympus IX73 inverted fluorescence microscope (Olympus).

*Confocal Microscopy*: Human nTregs and iTregs were 3D bioprinted as described as above with an empty core at $2 \times 10^6$ cells $mL^{-1}$. nTreg-laden and iTreg-laden structures were cultured in cX-vivo medium (+500 U $mL^{-1}$ of IL-2) overnight at 37 °C with 5% $CO_2$. Printed structures were stained with calcein AM (final concentration $1 \times 10^{-6}$ M; Thermo Fisher Scientific) and DAPI (300 ng $mL^{-1}$; Thermo Fisher Scientific) for 30 min at 37 °C with 5% $CO_2$ in the dark. 3D-bioprinted Tregs were washed in PBS and then imaged with Olympus FV3000 confocal laser scanning microscope (Olympus).

*Statistics*: Statistical significance ($P < 0.05$) was analyzed using the GraphPad Prism 7. One-Way ANOVA with Tukey's multiple comparisons test, Two-Way ANOVA with Tukey's multiple comparisons test, and paired two-tailed *T*-test were used to identify statistical significance. All replicates are biological replicates. All experiments utilized triplicates as technical replicates except for whole blood chemokine receptor phenotyping that used no technical replicates.

*Antibodies*: Antibody details are listed in Table S1 (Supporting Information).

## Supporting Information

Supporting Information is available from the Wiley Online Library or from the author.

## Acknowledgements

The authors wish to acknowledge funding from the Australian Research Council (ARC) Centre of Excellence Scheme (CE140100012) and The Hospital Research Foundation, Adelaide Australia; and support from the Australian National Fabrication Facility (ANFF)—Materials Node and Australian Red Cross Blood Services for providing human buffy coat for Treg isolation. J.K. acknowledges Dr. Randall Grose of South Australian Health and Medical Research Institute for operating fluorescence-activated cell sorter, Ms Ruth Williams from Adelaide Microscopy for help with TEM, and Prof. Shaun McColl and Dr. Iain Comerford of Chemokine Biology Group for their help with transwell migration assay. G.G.W. acknowledges the support of the ARC through an ARC Laureate Fellowship (FL110100196).

## Conflict of Interest

The authors declare no conflict of interest.

## Author Contributions

J.K. designed and performed all experiments, analyzed data, and wrote the manuscript. C.M.H. contributed to designing of experiments. C.M.H., N.G., G.B.P., S.O.S., Z.Y., X.L., A.U.A., F.D.K., and D.P. helped with experiments. C.M.H. contributed to chemokine receptor phenotyping. N.G. contributed to filament test and rheology. G.B.P. contributed to CD154 suppression assay. S.O.S and F.D.K. contributed to phenotyping of encapsulated Tregs. Z.Y. and X.L. contributed to hydrogel precursor synthesis. A.U.A. contributed to multilayer printing. D.P contributed to murine islet isolation. C.M.H., N.G., G.B.P., S.O.S., Z.Y., F.D.K., R.P.C., S.C.B, G.G.W., and P.T.C. edited the manuscript. S.O.S edited the figures. C.J.D., G.G.W., and P.T.C. conceptualized the project. C.J.D., R.P.C., S.C.B., G.G.W., and P.T.C. supervised the study. G.G.W. and P.T.C. attained funding.

## Keywords

3D bioprinting, biomaterials, immunotherapy, islet transplantation, regulatory t-cells

Received: January 19, 2020
Published online:

[1] S. Sakaguchi, T. Yamaguchi, T. Nomura, M. Ono, *Cell* **2008**, *133*, 775.
[2] R. Gershon, K. Kondo, *Immunology* **1971**, *21*, 903.
[3] S. Sakaguchi, N. Sakaguchi, M. Asano, M. Itoh, M. Toda, *J. Immunol.* **1995**, *155*, 1151.
[4] C. Baecher-Allan, J. A. Brown, G. J. Freeman, D. A. Hafler, *J. Immunol.* **2001**, *167*, 1245.
[5] S. Hori, T. Nomura, S. Sakaguchi, *Science* **2003**, *299*, 1057.
[6] J. D. Fontenot, M. A. Gavin, A. Y. Rudensky, *Nat. Immunol.* **2003**, *4*, 330.
[7] W. Liu, A. L. Putnam, Z. Xu-Yu, G. L. Szot, M. R. Lee, S. Zhu, P. A. Gottlieb, P. Kapranov, T. R. Gingeras, B. Fazekas de St Groth, C. Clayberger, D. M. Soper, S. F. Ziegler, J. A. Bluestone, *J. Exp. Med.* **2006**, *203*, 1701.
[8] N. Seddiki, B. Santner-Nanan, J. Martinson, J. Zaunders, S. Sasson, A. Landay, M. Solomon, W. Selby, S. I. Alexander, R. Nanan, A. Kelleher, B. Fazekas de St Groth, *J. Exp. Med.* **2006**, *203*, 1693.
[9] B. D. Singer, L. S. King, F. R. D. Alessio, *Front. Immunol.* **2014**, *5*, 46.
[10] M. Kanamori, H. Nakatsukasa, M. Okada, Q. Lu, A. Yoshimura, *Trends Immunol.* **2016**, *37*, 803.
[11] D. A. A. Vignali, L. W. Collison, C. J. Workman, *Nat. Rev. Immunol.* **2008**, *8*, 523.

[12] Q. Tang, J. A. Bluestone, *Cold Spring Harbor Perspect. Med.* **2013**, *3*, a015552.
[13] M. Romano, G. Fanelli, C. J. Albany, G. Giganti, G. Lombardi, *Front. Immunol.* **2019**, *10*, 43.
[14] C. B. Leitão, P. Cure, T. Tharvanji, D. A. Baidal, R. Alejandro, *Curr. Diabetes Rep.* **2008**, *8*, 324.
[15] N. Niemann, B. Sawitzki, *Curr. Transplant. Rep.* **2015**, *2*, 233.
[16] A. Fuchs, M. Gliwinski, N. Grageda, R. Spiering, A. K. Abbas, S. Appel, R. Bacchetta, M. Battaglia, D. Berglund, B. Blazar, J. A. Bluestone, M. Bornhäuser, A. ten Brinke, T. M. Brusko, N. Cools, M. C. Cuturi, E. Geissler, N. Giannoukakis, K. Golab, D. A. Hafler, S. M. van Ham, J. Hester, K. Hippen, M. Di Ianni, N. Ilic, J. Isaacs, F. Issa, D. Iwaszkiewicz-Grzes, E. Jaeckel, I. Joosten, D. Klatzmann, H. Koenen, C. van Kooten, O. Korsgren, K. Kretschmer, M. Levings, N. M. Marek-Trzonkowska, M. Martinez-Llordella, D. Miljkovic, K. H. G. Mills, J. P. Miranda, C. A. Piccirillo, A. L. Putnam, T. Ritter, M. G. Roncarolo, S. Sakaguchi, S. Sánchez-Ramón, B. Sawitzki, L. Sofronic-Milosavljevic, M. Sykes, Q. Tang, M. Vives-Pi, H. Waldmann, P. Witkowski, K. J. Wood, S. Gregori, C. M. U. Hilkens, G. Lombardi, P. Lord, E. M. Martinez-Caceres, P. Trzonkowski, *Front. Immunol.* **2018**, *8*, 1844.
[17] S. Todo, K. Yamashita, R. Goto, M. Zaitsu, A. Nagatsu, T. Oura, M. Watanabe, T. Aoyagi, T. Suzuki, T. Shimamura, T. Kamiyama, N. Sato, J. Sugita, K. Hatanaka, H. Bashuda, S. Habu, A. J. Demetris, K. Okumura, *Hepatology* **2016**, *64*, 632.
[18] S. Chandran, Q. Tang, M. Sarwal, *Am. J. Transplant.* **2017**, *17*, 2945.
[19] N. Safinia, G. Lombardi, *Front. Immunol.* **2015**, *6*, 438.
[20] P. J. O. Connell, D. J. Holmes-Walker, D. Goodman, W. J. Hawthorne, T. Loudovaris, J. E. Gunton, H. E. Thomas, S. T. Grey, C. J. Drogemuller, G. M. Ward, D. J. Torpy, P. T. Coates, T. W. Kay, *Am. J. Transplant.* **2013**, *13*, 1850.
[21] D. Penko, D. Mohanasundaram, S. Sen, C. Drogemuller, C. Mee, C. S. Bonder, P. T. H. Coates, C. F. Jessup, *Islets* **2011**, *3*, 73.
[22] D. Penko, D. Rojas-Canales, D. Mohanasundaram, H. S. Peiris, W. Y. Sun, C. J. Drogemuller, D. J. Keating, P. T. H. Coates, C. S. Bonder, C. F. Jessup, *Cell Transplant.* **2015**, *24*, 37.
[23] Z. Yue, X. Liu, P. T. Coates, G. G. Wallace, *Curr. Opin. Organ Transplant.* **2016**, *21*, 467.
[24] X. Liu, S.-S. D. Carter, M. J. Renes, J. Kim, D. M. Rojas-Canales, D. Penko, C. Angus, S. Beirne, C. J. Drogemuller, Z. Yue, P. T. Coates, G. G. Wallace, *Adv. Healthcare Mater.* **2019**, *8*, 1801181.
[25] J. Kim, K. Kang, C. J. Drogemuller, G. G. Wallace, P. T. Coates, *Curr. Diabetes Rep.* **2019**, *19*, 53.
[26] F. Lim, A. Sun, *Science* **1980**, *210*, 908.
[27] T. Y. Wuest, J. Willette-Brown, S. K. Durum, A. A. Hurwitz, *J. Leukocyte Biol.* **2008**, *84*, 973.
[28] D. Soler, T. R. Chapman, L. R. Poisson, L. Wang, J. Cote-Sierra, M. Ryan, A. McDonald, S. Badola, E. Fedyk, A. J. Coyle, M. R. Hodge, R. Kolbeck, *J. Immunol.* **2006**, *177*, 6940.
[29] S. F. Ziegler, F. Ramsdell, M. R. Alderson, *Stem Cells* **1994**, *12*, 456.
[30] D. Hill, N. Eastaff-Leung, S. Bresatz-Atkins, N. Warner, J. Ruitenberg, D. Krumbiegel, S. Pederson, N. McInnes, C. Y. Brown, T. Sadlon, S. C. Barry, *Immunol. Cell Biol.* **2012**, *90*, 812.
[31] Y. Barsheshet, G. Wildbaum, E. Levy, A. Vitenshtein, C. Akinseye, J. Griggs, S. A. Lira, N. Karin, *Proc. Natl. Acad. Sci. USA* **2017**, *114*, 6086.
[32] T. Gao, G. J. Gillispie, J. S. Copus, A. Kumar, P. Rajan, Y. Seol, A. Atala, J. J. Yoo, S. J. Lee, *Biofabrication* **2018**, *10*, 1.
[33] C. D. O'Connell, C. Onofrillo, S. Duchi, X. Li, Y. Zhang, P. Tian, L. Lu, A. Trengove, A. Quigley, S. Gambhir, A. Khansari, T. Mladenovska, A. O'Connor, C. Di Bella, P. F. Choong, G. G. Wallace, *Biofabrication* **2019**, *11*, 035003.
[34] N. Paxton, W. Smolan, T. Böck, F. Melchels, J. Groll, T. Jungst, *Biofabrication* **2017**, *9*, 044107.
[35] N. Soltan, L. Ning, F. Mohabatpour, P. Papagerakis, X. Chen, *ACS Biomater. Sci. Eng.* **2019**, *5*, 2976.
[36] R. Schwartz, M. Malpica, G. L. Thompson, A. K. Miri, *J. Mech. Behav. Biomed. Mater.* **2020**, *103*, 103524.
[37] A. Kumar, J. L. Moreau, M. Gibert, J. Theze, *J. Immunol.* **1987**, *139*, 3680.
[38] S. Létourneau, C. Krieg, G. Pantaleo, O. Boyman, *J. Allergy Clin. Immunol.* **2009**, *123*, 758.
[39] T. J. Sadlon, B. G. Wilkinson, S. Pederson, C. Y. Brown, S. Bresatz, T. Gargett, L. Melville, K. Peng, R. J. D. Andrea, G. Gary, G. J. Goodall, H. Zola, M. Frances, S. C. Barry, S. Bresatz, T. Gargett, E. L. Melville, K. Peng, *J. Immunol.* **2010**, *185*, 1071.
[40] M. Beyer, Y. Thabet, R. Müller, T. Sadlon, S. Classen, K. Lahl, S. Basu, X. Zhou, S. L. Bailey-bucktrout, W. Krebs, E. A. Schönfeld, J. Böttcher, T. Golovina, C. T. Mayer, A. Hofmann, D. Sommer, S. Debey-pascher, E. Endl, A. Limmer, K. L. Hippen, B. R. Blazar, R. Balderas, T. Quast, A. Waha, G. Mayer, M. Famulok, P. A. Knolle, C. Wickenhauser, W. Kolanus, B. Schermer, J. A. Bluestone, S. C. Barry, T. Sparwasser, J. L. Riley, J. L. Schultze, *Nat. Immunol.* **2011**, *12*, 898.
[41] T. Chinen, A. K. Kannan, A. G. Levine, X. Fan, U. Klein, Y. Zheng, G. Gasteiger, Y. Feng, J. D. Fontenot, A. Y. Rudensky, *Nat. Immunol.* **2016**, *17*, 1322.
[42] S. Gupta, T. B. Thornley, W. Gao, R. Larocca, L. A. Turka, V. K. Kuchroo, T. B. Strom, *J. Clin. Invest.* **2012**, *122*, 2395.
[43] S. Gupta, P. Samuels, S. Long, M. Tatum, J. Buckner, *Am. J. Transplant.* **2013**, *13*, 5.
[44] D. B. Hoelzinger, S. E. Smith, N. Mirza, A. L. Dominguez, S. Z. Manrique, J. Lustgarten, *J. Immunol.* **2010**, *184*, 6833.
[45] B. Kuehnemuth, I. Piseddu, G. M. Wiedemann, M. Lauseker, C. Kuhn, S. Hofmann, E. Schmoeckel, S. Endres, D. Mayr, U. Jeschke, D. Anz, *BMC Cancer* **2018**, *18*, 1278.
[46] E. Eruslanov, T. Stoffs, W. J. Kim, I. Daurkin, S. M. Gilbert, L. M. Su, J. Vieweg, Y. Daaka, S. Kusmartsev, *Clin. Cancer Res.* **2013**, *19*, 1670.
[47] A. Zingoni, H. Soto, J. A. Hedrick, A. Stoppacciaro, C. T. Storlazzi, F. Sinigaglia, D. D'Ambrosio, A. O'Garra, D. Robinson, M. Rocchi, A. Santoni, A. Zlotnik, M. Napolitano, *J. Immunol.* **1998**, *161*, 547.
[48] S. S. Tay, K. M. Plain, G. A. Bishop, *Curr. Opin. Organ Transplant.* **2009**, *14*, 16.
[49] Z. Liu, H. Fan, S. Jiang, *Immunol. Rev.* **2013**, *252*, 183.
[50] M. L. McCully, K. Ladell, R. Andrews, R. E. Jones, K. L. Miners, L. Roger, D. M. Baird, M. J. Cameron, Z. M. Jessop, I. S. Whitaker, E. L. Davies, D. A. Price, B. Moser, *J. Immunol.* **2018**, *200*, 1639.
[51] S. K. Chauhan, D. R. Saban, H. K. Lee, R. Dana, *J. Immunol.* **2009**, *182*, 148.
[52] S. Jhunjhunwala, G. Raimondi, A. J. Glowacki, S. J. Hall, D. Maskarinec, S. H. Thorne, A. W. Thomson, *Adv. Mater.* **2012**, *24*, 4735.
[53] D. A. Alagpulinsa, J. J. L. Cao, R. K. Driscoll, R. F. Sîrbulescu, M. F. E. Penson, M. Sremac, E. N. Engquist, T. A. Brauns, J. F. Markmann, D. A. Melton, M. C. Poznansky, *Am. J. Transplant.* **2019**, *19*, 1930.
[54] D. K. C. Cooper, R. Gatson, D. Eckhoff, J. Ladowski, T. Yamamoto, L. Wang, H. Iwase, H. Hara, M. Tector, A. J. Tector, *Br. Med.* **2018**, *125*, 5.
[55] Y. T. Ghebremariam, S. A. Smith, J. B. Anderson, D. Kahn, G. J. Kotwal, *Ann. N. Y. Acad. Sci.* **2005**, *1056*, 123.
[56] H.-T. Zhu, W.-L. Wang, L. Yu, B. Wang, *Front. Surg.* **2014**, *1*, 1.
[57] A. Schmidt, N. Oberle, P. H. Krammer, *Front. Immunol.* **2012**, *3*, 1.
[58] B. H. Nelson, *J. Immunol.* **2004**, *172*, 3983.
[59] H. Huang, Y. Ma, W. Dawicki, X. Zhang, J. R. Gordon, *J. Immunol.* **2013**, *191*, 1136.
[60] J. W. Griffith, C. L. Sokol, A. D. Luster, *Annu. Rev. Immunol.* **2014**, *32*, 659.
[61] E. G. Schmitt, C. B. Williams, *Front. Immunol.* **2013**, *4*, 152.

[62] J. R. Ghali, M. A. Alikhan, S. R. Holdsworth, A. R. Kitching, *Immunology* **2017**, *150*, 100.
[63] F. Mehrpouya, Z. Yue, T. Romeo, R. Gorkin, R. M. I. Kapsa, S. E. Moulton, G. G. Wallace, *J. Mater. Chem. B* **2019**, *7*, 556.
[64] M. Battaglia, A. Stabilini, B. Migliavacca, J. Horejs-Hoeck, T. Kaupper, M. G. Roncarolo, *J. Immunol.* **2006**, *177*, 8338.
[65] S. O. Stead, S. J. P. McInnes, S. Kireta, P. D. Rose, S. Jesudason, D. Rojas-Canales, D. Warther, F. Cunin, J. O. Durand, C. J. Drogemuller, R. P. Carroll, P. T. Coates, N. H. Voelcker, *Biomaterials* **2018**, *155*, 92.
[66] S. O. Stead, S. Kireta, S. J. P. McInnes, F. D. Kette, K. N. Sivanathan, J. Kim, E. J. Cueto-Diaz, F. Cunin, J. O. Durand, C. J. Drogemuller, R. P. Carroll, N. H. Voelcker, P. T. Coates, *ACS Nano* **2018**, *12*, 6637.
[67] M. Balyura, E. Gelfgat, M. Ehrhart-Bornstein, B. Ludwig, Z. Gendler, U. Barkai, B. Zimerman, A. Rotem, N. L. Block, A. V. Schally, S. R. Bornstein, *Proc. Natl. Acad. Sci. USA* **2015**, *112*, 2527.
[68] Y. Yang, E. C. Opara, Y. Liu, A. Atala, W. Zhao, *Exp. Biol. Med.* **2017**, *242*, 286.
[69] L. Picariello, S. Benvenuti, R. Recenti, L. Formigli, A. Falchetti, A. Morelli, L. Masi, F. Tonelli, P. Cicchi, M. L. Brandi, *J. Surg. Res.* **2001**, *96*, 81.
[70] D. Loessner, C. Meinert, E. Kaemmerer, L. C. Martine, K. Yue, P. A. Levett, T. J. Klein, F. P. W. Melchels, A. Khademhosseini, D. W. Hutmacher, *Nat. Protoc.* **2016**, *11*, 727.

 